STRENGTH AND DEFORMATION CHARACTERISTICS OF GEOCELL-FIBER REINFORCED GRANULAR SOIL

A THESIS

submitted by

AKASH PRIYADARSHEE

for the award of the degree

of

DOCTOR OF PHILOSOPHY

GEOTECHNICAL ENGINEERING
DEPARTMENT OF CIVIL ENGINEERING
INDIAN INSTITUTE OF TECHNOLOGY GUWAHATI

MARCH 2013

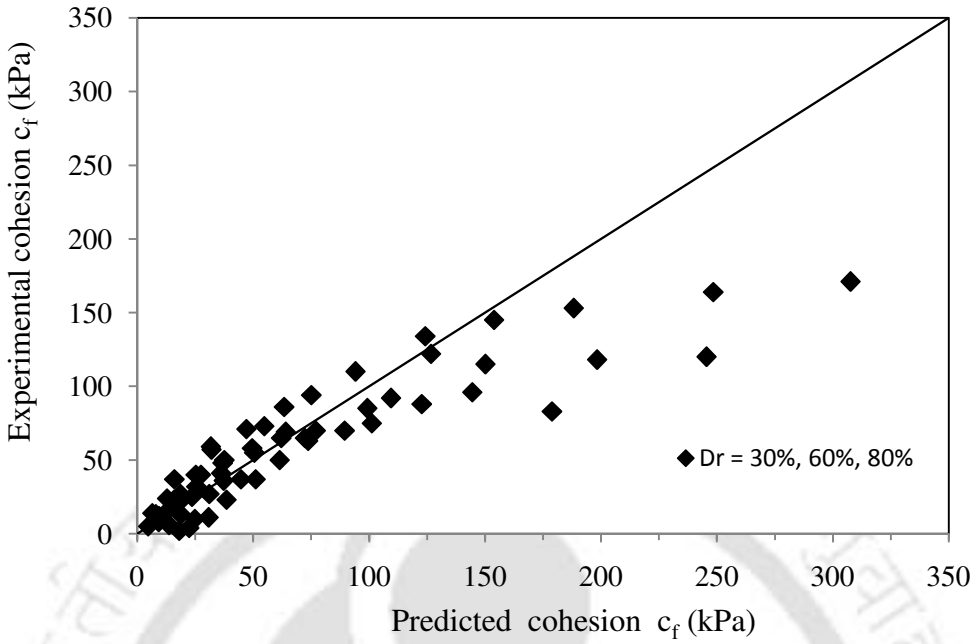

Fig. 5.49 Experimental versus predicted value of cohesion for fiber reinforced soil

TH-1123_10610407

CERTIFICATE

This is to certify that the thesis entitled **"Strength and Deformation Characteristics of Geocell-Fiber Reinforced Granular Soil"** submitted by **Akash Priyadarshee** Roll No. 10610407 to the Indian Institute of Technology Guwahati, for the award of the degree of Doctor of Philosophy in Civil Engineering is a record of bonafide research work carried out by him under my supervision and guidance. The thesis work, in my opinion, has reached the requisite standard fulfilling the requirement for the degree of Doctor of Philosophy.

The results contained in this thesis have not been submitted in part or full to any other University or Institute for award of any degree or diploma.

Dr. Sujit Kumar Dash
Associate Professor
Department of Civil Engineering
Indian Institute of Technology Guwahati
Guwahati – 781039, India

TH-1123_10610407

STATEMENT

I do hereby declare that the matter embodied in this thesis is the result of investigations carried out by me in the department of Civil Engineering, Indian Institute of Technology Guwahati, Guwahati, Assam, India.

In keeping with the general practice of reporting scientific observations, due acknowledgements have been made wherever the work described is based on the findings of other investigators.

Guwahati 781039 Akash priyadarshee

date

TH-1123_10610407

CHAPTER 1

INTRODUCTION

1.1 BACKGROUND

Different techniques being used for mitigating the problems due to weak soils primarily includes provision of piled foundation, excavation and replacement with good quality soil, preloading with vertical drains, stone columns, chemical stabilization, soil reinforcement etc. Among these soil reinforcement technique is relatively popular across the world. Since the pioneering work of Vidal (1969), numerous reinforced soil structures have been built across the world. In early days, the concept of reinforcing the earth was mainly pertaining to the use of metallic reinforcements (Sridharan 1990). Over the past two decades this concept has been extended to other materials like fabrics and grids, often termed as geotextiles and geogrids (Das and Khing 1994, Das et al. 1996), randomly distributed fibers (Puppala and Musenda 2007); manufactured mainly from polypropylene materials. The geocell reinforcement is a recently developed reinforcing technique, which is a three dimensional, polymeric, honeycomb like structure of cells interconnected at joints (Bush et al 1990). Compared to conventional techniques such as piling or chemical stabilization, the reinforced-soil doesn't need formwork, curing etc. resulting overall economy, ease of construction that provides added attraction to the practicing engineers. Geocell reinforcement technology was invented by the US Army Corps of Engineers for stabilization of beach sands for construction of roads (Webster 1979). Subsequently it has been widely applied in many areas of Geotechnical engineering such as highways, railways, foundations, embankments, retaining walls, pipeline

TH-1123_10610407

excavations etc. (Bathurst and Jarrett 1988, Bush et al. 1990, Bathurst and Crowe 1992, Cowland and Wong 1993, Chen and Chiu 2008).

The design of geocell structures need to account for the prevailing mechanisms of the fill material (Wesseloo et al. 2009). Indeed the beneficial effect of geocells in terms of the increase in stiffness and load carrying capacity is found to increase with increase in the density of the fill soil (Dash 2010). Fiber inclusion in soils can effectively improve their strength and stiffness (Gray and Al-Refeai 1986, Benson and Khire 1994), a technique that is being commonly in Geotechnical engineering projects (Gregory and Chill 1998, Refai, 2000, Park and Tan, 2005, Santoni et al. 2001). It is therefore imperative that if fiber reinforced soils can be sued as fill material, in geocells, would give rise to further improvement in performance, compared to that with soils alone. Indeed, Lambert et al. (2011) through model tests have reported that randomly reinforced tire chips in the sand fill of geocells can lead to substantial increase in compressive resistance of the geocell-soil system.

1.2 GEOCELL REINFORCED SOIL

The concept of geocell reinforcement is a recently developed one that has three dimensional, polymeric, honeycomb like structure of cells interconnected at joints. Geocells are broadly of two different types. When manufactured from high density polyethylene sheets (solid or perforated), ultrasonically welded at joint, is called geoweb, and is typically of 100 to 200 mm in height (Bathurst and Rajagopal 1993). Fig.1.1 shows a typical geoweb structure, available in the market. When required of higher height, is fabricated using geogrids, mechanically connected through bodkin joint (Bush et al. 1990). Such grid cells are popularly called geocells (Fig.1.2). The bodkin joint is formed by pulling the strands of transverse geogrid up through the diagonal geogrid and slipping a dowel through the loop created (Fig.1.3).

TH-1123_10610407

Geocells, when filled with soil and compacted, produce a composite mattress that redistributes the surcharge pressure over a wider area. Unlike planar reinforcements where the soil squeezes out laterally, the reinforcing mechanism in the geocells is by all-round confinement of soil within its pockets (Fig.1.4). The geocell walls intercept the shear planes in the soil and their rigidity forces them deeper into the foundation bed. As a result of which a higher surcharge loading is induced on the failure plane leading to enhanced load carrying capacity (Koerner 1990). A typical field installation of geocells is shown in Fig. 1.5. It is suggested that the geocells should be over filled by about 150 mm and be subjected to light rolling. The overfilling is to cater to compaction settlement (Bush et al 1990). With repeated passage of rolling and filling of potholes, a compact geocell-soil structure could be achieved. A cost comparison reported by Robertson and Gilchrist (1987) shows that the geocell mattress method of construction of road embankments over deep soft clay deposit could save 31% of the cost of conventional solutions.

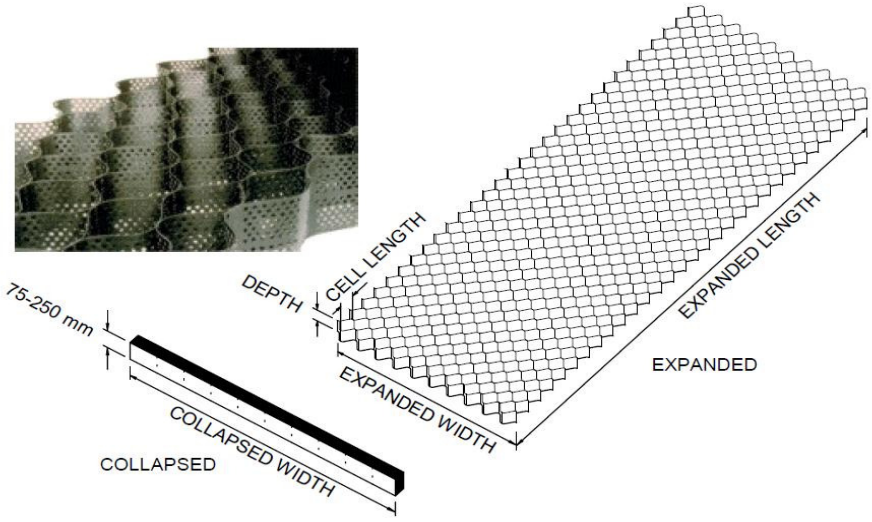

Fig. 1.1 Typical Geocell structure made of polymer sheets (Wesseloo 2004)

TH-1123_10610407

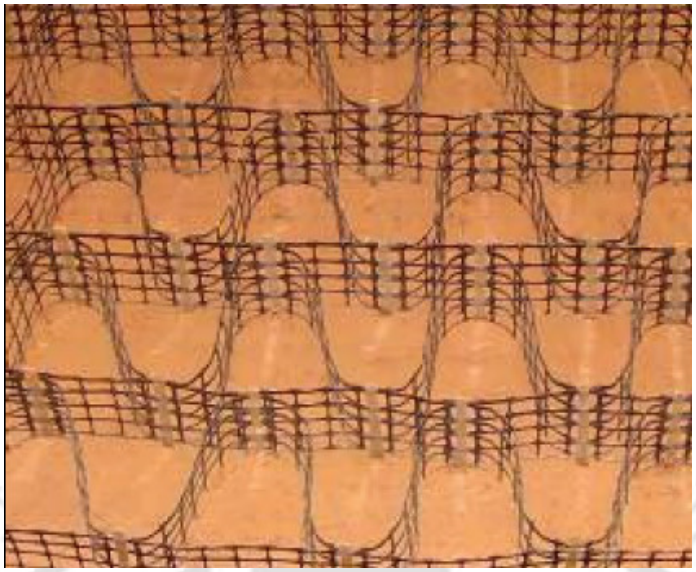

Fig. 1.2 Geocell system made of geogrid sheets (Minaxi 2010)

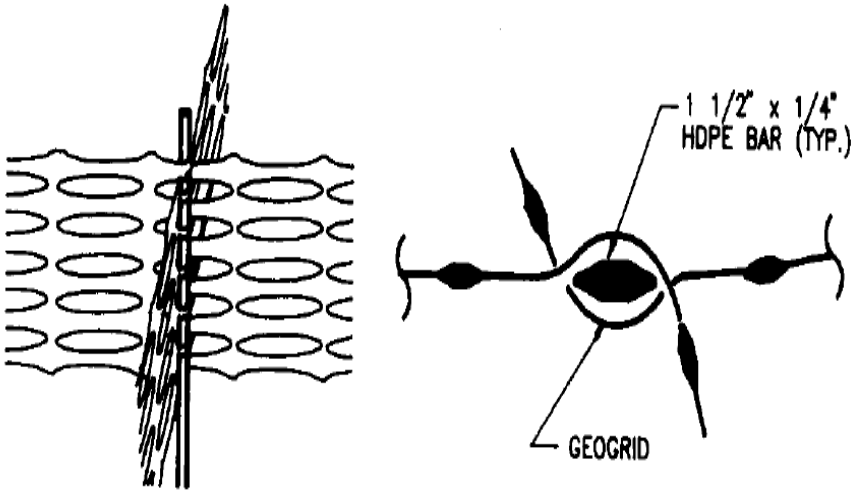

Fig. 1.3 Details of bodkin joint (Carroll Jr. and Curtis, 1990)

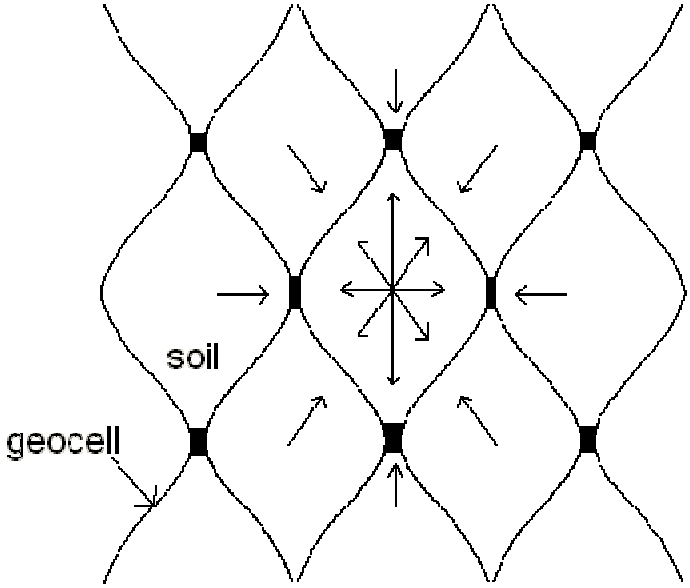

Fig.1.4 Confinement of soil by geocells

Fig. 1.5 Geocells being filled with soil (Emersleben and Meyer, 2008)

1.3 FIBER REINFORCED SOIL

Fiber reinforced soil is a mixture of soil and fibers. Fibers can be natural or synthetics. Natural fibers can be obtained from the plants, animals other natural source. Jute, Cotton, Silk are some examples of natural fibers. Petrochemicals are the major source of synthetic fibers. Polypropylene, polyester, polyamide etc. are the examples of such type of synthetic fiber. Other form of synthetic fiber is made of glass, the main constituent of which is silica. Since glass is an amorphous material, properties of glass fibers are uniform in all direction. Advantage of synthetic fibers over the natural fibers is less degradation, and therefore is widely being used in geotechnical applications.

A schematic sketch of fiber reinforced soil is depicted in Fig. 1.6. Major difference between the fiber reinforcement and other forms of soil reinforcement i.e. geogrid, geocell etc. is the orientation. While the geogrid is laid horizontally and geocells three dimensionally, the fiber is randomly distributed in the soil. Due to this random distribution, fiber reinforcement doesn't induce any clear cut potential plane of weakness as is the case with geogrid and geocells wherein there exists plane of weakness at the soil reinforcement interface.

The mechanism of fiber reinforcement is very much similar to the plant roots in soil. Fig. 1.7 shows a typical interaction between fiber and soil when stress is applied onto it. Under the stress imposed, the fiber deforms and thereby interlocks the soil. Besides, it mobilizes frictional resistance at the soil-fiber interface. These two factors are primarily responsible for the enhanced performance of fiber reinforced soils.

In the field the soil is scarified and fiber is placed over it (Fig. 1.8). Subsequently is mixed through rotary mixture (Fig.1.9) and compacted. When used in limited quantity

TH-1123_10610407

the soil fiber can be mixed in a centralized plant and transported to the construction site, in which case better quality control could be achieved.

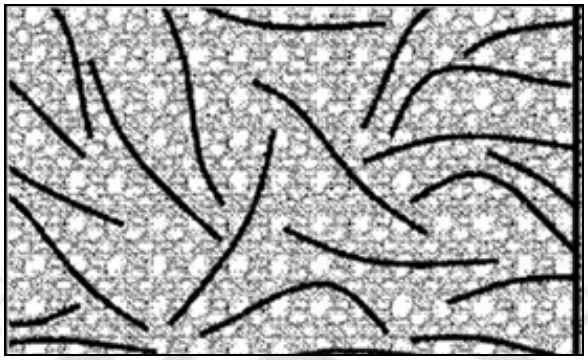

Fig. 1.6 Schematic diagram of soil-fiber matrix (Sadek et al., 2010)

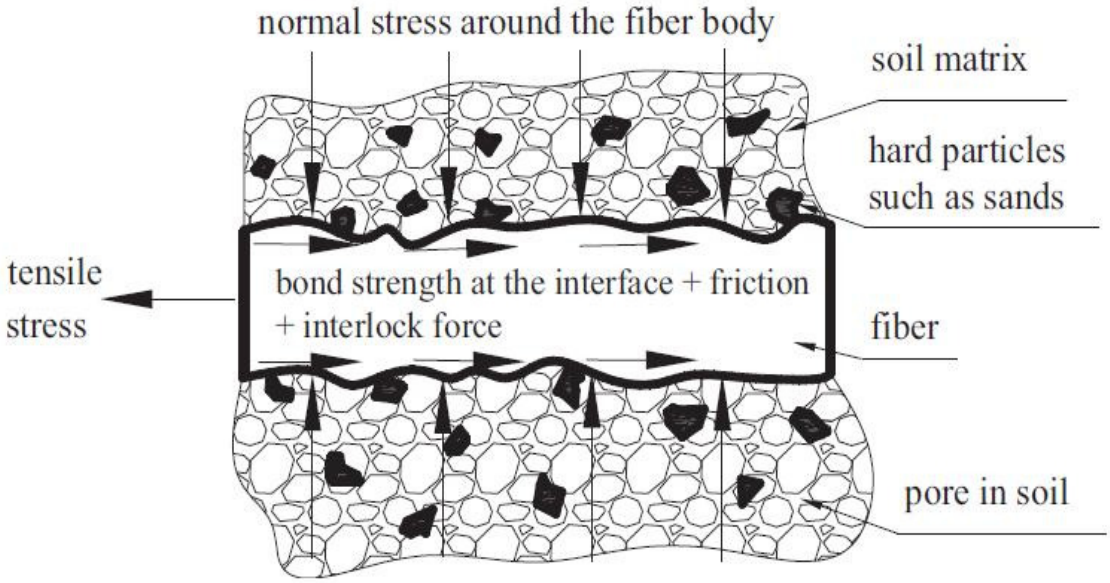

Fig. 1.7 Interaction between soil particle and fiber (Tang et al., 2007)

Fig. 1.8 Placement of fiber over scarified soil (Gregory, 2006)

Fig. 1.9 Mixing of fiber with soil (Gregory, 2006)

1.4 OBJECTIVE OF THE PRESENT STUDY

Objective of the present study is to develop an understanding of the strength and deformation characteristics of geocell, fiber and geocell-fiber reinforced granular soils.

1.5 ORGANISATION OF THE THESIS

A detailed review of literature pertaining to the present study is presented in Chapter 2. Subsequently, the scope of the present investigation has been brought out. In Chapter 3 characterization of the materials used, test details and planning of experiments are presented in detail. Chapter 4-6 present and discuss the results obtained. In Chapter 4, the results of the tests done with geocell reinforcement are presented. Chapter 5 deals with the test data on fiber reinforced soil. Chapter 6 brings out the performance improvement of soil due to the combined application of geocell and fiber reinforcement. Besides, dimensional analysis leading to the influence of different soil and reinforcement parameters on the behavior of the reinforced soils composites have also been presented and discussed. Subsequently, analytical model for predicting the performance improvement of soils due to the different forms of reinforcements is brought out. In Chapter 7 a summary of the present study and the major conclusions drawn, are presented.

TH-1123_10610407

CHAPTER 2

REVIEW OF LITERATURE AND SCOPE OF PRESENT STUDY

2.1 INTRODUCTION

Several studies have been reported on geocell and fiber reinforcement in soils. Presented here are the current literatures on these topics. The literature review is divided into two different sections. First is on geocell reinforcement and the second is on fiber reinforcement. Each of these sections has again been divided into three sub sections dealing with field applications, model tests and strength-stiffness behavior separately. An overview of the experimental procedures, details of test parameters and broad conclusions drawn from the reported studies are presented. At the end a critical summary of the literatures is made, based on which the scope of the present study is defined.

2.2 GEOCELL REINFORCEMENT

2.2.1 Applications

The pioneering work of Webster and Watkins (1977), Webster and Alford (1978), at the U.S. Army Engineers Experiment Station, Vicksburg, has lead to the development of commercial geocells of the present days. They carried out field tests on, sand filled, vertical, interconnected, shallow, thin-walled aluminium cells placed over soft subgrade. The loading applied was full scale traffic. It was observed that the geocell reinforced sand could provide significantly greater load carrying capacity than the compacted soil alone. The behaviour of the grid cell mattress resembles that of a slab. Based on the findings it is concluded that the performance of sand-filled grid cells

TH-1123_10610407

when used over very soft subgrade can be equivalent to that of a layer of crushed stone that is as much as 1.6 times thicker than the height of the geoecll mattress.

Johnson (1982) used geocell mattress concept in the construction of the Great ham Creek bridge, England wherein, the geocell mattress was placed under the 5 meter high approach embankment over soft estuarine silts running up to 7 meter depth. The settlements measured were less than 50% of the predicted values. The lateral strains were also found to be very small.

De Garidel and Morel (1986) evaluated the suitability of geotextile cells for construction of road. The geocell reinforced structures did not show much of improvement at small displacements. However, at large displacement the strengthening effect was remarkable.

Robertson and Gilchrist (1987) reported the geocell mattress application as the most cost effective and convenient solution for construction of a 4 meter high embankment over a 4 meter deep soft clay overlying mudstone, in the Auchenhowie road. The average undrained shear strength of the clay was 15 kPa. The selection of the geocell mattress solution was made after other methods were rejected under ground of practical difficulty or a much longer construction period. Cost analysis showed that, as compared to the conventional solutions, geocell mattress method of construction can provide up to 31% of cost saving.

Paul (1988) reported the use of geogrid formed geocell mattress to support an embankment over areas of deep soft deposits in Scotland. Four different methods of construction were examined; i.e. partial excavation of soft soil and replacement by backfill, installation of drainage followed by staged construction, complete excavation of the soft layer and replacement with a rock fill and construction of a geocell

TH-1123_10610407

mattress. Out of which, the geocell mattress option was found to be economical and most rapid way of construction without normal problems for mechanical plants and machinery. Settlement pins were installed within the embankment on top of the mattress. Approximately 90mm of initial settlement was recorded at the end of the embankment construction with no significant differential settlement noted either longitudinally or transversely.

Bush et al. (1990) reported the use of geocell foundation mattress in the construction of a full scale embankment over soft soil deposit (Fig. 2.1). The geocell were fabricated from polymer grid reinforcement, directly over the foundation soil, subsequently filled with granular material resulting in a semi rigid base of about 1 meter deep. Apart from, providing a working area for the construction, the geocell-soil mattress enhanced the bearing capacity substantially. The rough bottom of geocell mattress exerted a restraint against deformations in the foundation soil leading to increased stability of the system.

Fig. 2.1 Geocell mattress (Bush et al. 1990)

TH-1123_10610407

Dean and Lothin (1990) have reported the construction of an embankment over a deep soft deposit using geocell mattress. The geocells were fabricated using uniaxial geogrid and were filled with crushed rock. Among all other alternatives (i.e. construction of a viaduct, replacement of the soft deposit with rockfill, preconsolidation of the soft soil) the geocell mattress option was found to be the cheapest and convenient. Besides, it enabled the embankment to be constructed relatively rapidly.

Bathurst and Crowe (1992) described the use of geocell confinement systems in constructing flexible gravity walls and steepened slopes. They have conducted large scale unconfined compression tests in order to examine the stability of multiple layers of geocell mattress under vertical surcharge. The $1 \times 1 \times 1.44$ m sand-geocell column consisting of eight layers of geocell, was stable up to a maximum surcharge pressure of 155kPa (i.e. 10 m equivalent height of structure) with a corresponding vertical strain of 1.4%. Based on this input the authors have designed and built full scale retaining walls that didn't show any excessive deformation or collapse.

Cowland and Wong (1993) reported a case study of the performance of a geocell supported embankment on soft clay. The geocell mattress was formed using high density polyethylene and polypropylene geogrids. The geocell pockets were filled with 25mm down angular shaped rock fill. The embankment was fully instrumented with pneumatic piezometers, inclinometers, hydrostatic profile gauges, settlement plates, surface settlement markers and lateral movement blocks. The performance of the geocell mattress foundation was monitored during the construction of the embankment. The recorded extensions of the geocell mattress were found to be less

TH-1123_10610407

than 1%. This suggests that the geocell mattress has behaved as a raft foundation to the embankment.

Gupta and Somnath (1994) used the concept of geocells in the construction of box culverts over marine clay deposits in New Bombay area. The depth of the marine clay was more than 6 meters. First tubular gabions were constructed in the soft soil with their ends resting on hard moorum layer underlying. Next the geocell mattress was constructed on the clay surface. In this arrangement the gabions serve as granular piles and the geocell mattress as flexible pile cap. The performance of the geocell mattress has been reported to be satisfactory.

Forsman et al. (1998) have reported a case study on the performance of a geocell reinforced road over deep peat deposit. The geocells were fabricated using geogrids and were filled with light expanded clay aggregate. This lightweight fill was used because of expected large settlements in the peat deposit. The test structures were experimentally instrumented using vertical magnetic probe extensometers, horizontal hydrostatic profile gauges, settlement plates, horizontal extensometers and strain gauges. Plate load tests and falling weight deflectometer tests were conducted to measure the modulus of the subgrade. The results indicate that the tension is concentrated quite near the loading point. The geocell layer was found to be effective in increasing the bearing capacity and reducing differences in settlements. Even after a year and half, no significant differential settlement was observed on the road surface.

2.2.2 Model tests

Rea and Mitchell (1978) through laboratory model tests have investigated the performance of interconnected paper cells filled with sand as reinforced layer for

TH-1123_10610407

application in low cost highway construction. The cells were made of 0.203 mm thick paper and were square in shape when expanded. The width was kept constant at 51 mm. The subgrade was simulated using springs. The parameters studied are; radius of loaded area, cell width, cell height, subgrade stiffness and repetition of loading. Based on the test results, the different modes of failures identified are; cell penetration, cell bursting, cell wall buckling, bearing capacity failure, bending failure and excessive rutting.

Mhaiskar and Mandal (1996) investigated the effect of geocell geometry and relative density of the infill soil on the overall performance of the foundations. Fig. 2.2 shows the details of the test setup used in this study. Monotonic loading was applied in plate load tests. Considerable improvement in the load carrying capacity and reduction of settlement was observed.

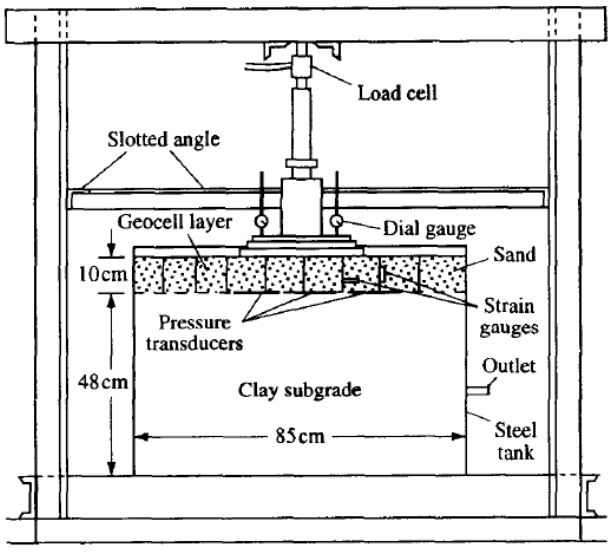

Fig. 2.2 Test setup used by Mhaiskar and Mandal (1996)

TH-1123_10610407

Krishnaswamy et al. (2000) conducted a series of laboratory model tests on geocell supported earth embankments constructed over soft clay bed (Fig. 2.3). The geocell layers were fabricated using different types of uniaxial and biaxial geogrids. The embankments were subjected to uniform surcharge pressure on the crest until failure. Test results indicated that the provision of a geocell layer at the base of the embankment improves the performance of the embankment to a large extent. A parametric study shows that the surcharge carrying capacity of the embankment depends on the stiffness of the geogrid, pocket opening size, height of geocell, type of soil filled inside the geocell and the pattern used to form the geocells.

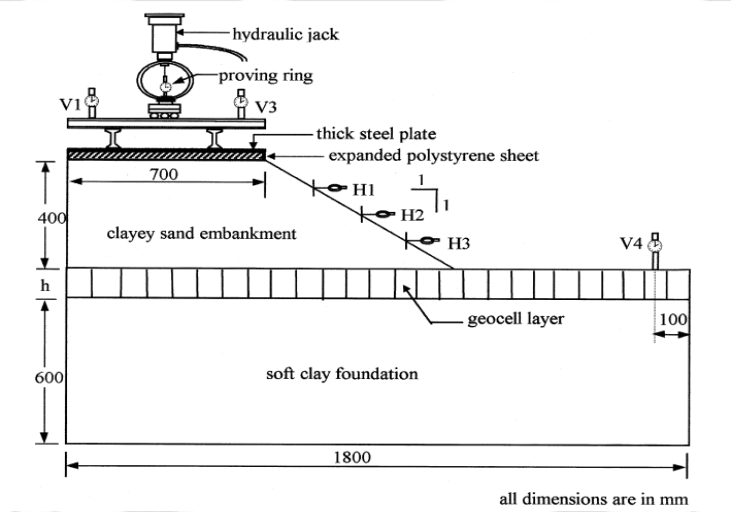

Fig. 2.3 Geocell reinforced model embankment tested by Krishnaswamy et al. (2000)

Dash et al. (2001) presented the results from laboratory-model tests on a strip footing supported by a sand bed reinforced with a geocell mattress. Fig. 2.4 shows the geometry of test setup used. Parameters studied are; pattern of geocell formation, pocket size, height and width of geocell mattress, the depth to the top of geocell mattress, tensile stiffness of the geogrids used to fabricate geocell mattress and the

TH-1123_10610407

relative density of the sand. With the provision of geocell reinforcement, failure was not noticed even at a settlement as high as 50% of the footing width, when there was about 8 fold increase in bearing capacity. Apart from the tensile strength of reinforcement, aperture size and orientation of ribs of the geogrid used to make the geocells to influence the bearing capacity improvement significantly.

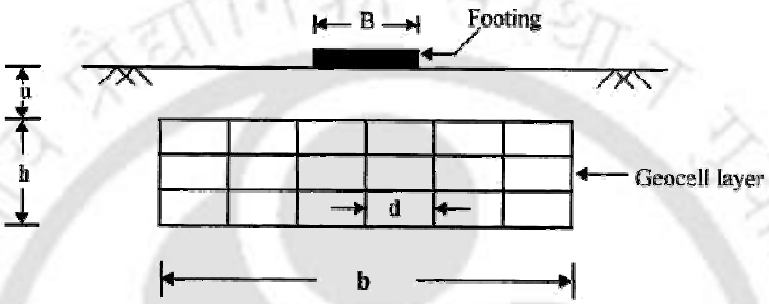

Fig.2.4 Geometry of model test done by Dash et al. (2001a)

The observed displacement pattern in the subgrade soil indicates that the geocell reinforcement intersects the potential failure planes in the foundation soil and its rigidity forces them deeper into the underlying soil layer thereby transmitting the footing pressures to deeper depth (Dash et al 2007). The proposed load dispersion mechanism is depicted in Fig. 2.5.

Pressure measurements, by Dash et al. (2003b), at the base of the geocell mattress indicates that the footing pressure is redistributed more uniformly over a wider area on the subgrade soil, indicating that the geocell-reinforced sand bed behaves as a stiffened composite body.

TH-1123_10610407

It is also observed that with the provision of geocell reinforcement, the subgrade modulus of sand bed can be increased as high as eight times that of the unreinforced soil (Dash et al. 2008).

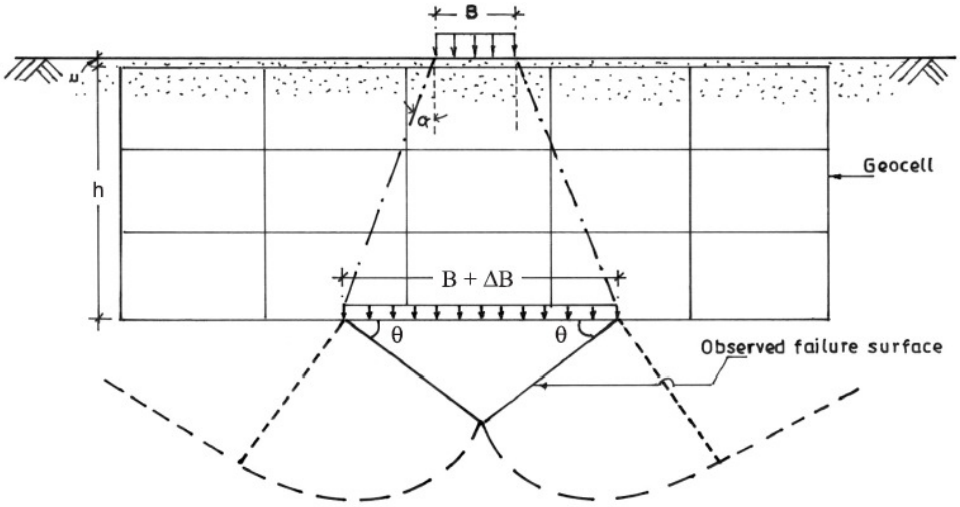

Fig. 2.5 Load dispersion mechanism in geocell mattress (Dash et al. 2007)

Effectiveness of geocell reinforcement placed in the granular fill overlying soft clay beds has been studied by Dash et al. (2003a). Fig. 2.6 shows the geometry of model test setup used. The test results indicate that with the provision of geocell reinforcement in the overlying sand layer, a substantial performance improvement can be obtained in terms of increase in the load carrying capacity and reduction in surface heaving of the foundation bed. An additional layer of geogrid placed at the base of the geocell mattress further enhances the load carrying capacity and stiffness of the foundation bed. Its beneficial effect decreases with the increase in the height of the geocell mattress. A seven-fold increase in the bearing capacity of the circular footing can be obtained by providing geocell reinforcement along with a basal geogrid layer in the sand bed underlying soft clay.

TH-1123_10610407

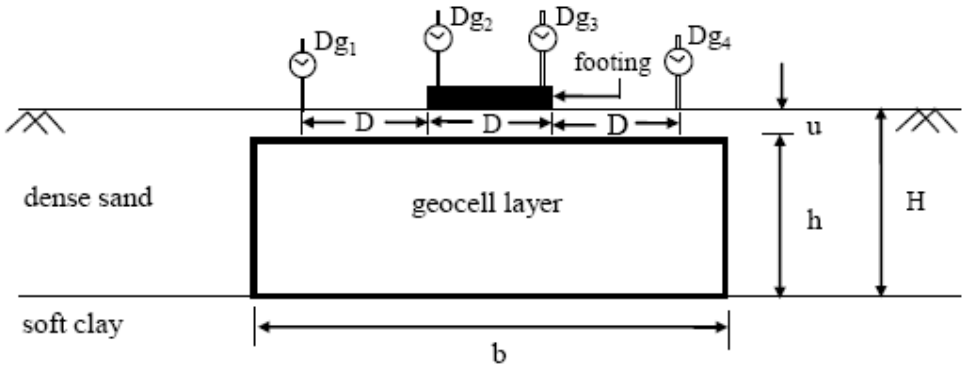

Fig. 2.6 Schematic sketch of test set up used by Dash et al. (2003a)

Through laboratory tests Dash et al. (2004) have studied the relative performance of different forms of reinforcement i.e. geocell, planar and randomly distributed mesh elements, in sand beds under strip loading. The results demonstrate that geocell reinforcement is the most advantageous one. With its provision, failure was not observed even at a settlement equal to about 45% of the footing width and a load as high as eight times the ultimate capacity of the unreinforced soil, whereas, with planar reinforcement, failure took place at a settlement of about 15% of the footing width and a load of about four times the ultimate capacity of the unreinforced soil. For the case with randomly distributed reinforcement mesh, failure was recorded at a load of about 1.8 times the ultimate capacity of the unreinforced soil and at a settlement of about 10% of the footing width. Latha and Somwanshi (2009) through model tests and numerical studies too have arrived at similar conclusions regarding the superiority of the geocells over the planar and randomly distributed reinforcement in the foundations.

Sireesh et al. (2009) have studied the potential benefits of providing geocell reinforced sand mattress over a void (Fig.2.7). The test results indicate that substantial improvement in performance can be obtained with the provision of geocell mattress,

TH-1123_10610407

of adequate size, over the subgrade with void. However, the geocell mattress must spread beyond the void at least a distance equal to its diameter. The influence of the void over the performance of the footing reduces for height of geocell mattress greater than 1.8 times the diameter of the footing. Better improvement in performance is obtained when the geocells are filled with dense soil.

Xie and Yang (2009) have evaluated the performance of flexible geocell retaining walls, constructed on an expressway in central north China's Shanxi Province. The horizontal stress of tied reinforced layers developed in three phases: bending, stretching–bending, and stretching as the external load increased. An economic analysis demonstrated that the geocells can reduce the overall cost of the retaining walls by about 24%.

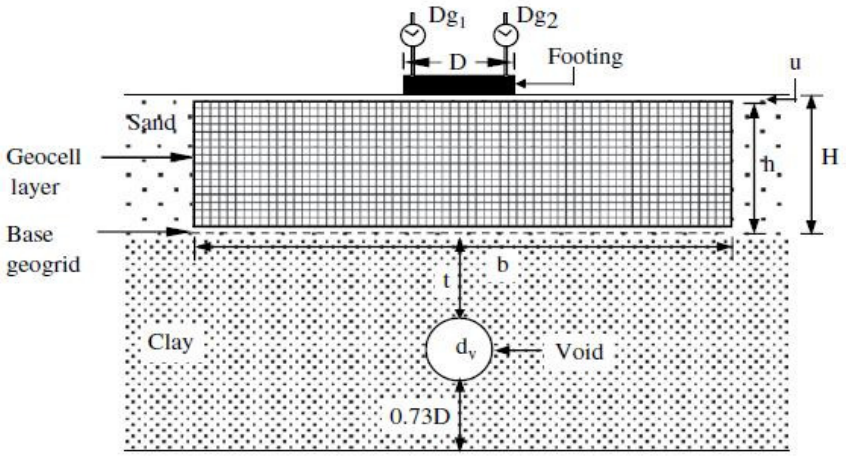

Fig. 2.7 Geometry of model tests used by Sireesh et al. 2009

TH-1123_10610407

Through model load tests on geocell-reinforced and unreinforced sand beds, Dash (2010) has brought out the influence of relative density of the foundation soil on the overall performance of the foundations. Tests were carried out for five different relative densities of sand 30, 40, 50, 60, and 70%. It is observed that the beneficial effect of geocell reinforcement, in terms of increase in stiffness, bearing capacity, and load dispersion angle of the foundation bed, though is felt over a wide range of relative density; is higher for dense condition of foundation soil. With geocell reinforcement offering three-dimensional confinement, the dilation induced benefit is substantially high for dense soil fill. Therefore, for effective utilization of geocell reinforcement, the foundation soil should be compacted to higher density.

Pokharel et al. (2010) have experimentally investigated the factors influencing the behavior (stiffness and bearing capacity) of single and multiple geocell-reinforced bases. The test results indicate that geocell of circular shape have higher stiffness and bearing capacity than the elliptical one. Besides, the performance of the geocell-reinforced base depends on the elastic modulus of the geocells, Single geocell-reinforced base is found to have lower stiffness and bearing capacity than the multiple geocell-reinforced bases.

Tafreshi and Dawson (2010a, 2010b) have reported the results of a series of laboratory model tests on strip footings supported on 3D geocell and planar geotextile-reinforced sand beds under static and repeated loads. On the whole, the results indicate that, for the same mass of geotextile material used in the tests, the 3D geotextile reinforcement system behaves more effectively than the planar reinforcement. Thus, a specific improvement in footing settlement can be achieved using a lesser quantity of 3D geotextile material (i.e. geocell) as compared to that with planar geotextile.

TH-1123_10610407

2.2.3 Strength-stiffness behavior

Bathurst and Karpurapu (1993) have carried out a series of large-scale triaxial compression tests on isolated geocell encased soil specimens of 100 mm diameter and 200 mm height. The results indicate an increase in stiffness and strength of the soil due to the geocell. Comparison of reinforced and unreinforced soil specimens shows that the frictional resistances, described by the peak friction angle, of the both are comparable. They have quantified the strength gain due to geocells through an apparent cohesion, the expression for which is given by

$$c_g = \frac{\Delta\sigma_3}{2}\tan\left(45 + \frac{\emptyset}{2}\right) \quad (2.1)$$

Where; c_g is the apparent cohesion due to geocell, Ø is the internal angle of friction of the soil, $\Delta\sigma_3$ is the induced confinement due to the geocell which is obtained using the elastic membrane model proposed by Henkel and Gilbert (1952), Equation 2.2.

$$\Delta\sigma_3 = \frac{2.M}{D_0}\left[\frac{1-\sqrt{(1-\varepsilon_a)}}{1-\varepsilon_a}\right] \quad (2.2)$$

Where; M is the compression modulus of rubber membrane, ε_a is the axial strain of the specimen, D_o is the initial diameter of the specimen.

Rajagopal et al. (1999) studied the influence of multiple geocell confinement system on the strength and stiffness behaviour of granular soils. A large number of triaxial compression tests were performed thereof. Fig. 2.8 shows the picture of a typical test specimen with multiple geocells and Fig.2.9 shows the stress strain responses.

TH-1123_10610407

Fig 2.8 Typical test specimen with multiple geocells (Rajagopal et al. 1999)

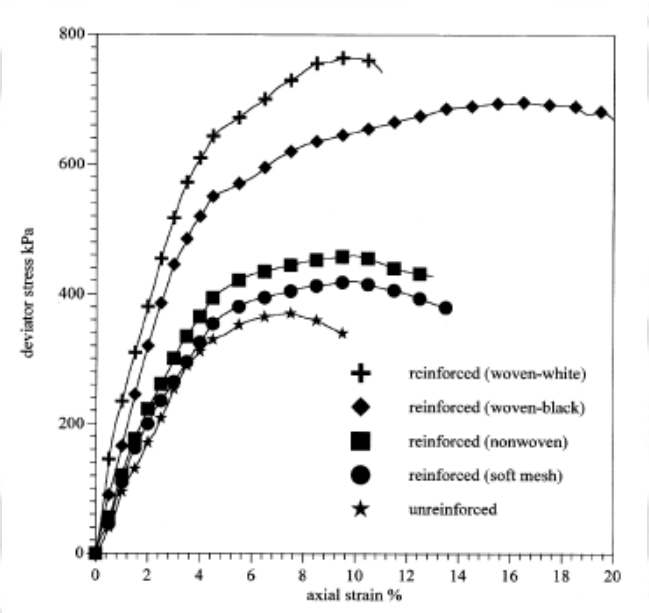

Fig. 2.9 Stress-strain responses of geocell encased sand (Rajagopal et al. 1999)

The strength and stiffness of the encased soil is found to have increased substantially with increase in the strength and stiffness of the geocell reinforcement. It was observed that the granular soil develops a large amount of apparent cohesive strength due to the confinement by the geocell. Similar to Bathurst and Karpurapu (1993), the authors proposed the use of the hoop-stress theory of Henkel and Gilbert (1952) for calculating the apparent cohesion. The value of apparent cohesion was found to

TH-1123_10610407

increase with increase in the number cells till about 3 to 4, beyond which further improvement was marginal. Therefore there interconnected cells in the triaxial compression tests may represent the mechanism of having a large number of inter connected cells.

Latha and Murthi (2007) studied the influence of different forms of reinforcement i.e. horizontal layers, geocells, and randomly distributed discrete fibers; on the strength improvement of sand, through triaxial compression tests. Among the three, cellular form of reinforcement is found to be most effective one in improving the strength, while, the discrete fiber was found to be inferior as compared to the other two forms of reinforcement i.e. geocell and planar.

Wang et al. (2008) have evaluated the shear parameters of geocell reinforced soils using large-scale direct shear tests. Three different specimens i.e. silty gravel, geocell reinforced silty gravel soil and geocell reinforced cement stabilizing silty gravel soil were tested. The shear stress-displacement behavior, the shear strength and the strengthening mechanism of geocell reinforced soils were evaluated. The comparisons of large-scale shear test responses with that from triaxial compression tests were conducted, in order to evaluate the influences of testing method on the shear strength as well. The test results indicate that both the unreinforced soil and geocell reinforced soil give similar nonlinear responses in their shear-strain behaviour. The geocell reinforced cement stabilized soil showed quasi-elastic characteristic when the normal stress was in the range of 1.0 Gpa. The geocell reinforcement resulted in an increase of cohesion of sand by about 244%, while it resulted about 10 fold increase in cohesion in case of the cement stabilized soil. The friction angle does not undergo much of change.

TH-1123_10610407

Khedkar and Mandal (2009) investigated the behavior of sand, confined with geocells, under triaxial loading conditions. Peak deviator stress is found to increasing with increasing height of cellular reinforcement, which is attributed to the induced confining effect of the cellular reinforcement. Horizontal displacement pattern of the reinforced samples indicated multi-zoned failures. Besides, the cellular reinforcement was found to provide performance improvement than the planar one.

Wesseloo et al. (2009) reported the results of uniaxial compression tests performed on soil filled geocell packs of varying size. The packs were instrumented to record the strength and deformations, as the test progressed. The test results indicate that the strength of the geocell composite structure is indirectly proportional to the size of the individual cells and that the strength reduces with an increase in the number of cells in the structure.

2.3 FIBER REINFORCEMENT

2.3.1 Applications

The application of fiber reinforcement in geotechnical engineering is spreading rapidly. Several case studies are being reported thereof. Prominent among them is the construction of embankments (Gregory and Chill 1998), land fill liners (Refai 2000), earth retaining walls (Park and Tan 2005) and roads (Lindh and Eriksson 1990, Santoni et al. 2001).

Tingle et al. (2002) conducted full scale tests to study the performance of fiber reinforced soil in low volume roads. Military truck was used to load the test track. Other than rut resistance, performance based on construction and maintenance was also checked. It was found that use of 0.8% of fiber content and 51mm fiber length was the optimum value giving maximum performance improvement in terms of reducing rutting and enhancing the serviceability of the road.

TH-1123_10610407

Gregory (2006) reported the performance of fiber reinforced soil used in two different projects. In first project, a fiber reinforced road was constructed on clay embankment. Second project was the repair of a slope, in the Lake Ridge Parkway at Texas. In both the cases fiber reinforced soil was used. It was observed that fiber reinforced soil yields better performance when the slope is shallow. It was recommended that the fiber reinforcement can be used as a secondary reinforcement, in the soil, with planar geogrid as the main reinforcement.

Dronamraju (2008) studied the performance of the different admixtures used to treat soil for slope stabilization of the two dam sites Joepool dam and Grapavine dam. Performance of soil with 8% lime with 0.15% polypropylene fiber was found most effective against the wetting and drying cycle.

Zhand et al. (2008) have studies the long term performance of the two reinforcement method first with randomly oriented fibers and second with non-wooven fabric used for slope stabilization in field. No significant long term movement was observed in both cases. Use of fabric was recommended over fiber to prevent the development of pore pressure by providing horizontal drainage through fabric.

Maheshwari et al. (2011) reported the results of laboratory test and field test of fiber reinforced soil under foundation. Significant improvement in the bearing capacity was found at the fiber content of 0.5% which was found optimum during laboratory testing.

2.3.2 Model tests

Al-Refeai (1992) performed bearing capacity tests on model strip footing on sand reinforced with polypropylene fiber. Tests were carried out by varying the width and depth of the reinforced zone. The test results indicate a significant increase in the bearing capacity and stiffness of the foundation bed. With size of the reinforced zone

TH-1123_10610407

extending vertically till about 2B (B: width of footing) and horizontally until 4B, the increase in bearing capacity was substantial beyond which further improvement was marginal. Hence for all practical purposes, the optimal width and depth of the randomly reinforced zone, in foundations, can be taken as 4B and 2B respectively.

Wasti and Butun (1996) performed a series of model tests on strip footing placed over randomly reinforced sand beds. Polypropylene fiber and mesh elements were used as the reinforcing material. The randomly distributed inclusions were found to have increased the ultimate bearing capacity and settlement as well (Fig. 2.10). The effectiveness of the reinforcing elements was observed to be dependent on the shape of the inclusions. The larger mesh size was found to be superior, to other inclusions, in terms of increase in ultimate bearing capacity. While the mesh elements had an optimum percentage of inclusion, giving maximum performance improvement, the fibers exhibited a linearly increasing trend, for the range of reinforcement content tested. Consoli et al. (2003) too have reported similar observations that addition of polypropylene fibers significantly improved the bearing capacity behavior of the soil.

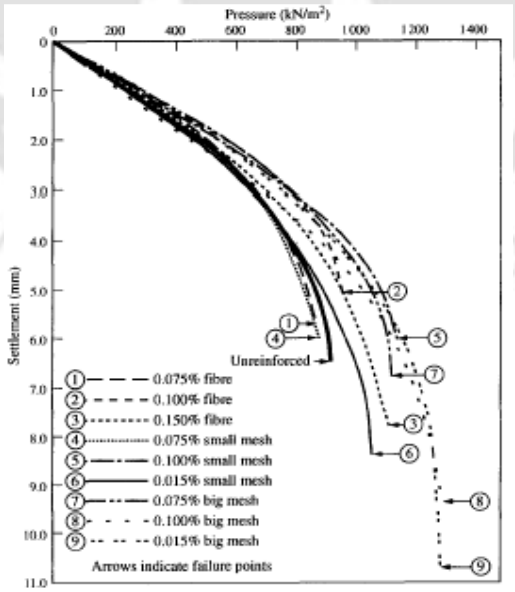

Fig. 2.10 Bearing pressure-settlement response of randomly reinforced sand beds (Wasti and Butun 1996)

TH-1123_10610407

Bahloul (2004) investigated effect of using randomly distributed fibers for reinforcing sand cushion over soft clay slope. The results obtained establish that use of randomly reinforced sand cushion, over a clay slope, can effectively increase the bearing capacity of the footing supported over. The maximum increase bearing capacity due to the sand cushion is of the order of 241% that of the clay slope alone. With addition of fiber reinforcement the bearing was further enhanced by 28%.

Park and Tan (2005) have studied the effects of the inclusion of short fiber in sandy silt soil on the performance of reinforced walls. Short fiber of 60mm length was used and the mixing ratio of the fiber was 0.2% by weight of the soil. The inclusion of short fiber in soil is found to have increased strength and stability of the system. Besides the earth pressures and displacements on the wall face too were found to have reduced. These effects were more significantly observed when the fiber soil is used in combination with geogrid.

2.3.3 Strength-stiffness behavior

Gray and Ohashi (1983) studied the strength-stiffness behavior of fiber reinforced sand using direct shear tests. The fiber reinforcement is found to have increased the shear strength of the soil. Experimental behavior was compared with theoretical predictions based on a force equilibrium model of fiber reinforced sand as depicted in Fig. 2.11. It was assumed that tensile strength mobilized has two components; one directly resists the deformations and the other increase the confinement, leading to increase in the overall shear strength of the soil. The increased shear strength (ΔS) due to fiber reinforcement can be estimated as

$\Delta S = t_r[sin\theta + cos\theta\ tan\emptyset]$, for perpendicular fibers

$\Delta S = t_r[\sin(90 - \varphi) + \cos(90 - \varphi)\ tan\emptyset]$, for fibers at some angle

TH-1123_10610407

Where,

$$\varphi = angle\ of\ shear\ distortion = \tan^{-1}[\frac{1}{k + (\tan^{-1} i)^{-1}}]$$

Ø = angle of internal friction of sand, i = angle of orientation of fiber with shear surface, x = horizontal component of shear displacement, z = thickness of shear zone, k= shear distortion ratio = x/z, t_r = tensile strength per unit area of soil = $(A_r/A)\sigma_r$, σ_r = tensile stress at fiber plane.

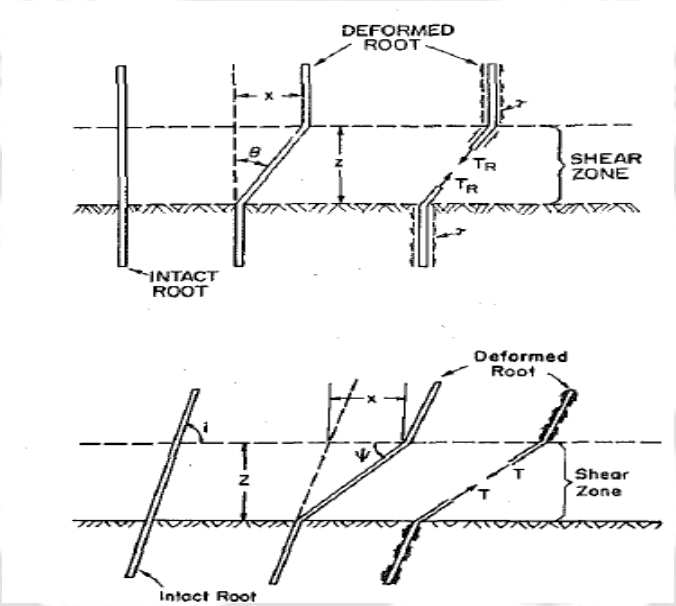

Fig.2.11 Fiber reinforcement model (Gray and Ohashi 1983)

Gray and Al-Refeai (1986) studied the influence of both continuous oriented fabric layers and randomly distributed discrete fibers; on the stress-strain responses of sand under triaxial compression tests. The parameters investigated are; amount of reinforcement, confining stress, reinforcement modulus and surface friction. Test results have shown that both the reinforcement types have improved the strength and reduced the post-peak loss of strength. At low strains (i.e. less than 1%) fabric

TH-1123_10610407

inclusions resulted in a loss of compressive stiffness. This effect was however not observed in the case of fiber reinforcement. Strength increase was proportional to the quantity of reinforcement, up to a certain limit beyond which further improvement was marginal. Fiber-reinforced samples failed along a prominent planar shear plane, whereas fabric-reinforced sand failed by bulging between layers.

Influence of fiber on mechanical properties of kaolinite has been studied by Maher and Gray (1990) through a series of unconfined-compression, splitting-tension, three-point-bending tests. The inclusion of randomly distributed fibers significantly increased the peak compressive strength, ductility, splitting tensile strength, and flexural toughness of the compacted kaolinite clay. The increase in the strength and toughness was a function of fiber length and content, and the water content of the composite. Increasing fiber content increased the compressive and tensile strength, and toughness index of kaolinite clay, with the effect being more pronounced at lower water contents. Increase in fiber length is found to have reduced the peak compressive and tensile strengths but has improved the ductility of the soil mass.

Shewbridge and Sitar (1990) have developed a closed form theoretical model simulating the behavior of fiber reinforced soils. The model accounts for the plastic work to deform the soil and the elastic work to deform the reinforcements in tension and bending. The analysis shows that the mobilization of tension in the reinforcements is a function of the reinforcement properties and the deformation characteristics of the reinforced soil. The reinforcement properties that influence the increase in the strength of the reinforced soil is not linearly proportional to the reinforcement concentration. The contribution of reinforcement tensile stresses to the increased strength of the reinforced soil is as much as one order of magnitude greater

TH-1123_10610407

than the bending stresses. Thus, the use of limit equilibrium methods for analysis of reinforced structures, ignoring the bending moment contribution, is recommended.

Al-Refeai (1991) performed triaxial tests on fine sand with subrounded particles and medium sand with subangular particles reinforced with glass fibers and polypropylene pulp and mesh elements. Tests were performed on sand specimens with inclusions in varying lengths and contents, at different confining stresses. Soil-reinforcement friction interaction is found to be dependent mainly on the extensibility of the inclusions. Fine sand with subrounded particles showed a more favorable response to fiber reinforcement than medium sand with subangular particles. The mesh elements were superior to glass fibers in improving sand strength especially in case of fine sand.

Michalowski and Zhao (1996) using an energy-based homogenization scheme have developed a model for estimating the macroscopic failure stress of the fiber reinforced granular soils. The model has considered cylindrical shaped monofilament fibers with an isotropic distribution. Five different parameters i.e. volumetric fiber content, fiber aspect ratio, fiber yield, stress, soil/fiber interface friction angle, and internal friction angle of soil, are required to predict the failure stress. The model's predictions were in good agreement with the test data.

Ranjan et al. (1994, 1996) have performed a series of triaxial compression tests on cohesion less soils reinforced with discrete, randomly distributed fibers. The parameters studied are the influence of fiber characteristics (i.e. weight fraction, aspect ratio, and surface friction), soil characteristics and its density, and confining stress on shear strength of reinforced soils. The fiber inclusions increase the shear strength of the soil significantly (Fig. 2.12). The failure envelopes of soil-fiber

TH-1123_10610407

composites are found to be curvilinear failure in shape, with a transition occurring at a certain confining stress, termed as "critical confining stress," below which the fibers tend to slip. The increase in strength is function of fiber weight fraction, aspect ratio and soil grain size. In order to estimate the strength of fiber reinforced soil, regression analysis of the test data was carried out and a mathematical model was developed. The model predictions are in good agreement with the experiment results.

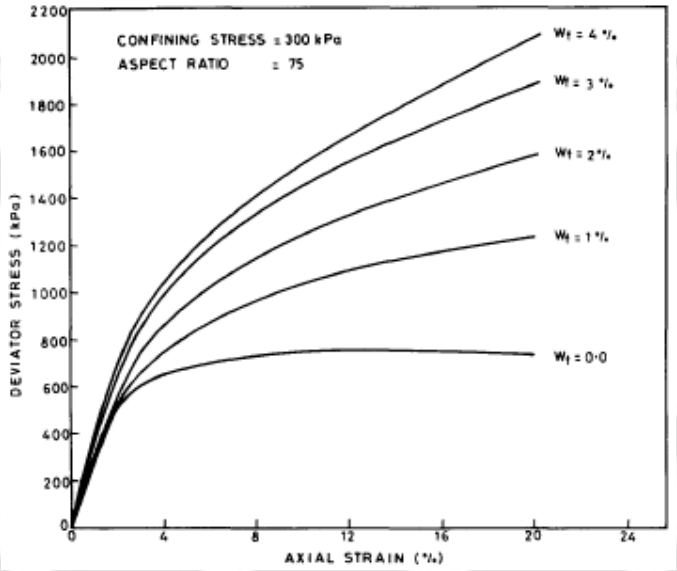

Fig. 2.12 Stress-strain behavior of fiber reinforced sand (Rajan et al 1994)

For design and construction of fiber reinforced structures it is essential to quantify the soil-fiber interface characteristics. Frost and Han (1999) have presented the results of experiments on the behavior of sand-fiber interface. It is observed that the interface shear behavior is highly depended on the relative roughness i.e. surface roughness of fiber/particle mean size, the normal stress applied, density of soil mass, and angularity of soil particles. Thickness of the test specimen and rate of shearing had little influence on the measured interface friction values.

TH-1123_10610407

In order to identify and quantify the effect of several variables on the performance of fiber-stabilized soils Santoni et al. (2001) carried out compression tests. It was observed that the inclusion of randomly oriented discrete fibers can significantly improve the compressive strength of sands. The optimum fiber length giving maximum performance improvement is about 51 mm. Similarly fiber content in the range of 0.6 to 1.0% by dry weight, gave best performance. Specimen performance was enhanced in both wet and dry of optimum conditions and silt content up to about 8% does not affect the performance of the fiber reinforcement.

Michalowski and Cermak (2003) have reported the results of triaxial compression tests on specimens of fiber-reinforced sand. Addition of even a small amount of synthetic fibers increases the failure stress substantially. The increase is as much as 70% at a fiber concentration of just 2% by volume. Apart from fiber concentration, length and aspect ratio, the performance improvement is found to be dependent on the relative size of the soil grains. A larger improvement in the peak shear stress was observed in fine sand, as compared to that in coarse sand, when the fiber concentration was small i.e. 0.5%. This trend was however reversed for relatively a large content of fibers i.e. 1.5%. The failure envelope has two segments: a linear part associated with fiber slip, and a nonlinear one related to yielding of the fiber material.

Yetimoglu and Salbas (2003) through direct shear tests have investigated the effect of fiber reinforcement on the shear strength of sands. The results of the tests indicated that fiber reinforcements can provide smaller loss of post-peak strength leading to increased ductility of the system. Besides, the fiber reinforcement is reported to have increased the residual shear strength angle of the sand.

TH-1123_10610407

The influence of fiber reinforcement on soft clay has been studied by Kumar et al. (2006) through unconfined compression tests. The results indicate that the degree of compaction affected the relative benefits of fiber reinforcement for the subject soil. Samples compacted after mixing various proportions of sand into clay (varying from 0% to 12% of clay) was also tested. It was observed that unconfined compressive strength of clay increases with the addition of fibers and it further increases when fibers are mixed in clay sand mixture.

Influence of fiber reinforcement on strength, swell, and shrinkage characteristics of expansive clays have been studied by Puppala and Musenda (2007). Fiber reinforcement of varied dosages (i.e. 0, 0.3, 0.6, and 0.9 percent by dry weight of soil) was considered. Both unreinforced and fiber-reinforced clayey specimens were tested for unconfined compressive strength (UCS), volumetric shrinkage, three-dimensional swell, and swell pressure. It was observed that the fiber reinforcement can substantially improve the compressive strength and reduce the shrinkage strains of the expansive soil. In the presence of fiber reinforcement, the swell pressure of the soil too was found to have reduced.

Influence of randomly distributed fibers on the strength of silty sand has been studied by Ahmad et al. (2010). Fiber doses of varied content and length was mixed with the soil and triaxial compression tests were performed. Inclusion of randomly distributed discrete fibers significantly improved the shear strength of silty sand. Coating of fibers with thermoplastics is found to have increased the interface friction between the fiber and soil particles, through increase in the surface area. Reinforced silty sand containing 0.5% coated fibers of 30mm length exhibited approximately 25% increase in friction angle and 35% in cohesion compared to that of unreinforced silty sand.

TH-1123_10610407

2.4 CONCLUDING REMARKS AND SCOPE OF PRESENT STUDY

The review of literature shows that both geocell and fiber reinforcement are effective means of improving the engineering performance of granular soils. With geocell reinforcement the reinforcing action is through overall confinement while with fiber reinforcement it is through surface interaction. Therefore, in case of geocells it is the strength and stiffness whereas in case of fiber it is the length and content that significantly contributes to the performance improvement of soils. The influence of these parameters on the strength and deformation characteristics of reinforced soils, with specific reference to the density of soils hasn't yet been understood properly. It is therefore proposed to study this aspect in detail. Apart from this influence of geocell strength and stiffness on the performance improvement of the encased soil has also been studied. The optimum fiber content that gives maximum performance improvement is expected to be dependent on the fiber length and density of soil which has been investigated herein.

Gregory (2006), Park and Tan (2005) have observed that fiber reinforcement when used along with planar geogrid can lead to increased performance improvement. Geocell being a three dimensional system is expected to perform better when filled with fiber reinforced soil. It is therefore envisaged to investigate, under this research work, if the fiber reinforcement can be used as a secondary reinforcement, in the soils, with geocell as the main reinforcement. A series of triaxial compression tests have been conducted thereof.

TH-1123_10610407

CHAPTER 3

DETAILS OF EXPERIMENTS: MATERIALS AND METHODS

3.1 INTRODUCTION

In order to understand the behavior of soil-geocell-fiber composite system it is essential to understand and quantify the mechanical properties of the constituent materials i.e. soil, geocell, fiber; that has been brought out in this chapter. Besides, planning of experiments, preparation of specimens and details of test procedures are presented and discussed.

3.2 TEST MATERIALS

3.2.1 Soil

The soil used in this study is a locally available river sand. It was cleaned and air dried before the tests were performed. Its specific gravity was determined as per the ASTM D 0854-06 (IS: 2720 part 3) and is found to be 2.68. The particle size analysis of this soil was determined using the dry sieve analysis, as per ASTM D 6913-04 (IS: 2720 part 4) and the obtained particle size distribution is depicted in Fig. 3.1. The soil particles have a mean diameter (D_{50}) of 0.39 mm, uniformity coefficient (C_u) of 2.61 and coefficient of curvature (C_c) of 0.93. As per the Unified Soil Classification System USCS ASTM D 2487-06 (IS: 1498), it is classified as poorly graded sand (SP). The maximum dry density and minimum dry density, of this soil, as determined according to ASTM D 4253-00 and ASTM D 4254-00 (IS: 2720 part 14), are 16.5 kN/m^3 and 13.9 kN/m^3, respectively.

TH-1123_10610407

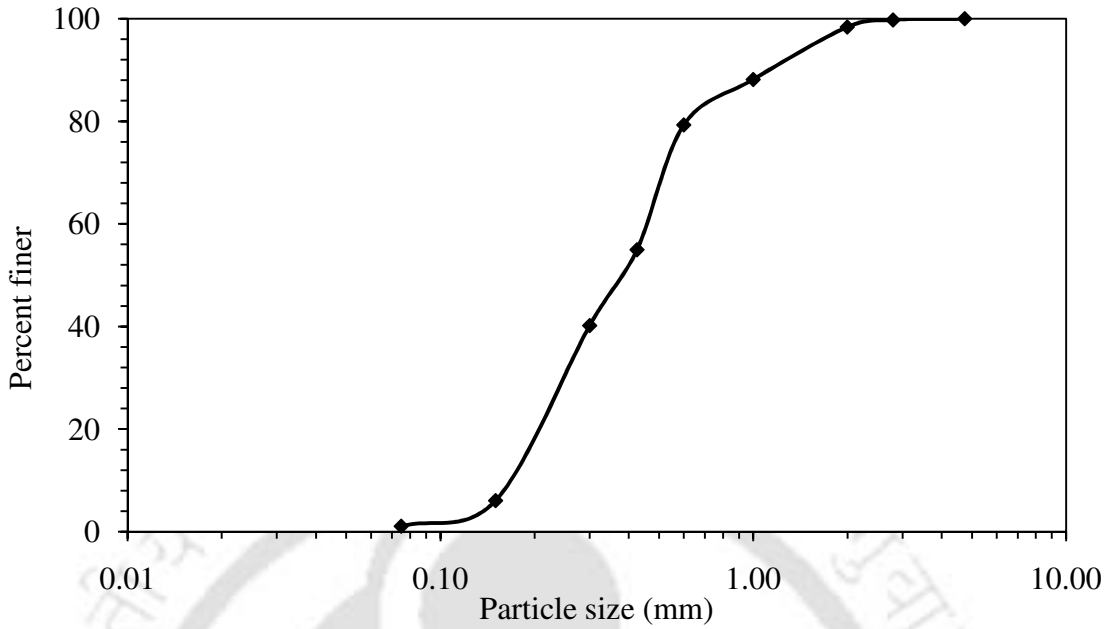

Fig. 3.1 Particle size distribution of the soil

3.2.2 Geocell

Geocell used in this study is prepared in lab. Four different geosynthetics were considered, in this test program, for making the geocells, out of which two are geotextile and two are geomesh (Fig. 3.2). The geotextiles are woven polymer, dark and white in colour and are named as GT_1 and GT_2 respectively. The geomeshes are meshes made of unoriented polymer, named as GM_1 and GM_2. The mesh GM_1 has a diamond shaped aperture with opening size of 1.5 mm × 1.5 mm, whereas GM_2 has hexagonal shaped apertures with opening size of 1mm × 1mm.

The geosynthetics in the geocells are stretched in the direction normal to the cell axis while being allowed to contract parallel to the cell axis, thereby it deforms under plane stress conditions, similar to that under uniaxial loading. The load-strain behaviour of the geosynthetics was, therefore, evaluated through uniaxial wide width tension tests as per the ASTM D 4595 (IS: 13162 part 5). The obtained responses are presented in Fig.3.3.

TH-1123_10610407

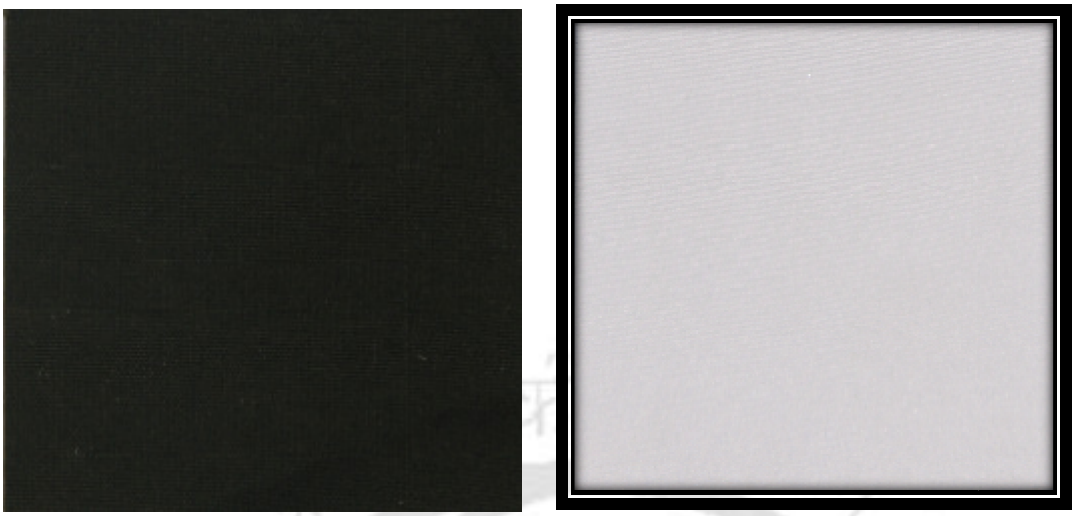

(a) GT_1 (b) GT_2

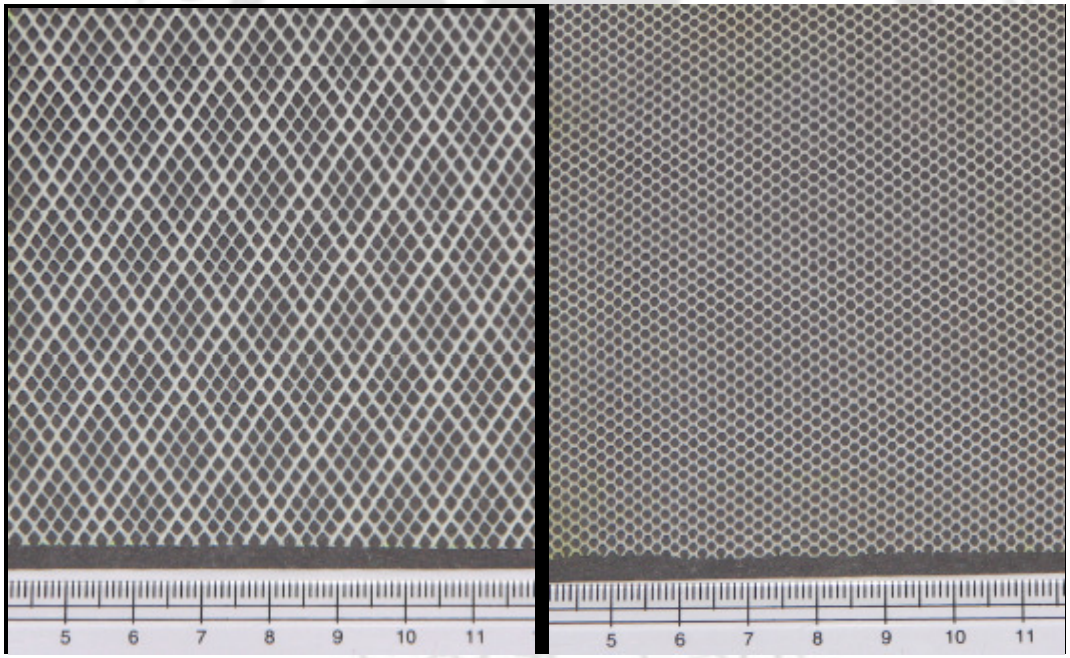

(c) GM_1 (d) GM_2

Fig. 3.2 Pictures of geosynthetics used for making geocells.

TH-1123_10610407

Thickness of the geosynthetics was determined according to ASTM D 5199-11 (IS: 13162 part 3) and mass per unit area as per the ASTM D 5261-10 (IS: 14716). These properties along with the tensile strength and modulus of all the geocell materials are summarized in Table 3.1. It could be observed that the geocell materials used have a wide range of strength and stiffness.

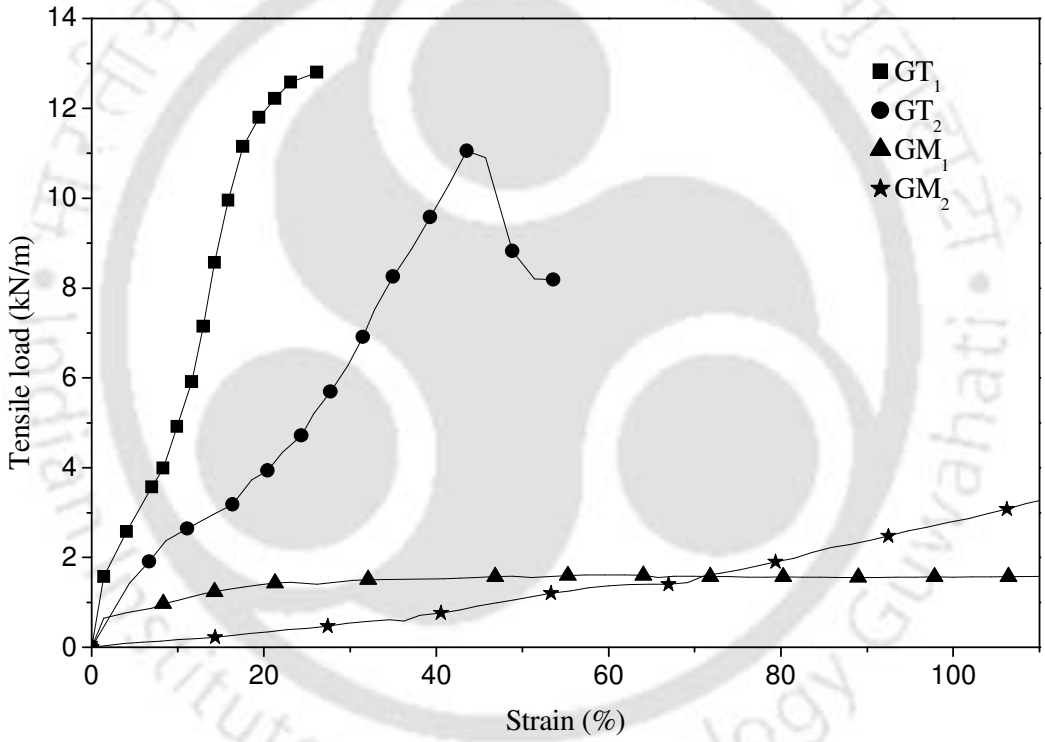

Fig. 3.3 Load-strain behavior of geosynthetics used for making geocells

The geocells were formed by stitching the geosynthetics in cylindrical shape with height and diameter equal to that of the soil specimen i.e. 100 mm in diameter and 200 mm in height. This was done by overlapping the geosynthetics, to required diameter, over 15

TH-1123_10610407

mm wide section and then stitching over it. To maintain uniformity, the number of stitches and the thread used in fabricating the geocells, was kept constant in all the tests. The strength of the seam was tested through wide width tensile test (ASTM D 4884, IS: 15060), wherein the seam was kept at mid depth of the test specimen. The load-strain responses of the geosynthetics, with seam, are shown in Fig. 3.4. The strength and stiffness (i.e. modulus) of the seamed geosynthetics are presented in Table 3.2.

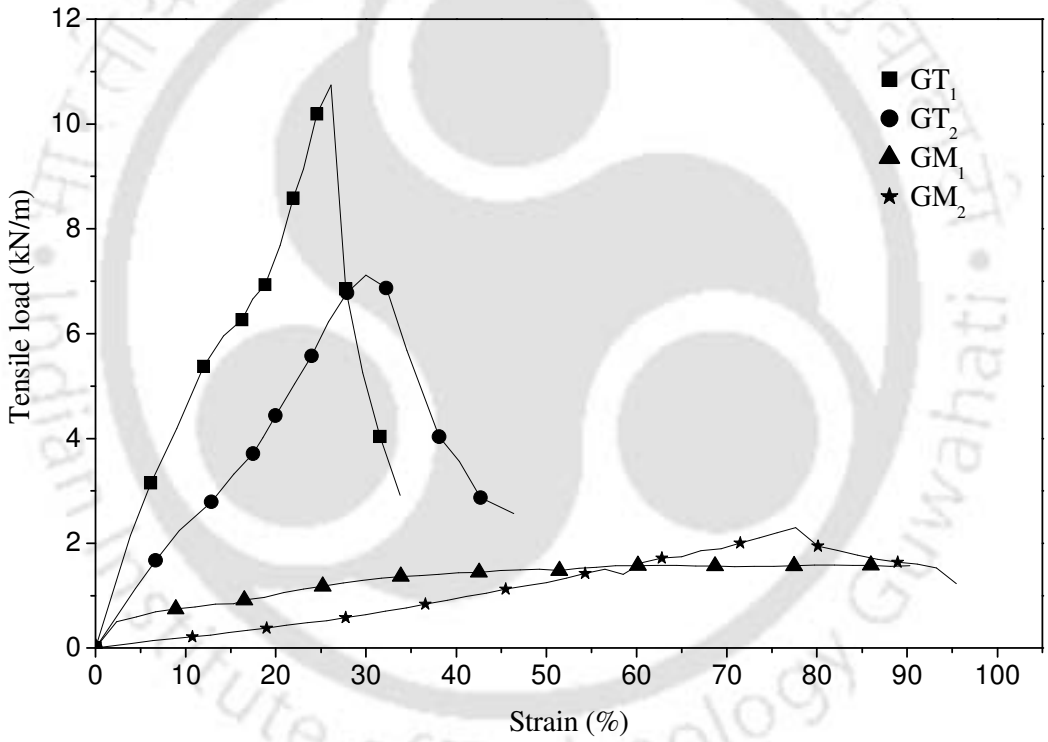

Fig. 3.4 Load-strain behavior of the geosynthetics with seam

TH-1123_10610407

Table 3.1: Properties of the geosynthetics used to make geocells.

Type of Geosynthetics	Thickness (mm)	Mass per unit area (g/m^2)	Tensile strength (kN/m)	Secant modulus at 5% strain (kN/m)
GT_1	0.6	344	12.5	58
GT_2	0.3	114	11	31
GM_1	1	232	1.6	13.5
GM_2	0.3	61	2.9	2.4

Table 3.2: Properties of the geosynthetics with seam.

Geosynthetics with seam	Strength (kN/m)	Secant modulus at 5% strain: M (kN/m)
GT_1	11.5	51
GT_2	7.1	25
GM_1	1.5	12.5
GM_2	2.4	2.2

3.2.3 Fiber

The fibers used in this study are commercially available glass fibers, cut into lengths of 10mm, 20mm, 40mm and 80mm. Fig. 3.5 shows typical of these fibers, both in fasciculus and singles form. Scanning electron micrograph, of two typical fibers is depicted in Fig. 3.6 that provides a visual appreciation of the surface texture of the fiber reinforcement. The average diameter of the fiber is found to be 0.15 mm. Its specific gravity, determined as per the ASTM-D792 (IS: 326 part 3), is 2.57.

TH-1123_10610407

(a) Fasciculus

(b) Singles

Fig. 3.5 Pictures of glass fibers used in the experiments

TH-1123_10610407

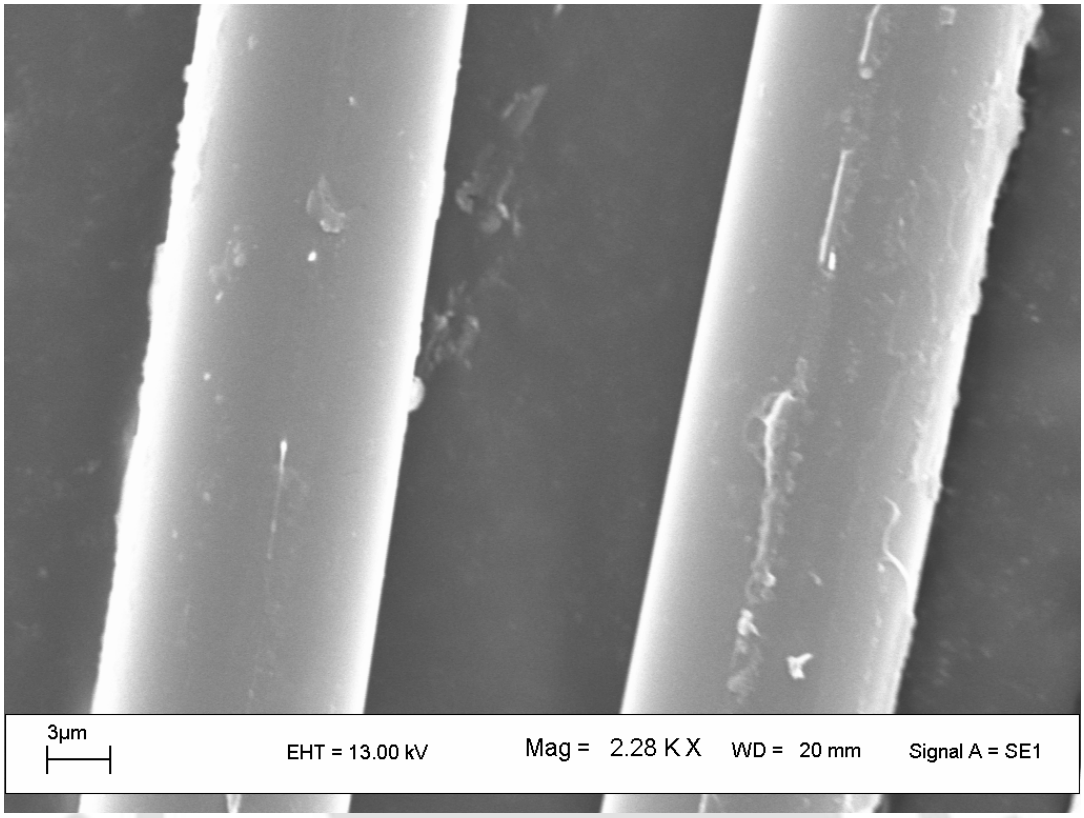

Fig.3.6 SEM micrograph of the fiber

The tensile properties of the yarn were determined by the single-strand method, as per the ASTM-D2256 (IS: 235). A typical stress-strain response for a single fiber as obtained from the tensile test is depicted in Fig.3.7. From this response, the ultimate tensile strength and elongation at break of a single fiber are found to be 1.53 GN/m^2, 1.8% respectively. The modulus of elasticity of the single fiber was determined using the tangent method as suggested in the ASTM-D2256 and is found to be 112.3 GN/m^2. The fiber-soil interaction parameter was evaluated through pullout tests performed in a modified direct shear box apparatus. The obtained peak interface friction angle (δ) for soil relative density of 30%, 60% and 80%, are found to be 19.5°, 22.5° and 25° respectively.

TH-1123_10610407

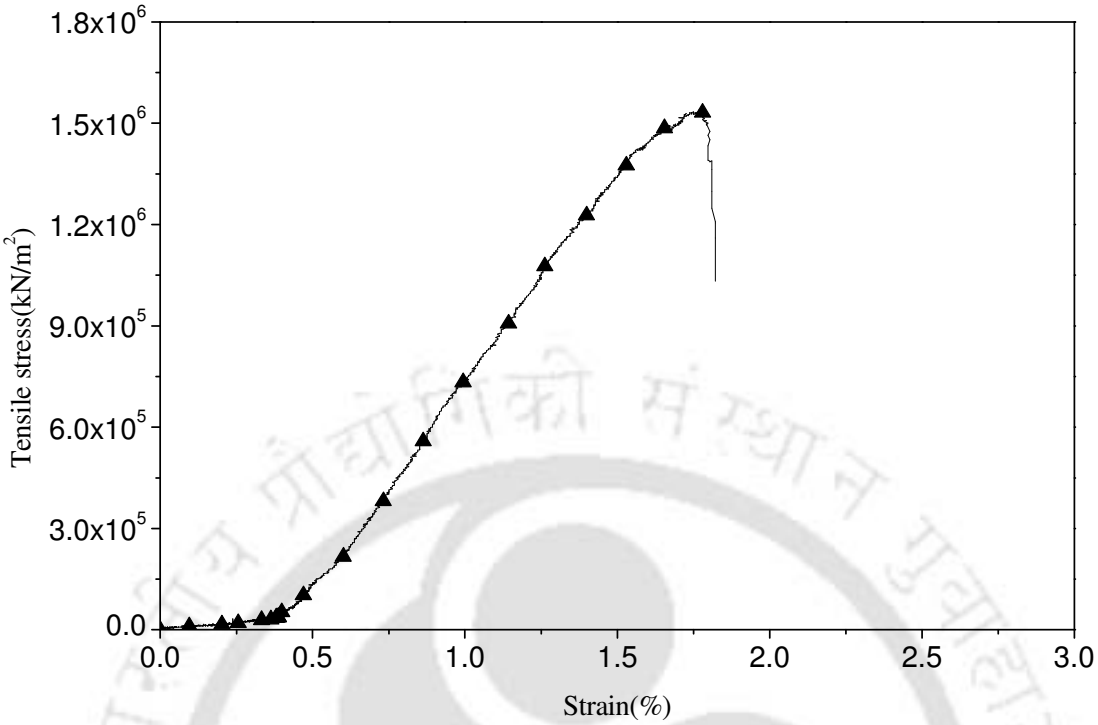

Fig. 3.7 Tensile stress-strain responses of single fiber

Glass fibers have far better fire resistant capability than their counterpart i.e. polymer fibers and natural fibers. In deed the glass fibers used in the present investigation was placed in an oven maintained at 800 °C for 12 hours and no weight loss was found. This indicates that such fibers can be used very hot weather climates such as India where summer is intensely felt. Besides they are highly resistant against aggressive chemical environment. In view of this glass fibers can be of great use in industrial constructions susceptible to fire and chemical hazards.

3.3 TEST PROGRAM

In order to study the influence of different forms of reinforcements i.e. geocell, fiber, geocell-fiber composite; on the strength and stiffness behavior of soils, several series of

TH-1123_10610407

tests have been carried out, using the conventional triaxial compression test setup. In all the tests dry sand was used and the tests were performed under at different confining pressures i.e. 49, 98, 196, and 392 kPa. Within each series, only one parameter was varied while the others were kept constant. This is to understand the influence of that particular parameter on the overall behavior of the reinforced soil system. In total 348 triaxial compression tests, under 16 different series, were carried out, the details of which are presented in Table 3.3. Many of these tests were repeated to ensure the repeatability of the results.

Tests in series A_1 were carried out on unreinforced soil specimens with relative densities (D_r) of 30%, 60%, 80%; representing loose, medium dense and dense conditions. Results obtained from these tests are primarily used as reference data in order to quantify the improvement due to the different forms of reinforcements used i.e. geocell, fiber, geocell-fiber composite; as studied in the successive test series.

Behaviour of geocell reinforced soils was studied in tests under series B_1-B_4. The parameters investigated are the influence of geocell strength, stiffness and density of the infill soil, on the overall performance of the soil-geocell system. Tests were carried out both at low and high confinement pressures (49-392 kPa). In order to maintain uniformity the stiffness of geocells is expressed as the secant modulus of geocell seam at 5% of strain, designated through the letter symbol 'M', as detailed in Table 3.2.

TH-1123_10610407

Table 3.3 Test details

Test series	Reinforcement	Details of test parameters	
		Constant parameters	Variable parameter
A_1	Unreinforced	-	D_r = 30%, 60%, 80%
B_1	Geocell, GM_2	M = 2.2 kN/m	D_r = 30%, 60%, 80%
B_2	Geocell, GM_1	M = 12.5 kN/m	D_r = 30%, 60%, 80%
B_3	Geocell, GT_2	M = 25 kN/m	D_r = 30%, 60%, 80%
B_4	Geocell, GT_1	M = 51 kN/m	D_r = 30%, 60%, 80%
C_1	Fiber	D_r = 30%, L = 10mm	f_c = 1%, 2%, 3%, 4%, 5%
C_2	Fiber	D_r = 30%, L = 20mm	f_c = 1%, 2%, 3%, 4%, 5%
C_3	Fiber	D_r = 30%, L = 40mm	f_c = 1%, 2%, 3%, 4%, 5%
C_4	Fiber	D_r = 30%, L = 80mm	f_c = 1%, 2%, 3%, 4%, 5%
C_5	Fiber	D_r = 60%, L = 10mm	f_c = 1%, 2%, 3%, 4%, 5%
C_6	Fiber	D_r = 60%, L = 20mm	f_c = 1%, 2%, 3%, 4%, 5%
C_7	Fiber	D_r = 60%, L = 40mm	f_c = 1%, 2%, 3%, 4%, 5%
C_8	Fiber	D_r = 60%, L = 80mm	f_c = 1%, 2%, 3%, 4%, 5%
C_9	Fiber	D_r = 80%, L = 10mm	f_c = 1%, 2%, 3%, 4%, 5%
C_{10}	Fiber	D_r = 80%, L = 20mm	f_c = 1%, 2%, 3%, 4%, 5%
C_{11}	Fiber	D_r = 80%, L = 40mm	f_c = 1%, 2%, 3%, 4%, 5%
C_{12}	Fiber	D_r = 80%, L = 80mm	f_c = 1%, 2%, 3%, 4%, 5%
D_1	Geocell + fiber	D_r = 30%, L = 40mm, f_c = 3%	M = 2.2, 12.5, 25, 51 kN/m
D_2	Geocell + fiber	D_r = 60%, L = 40mm, f_c = 3%	M = 2.2, 12.5, 25, 51 kN/m
D_3	Geocell + fiber	D_r = 80%, L = 40mm, f_c = 4%	M = 2.2, 12.5, 25, 51 kN/m

Note: All tests are conducted for confinement pressures of; 49, 98, 196, and 392 kPa.

Tests under series C_1-C_{12} have studied the influence of fiber reinforcement on the strength and stiffness of the soils at varied relative densities. The different lengths (L) of

TH-1123_10610407

the fiber reinforcement used are 10, 20, 40 and 80 mm and their contents (f_c) were varied through 1, 2, 3, 4 and 5% by dry weight of the soil.

Tests in series D_1-D_3 are carried out to study the influence of the composite reinforcement system comprising of fiber mixed soils filled into geocell. The fiber reinforcement herein serves as a secondary reinforcement. The length and content of fibers, in these tests, were kept at the optimum value that gives maximum performance improvement, as determined from test series C_1-C_{12}.

3.4 EXPERIMENTAL DETAILS

All the tests in this investigation are carried out using a standard triaxial compression test apparatus wherein a cylindrical soil specimen is sealed in a watertight rubber membrane, placed in a cylindrical chamber and subjected to an all round confining pressure. Fig. 3.8 depicts a schematic diagram of the test set up and photographic view of the same is shown in Fig. 3.9. The test specimens (i.e. both unreinforced soil and fiber reinforced soil) are 100 mm in diameter and 200 mm in height.

The unreinforced specimens were prepared as per the ASTM 5311-92(04) using the vibratory method. Weight of dry sand required to obtain a desired density was determined based on the volume of the spilt mould. The soil was divided into 15 equal parts. Each part was spooned into the membrane lined split mould, attached to the bottom plates of the triaxial cell, and compacted to the desired dry unit weight by vibration. In order to produce a relatively homogeneous sample an under-compaction method as suggested by Ladd (1978) was adopted. Fig. 3.10 shows the picture of a typical unreinforced specimen in the membrane lined mold. For clarity the picture is taken with partial fill.

TH-1123_10610407

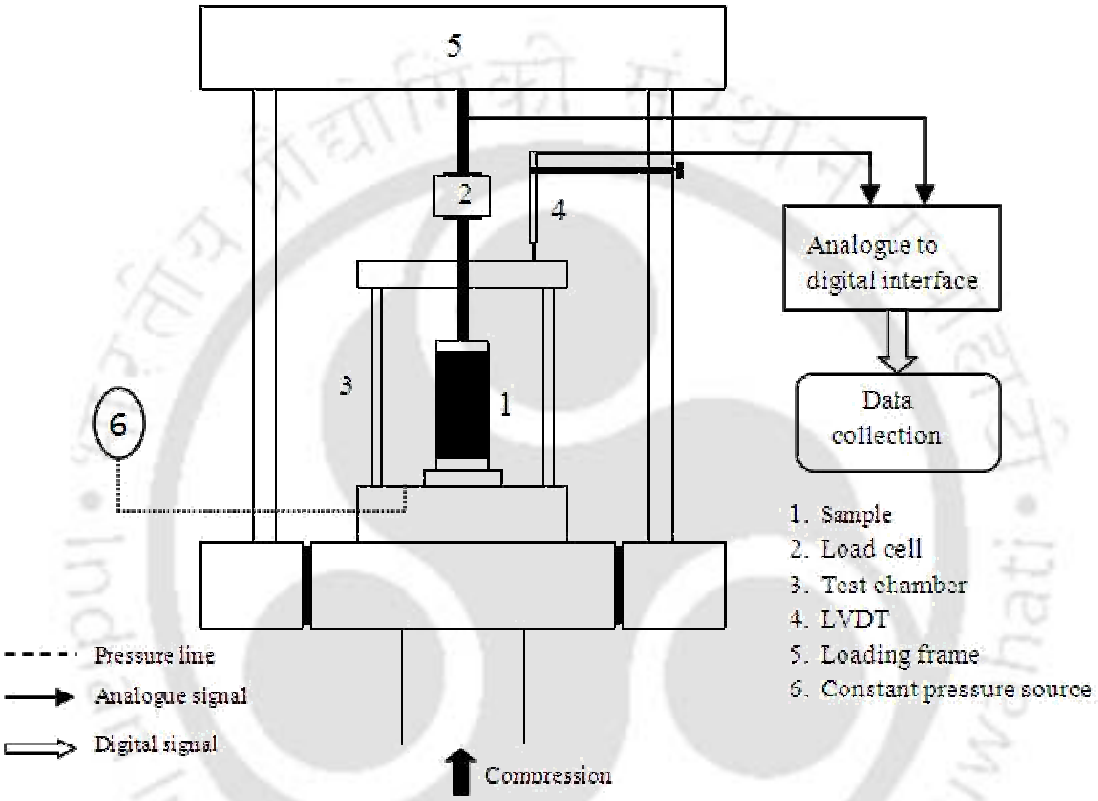

Fig. 3.8 Schematic diagram of the triaxial compression test setup

TH-1123_10610407

Fig. 3.9 Overall view of the test setup

Fig. 3.10 Typical unreinforced soil specimen

TH-1123_10610407

In case of geocell reinforcement, the prefabricated geocell is placed within the mold with rubber membrane, following which sand was poured in and compacted in layers. While with fiber reinforcement, soil and fiber were mixed thoroughly, before it was placed into the mold, lined with rubber membrane. Quantity of fibers to be added is taken as the percentage of the dry weight of the soil solids (Kaniraj and Gayathri 2003) i.e. $W_f = f_c W_s$; where, W_f is the weight of fibers, f_c is fiber content and W_s is the weight of dry soil. The total weight of the specimen (W) that can be obtained from the volume of the mold and placement density (γ_d) = $W_f + W_s$. Therefore, weight of dry soil, for a particular content of fiber (f_c), can be taken as $W/(1+f_c)$.

It is difficult to mix fiber with the cohesionless sand for they get segregated during the process. In order to avoid this, it is necessary to add a little amount of water into the mix (Gray and Al-Refai 1986, Maher and Gray 1990, Al-Refeai 1991). In the present investigation 3% water (by weight) was added to the soil-fiber mix. It should be mentioned here that the soil used is coarse grained sand and didn't contain any fines. Therefore, a low water content of 3% had no measurable effect on its stress-strain behavior. Similar observation has been reported by many other researchers as well (Maher and Gray 1990, Gray and Al-Refai 1986).

Mixing was done manually and adequate care was taken, at each stage, that homogeneous mixtures are prepared. Subsequently, the sand-fiber mixture was poured into the spilt mold, and was compacted to the desired thickness. The little amount of water added during mixing helped preventing the segregation of fibers while transferring the mixture into the mold and during compaction as well. With geocell-fiber combined reinforcement, first the geocell was placed in the rubber lined mold, following which the

TH-1123_10610407

sand-fiber mix was poured into and compacted in layers as has been mentioned earlier. Schematic diagram of soil specimen with different forms of reinforcement are depicted in Fig. 3.11 and the pictorial view of the same is shown in Fig. 3.12.

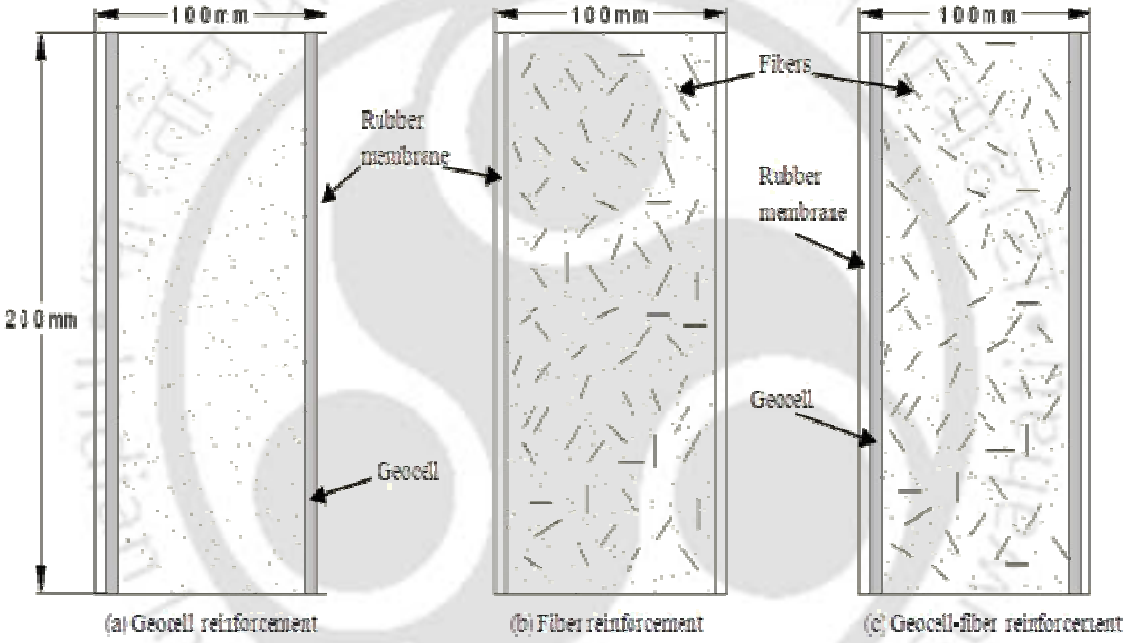

Fig. 3.11 Schematic diagram of test specimen with different reinforcements

TH-1123_10610407

(a) Geocell reinforcement

(b) Fiber reinforcement

(c) Geocell-fiber reinforcement

Fig. 3.12 Photograph of soil specimen with different forms of reinforcement

TH-1123_10610407

After compaction of the last layer, the top cap was placed on the soil sample and two O-rings were fixed onto it. The other set of O-rings originally placed at the bottom of the mold were rolled back and fixed onto the base cap. This was done in order to seal the specimen against intrusion of water. Subsequently the internal vacuum that held the rubber membrane flush with the mold was released and the split mold was opened up. Fig. 3.13 shows the general view of a typical test specimen thus prepared. Subsequently it was placed in the triaxial compression tests chamber (Fig. 3.14) for the tests to be conducted.

Fig. 3.13 General view of a typical test specimen

TH-1123_10610407

Fig.3.14 View of the test specimen placed in the traixial compression cell.

The tests were carried out as per ASTM D 2850-03 (IS: 2720 part 11). Having placed the specimen in the test chamber, it was filled with water that acts as the confining medium. Initially a pressure is applied onto the water in the cell that an equal stress is felt by the specimen in all directions. Subsequently, vertical loading was applied onto the top platen, over the specimen, which increases the axial stress that the sample is subjected to shearing. The loading was applied in strain controlled manner, at a rate of 1.2 mm/min. The load transferred onto the test specimen was measured through a load cell supported against the reaction frame. It has a capacity of 50 kN with least count of 0.5N. The deformation in the soil specimen was measured using a Linear Variable Differential Transducer, LVDT, as shown in Fig. 3.7, which has a maximum travel of 50 mm with a

TH-1123_10610407

least count of 0.5 micron. All these transducers are connected to a computerized data acquisition system through a multi channel carrier frequency amplifier of HBM, Germany. In the absence of a clear failure vertical loading was applied until the axial deformation reached 40 mm that's equal to an average strain of 20%.

3.5 SUMMARY

Presented in this chapter are the details of the materials used in the laboratory tests. Evaluation of their properties and characterization has been carried out using the standard procedures as per the ASTM codes of practice. Methods of sample preparation, test program and test procedures are discussed in detail. The obtained results are systematically analyzed and discussed in the subsequent chapters.

TH-1123_10610407

CHAPTER 4

RESULTS AND DISCUSSION-I: GEOCELL REINFORCED SOIL

4.1 INTRODUCTION

In this chapter, the results obtained from triaxial compression tests on geocell reinforced soil along with the unreinforced one are presented and discussed. The influence of various parameters, such as density of fill soil and modulus of geocell material, on the strength and stiffness behavior of the reinforced soil system has been brought out.

4.2 UNREINFORCED SOIL

In order to evaluate the performance improvement due to reinforcements, reference tests were carried out with unreinforced soils as well. The obtained results are plotted as deviator stress and axial strain. The stress-strain responses of the unreinforced soils at different confining pressures, for relative densities of 30%, 60% and 80% are depicted in Figs. 4.1, 4.2 and 4.3 respectively. The deviator stress is taken equal to $\sigma_1 - \sigma_3$, wherein σ_1 is the major principal stress and σ_3 is the minor principal stress. Axial strain is the axial deformation expressed as percentage of the original length of the test specimen.

The stress-strain responses for 30% relative density, particularly at low confining pressures have not shown any clear peak, but at very high confining pressure (i.e. 392 kPa) has exhibited a mild peak (Fig. 4.1). This is typical of sand behavior when it is in loose state. However at 80% relative density the soil has exhibited clear peak even at low confining pressures (98 and 196 kPa), indicating a dense behavior of the soil

TH-1123_10610407

matrix. The specimen at 60% relative density has shown an intermediate behavior (Fig.4.2).

The strength envelopes for different soil specimens as obtained from triaxial compression test data are shown in Fig. 4.4. These strength envelops are based on peak shear resistance and are plotted in terms of the shear and hydrostatic stress invariants, q and p. Where, q is defined as $(\sigma_{1max} - \sigma_{3max})/2$ and p is defined as $(\sigma_{1max} + \sigma_{3max})/2$. The peak major principal stress, σ_{1max}, is the maximum axial stress on the specimen and $\sigma_{3max,}$ the peak minor stress acting on the test specimen is the confining pressure applied onto it. The cohesion (c) and friction angle (Φ) are found out through the relationships, $c = a/cos\Phi$, $sin\Phi = tan\alpha$; where, a and α are the intercept and slope of the p-q plot respectively (Lambe and Whitman 1979). The soil is found to have exhibited zero intercept and therefore has zero cohesion. The friction angles at relative densities of 30%, 60% and 80% are found to be 35°, 38° and 40° respectively.

Typical failure modes observed for the soil specimens are depicted in Fig. 4.5. The specimen at loose state of packing (D_r = 30%) has undergone bulging failure while both medium dense (D_r = 60%) and dense specimens (D_r = 80%) have developed clearly defined shear planes.

These test data on unreinforced soils are used as reference for comparing and quantifying the performance improvement due to the reinforcements i.e. geocell, fiber and geocell-fiber composite. However, in this chapter only the results pertaining to geocell reinforcement have been studied, the details of which are presented in the following sections.

TH-1123_10610407

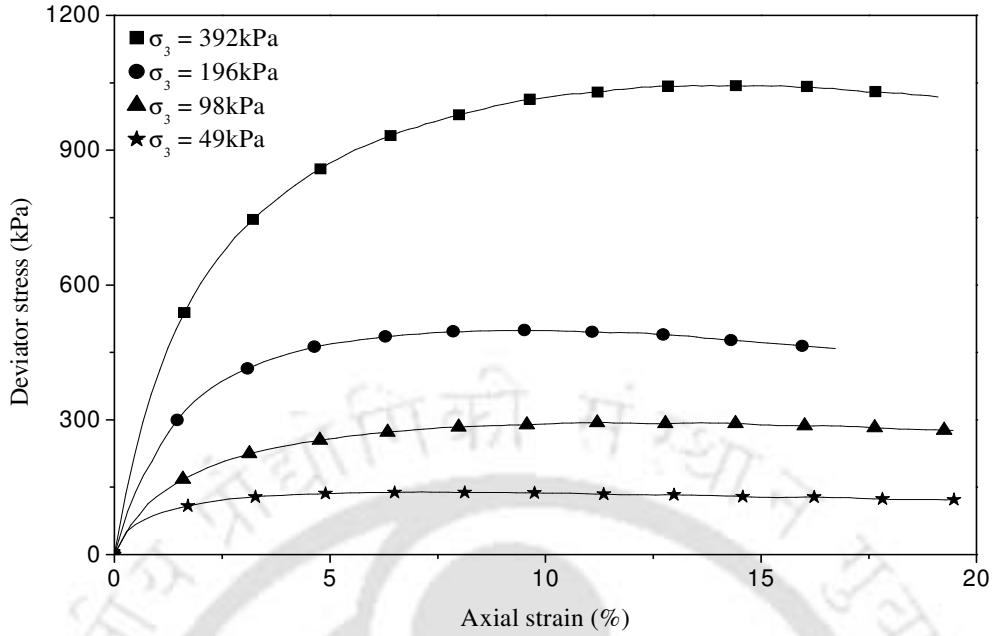

Fig. 4.1 Stress-strain behavior of unreinforced soil (D_r = 30%)

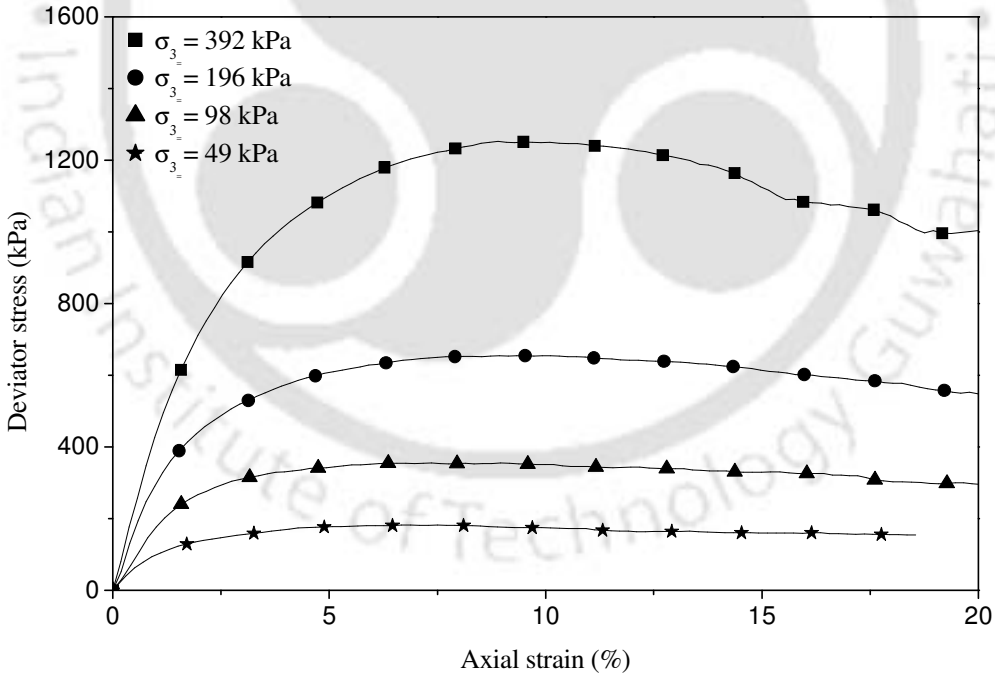

Fig. 4.2 Stress-strain behavior of unreinforced soil (D_r = 60%)

TH-1123_10610407

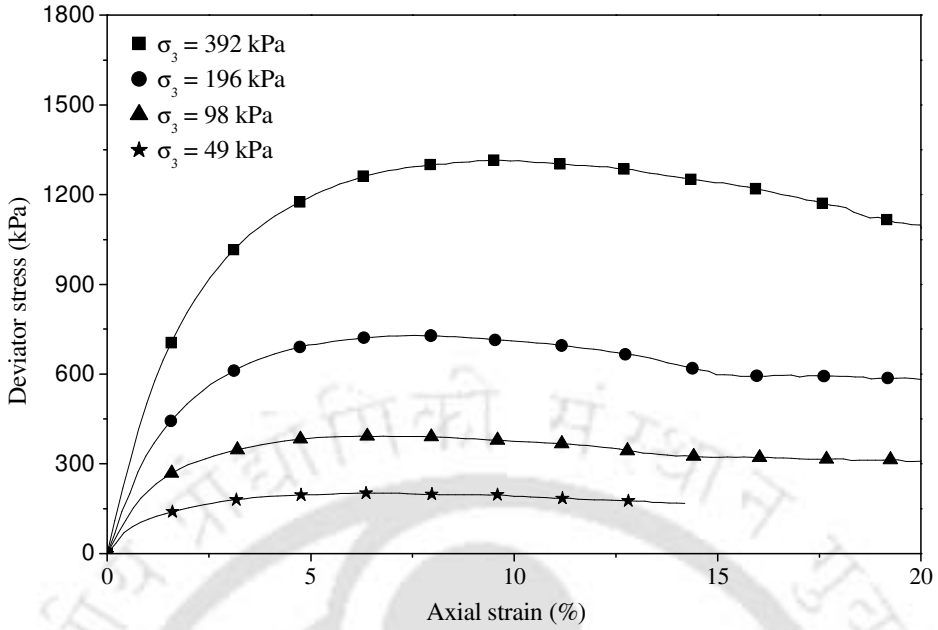

Fig. 4.3 Stress-strain behavior of unreinforced soil (D_r = 80%)

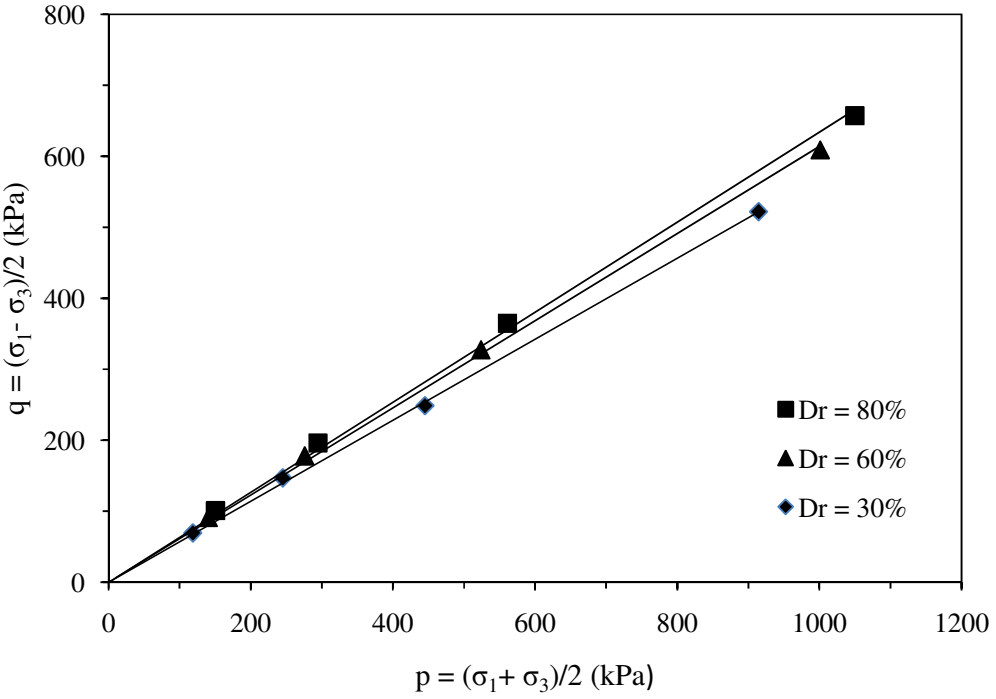

Fig. 4.4 p-q diagrams for unreinforced soils

TH-1123_10610407

(a) D_r = 30% (b) D_r = 60% (c) D_r = 80%

Fig. 4.5 Typical failure mode of the soil specimens (σ_3 = 196 kPa)

4.3 GEOCELL REINFORCED SOIL

Four series of tests were carried out to study the influence of geocell reinforcement on the performance of soils. Over these tests the stiffness of the geocell was varied through 2.2-51 kN/m and the relative density of the soil was varied from 30% to 80%. Typical stress-strain responses of geocell reinforced soil, with dense infill (D_r = 80%) and geocell made of GT_1 geotextile, are depicted in Fig. 4.6. It is of interest to note that the unreinforced sand, after about 7% strain has undergone strength reduction indicating that failure has taken place. However, with geocell encasement the soil has continued to take load until axial strain as high as 17%. This is because soil particles under shearing tend to slide apart leading to a relatively weak matrix and thereby manifesting the strain softening responses. While with a stiff geocell around the soil grains are held tight against the shearing that the system continues to sustain increased

TH-1123_10610407

loading, similar to that of strain hardening behaviour. Hence it can be said that an increase in the permissible strain limit in the design of structures made of geocell-reinforced soils is not likely to cause much of inconvenience. The sudden drop in the strength at about 17% strain is attributed to local rupture of the geocell at its seam, primarily due to stress concentration effect (Fig. 4.9).

In comparison to that of soil alone (Fig. 4.3), with geocell reinforcement the strength is found to have increased substantially (Fig. 4.6). This can better be explained through the observed failure pattern as shown in Fig. 4.7. It can be seen that the geocell reinforced specimen has exhibited a mild bulging in the central region otherwise has almost stood intact. In contrast the unreinforced soil had undergone a clear shear failure (Fig.4.5c). Hence it is established that the geocell reinforcement through its three dimensional confinement has effectively inhibited the formation of rupture planes in the soil mass leading to increased performance improvement.

The failure strength envelopes, i.e. p-q diagram, depicted in Fig. 4.8 shows that the geocell reinforced soil has almost a similar friction angle (Φ) as that of the unreinforced soil but has displayed a significant cohesion intercept (c). Similar such behavior is observed in all other cases which is in agreement with the findings of other researchers as well (Bathurst and Rajagopal 1993, Rajagopal et al. 1999). In the shear strength of soils, parameter c represents the portion of strength that is independent of the applied normal stress while the parameter Φ refers to the increase in shear strength due to increased normal stress. The reinforcing action of geocells is primarily through mobilization of hoop stress. As the hoop stress generated in the reinforcement is independent of the applied normal stress its contribution in strength

TH-1123_10610407

improvement is similar to that of the parameter *c,* as has been manifested in form of the cohesion intercept in the p-q diagram.

The shear parameters of geocell reinforced soil for the present case with D_r = 80% and M = 51kN/m, as obtained from the p-q plot (Fig. 4.8) are cohesion = 142 kPa and friction angle = 38°. The corresponding value of the bearing capacity factor, N_c, is found to be 61.35 (Vesic 1973). Therefore, the improvement in bearing capacity (i.e. cN_c) is of the order of 8712 kPa. Such large increase in bearing capacity establishes the potential benefit of geocell reinforcement in improving the performance of geotechnical structures.

The influence of different parameters on the overall behavior of the geocell reinforced soil system and the possible mechanisms are presented and discussed in the following sections.

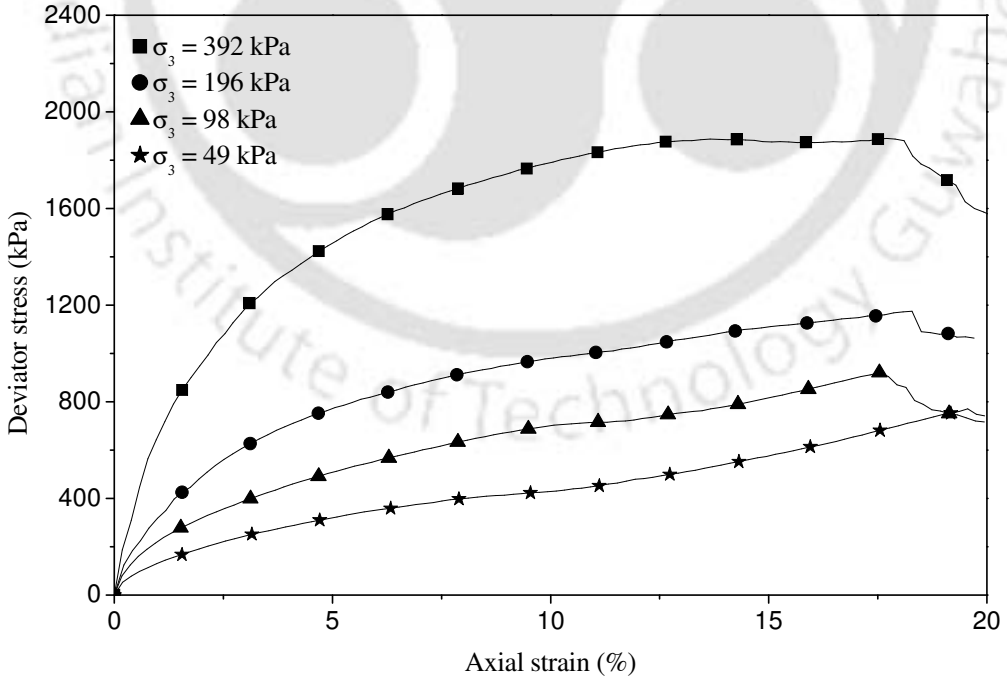

Fig. 4.6 Stress-strain behavior of geocell reinforced sand (D_r = 80%, Geocell made of GT_1)

TH-1123_10610407

Fig. 4.7 Typical failure mode of geocell reinforced soil specimen (D_r = 80%, Geocell made of GT_1, σ_3 = 196 kPa)

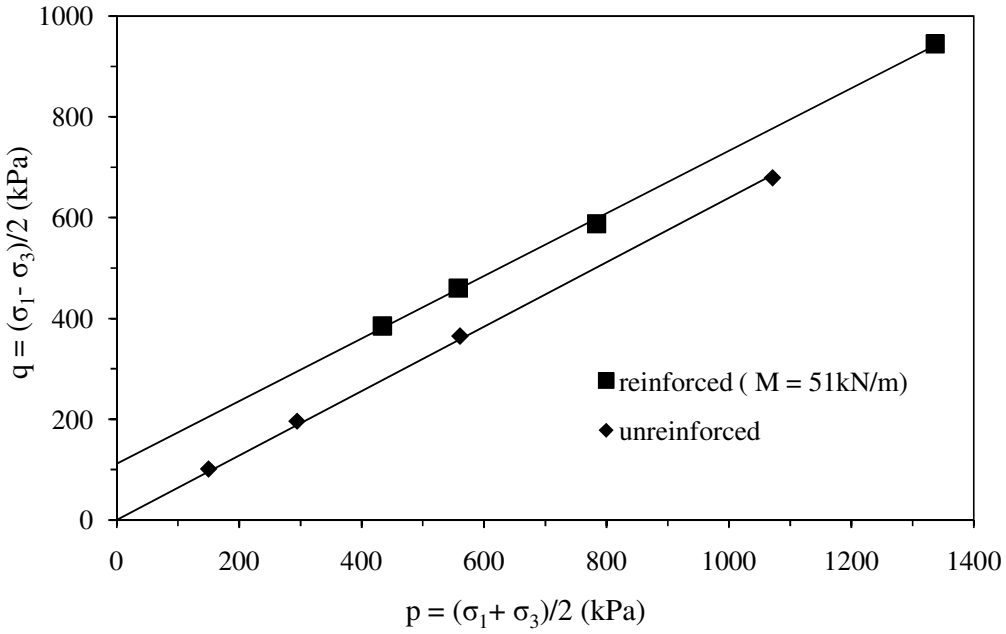

Fig. 4.8 Typical failure strength envelopes of unreinforced and geocell reinforced soils (D_r = 80%, Geocell made of GT_1)

TH-1123_10610407

Fig. 4.9 Rupture of seam of geocell after test (Geocell made of GT_1)

4.3.1 Influence of stiffness of geocell

Typical stress-strain responses for the medium dense soil (D_r = 60%) with geocell reinforcement of varied stiffness i.e. M = 2.2, 12.5, 25 and 51 kN/m are depicted in Fig. 4.10, 4.11, 4.12 and 4.13 respectively. It can be seen that with geocells of relatively low strength (M = 2.2, 12.5 kN/m) the specimens have undergone a strength reduction at about 10-12% of axial strain. This behavior is almost similar to that of the unreinforced soil. Indeed the strength envelopes depicted in Fig.4.14-4.16 and the cohesion values presented in Table 4.1 show that irrespective of the density of the fill soil i.e. loose, medium dense, dense; the strength improvement due to the weak geocells is very small. While with relatively stiff geocell (M = 51 kN/m) the stress strain responses have shown a sharp increase in strength, typically of a strain hardening behavior (Fig. 4.13). The same is also noticed in the p-q plots and the values depicted in Table 4.1 that the induced cohesion, in case of this geocell (i.e. M = 51 kN/m), is substantially high. Hence it can be said that there is threshold strength

TH-1123_10610407

for the geocell reinforcement beyond which the strength improvement is visibly high. The possible mechanism for the same can be figured out through the failure patterns observed in the post test specimens (Fig. 4.17). It can be seen that with geocell having stiffness 12.5 kN/m, there has developed a clear shear plane in the medium dense soil encased within. In other words the soil is strong enough to rupture through the geocell reinforcement. However, with relatively stiff geocell (M = 51 kN/m) even the dense soil matrix (D_r = 80%) hasn't shown any visible shear failure that the geocell is strong enough to prevent rupture in the soil mass. Therefore, the geocell reinforced soil specimen has exhibited a steep increase in strength until a large strain, as high as 17%, when there has happened sudden failure. This sudden failure is primarily attributed to the local rupture of geocell seam due to high stress concentration taking place in the region right under loading. When the specimen is subjected to higher deviator stress and hence larger shear stress, it is likely to have higher stress concentration effect leading to failure at an earlier stage. Indeed, for failure deviator stress of 1690 kPa the axial strain is about 17% while with peak deviator stress of 711 kPa the failure axial strain is in the order of 20% (i.e. σ_3 = 392 kPa and 49 kPa respectively, Fig. 4.13).

Another feature of interest to note that invariably for all cases, unreinforced and reinforced, the stress-strain responses have undergone an increase in their slope when the axial strain is in the order of 5%. This is the stage when the soil tends to be yielding. When unreinforced, the yielding of soil continues, that the stress-strain response tends to be nearly asymptotic indicating that the specimen with just little increase in the applied stress continues to strain leading to failure. Nearly similar is the situation with weak geocells, M = 2.2 kN/m and 12.5 kN/m. This is because with the onset of yielding the soil tends to dilate that its ability to sustain surcharge loading

TH-1123_10610407

reduces (Bolton 1986). As the weak geocell tends to deform away, under the soil pressure and allows formation of shear bands, it is therefore the behavior of soil that dominates the overall behavior of the geocell-soil composite structure. However, with geocell of adequate stiffness (M = 51 kN/m) the expansion of the soil mass is effectively suppressed that it continues to sustain increased loading As a result of which the stress-strain responses have continued to exhibit an ascending tendency until the failure, which takes place due to the stress localization in the geocells.

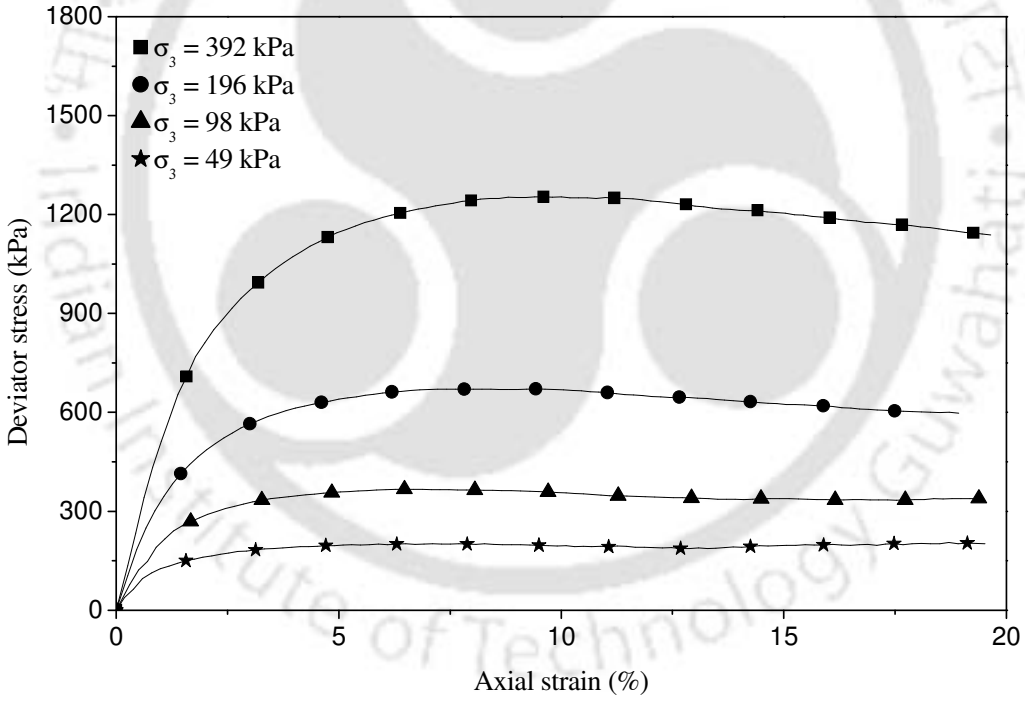

Fig. 4.10 Stress-strain behavior of geocell reinforced sand (D_r = 60%, M = 2.2kN/m).

TH-1123_10610407

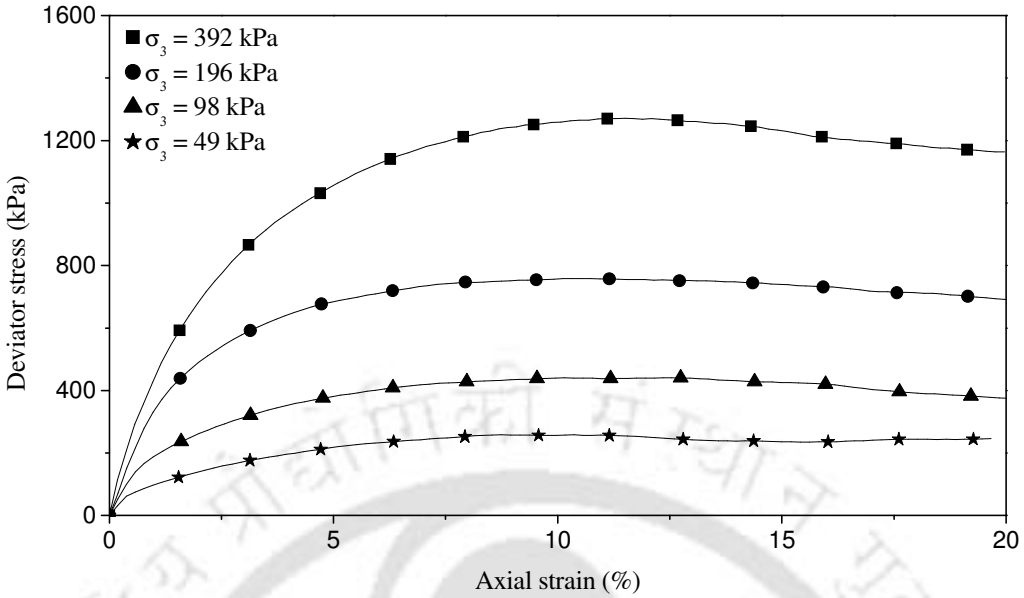

Fig. 4.11 Stress-strain behavior of geocell reinforced sand (D_r = 60%, M = 12.5kN/m)

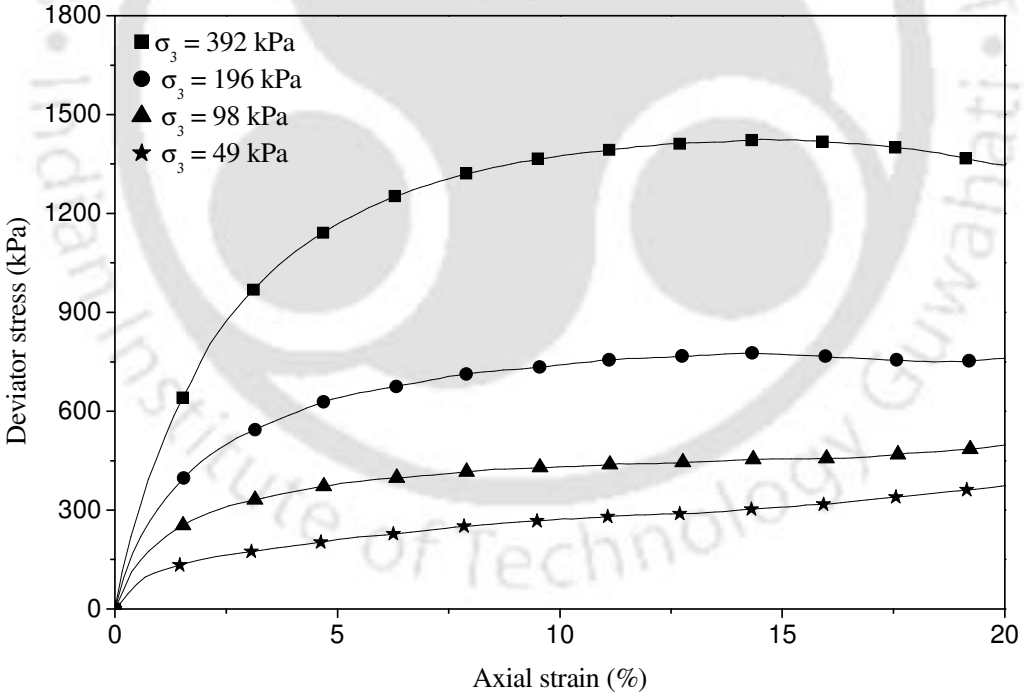

Fig. 4.12 Stress-strain behavior of geocell reinforced sand (D_r = 60%, M = 25kN/m).

TH-1123_10610407

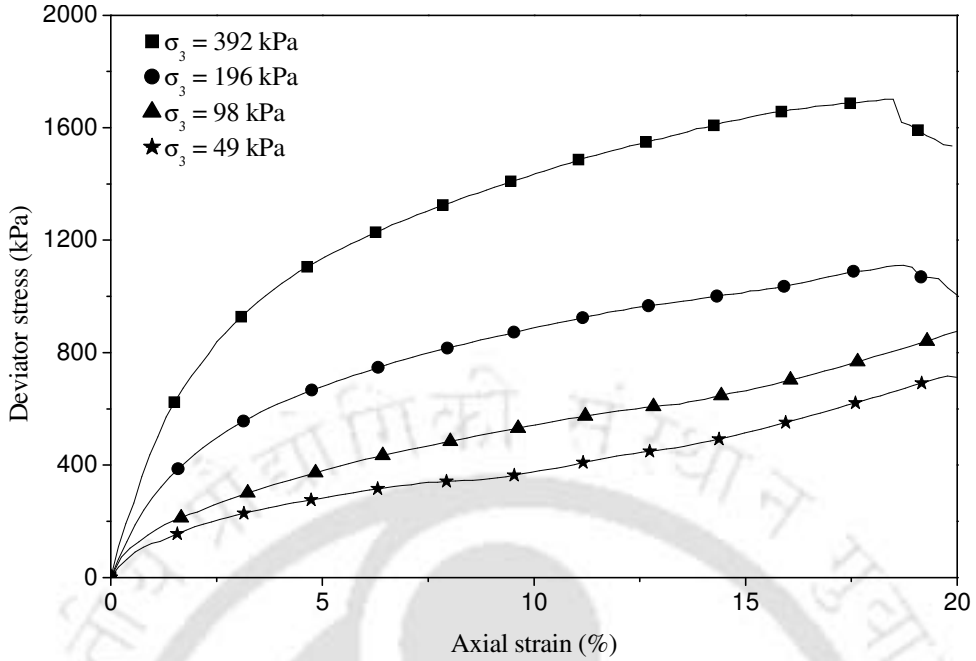

Fig. 4.13 Stress-strain behavior of geocell reinforced sand (D_r = 60%, M = 51kN/m)

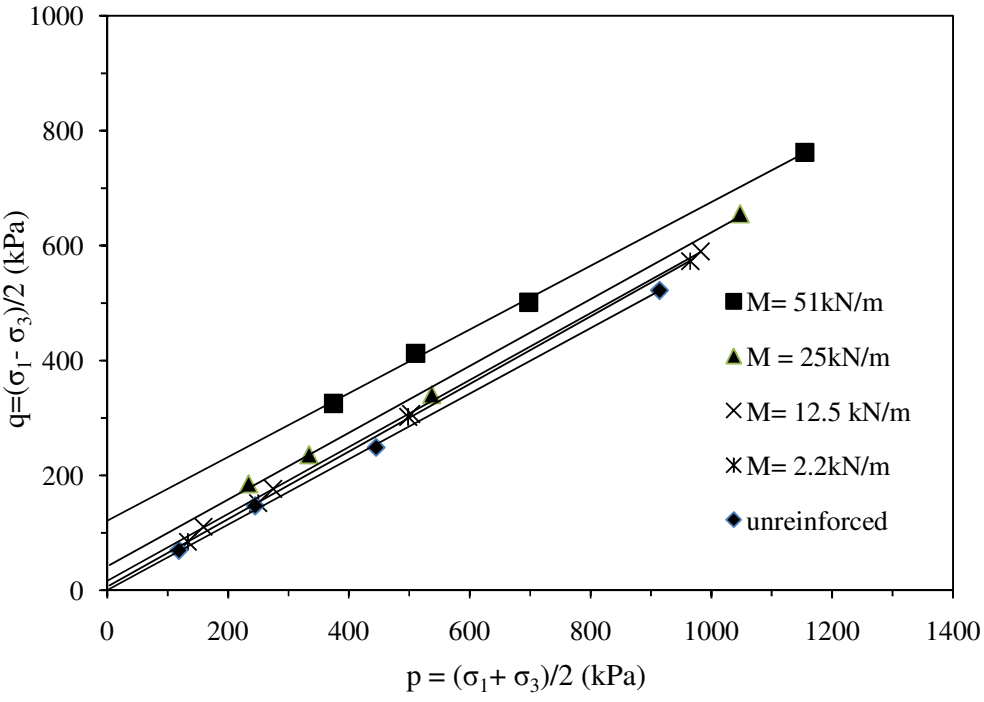

Fig. 4.14 Failure strength envelopes of geocell reinforced soils: Influence of stiffness of geocell on loose soil (D_r = 30%).

TH-1123_10610407

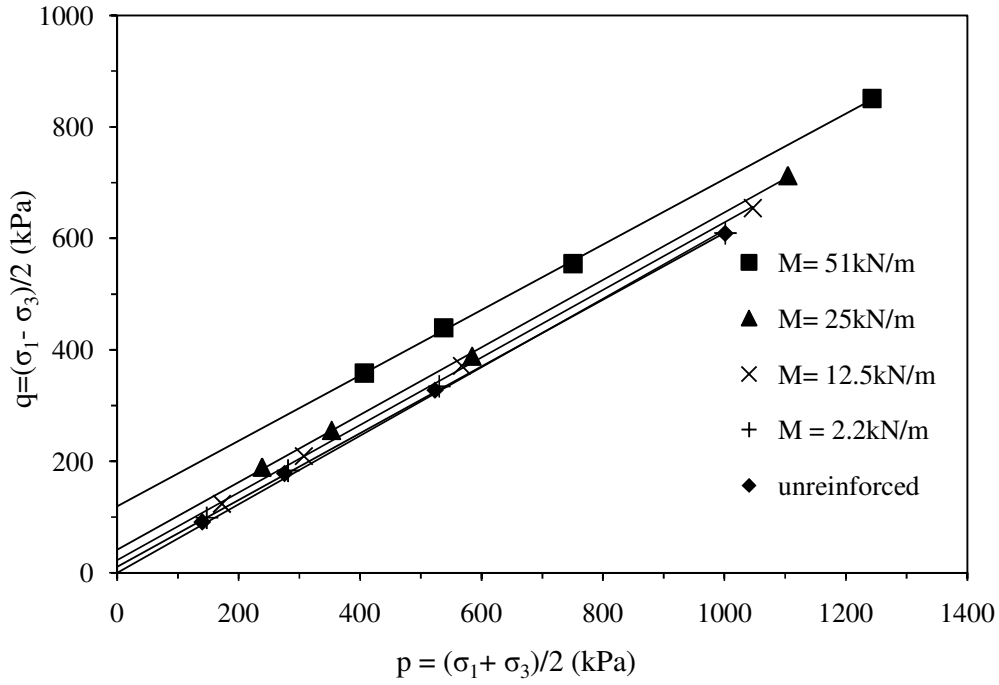

Fig. 4.15 Failure strength envelopes of geocell reinforced soils: Influence of stiffness of geocell on medium dense soil (D_r = 60%)

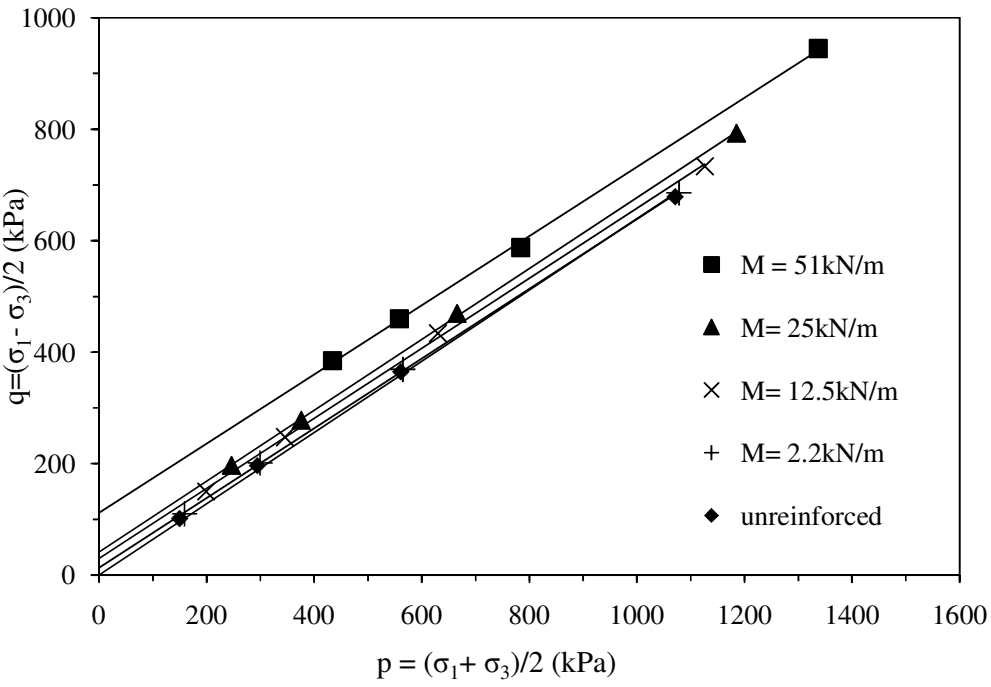

Fig. 4.16 Failure strength envelopes of geocell reinforced soils: Influence of stiffness of geocell on dense soil (D_r = 80%)

TH-1123_10610407

Table 4.1 Summary of shear strength parameters of geocell reinforced soil: Influence of stiffness of geocell reinforcement

Density of soil D_r (%)	Type of geocell	Stiffness of geocell M (kN/m)	Failure axial strain (%)	Friction angle Φ(°)	Cohesion c_g (kPa)
30	GM_2	2.2	12	36	8
	GM_1	12.5	18	36	20
	GT_2	25	20	36	51
	GT_1	51	20	34	146
60	GM_2	2.2	8	37	15
	GM_1	12.5	11	37	28
	GT_2	25	17.5	37	51
	GT_1	51	19.5	36	147
80	GM_2	2.2	7.5	39	16
	GM_1	12.5	9	39	38
	GT_2	25	16	39	53
	GT_1	51	18	38	142

TH-1123_10610407

(a) M = 12.5 kN/m, D_r = 60% (b) M = 51 kN/m, D_r = 80%

Fig. 4.17 Failure mode of geocell reinforced soil: Influence of stiffness of geocell (σ_3 = 196 kPa).

4.3.2 Influence of relative density of fill soil

Stress-strain responses of geocell-sand composite, with loose (relative density of 30%), medium dense (relative density of 60%) and dense (relative density of 80%), for a typical case (geocell stiffness of 25 kN/m), are shown in Fig.4.18, Fig.4.19 and Fig.4.20 respectively. It could be observed that the responses with loose soil, irrespective of the confinement pressure, have generally shown an increasing trend leading to a nearly asymptotic state (i.e. constant deviator stress) at relatively large strain. While specimens with dense infill (D_r of 60% and 80%), after showing an initial increase, have undergone a stress drop. This is because the loose soil when subjected to shearing undergoes volume compression leading to an increasingly dense

TH-1123_10610407

matrix that sustains increased loading. On the other hand the dense infill tends to dilate forcing the weak geocell to yield. As a result of which the soil gets unloosened leading to the stress drop. However, if the geocell is strong enough to stand against the soil pressure such a phenomenon of strain softening would not take place. Indeed, the stress-strain responses with a relatively stiff geocell (M = 51 kN/m) as depicted in Figs. 4.21-4.23 haven't exhibited such post yield strain softening behaviour. Even with loose soil infill the rise in the deviator stress is much steeper as compared to that with the geocell having lower stiffness i.e. M = 25 kN/m (Fig. 4.21 vs. Fig. 4.18). This is attributed to the strengthening effect of the geocell reinforcement that increases with the increase in its stiffness. Hence it can be said that both at loose and dense state of the infill soil the influence of geocell reinforcement is prominently felt.

The results can further be analysed through the strength envelopes depicted in Figs. 4.24-4.27 and the values of apparent cohesion reported in Table 4.2. With relatively weak geocells, M = 2.2 and 12.5 kN/m, the apparent cohesion is found to have increased with increase in the density of the fill soil (Figs. 4.24 and Fig.4.25, Table 4.2). This is because the weak geocell tends to expand with the soil. As a dense soil matrix expands more so is the geocell around is subjected to increased membrane straining induces increased membrane stress onto the soil mass leading to increased induced cohesion.

However, with relatively stiff geocell, Figs. 4.26 and 4.27, the cohesion intercepts for all the relative densities are almost the same indicating that the placement density of the fill soil has a marginal influence on the apparent cohesion of the geocell-soil composite. Indeed the data presented in Table 4.2, corresponding to M = 25 and 51 kN/m, shows that the apparent cohesion values for different relative densities are

TH-1123_10610407

comparable. This is because a loose soil matrix in the process of loading gets compacted and thereby attains a dense state that it derives a similar order of hoop stress from the geocell as that of the soil initially packed dense. In view of this, there is not much of difference in the peak cohesion values for different initial densities of the fill soil. However, the loose specimens generally have undergone large strain before they have mobilised such large apparent cohesion. This indicates that a geocell mattress with loose infill if used in foundations shall undergo large settlements before it can mobilise large bearing capacity. But, given the serviceability of the structures, this is likely to be unacceptable in most of the cases. In view of this the geocells must be dense filled. Besides, the other advantage of dense infill is that there is an increase in the friction component with increase in the relative density, as is evident through the increase in slope of the strength envelopes (Fig.4.24-4.27). As a result of which there is an overall improvement in the load carrying capacity of the geocell-soil system. Therefore, the soil in the geocells should be compacted to higher density.

In actual field applications, particularly with geocells of larger height, it is relatively difficult to compact the soil inside geocell pockets. In view of this, as has been suggested by Bush et al 1990, the geocells with little over filling (i.e. about 150 mm) should be subjected to light rolling. This overfilling is meant to cater for the compaction induced settlements. With repeated passage of rolling and filling of potholes, a compact geocell-soil structure could be achieved. It should be mentioned here that using this method Bush et al. (1990) have reported the construction of geocells of one meter height, in an embankment foundation over soft clay.

TH-1123_10610407

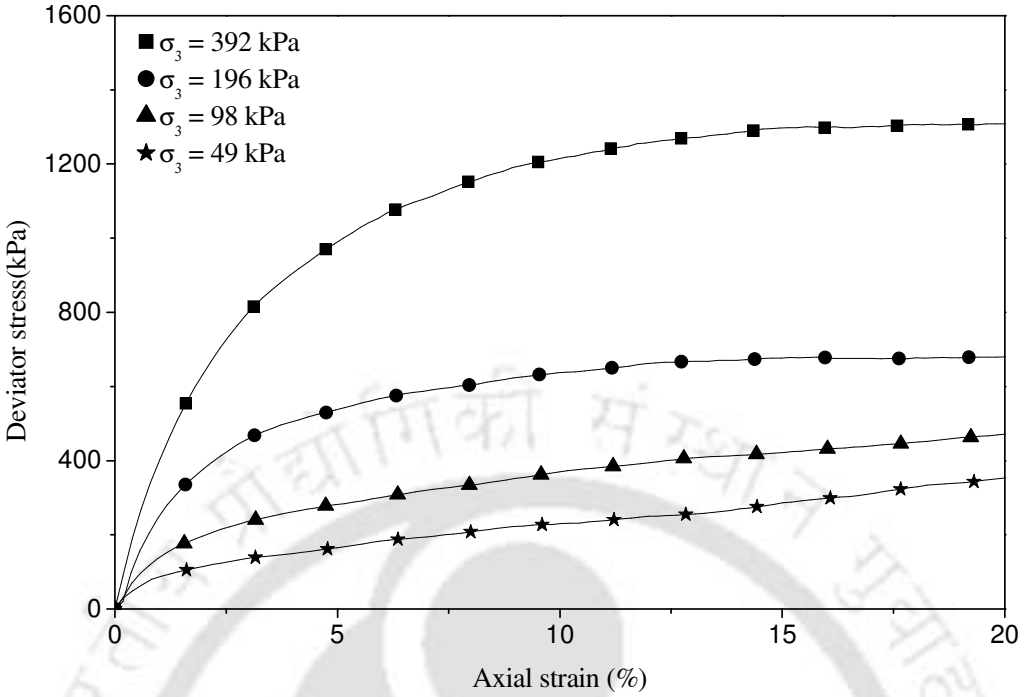

Fig. 4.18 Stress-strain behavior of geocell reinforced sand (M= 25kN/m, D_r = 30%)

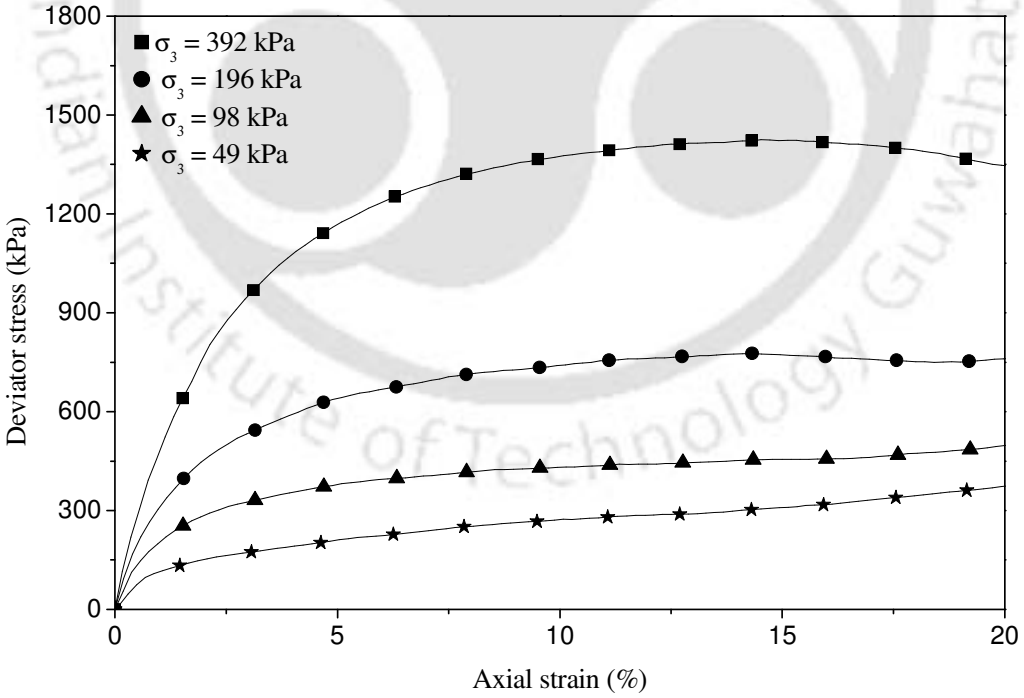

Fig. 4.19 Stress-strain behavior of geocell reinforced sand (M= 25kN/m, D_r = 60%)

TH-1123_10610407

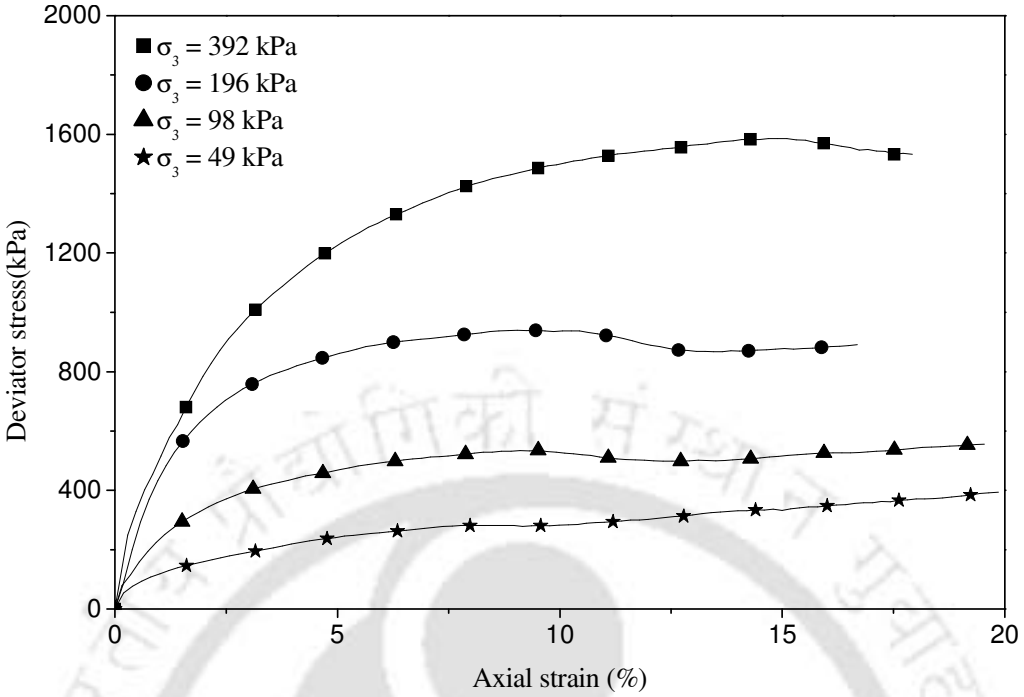

Fig. 4.20 Stress-strain behavior of geocell reinforced sand (M= 25kN/m, D_r = 80%)

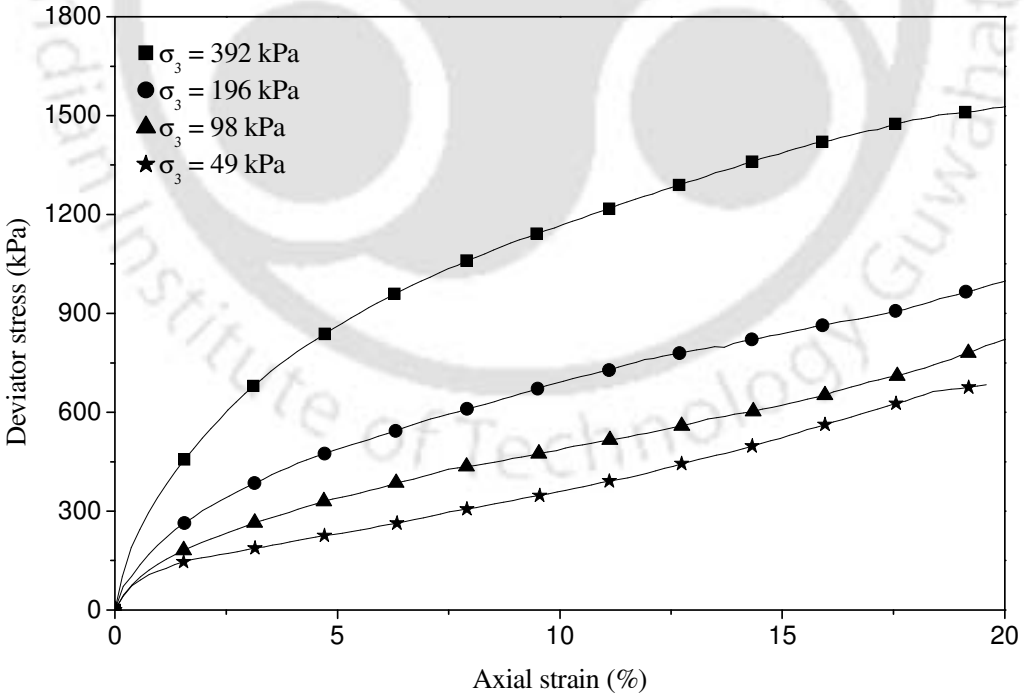

Fig. 4.21 Stress-strain behavior of geocell reinforced sand (M= 51kN/m, D_r = 30%)

TH-1123_10610407

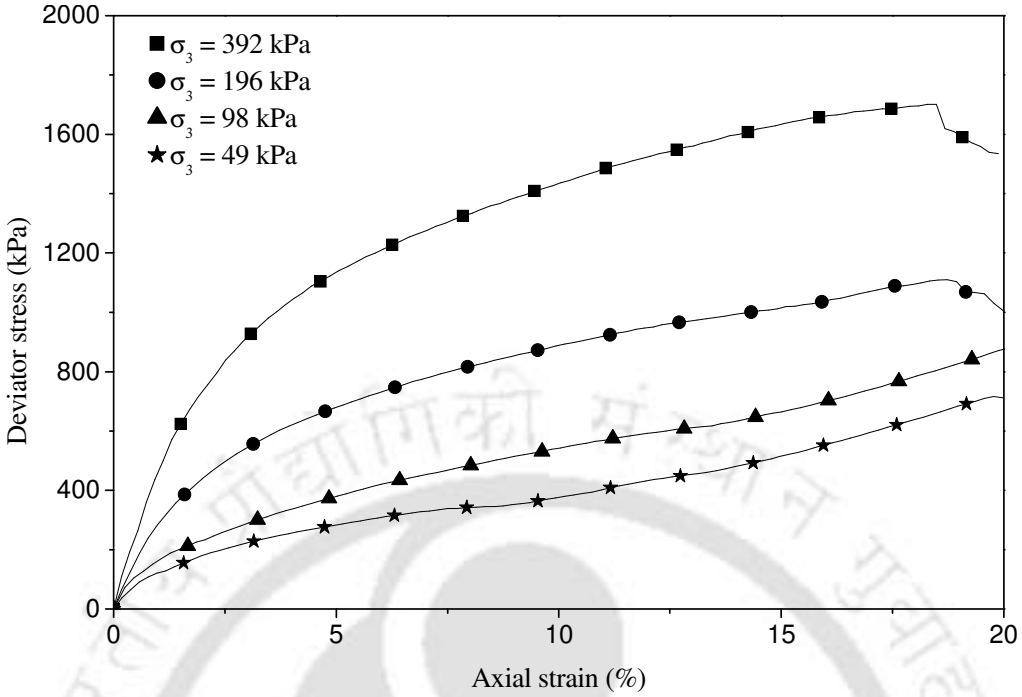

Fig. 4.22 Stress-strain behavior of geocell reinforced sand (M= 51kN/m, D_r = 60%)

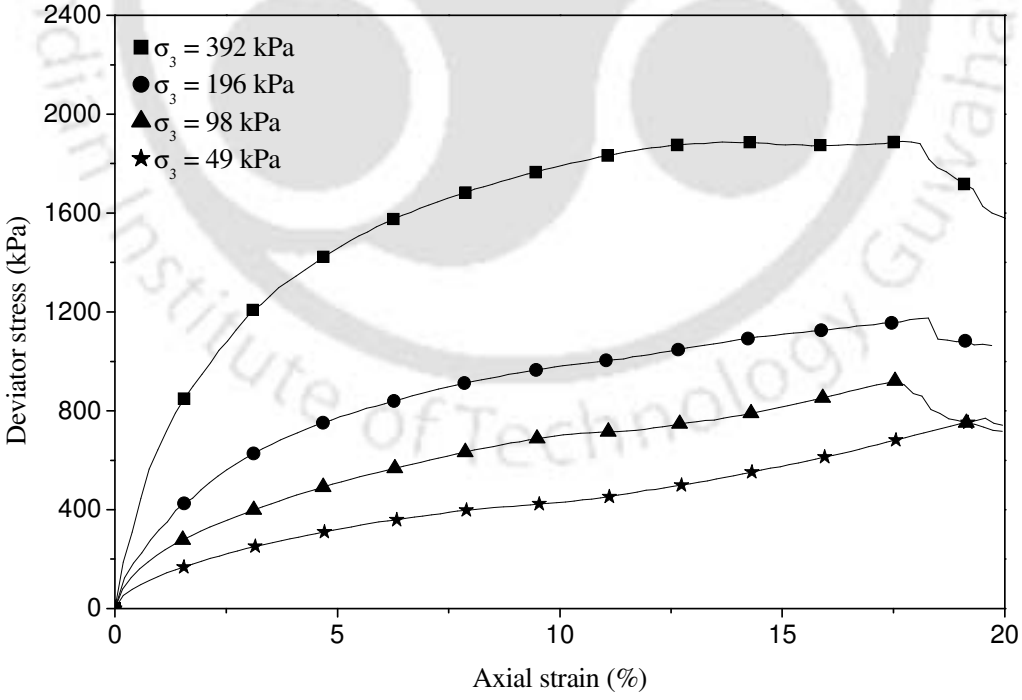

Fig.4.23 Stress-strain behavior of geocell reinforced sand (M = 51kN/m, D_r = 80%)

TH-1123_10610407

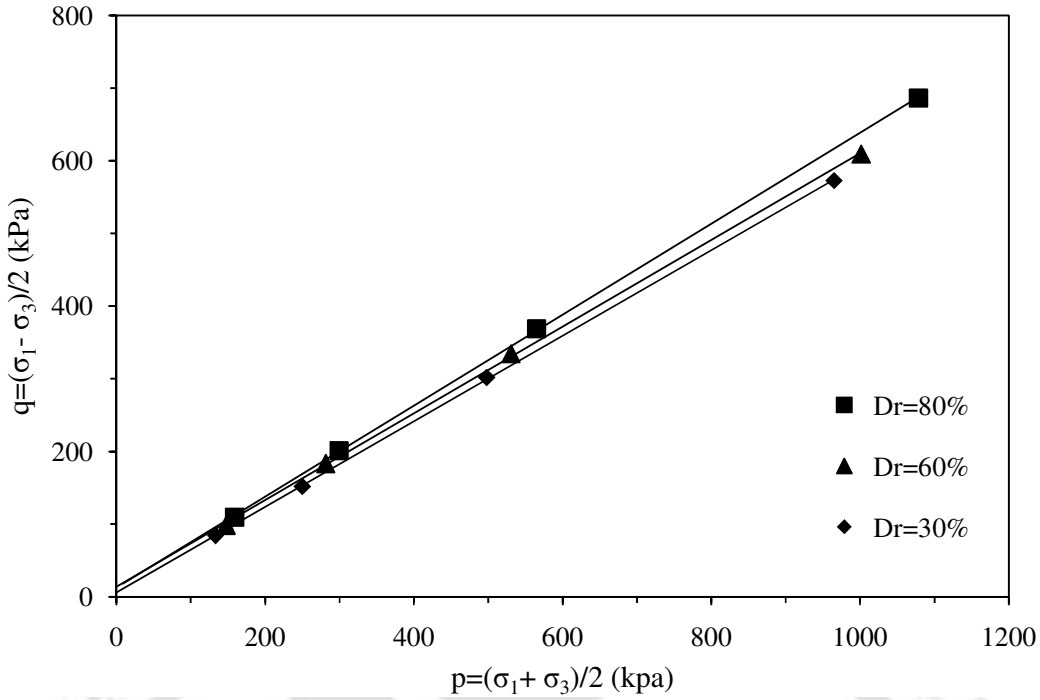

Fig.4.24 Failure strength envelopes of geocell reinforced soils: Influence of density of soil (M =2.2kN/m)

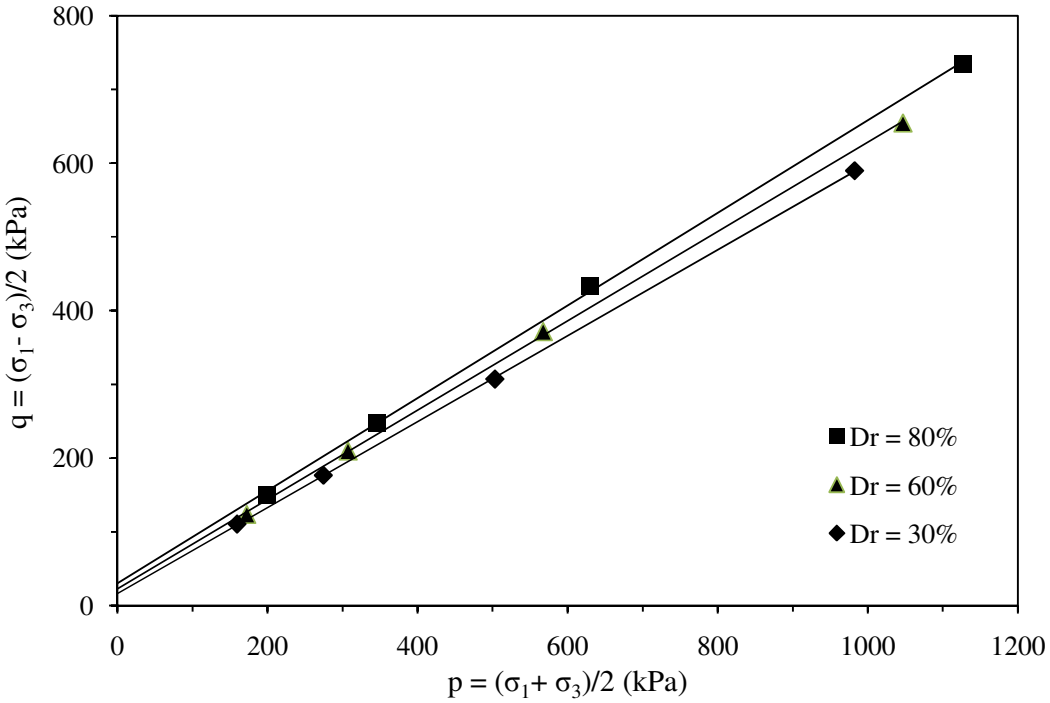

Fig.4.25 Failure strength envelopes of geocell reinforced soils: Influence of density of soil (M =12.5kN/m)

TH-1123_10610407

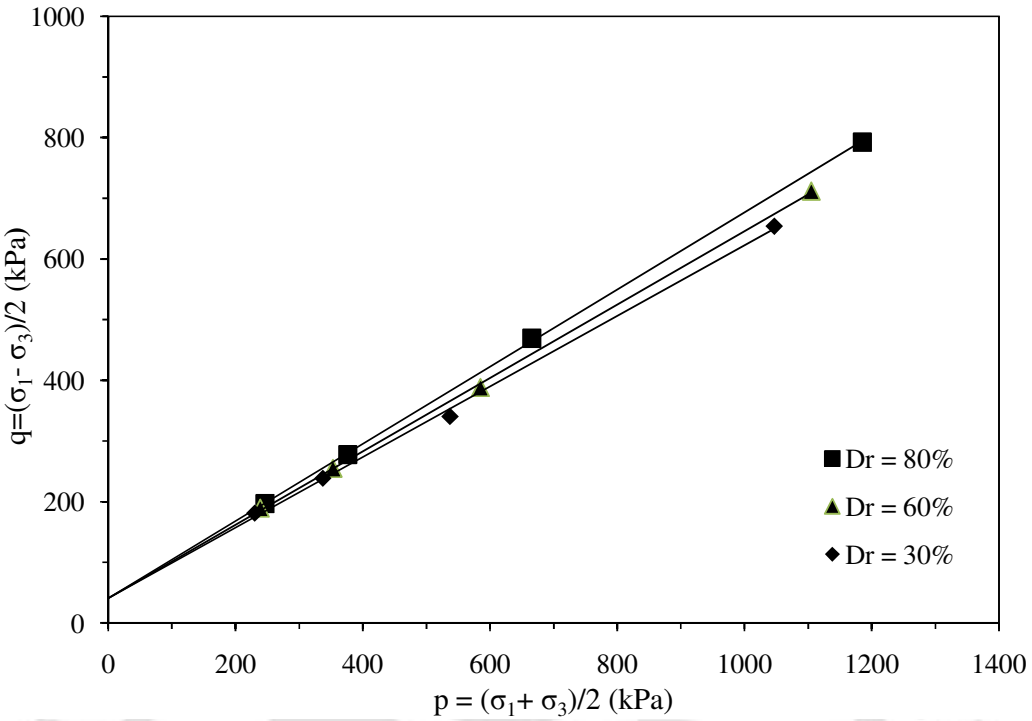

Fig. 4.26 Failure strength envelopes of geocell reinforced soils: Influence of density of soil (M =25kN/m)

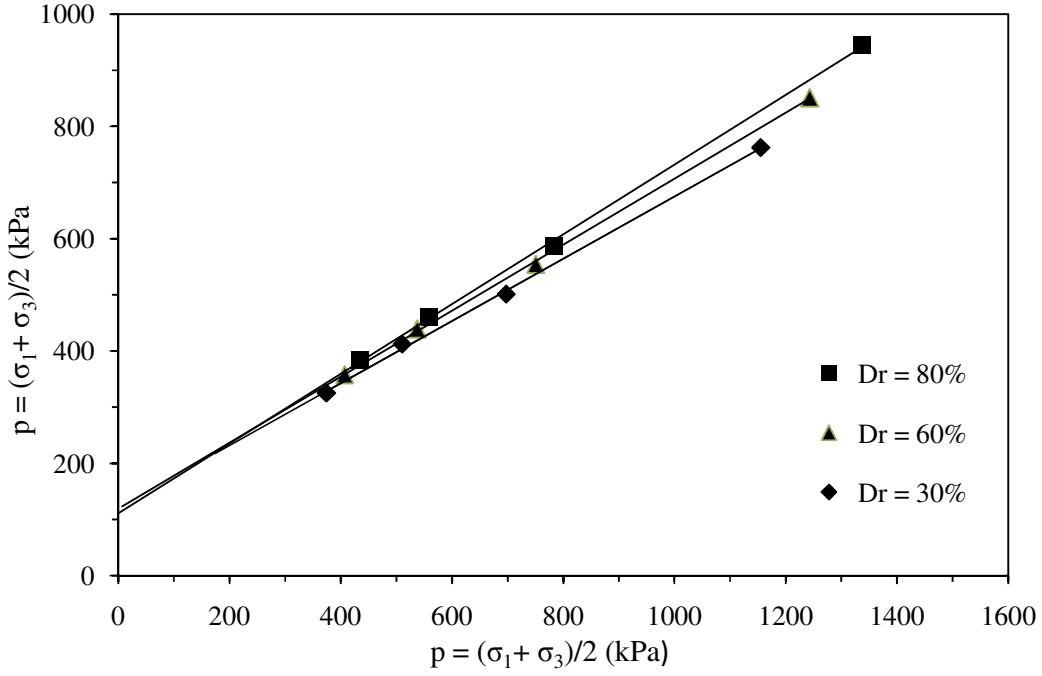

Fig. 4.27 Failure strength envelopes of geocell reinforced soils: Influence of density of soil (M = 51 kN/m)

TH-1123_10610407

Table 4.2 Summary of shear strength parameters of geocell reinforced soil obtained from triaxial compression tests: Influence of density of soil

Type of reinforcement	Stiffness of geocell M (kN/m)	Density of soil D_r (%)	Friction angle Φ (°)	Cohesion c_g (kPa)
Unreinforced	_	30	35	0
	_	60	38	0
	_	80	40	0
Geocell	2.2	30	36	8
		60	37	15
		80	39	16
	12.5	30	36	20
		60	37	28
		80	39	38
	25	30	36	51
		60	37	51
		80	39	53
	51	30	34	146
		60	36	147
		80	38	142

4.3.3 Influence of confining pressure

Typical stress-strain responses of geocell reinforced soils for a low confining pressure i.e. σ_3 = 49 kPa and a relatively high confining pressure i.e. σ_3 = 392 kPa, for different relative densities of fill soil, are presented in Figs. 4.28 and 4.29 respectively. Similar responses were observed in other cases as well. It is of inertest to note that when the applied confining pressure is less (σ_3 = 98 kPa) the stress-strain responses have shown an ascending trend, similar to that of strain hardening (Fig. 4.28). This is more

TH-1123_10610407

prominently observed in case of stiff geocells. However, with high confining pressure (σ_3 = 196 kPa), the stress responses are mostly of strain softening type. It indicates that in situations where the ambient confining stress is less the geocell has a greater influence on the overall behavior. In other words it can be said that under the condition of low ambient confinement pressure the geocell is free to expand under the applied surcharge loading that it mobilises higher hoop stress inducing a stiffened behavior onto the encapsulated soil mass.

With increased confinement pressure the membrane action of the geocells is suppressed that the hoop stress mobilized is substantially less. As a result of which the encapsulated soil plays the dominant role that is amenable to strain softening in the post failure stage. Indeed, the geocell-soil responses with higher confinement pressure (Fig.4.29) are mostly similar to that of the unreinforced soil (Fig.4.1-4.3). Hence it can be said that in situations where the surrounding pressure is relatively less, for example in reinforced soil walls lying over ground, the geocells can perform better as compared to the underground structures such as foundations where the ambient confining pressure is generally much higher.

TH-1123_10610407

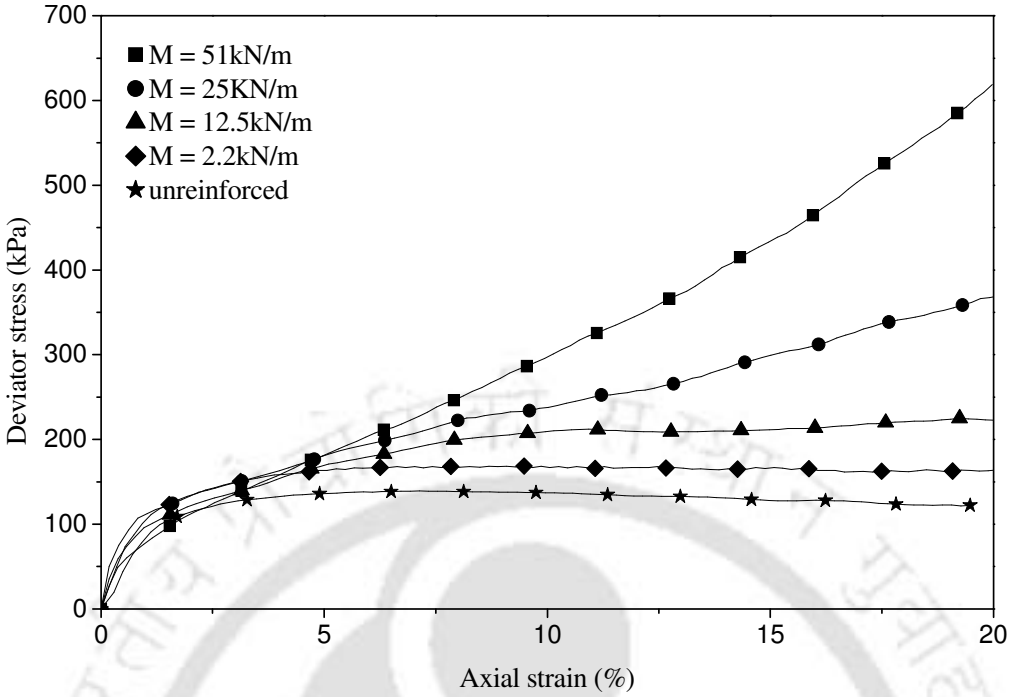

(a) D_r = 30%

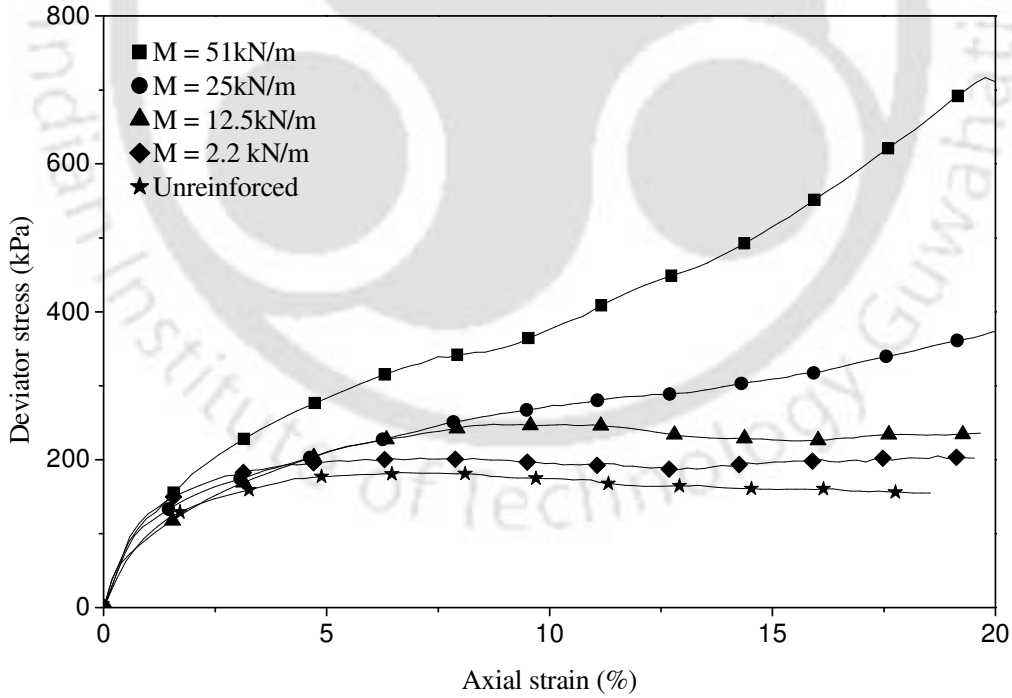

(b) D_r = 60%

Fig. 4.28 Stress-strain behavior of geocell reinforced soils at low confinement pressure (σ_3 = 49 kPa)

TH-1123_10610407

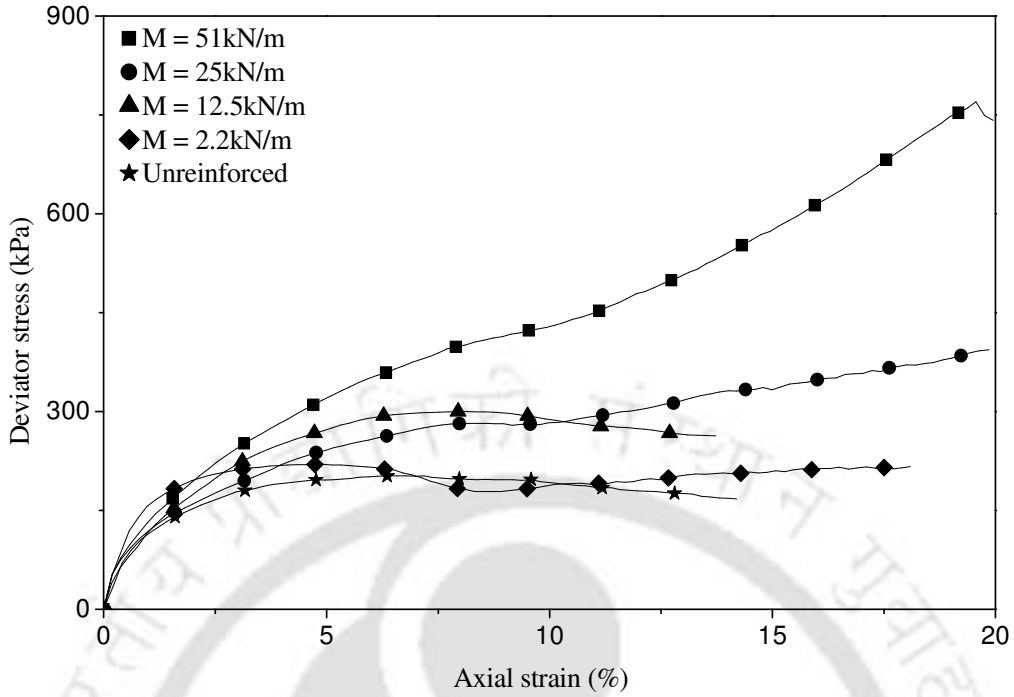

(c) D_r = 80%

Fig. 4.28 (Contd.) Stress-strain behavior of geocell reinforced soils at low confinement pressure (σ_3 = 49 kPa)

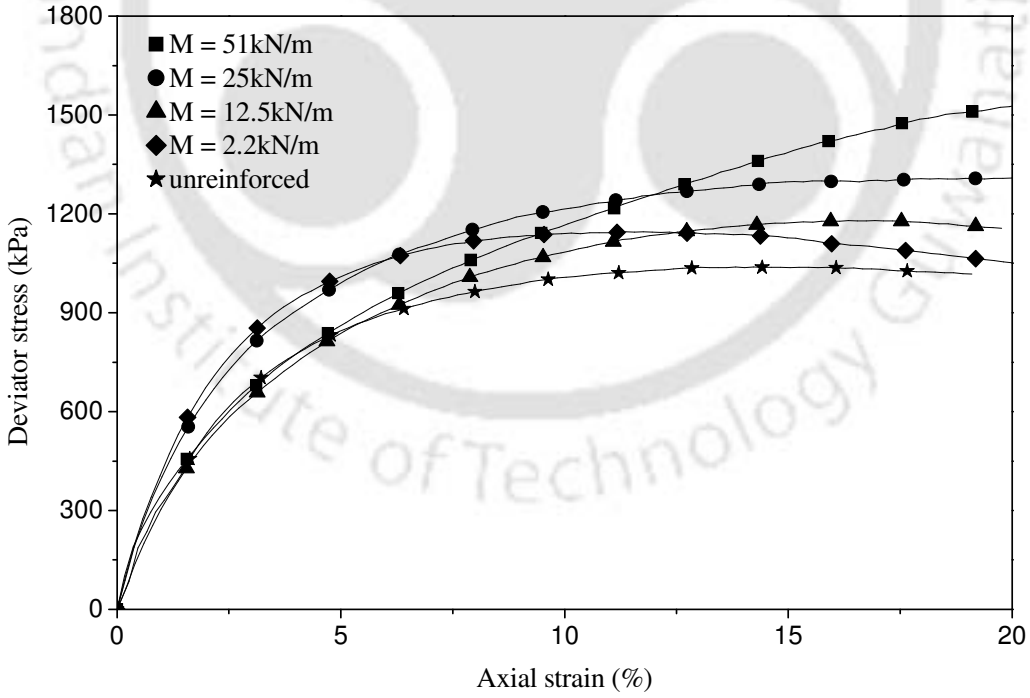

(a) D_r = 30%

Fig. 4.29 Stress-strain behavior of geocell reinforced soils at high confinement pressure (σ_3 = 392 kPa)

TH-1123_10610407

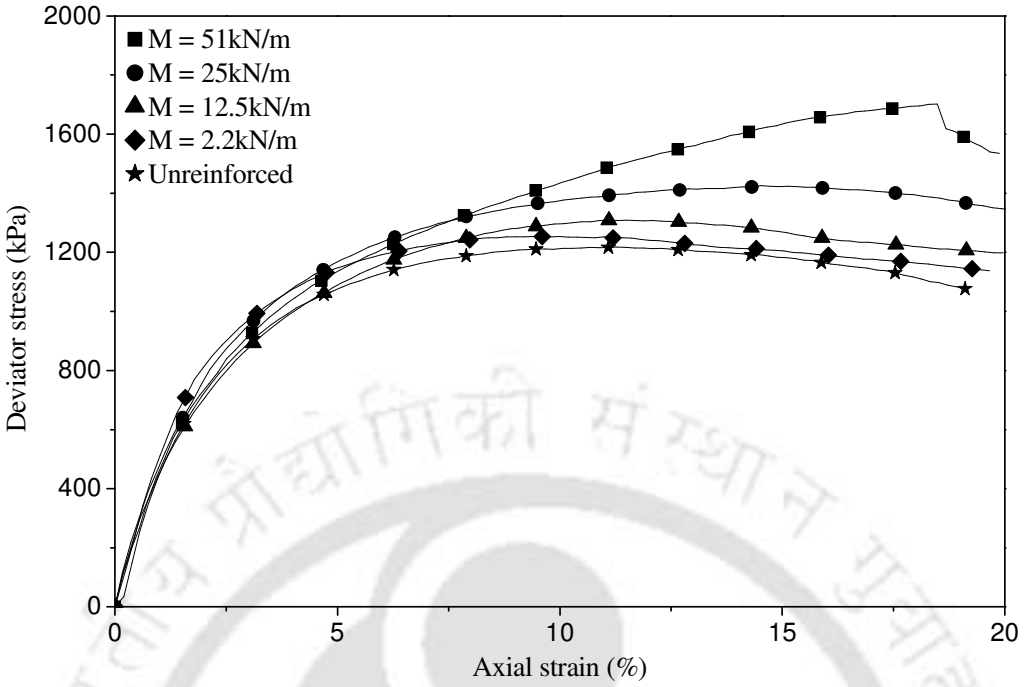

(b) D_r = 60%

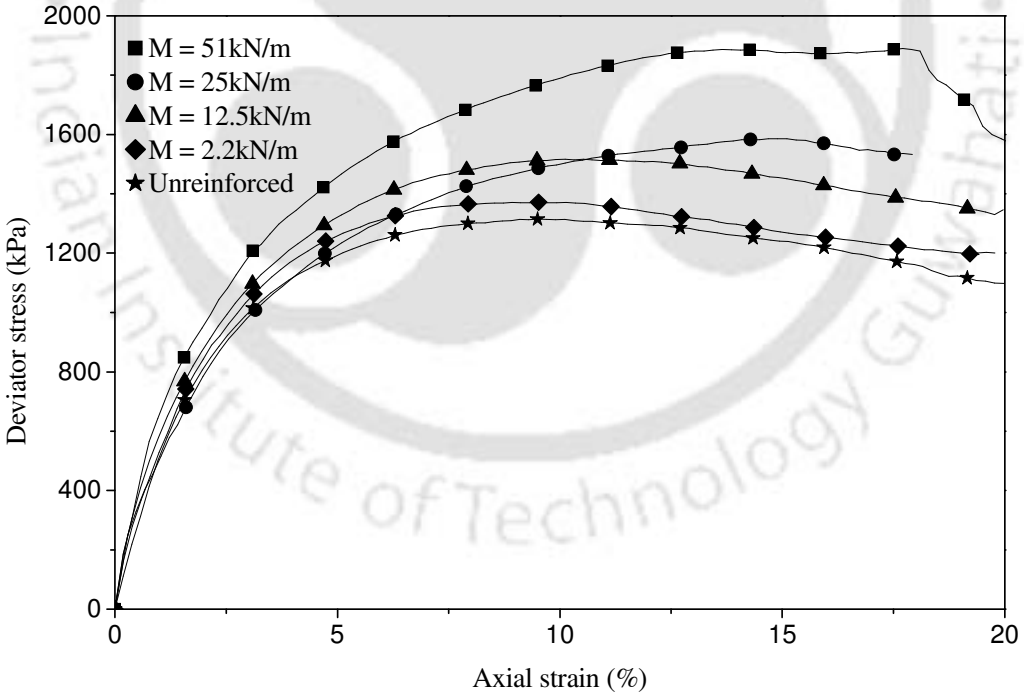

(c) D_r = 80%

Fig. 4.29 (Contd.) Stress-strain behavior of geocell reinforced soils at high confinement pressure (σ_3 = 392 kPa)

TH-1123_10610407

4.4 SCALE EFFECT

The important parameters that influence the behavior of the geocell reinforced soil system can be taken as: D, h, S_{gc},γ, ϕ, G, σ_1, σ_3. Herein, D is the diameter of the geocell which is equal to the diameter of the specimen, h is the height of the geocell, S_{gc} is the strength/stiffness of the geocell reinforcement, γ is the unit weight of soil, ϕ is the friction angle of the soil, G is the shear modulus of soil, σ_1 is the major principal stress i.e. the vertical surcharge pressure, σ_3 is the minor principal stress i.e. the ambient confinement pressure. The function (f) that governs the system can be written as

$$f(D, h, S_{gc}, \gamma, G, \sigma_1, \sigma_3, \phi) = 0 \qquad (4.1)$$

The eight parameters in Eq.4.1 are having three fundamental dimensions (i.e. mass, length and time) i.e. D = {M, L, T}. In terms of these three fundamental dimensions, the dimensions of the parameters can be written as; L, L, MT^{-2}, $ML^{-2}T^{-2}$, $ML^{-1}T^{-2}$, $ML^{-1}T^{-2}$, $ML^{-1}T^{-2}$ and 0, respectively. As per the theory of Langhaar (1951) this system can be studied by any complete set of five (i.e. 8 – 3) independent parameters. Herein {D, h} and {G, σ_1, σ_3} have similar dimensions. Hence, R which is the set of parameters having totally distinct dimensions will be {D, γ, σ_3} and Q which is set of repeated variables can be { D, γ, σ_3} (Butterfield R. 1999). But these repeated variables can make dimensional group ($D\gamma/\sigma_3$), so dimensional analysis will fail. According to Bridgman (1931) dimensional analysis will fail if $D > D_{min}$. Here D_{min} can be obtained by considering D = {F, L} i.e. force and length, where dimension of F is $[MLT^{-2}]$.

TH-1123_10610407

Now here there will be six independent parameters (i.e. 8-2) π_1, π_2, π_3,…….π_6 (Bukingham 1914) and dimensions of the parameters in equation 4.1 can be expressed as; L, L, FL^{-1}, FL^{-3}, FL^{-2}, FL^{-2}, FL^{-2} and 0, respectively. Hence, R will be {D,γ, σ_3} and in Q it can be any two parameters from the R, here it is taken { D, σ_3}. Therefore, the isolated variable function will be {h, S_{gc},γ, G, σ_1, ϕ}. Dimensionless groups are formed by repeated and isolated variables, for example $\pi_1 = (hD^{a1}\sigma_3^{a2})$. Conventionally in dimensional group, isolated variable is expressed with raised to the first power and repeated variables are expressed with indices (here in π_1 term a1 and a2 are indices of D and σ_3 respectively). Indices of these variables can be determined by equating indices of [F, L] separately to zero. Similar way we can obtained other pi terms. Hence Eq.4.1 can be reduced to the following form

$$g(\pi_1, \pi_2, \pi_3, \ldots\ldots \pi_6)$$

$$= \quad g\left[\left(\frac{h}{D}\right),\left(\frac{S_{gc}}{D\sigma_3}\right),\left(\frac{D\gamma}{\sigma_3}\right),\left(\frac{G}{\sigma_3}\right),\left(\frac{\sigma_1}{\sigma_3}\right),\phi\right] = 0 \qquad (4.2)$$

For a prototype geocell (p) with diameter N times higher than the model (m)

$$\frac{D_p}{D_m} = N \qquad (4.3)$$

For similarity to be satisfied all the π terms should be same both for the prototype and the model.

$$(\pi_3)_p = (\pi_3)_m \quad \Rightarrow \quad \frac{D_p\gamma_p}{\sigma_{3p}} = \frac{D_m\gamma_m}{\sigma_{3m}} \qquad (4.4)$$

In the case of, soils in the model and prototype to be of same density Eq.4.4 reduces to

TH-1123_10610407

$$\frac{\sigma_{3p}}{\sigma_{3m}} = \frac{D_p}{D_m} = N \tag{4.5}$$

$$(\pi_2)_p = (\pi_2)_m \quad \Rightarrow \quad \frac{S_{gcp}}{D_p \sigma_{3p}} = \frac{S_{gcm}}{D_m \sigma_{3m}} \quad \Rightarrow \quad \frac{S_{gcp}}{S_{gcm}} = \frac{D_p \sigma_{3p}}{D_m \sigma_{3m}} = N^2 \tag{4.6}$$

It could be observed that while the geometric parameters have a linear variation the strength and stiffness parameters vary in second order. Hence, for the present results to be valid, the strength of the reinforcement in the prototype reinforced soil foundation bed should be of N^2 times the strength of the reinforcement used in the model test.

4.5 PREDICTION OF STRENGTH OF THE GEOCELL-SOIL COMPOSITE

As has been observed in the tests results discussed above the increase in strength of granular soil due to geocell confinement is primarily through development of an apparent cohesion. For estimating the induced apparent cohesion due to geocells several researchers such as; Bathurst and Karpurapu 1993, Rajagopal et al. 1999 have used the membrane correction theory of Henkel and Gilbert (1952). The same has been adopted here as explained below.

The increase in the major principal stress in a typical soil specimen due to the geocell reinforcement can either be idealized due to an increase in the confining pressure i.e. $\Delta\sigma_3$' or through an induced cohesion i.e. c_g, as has been depicted through the Mohr circles shown in Fig. 4.30.

TH-1123_10610407

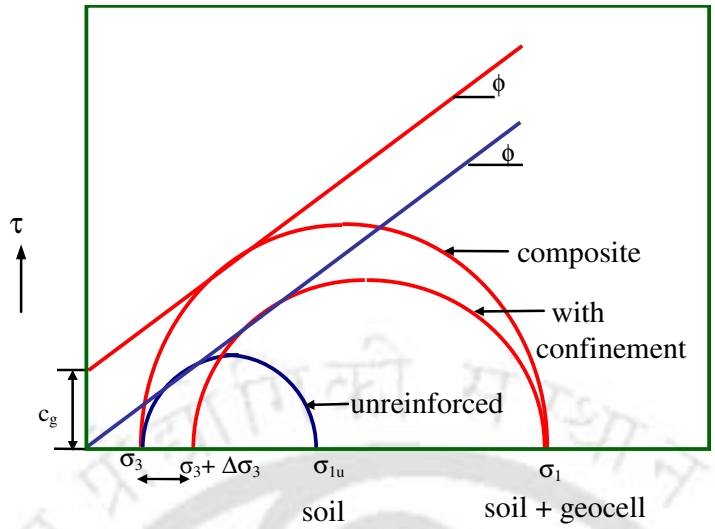

Fig. 4.30 Mohr circle representation of geocell reinforced soil

The ultimate stress, σ_1; that can be applied to the soil having the geocell induced cohesion of c_r, subjected to a confinement pressure of σ_3, can be written as

$$\sigma_1 = \sigma_3 tan^2\left(45 + {}^{\emptyset}/_{2}\right) + 2c_g tan\left(45 + {}^{\emptyset}/_{2}\right) \quad (4.7)$$

While if the geocell reinforcing effect is considered as an enhanced confining pressure, $\Delta\sigma_3$; mobilized through the hoop stress, the ultimate stress that the soil can sustain will be as given below

$$\sigma_1 = (\sigma_3+\Delta\sigma_3) tan^2\left(45 + {}^{\emptyset}/_{2}\right) \quad (4.8)$$

As the ultimate stress of soil at failure is a unique value both the expressions can be equated and thereby the following relation can be obtained

TH-1123_10610407

$$c_g = \frac{\Delta\sigma_3}{2}\tan\left(45 + {}^{\emptyset}/_{2}\right) = \frac{\Delta\sigma_3}{2}\sqrt{K_p} \quad (4.9)$$

The additional confining pressure, $\Delta\sigma_3$, imposed onto the soil, due to the geocell, is estimated using the membrane correction theory of Henkel and Gilbert (1952). The free body diagram of a typical geocell-encased soil specimen, used in the triaxial compression tests, is shown in Fig. 4.31.

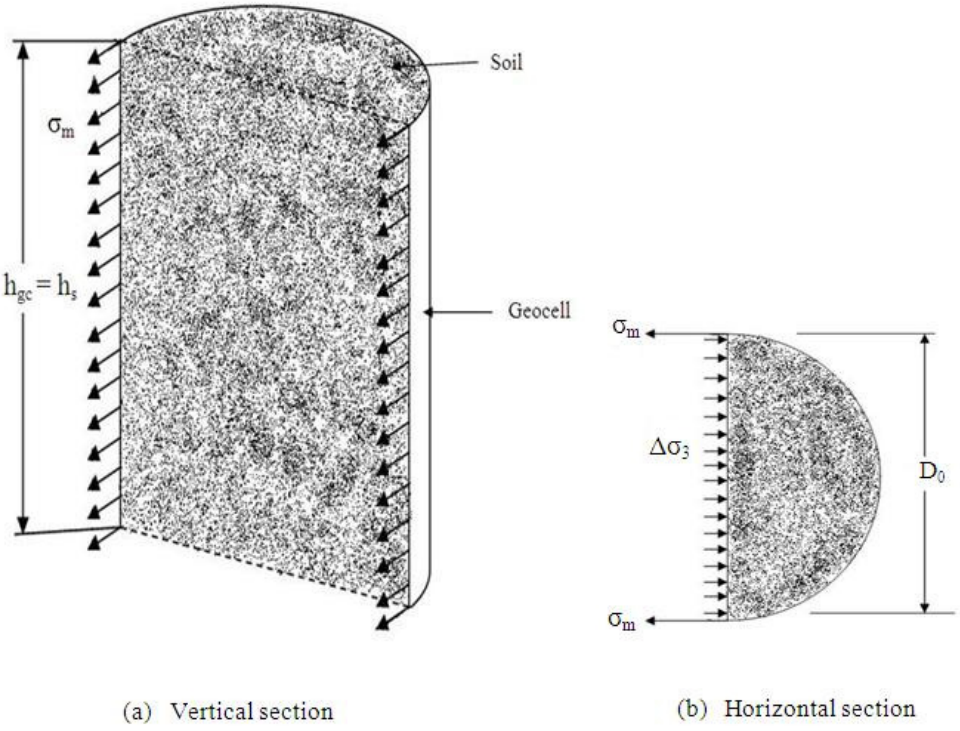

Fig. 4.31 Free body diagram of geocell encased soil specimen

TH-1123_10610407

Assuming equilibrium of forces in the horizontal direction i.e. soil pressure $\Delta\sigma_3$ and the membrane stress, it can be written as

$$2th_{gc} \times \sigma_m = D_o h_s \times \Delta\sigma_3 \tag{4.10}$$

Where, t is the initial thickness of the geocell, h_{gc} is the initial height of the geocell, σ_m is the membrane stress developed in the geocell, D_o is the initial diameter of the soil specimen and h_s is the initial height of the soil cylinder.

Rearranging the above equation the induced confining stress can be obtained as

$$\Delta\sigma_3 = \frac{2t}{D_o}\sigma_m \frac{h_{gc}}{h_s} \tag{4.11}$$

As the specimen is loaded and thereby undergoes deformation its geometry changes. If, with an axial strain of ε_a, the soil specimen diameter and height changes to D' and h_s' respectively and geocell length and thickness changes to h_{gc}' and t' respectively then the induced confining pressure will be

$$\Delta\sigma_3 = \frac{2t'}{D'}\sigma_m' \frac{h_{gc}'}{h_s'} \tag{4.12}$$

The changed height of the soil specimen, $h_s' = h_s(1-\varepsilon_a)$; while the changed height of the geocell, $h_{gc}' = h_{gc}(1-\varepsilon_c\nu_{gc})$, where ε_c is the circumferential strain in the geocell and ν_{gc} is the passions ratio of the geocell material. Hence the ratio of the membrane height to that of the soil can now be written as

$$\frac{h_{gc}'}{h_s'} = \frac{h_{gc}}{h_s}\left(\frac{1-\varepsilon_c\nu_{gc}}{1-\varepsilon_a}\right) \tag{4.13}$$

TH-1123_10610407

Since initial height of the soil, at the beginning of the test, is equal to the height of geocell; h_{gc} is equal to h_s. Besides, the factor $\varepsilon_c \nu_{gc}$ is too small and hence can be neglected. Therefore, the Equation 4.13 reduces to

$$\frac{h_{gc}^{'}}{h_s^{'}} = \frac{1}{(1-\varepsilon_a)} \tag{4.14}$$

Substituting Equation 4.14 into Equation 4.12, the induced confinement by the geocell under an axial strain of ε_a can be written as

$$\Delta\sigma_3 = \frac{2t^{'}}{D^{'}}\sigma_m^{'}\left(\frac{1}{1-\varepsilon_a}\right) \tag{4.15}$$

The membrane stress, $\sigma_m^{'}$, in the geocell is equal to $E_m\varepsilon_c$. Where, E_m is the elastic modulus of the geocell material, that can be obtained by dividing the secant modulus with the thickness of the geocell i.e. M/t'. M is the secant modulus corresponding to the circumferential strain in the geocell, ε_c. Substituting these values into Equation 4.15 the final relation for estimating the geocell induced confining stress can be obtained as

$$\Delta\sigma_3 = \frac{2M\varepsilon_c}{D^{'}}\left(\frac{1}{1-\varepsilon_a}\right) \tag{4.16}$$

The circumferential strain developed in the geocell can be written as

$$\varepsilon_c = \frac{\pi D^{'} - \pi D_o}{\pi D_o} = \frac{D^{'} - D_o}{D_o} \tag{4.17}$$

Under the condition that the volume of the soil mass in the specimen does not change under loading; the diameter, D', at an axial strain ε_a cab be obtained by comparing the initial volume with the final one.

TH-1123_10610407

$$\frac{\pi}{4}D_o^2 h_s = \frac{\pi}{4}D'^2 h_s' \tag{4.18}$$

Rearranging the above equation, the final diameter D' of the specimen can be written as

$$D' = \frac{D_o}{\sqrt{h_s'/h_s}} = \frac{D_o}{\sqrt{1-\varepsilon_a}} \tag{4.19}$$

Substituting Equation 4.19 into Equation 4.17, the circumferential stress can be obtained as

$$\Delta\sigma_3 = \frac{2M}{D_0}\left[\frac{1-\sqrt{1-\varepsilon_a}}{(1-\varepsilon_a)}\right] \tag{4.20}$$

Substituting Equation 4.20 into Equation 4.9 the apparent cohesion induced by the geocell reinforcement into the soil can be obtained as

$$c_g = \frac{M}{D_o}\left[\frac{1-\sqrt{1-\varepsilon_a}}{1-\varepsilon_a}\right]\sqrt{K_p} \tag{4.21}$$

This model is used to estimate the apparent cohesive strength, c_g, developed by the geocells used in different tests under series-B_1-B_4. A comparison of the experimentally obtained values of the apparent cohesion with the theoretically obtained ones, are shown in Table 4.3 (Fig. 4.32). It could be observed that while with relatively stiff geocells (i.e. GT_1, GT_2) the predicted values of apparent cohesion have a relatively close match with the experimentally obtained ones but with weak geocells (i.e. GM_1 and GM_2) there is large difference between the two. This is attributed to the difference in the failure mechanism between the two cases. While with stiff geocell the failure is primarily through local rupture due to stress concentration right under the loading that the geocell-soil system almost stands intact. As result of which the distortion in the geocell-soil system, under loading, is minimal leading to uniform strain distribution over a majority portion of the geocell membrane which is in close match with assumptions considered in the proposed theory.

TH-1123_10610407

But with weak geocell there takes place visible bulging and slip deformation leading to large strain in the central zone as compared to that at top and bottom region. Therefore the membrane strain in the geocell and thereby the hoop stress developed in the central region of the geocell-soil specimen will be large than that in the region above and below (i.e. top and bottom zone). As the proposed model does not take into account such difference in the strain over the specimen, therefore, the hoop stress developed in the geocell and the predicted apparent cohesion has a shown large variation from the measured values. Indeed with loose soil, i.e. D_r of 30%, wherein central bulging of specimen is much less the comparison between the two (i.e. c_g predicted and measured) is relatively close (Table 4.3, Test B_1 and B_2).

Hence it can be said that the proposed model, for estimating the apparent cohesion, is more suitable with relatively stiff geocells which can effectively prevent the bulging of soil that the strain over the specimen is relatively uniform, which is a prominent assumption in this model.

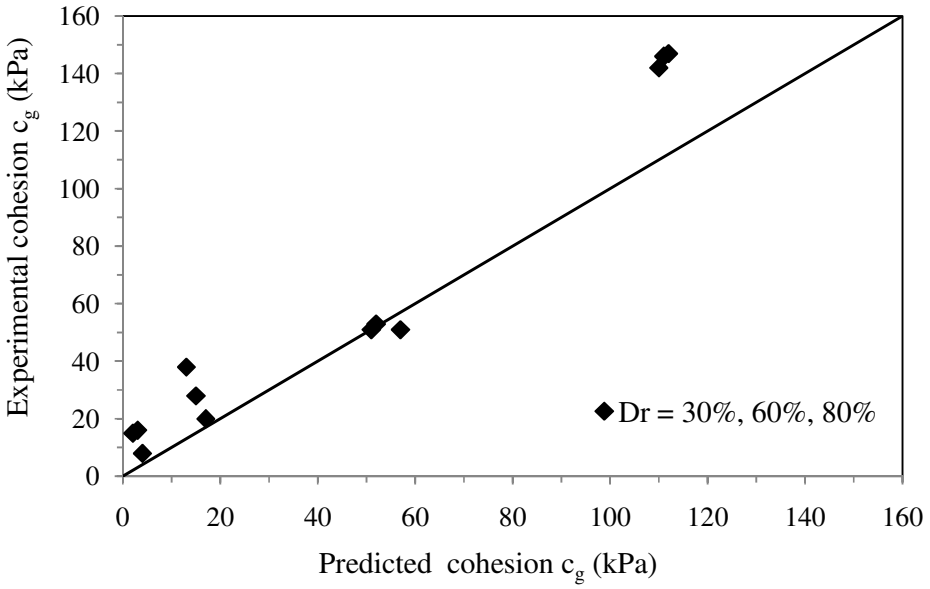

Fig. 4.32 Experimental versus predicted value of cohesion for geocell reinforced soil

TH-1123_10610407

Table 4.3: Apparent cohesion of geocell reinforced soil: Comparison of experimental data with the theoretically predicted values.

Test series	Type of geocell	Density of soil, D_r (%)	Cohesion, c_g (kPa) from experiment	Cohesion, c_g (kPa) predicted: Eq. 4.21
B_1	GM_2	30	8	4
		60	15	2
		80	16	3
B_2	GM_1	30	20	17
		60	28	15
		80	38	13
B_3	GT_2	30	51	57
		60	51	51
		80	53	52
B_4	GT_1	30	146	111
		60	147	112
		80	142	110

4.6 SUMMARY

In this chapter triaxial compression test data pertaining to unreinforced and geocell reinforced soils are presented and discussed. The influence of major parameters studied are, the stiffness of geocell reinforcement, density of fill soil and the ambient confinement pressure. The test results are carefully analyzed to understand the strength and stiffness behavior of the encased soils. The geocell reinforcement is found to have induced an apparent cohesion to the granular soil mass. A theoretical model based on the membrane correction theory of Henkel and Gilbert (1952) is used to predict the apparent cohesion. It is found that while the theory can satisfactorily estimate the apparent cohesion when the geocell are relatively stiff but with weak geocell the prediction is substantially in the lower side of the observed value.

TH-1123_10610407

CHAPTER 5

RESULTS AND DISCUSSION-II: FIBER REINFORCED SOIL

5.1 INTRODUCTION

The strength-deformation characteristics of fiber reinforced soils have been studied through several series of laboratory triaxial compression tests the details of which are given Table 3.3. The tests results are presented and discussed in this chapter. The fiber reinforcement used is discrete and randomly distributed glass fiber. Effect of different parameters studied are; the length and content of fiber, density of soil and ambient confining pressure. The influence of these parameters on the overall behavior of the reinforced soil is brought out in the following sections.

5.2 UNREINFORCED SOIL

Triaxial compression tests on unreinforced soil at different relative densities were conducted under the test series A_1 (Table 3.3.). The results obtained are presented in Figs. 4.1-4.3. The friction angles at relative densities of 30%, 60% and 80% are found to be 35°, 38° and 40° respectively and no cohesion was observed. Besides, the medium dense (D_r = 60%) and dense soil (D_r = 80%) had exhibited a clear shear failure while the loose specimens (D_r = 30%) had undergone bulging failure. Detailed discussions of these test data, with specific reference to strength and deformation characteristics, have already been presented in Chapter 4 under section 4.2. The same is being referred herein in order to bringing out the performance improvement due to the fiber reinforcement.

TH-1123_10610407

5.3 FIBER REINFORCED SOIL

Twelve series (C_1-C_{12}, Table 3.3) of triaxial compression tests were carried out to investigate the influence of various soil and reinforcement parameters on the strength and deformation behavior of fiber reinforced soils. In each series, for a specific length of fiber and density of soil, the content of fiber was varied in five different percentages (i.e. f_c = 1, 2, 3, 4, 5%). Across the test series the length of fiber was varied from 10 mm to 80 mm while the density of soil was varied from lose to dense (i.e. D_r = 30-80%). The obtained test results are analysed herein.

Figure 5.1 depicts stress-strain responses of fiber reinforced soil for a typical case with soil relative density of 80%, fiber length of 40 mm and fiber content of 4%, tested at varied confining pressures i.e. 49, 98, 196, 392 kPa. The corresponding responses with unreinforced soil are presented in Fig. 5.2. It could be observed that with fiber reinforcement the stress-strain responses have exhibited a prominent peak with large strength improvement. But, the increase in failure strain due to fiber reinforcement is not very significant indicating that the ductility of the soil hasn't improved much. Besides the responses in the post yield stage have exhibited strain softening behavior. These observations are in contrary to the findings with the geocell reinforcement wherein the failure strain and thereby the ductility of the soil had improved visibly. Besides, the geocell-soil composite had exhibited strain hardening behavior (Section 4.3). This disparity is attributed to the difference in the reinforcing mechanism of these two forms of reinforcement. The geocell reinforcement owing to its cellular structure contains and confines the soil more effectively and thereby inhibits the formation of shear planes in the soil mass until large deformations. While, with fibers the reinforcing action is primarily through local stitching of the potential

TH-1123_10610407

slip planes by mobilization of friction and interlocking resistance over its surface. At one stage the fiber overcomes this limited resistance and thereby suffers pullout failure else undergoes breakage leading to rupture in the specimen (Fig. 5.3). Similar behavior is noticed in most other cases of fiber reinforced soils as well. At this stage the reinforcing action being lost the soil-fiber composite behaves similar to that of the soil. This aspect has been discussed in more detail in the subsequent sections.

In general, with fiber reinforcement, the load carrying capacity of the soil is found to have improved significantly. Fig. 5.4 depicts the typical failure strength envelopes for both fiber reinforced and the corresponding unreinforced soil. It could be observed that similar to geocell reinforcement the fiber reinforcement too has induced significant apparent cohesion (c_f) onto the granular soil. However, the friction angle, as compared to the unreinforced case ($\Phi = 40°$), has reduced little with the fibers ($\Phi = 37°$). This is attributed to the breakage of the fibers at higher confinement stress. Indeed the strength envelop has exhibited reduced shear strength (q) at increased confinement pressure (p) leading to reduced slope as compared to the unreinforced case. The apparent cohesion in this case is found to be 134 kPa that is equivalent to an increase in the bearing capacity in the order of 7554 kPa (i.e. $c_f N_c = 134 \times 55.63$). It is of interest to note that even the post failure residual strength of the fiber reinforced soil is much higher than that of the unreinforced soil. For example with a confining pressure of 392 kPa the residual strength of unreinforced soil is about 1200 kPa (Fig.5.2) while with fiber reinforcement its of the order of 1500 kPa (Fig. 5.1). Hence it can be said that, through introduction of fiber reinforcement, chances of catastrophic failure of soils can significantly be reduced. After test soil-fiber mixture was carefully observed for different conditions and failure due to breakage of pullout was clearly observed by comparing the size of the fibers after test and before test. The

TH-1123_10610407

amount of the fiber undergoes breakage depends upon the different conditions like fiber content, length of fiber, relative density of soil and confining pressure. SEM images of fibers after test are presented in Fig. 5.5. Fig. 5.5 (a) shows the breaking of the fiber and 5.5 (b) shows the surface rupture of fibers. The influence of different parameters, such as content of fiber, length of fiber, density of soil and confining pressure; on the overall behavior of the fiber reinforced soils are brought out in the following sections.

TH-1123_10610407

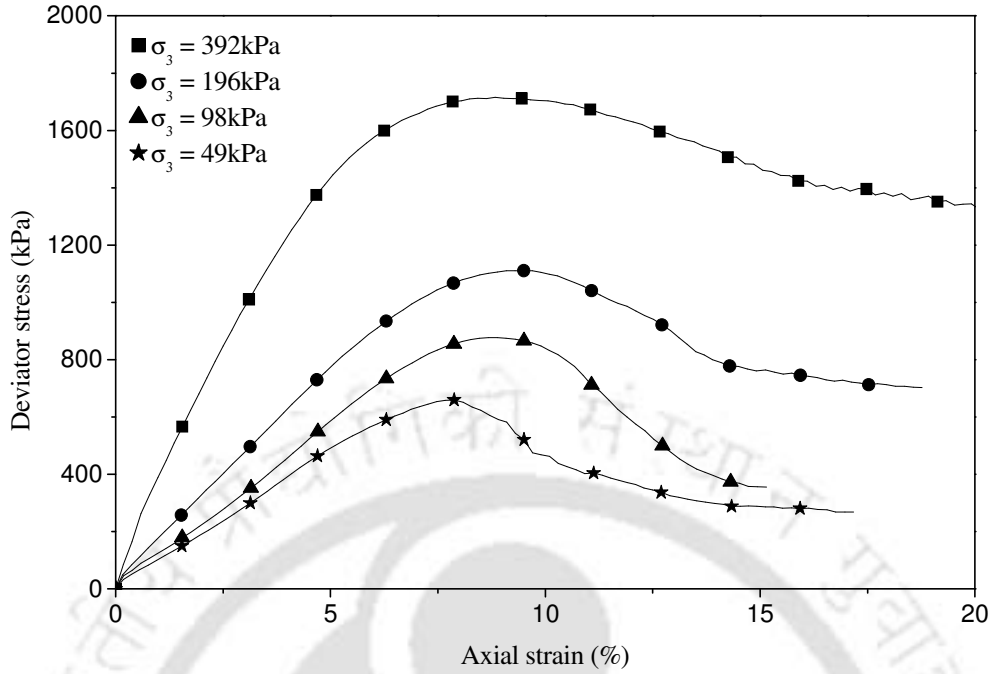

Fig. 5.1 Stress-strain behavior of fiber reinforced soil (D_r = 80%, L = 40mm, f_c = 4%)

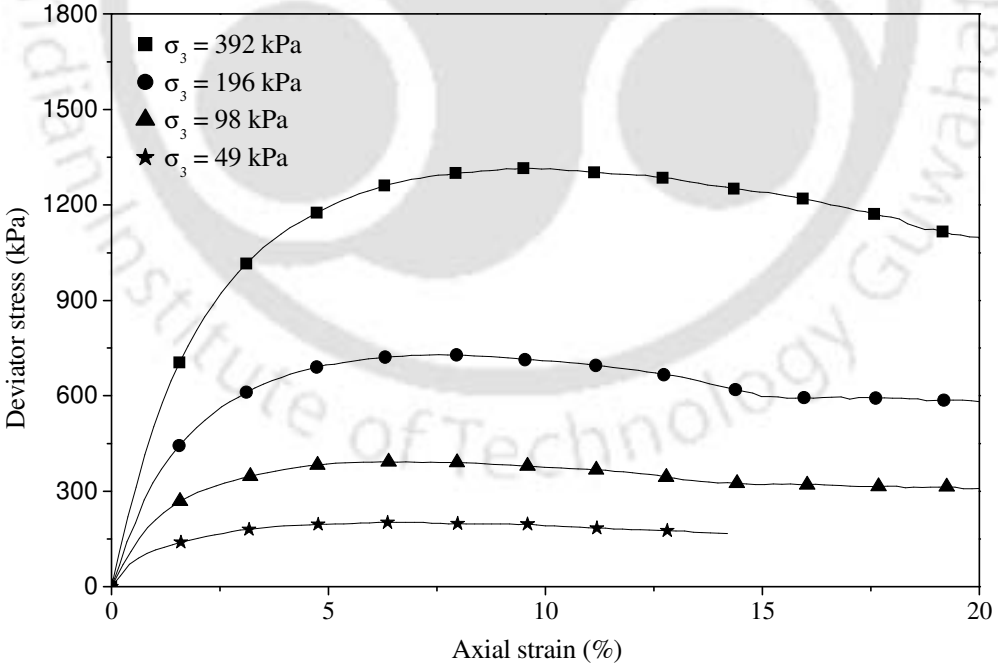

Fig. 5.2 Stress-strain behavior of unreinforced soil (D_r = 80%)

TH-1123_10610407

Fig. 5.3 Typical failure mode of fiber reinforced soil (D_r = 80%, L = 40mm, f_c = 4%, σ_3 = 196 kPa)

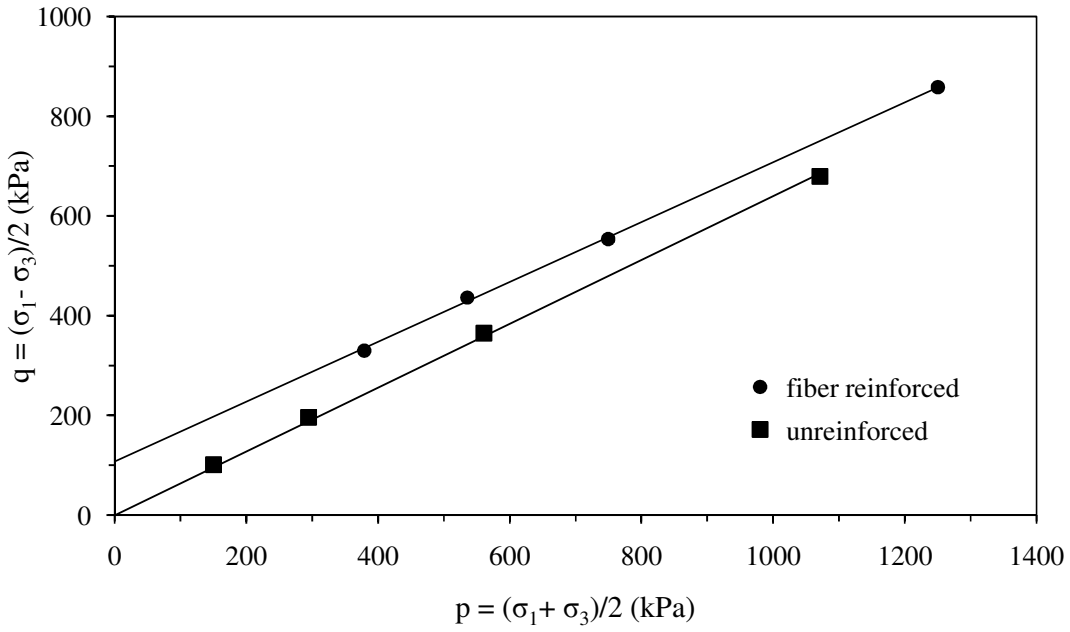

Fig. 5.4 Typical failure strength envelopes of unreinforced and fiber reinforced soils (D_r = 80%, L = 40mm, f_c = 4%)

TH-1123_10610407

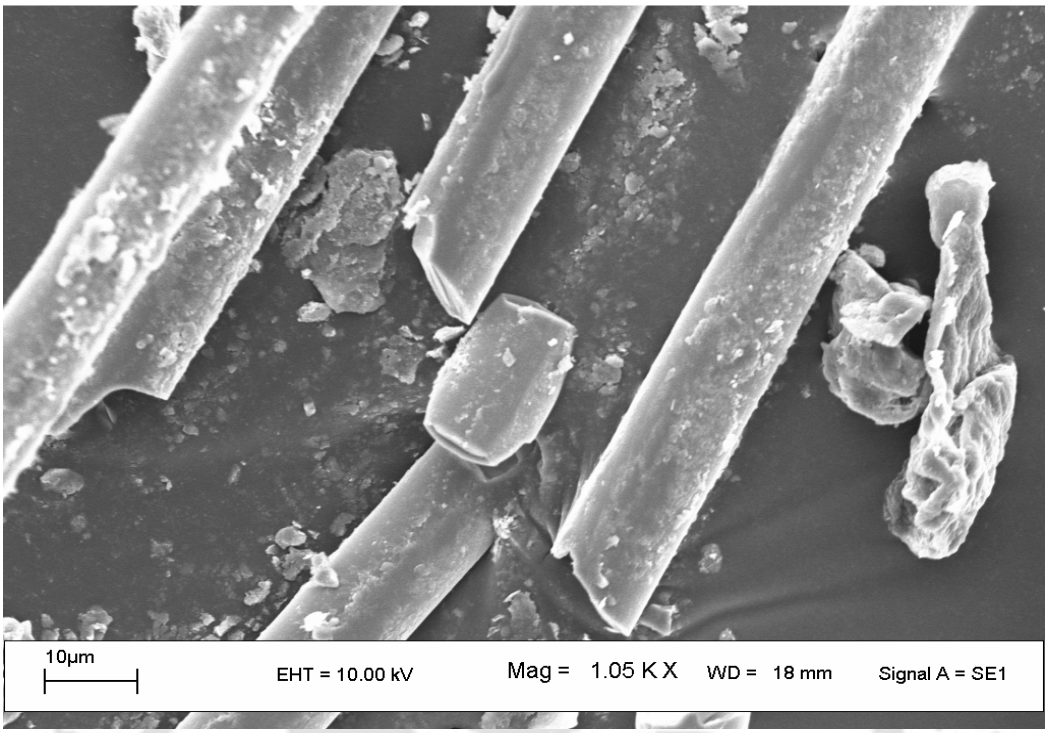

(a)

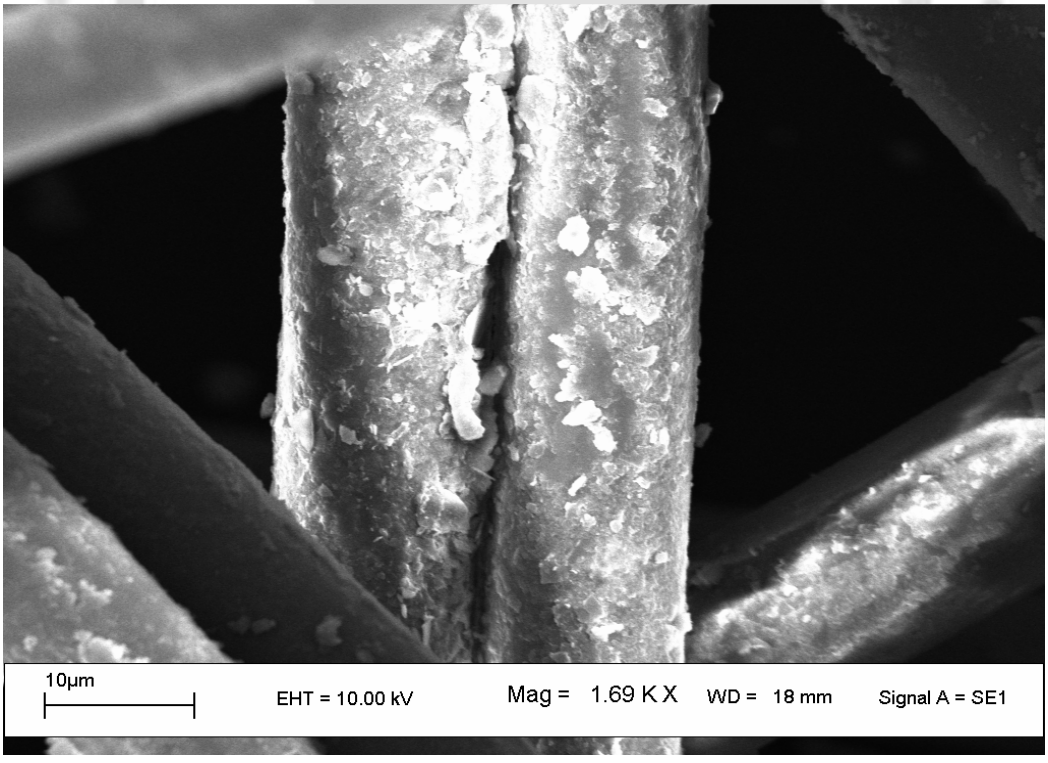

(b)

Fig. 5.5 SEM images of fibers after test

TH-1123_10610407

5.3.1 Influence of content of fiber

As is mentioned earlier, the influence of content of fiber on the performance of granular soils was evaluated by conducting tests at varied rate of fiber dosage, while all other significant tests parameters were kept constant. Typical stress strain responses for three different fiber contents i.e. low (1%), medium (3%) and high (5%), are depicted in Figs.5.6, 5.7 and 5.8 respectively. It may be observed that irrespective of the confining pressure applied the constitutive (i.e. stress-strain) behavior of the reinforced soils, both at low and high content of fiber, is almost the same. However the peaks in the responses are more prominent when the fiber content is high.

Comparison of stress-strain responses depicting the influence of content of fiber, for two typical cases i.e. short (L = 20 mm) and long (L = 40 mm) fibers, are shown in Figs. 5.9 and 5.10 respectively. It could be observed that in both the cases the load carrying capacity has continued to increase with increase in fiber content. Even after failure there is substantial amount of strength retained in the specimen and it is higher than that with soil alone indicating that with fiber reinforcement the residual soil too can be increased. However the post failure strength loss is relatively higher with very high content of fiber (i.e. 4-5%). This is because with higher content of fibers there is relatively less soil to soil interaction and fiber to fiber interaction is likely to be more. As long as the fiber is able to stand against the surcharge loading the performance improvement continues to increase. At the critical stage when the fiber suffers failure, either through pull out or breakage, the performance improvement is primarily through interface frictional interaction. With higher content of fiber the chances of fibers coming in contact with themselves is more that the soil-fiber interaction is less. As the fiber-fiber friction is less compared to that of soil-fiber friction the overall

TH-1123_10610407

residual strength of the specimen has shown a reduction with increased content of fiber.

It can further be noted that the apparent cohesion (c_f) increases with increase in the quantity of fibers until a certain percentage, beyond which further improvement is practically negligible. This indicates that there is a fiber content at which the performance improvement is the maximum. It may be noted that the strain required to mobilize the peak strength is relatively higher with higher content of fiber (i.e. 4-5%). This is possibly due to the manifestation of a sponge like effect, at higher dosage of fiber, that tends to require relatively larger deformation in order to mobilise the reinforcing action and thereby the load carrying capacity. Similar behavior of fiber reinforced soil has been reported by Webster and Santoni (1997).

Typical failure modes in fiber reinforced soil specimens with varied content of fiber are shown in Fig. 5.11. It could be seen that both at low and higher fiber content the specimen has undergone shear failure with development of a clear rupture plane. Hence it can be said that the fiber reinforced soil during failure tends to behave similar to that of the unreinforced soil. This is because the randomly distributed fibers locally stitch up the potential rupture planes in the soil mass that the fiber soil composite exhibits improved performance. However, the reinforcing action of the fiber is through mobilization of friction at the fiber soil interface that when is exceeded up, due to increased surcharge loading, the fiber gets pulled out leading to loss of reinforcing action. Similarly relatively long fibers although have large resistance against pullout but undergo breakage when the applied stress exceeds its tensile strength, leading to loss of reinforcing action. With reinforcing action gone,

TH-1123_10610407

the fiber-soil composite structure breaks that it ruptures in similar way as that of the unreinforced soil.

It can further be observed that while with unreinforced soil the failure plane runs right from top to bottom of the specimen (Fig. 4.5d) with fiber reinforcement the rupture is localized in the central region. This effect is more prominently observed with relatively higher content of fibers i.e. 4% and 5% (Fig.5.11c, d) wherein a column like structure, right under the loading, appears to be pushing into the rest of the soil mass. This indicates that with fiber reinforcement failure is contained in a relatively smaller region.

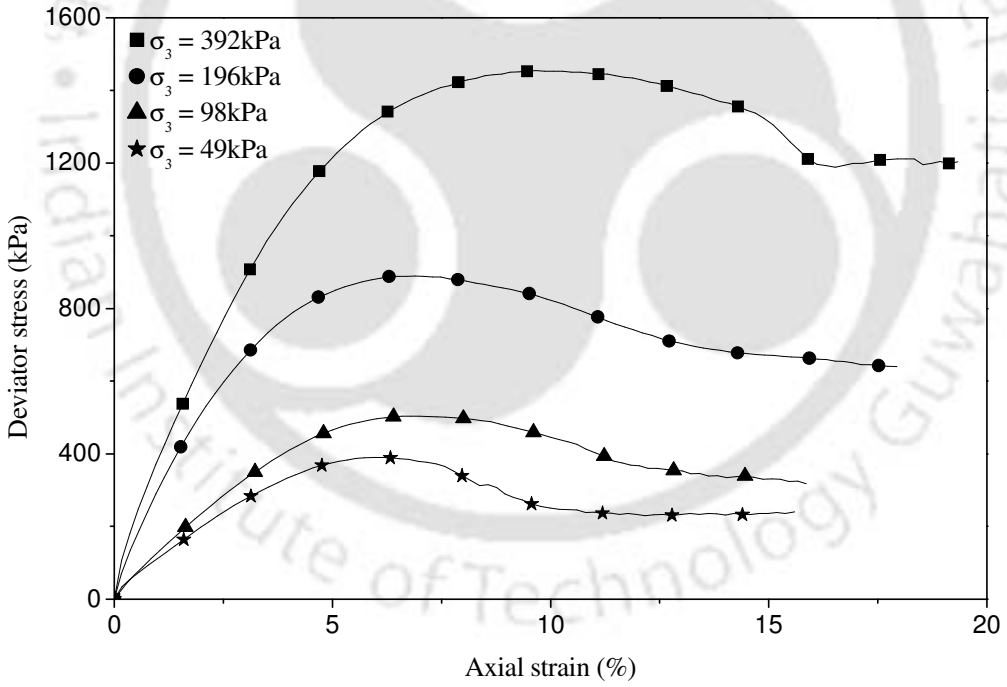

Fig. 5.6 Stress-strain behavior of fiber reinforced soil (D_r = 80%, L = 40mm, f_c =1%)

TH-1123_10610407

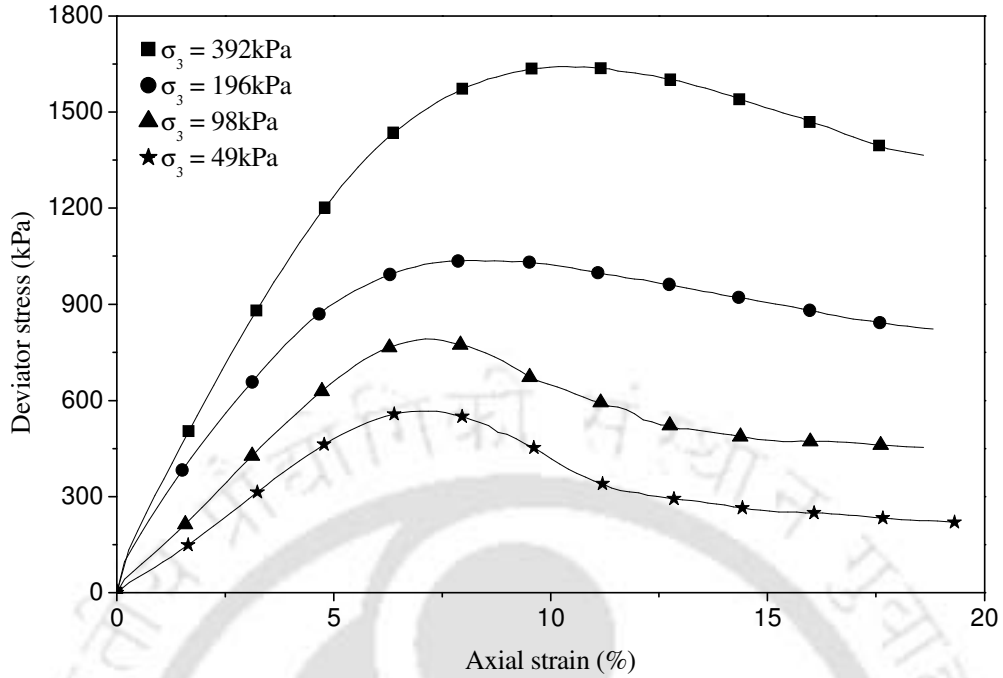

Fig. 5.7 Stress-strain behavior of fiber reinforced soil (D_r= 80%, L = 40mm, f_c= 3%)

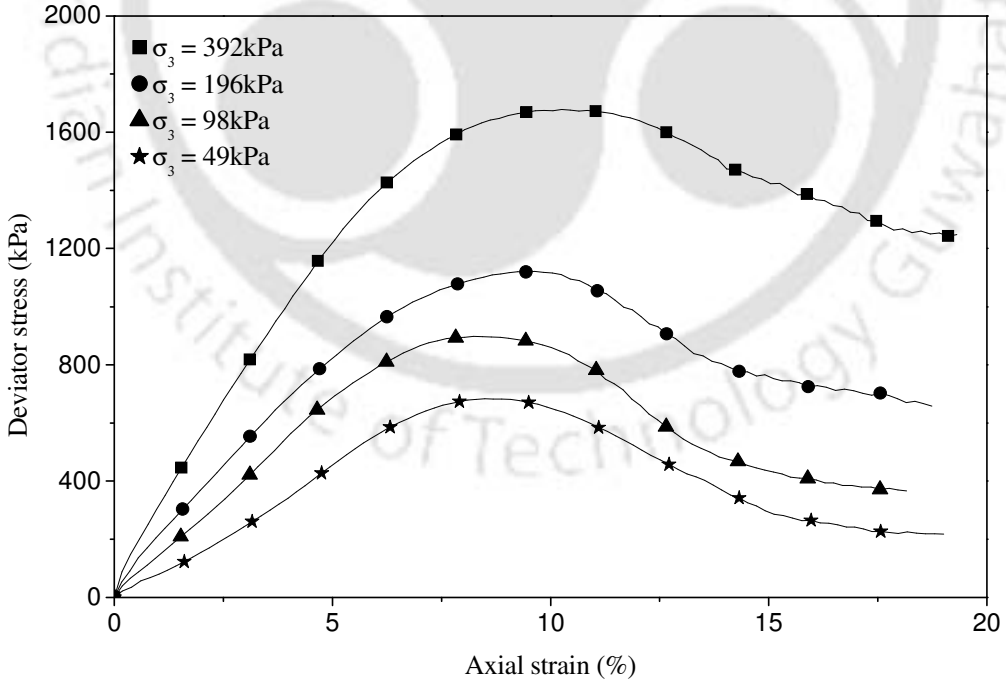

Fig. 5.8 Stress-strain behavior of fiber reinforced soil (D_r = 80%, L = 40mm, f_c = 5%)

TH-1123_10610407

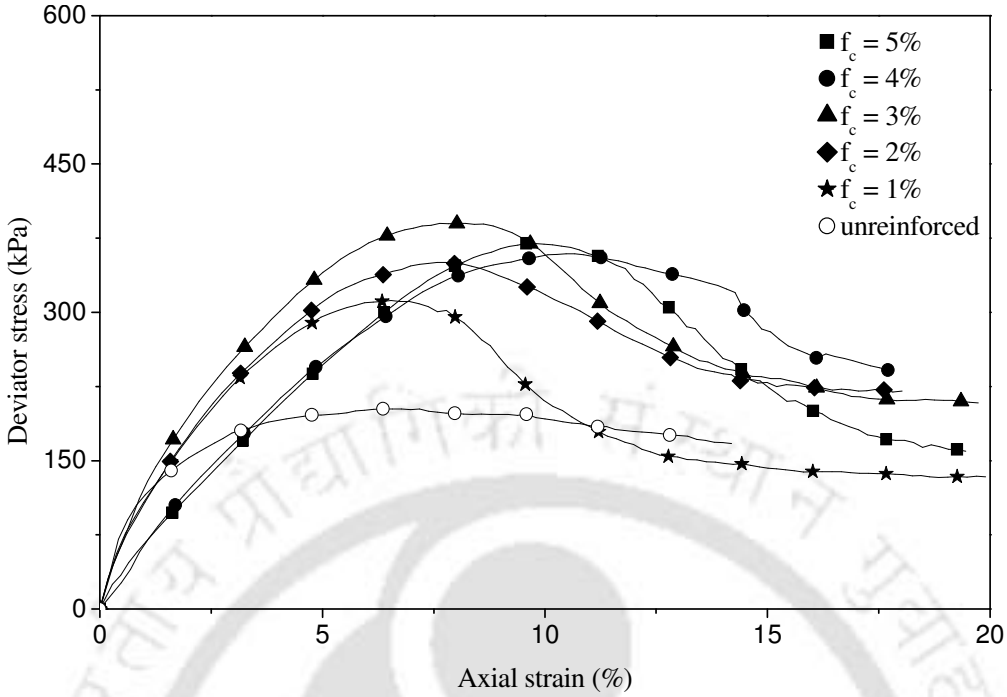

Fig. 5.9 Stress-strain behavior of fiber reinforced soil (D_r = 80%, L = 20mm, σ_3 = 49kPa): Influence of fiber content

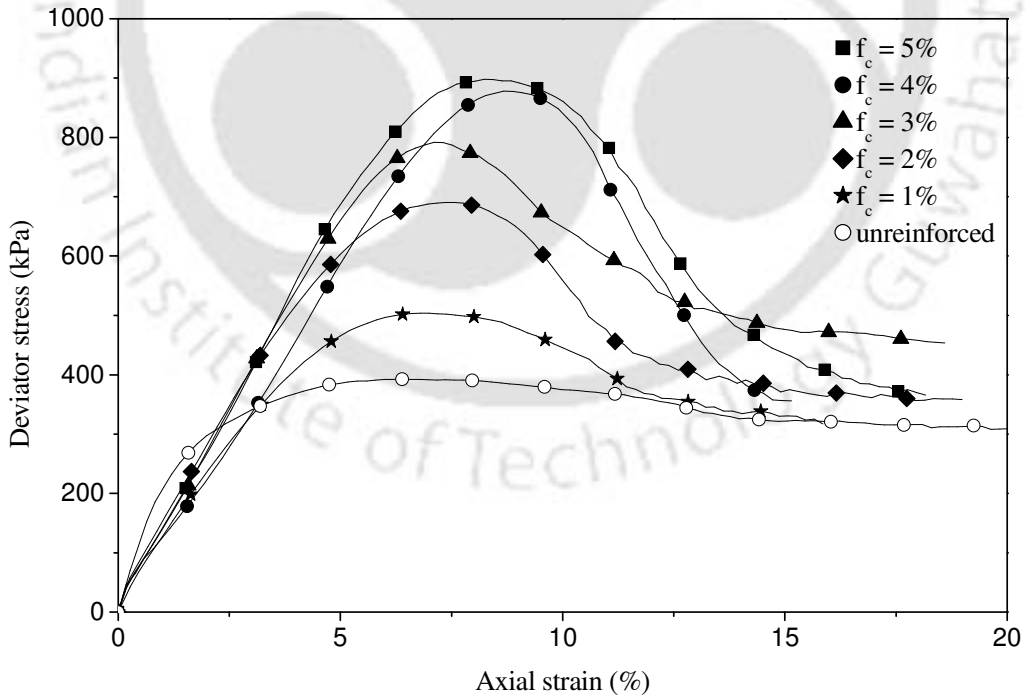

Fig. 5.10 Stress-strain behavior of fiber reinforced soil (D_r = 80%, L = 40mm, σ_3 = 98kPa): Influence of fiber content

TH-1123_10610407

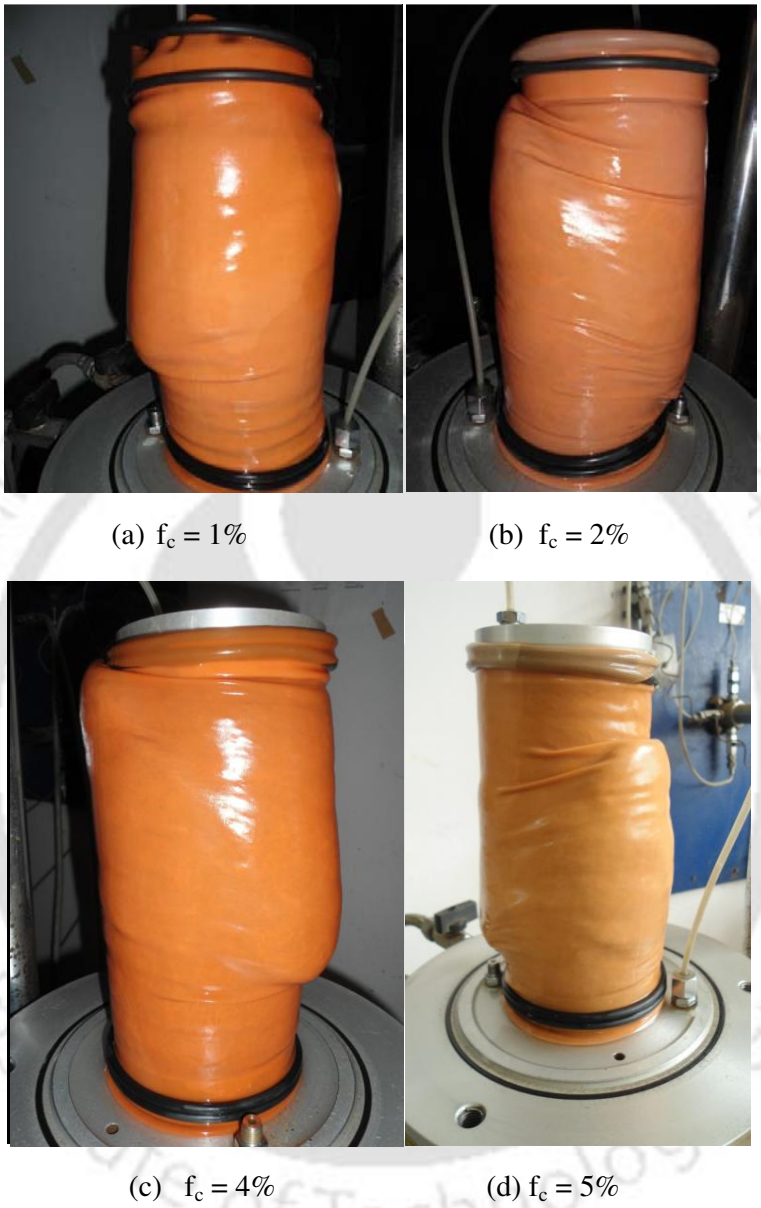

(a) f_c = 1% (b) f_c = 2%

(c) f_c = 4% (d) f_c = 5%

Fig. 5.11 Failure mode of fiber reinforced soil (D_r = 80%, L = 40 mm, σ_3 = 98 kPa): Influence of fiber content

TH-1123_10610407

Typical strength envelopes depicting the influence of fiber content on dense soil matrix (i.e. relative density of 80%) for fiber lengths of 10 mm, 20 mm, 40 mm and 80 mm are depicted in Figs. 5.12, 5.13, 5.14 and 5.15 respectively. It could be observed that in general with increased fiber content the strength envelopes have shown increased intercept while their slope hasn't altered much. This indicates that the improvement in performance of soil due to fiber reinforcement is mostly through inducement of apparent cohesion while the friction contribution doesn't change much. Nearly similar trend was observed in case of medium dense and loose soils (i.e. relative density of 60 % and 30%) as well.

A summary of the shear parameters i.e. cohesion and friction, for different cases, with varied fiber content, are presented in Table 5.1. A comparison shows that, in all the cases, the induced cohesion in the granular soil has increased with increase in the fiber content. This indicates that irrespective of the fiber length and soil density, the fiber content has a prominent role in improving the soil performance. However, beyond a certain limit further increase in fiber content doesn't produce much of improvement and in some cases even leads to strength loss. The optimum fiber content giving maximum apparent cohesion is about 2-3% when the fiber length is short i.e. 10 mm, 20 mm. But with long fibers i.e. 40 mm and 80 mm the optimum fiber content is relatively high i.e. of the order of 4-5%. With the reinforced soil specimen subjected to loading and thereby getting strained, the frictional resistance at sand-fiber interface gets mobilized resulting in development of tensile stress in fibers that produces an internal confinement in the soil mass leading to the inducement of apparent cohesion. The short fibers, due to inadequate bond capacity, suffer a premature failure through pullout. As the frictional resistance at the fiber-soil interface is considerably lower than that of the soil, a fiber that is pulled out will cause

TH-1123_10610407

a local reduction in strength. With increased fiber content the percentage of these failed fibers increases leading to an overall strength reduction. However, relatively long fibers (40 mm and 80 mm) due to increased anchorage resistance, mobilized through interface friction and bond, over their long length, do effectively stand against pullout failure. In the absence of redundant fibers (i.e. pulled out) the performance improvement has increased considerably until large fiber content. However fiber content reaching about 4-5% even the long fibers do not so much of additional improvement with increased fiber content. This may be because at this stage there has taken place saturation that the fiber quantity has almost reached the reinforcing requirement of the soil that any addition of fiber beyond this point doesn't give rise to any tangible increase in performance improvement.

Overall the induced cohesion with short fibers is much less as compared to that with the long fibers. For example with fibers of 10 mm length the maximum cohesion (c_g) is just about 27 kPa while with 80 mm long fiber it is as high as 171 kPa (Table 5.1). Another behavior worth noting is that when fiber length is short the increase in cohesion intercept with increased fiber content is not very prominent (Fig. 5.12). The same is also observed in terms of the induced cohesion values depicted in Table 5.1. This is attributed to the premature pullout of the short fibers due to inadequate frictional resistance that any amount of increase in fiber content does not lead to much of benefit. But with increase in length of fibers the cohesion intercept as well as the apparent cohesion values have shown increasing higher values with increased fiber content. As the long fibers mobilise increasingly higher tension through increased frictional resistance when increased in quantity lead to increasingly higher performance improvement.

TH-1123_10610407

It can further be observed that there happens to be a reduction in the friction angle of the fiber-soil composite with increased fiber content. This is possibly due to reduced soil to soil contact because of increased fiber content. This trend is more prominently observed when the soil is dense (D_r = 80%) and the fibers are long (L = 80mm). When the soil is dense it has fewer voids to accommodate the large volume of fibers within that the fibers visibly obstruct the soil to soil contact leading to reduced friction angle. Similarly long fibers are likely to have relatively higher folding and bending that hinders soil to soil contact giving rise to reduced frictional interaction. With reduced density of soil the inter-particle voids are increased that accommodates the fibers within, that the fiber induced obstruction to soils is much less and so is the reduction in friction angle. Indeed for loose soil i.e. 30% relative density, the reduction in friction angle with increased fiber content is almost negligible (Table 5.1).

The other possible reason for such a behavior could be due to breakage of fibers. In dense soil with long fibers there is likely to be high interface frictional resistance at high confinement pressures that in this situation the mode of fibers is mostly due to breakage. This is because the shear resistance of the soil-fiber composite is dependent on the tensile stress developed in the fibers. When the fiber suffers breakage there is loss of shear resistance in spite of the ambient confining pressure remaining unchanged. As result of which 'friction angle' that indicates the proportional variation of shear stress with normal stress, is reduced.

TH-1123_10610407

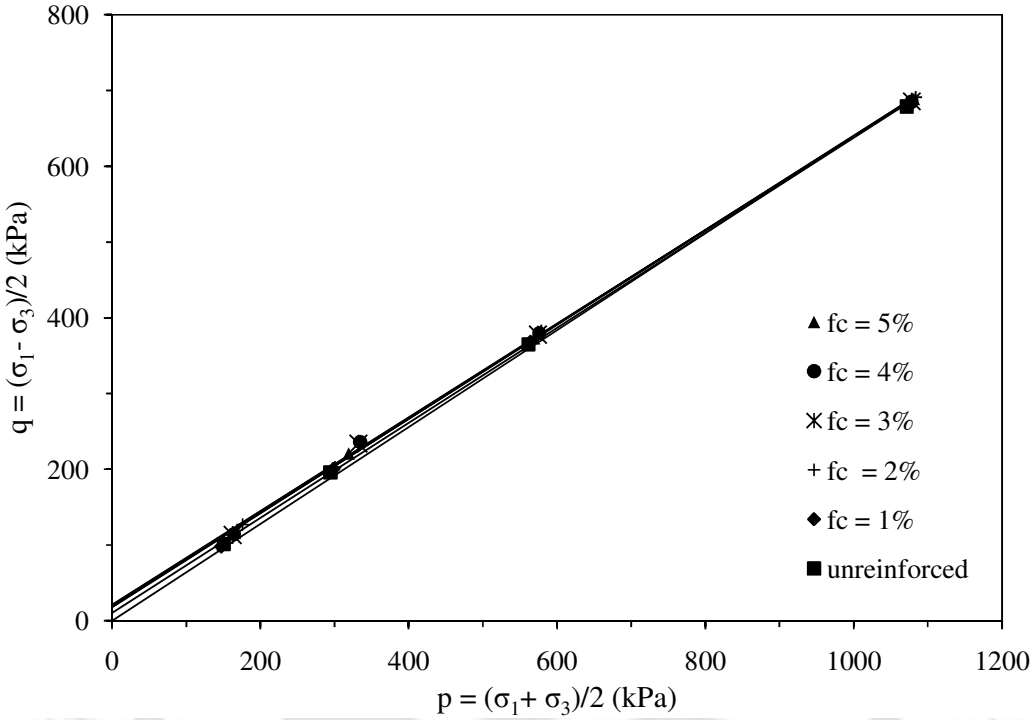

Fig. 5.12 Failure strength envelopes of fiber reinforced soil (D_r = 80% L = 10mm): Influence of fiber content

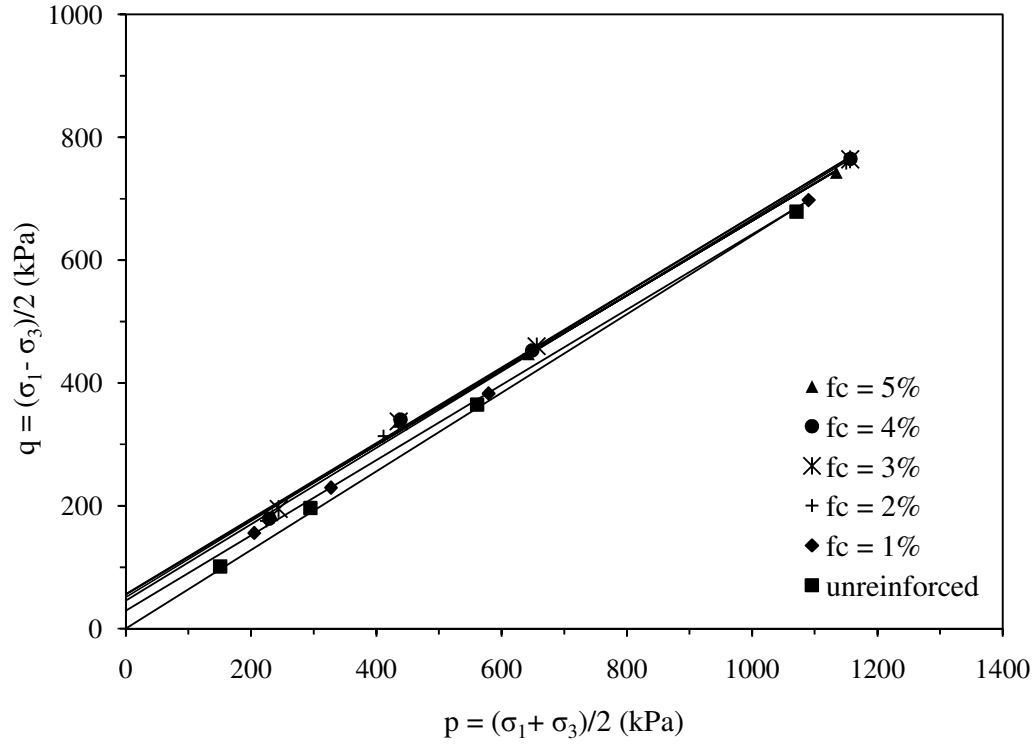

Fig. 5.13 Failure strength envelopes of fiber reinforced soil (D_r = 80%, L = 20mm): Influence of fiber content

TH-1123_10610407

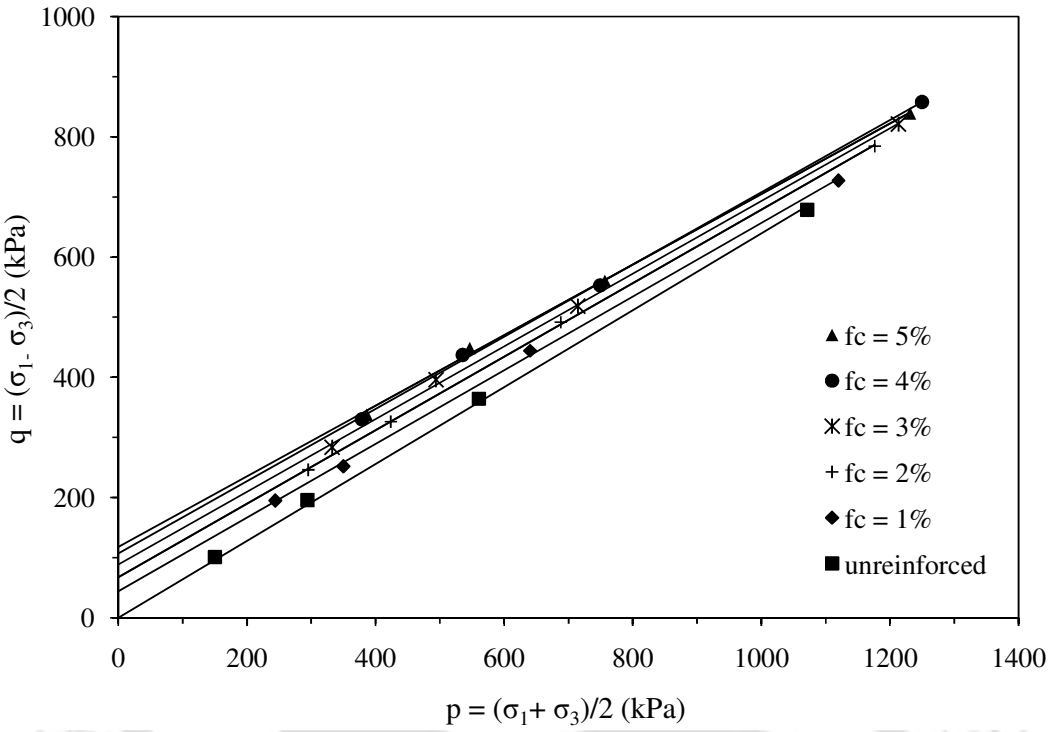

Fig. 5.14 Failure strength envelopes of fiber reinforced soil (D_r = 80%, L = 40mm): Influence of fiber content

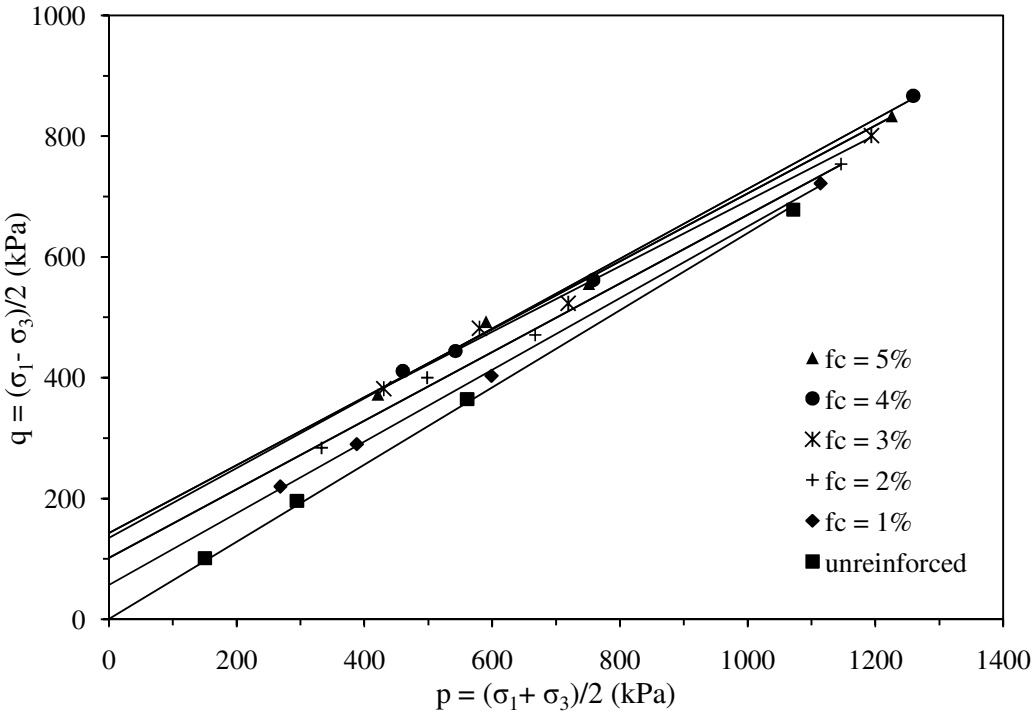

Fig. 5.15 Failure strength envelopes of fiber reinforced soil (D_r = 80% L = 80mm): Influence of fiber content

TH-1123_10610407

Table 5.1 Summary of shear strength parameters of fiber reinforced soil obtained from triaxial compression tests: Influence of content of fiber

Soil density D_r (%)	Fiber length L (mm)	Fiber content f_c (%)	Friction angle Φ (°)	Cohesion c_f (kPa)
80	10	1	39	13
		2	39	23
		3	38	25
		4	38	27
		5	38	23
	20	1	38	37
		2	38	59
		3	38	71
		4	38	65
		5	37	70
	40	1	38	57
		2	38	86
		3	37	110
		4	37	134
		5	36	145
	80	1	36	69
		2	35	122
		3	35	153
		4	35	164
		5	34	171
60	10	1	37	14
		2	37	15
		3	37	13
		4	37	10
		5	37	11
	20	1	37	24
		2	37	40
		3	37	50
		4	36	58
		5	36	50
	40	1	37	32
		2	37	55
		3	36	94
		4	36	85
		5	36	88
	80	1	36	37
		2	35	75
		3	34	115
		4	34	118
		5	34	120

TH-1123_10610407

Table 5.1 (**contd.**) Summary of shear strength parameters of fiber reinforced soil obtained from triaxial compression tests: Influence of content of fiber

Soil density D_r (%)	Fiber length L (mm)	Fiber content f_c (%)	Friction angle Φ (°)	Cohesion c_f (kPa)
30	10	1	35	5
		2	35	8
		3	35	6
		4	35	2
		5	35	4
	20	1	35	12
		2	35	22
		3	35	40
		4	35	41
		5	35	37
	40	1	35	27
		2	34	48
		3	34	73
		4	34	65
		5	34	70
	80	1	34	36
		2	34	63
		3	33	92
		4	33	96
		5	34	83

5.3.2 Influence of length of fiber

Typical stress-strain responses of reinforced soils with short fibers (i.e. length of 10 mm) and long fibers i.e. length of 80 mm are presented in Fig. 5.16 and Fig.5.17 respectively. In both the cases the relative density of soil was kept at 80% while fiber content was kept at 5%. It could be observed that the stress-strain responses with short fibers after about 10% stain have shown a nearly asymptotic behavior. But with long fibers there has developed prominent peak followed by a distinct stress drop. The short fibers locally stitch up the slip planes leading to increased load carrying capacity of the soil mass. However due to inadequate bonding capacity owing to short length

TH-1123_10610407

they get pulled out. With the fiber getting pulled the load carrying capacity doesn't increase further. This primarily happens in local pockets where the induced stress is relatively higher that it exceeds the bond capacity of the reinforcement. However the pulled fibers still poses some amount of resistance (i.e. residual). Besides in the adjacent regions the fibers are still intact that they share the unbalanced stress from the pulled out region that the specimen continues to sustain the imposed loading. However due to continuous pull out of the fibers the soil-fiber composite has undergone increased strain. Whereas the long fibers having large frictional resistance enables the soil mass to sustain a relatively large load but beyond certain stage undergoes breakage failure leading to the stress drop (Fig.5.17).

The above findings can further be explained through the observed failure patterns depicted in Fig. 5.18. With short fibers (i.e. L = 10 mm) the failure is in mixed mode that there is prominent budging with mild rupture. The budging establishes that the fibers are getting pulled out that the specimen has undergone large deformation. Absence of a clear shear plane indicates that rupture has been arrested. At large very large deformation with substantial amount of fiber tending to get pulled out there has taken place a mild rupture indicated through a small shearing. But with increased length the fiber exhibits increased resistance against pull out that it holds the soil mass against volume expansion. As a result the soil-fiber composite stands like a column sustaining the surcharge loading. But at some stage the fibers start breaking up, mostly on the critical plane where the induced shear stress exceeds its tensile strength. With the fibers breaking away there has developed local rupture in the specimen giving rise to the stress drop. It may be observed that the column like beahviour is more prominently observed in case of long fibers (40 mm, 80 mm; Fig.5.18 c,d), which establishes the increased reinforcing efficiency of the fibers, with increase in

TH-1123_10610407

their length. This aspect is more clearly brought out in the following analysis of test data.

Stress-strain responses depicting the influence of fiber length on the performance of soil, for three different fiber contents i.e. 1%, 3% and 5% are shown in Figs. 5.19, 5.20 and 5.21 respectively. For the sake of comparison the corresponding unreinforced test data are also presented therein. It can be seen that in all the cases there is visible increase in deviator stress with increase in fiber length. But the post failure residual strength retained by the specimen is relatively high with medium fiber content i.e. 3% while both with low and high fiber content (i.e. 1% and 5%) it is much less. This may be because with fewer fibers there is inadequate reinforcement that with the loss of this limited reinforcing action the specimen behaves similar to that of the soil that it doesn't exhibit enhanced residual strength. At high fiber content, in the post failure stage, when large percentage of fibers are broken the load carrying capacity is primarily dependent on inter particle frictional resistance. Due to high density of fibers there is less soil to soil interaction that the overall frictional resistance on the slip plane is relatively low leading to reduced residual strength.

Typical failure envelopes showing the influence of fiber length in dense soil matrix of (D_r = 80%), for three different fiber contents i.e. 1%, 3% and 5%; are shown in Figs.5.22, 5.23 and 5.24 respectively. It can be seen that the strength of the soil has continued to increase with increase in fiber length till about 40 mm beyond which further improvement is marginal. This is because the long fibers tend to break. This particularly happens when the fiber is subjected to increased normal stress (through increased confining pressure) that it mobilizes high frictional resistance against pull out and thereby effectively stands against the applied loading until the induced stress

TH-1123_10610407

exceeds its strength when it undergoes breakage. The breakage of the fibers, observed in the post test specimen, is also reflected through the reduced slope of the failure envelope, more prominently at relatively higher confinement pressure. As a result of which the additional frictional reentrance, owing to increased length of fiber, remains immobilized leading to marginal performance improvement. Similar behavior is also observed with medium dense soil (i.e. D_r = 60%, Fig. 5.25). But, in case of loose soil (D_r = 30%, Fig. 5.26) the failure stress envelopes do not exhibit any such reduction in its slope. This is because the fibers due to inadequate frictional resistance (owing to loose soil mass around) mostly get pulled out. A pulled out fiber, however, does not suffer complete loss of strength as in case of breakage. This is because even after pull out the fiber continues to mobilize certain amount of frictional resistance i.e. the residual strength. As a result the loss of strength is minimal that the strength envelope continues to maintain nearly constant slope even at very high confinement pressure. However, the performance improvement with fiber length increasing beyond 40 mm is relatively less. Hence it can be said that the critical length of the fibers that gives maximum performance improvement is about 40 mm.

Summary of shear parameters i.e. friction angle and cohesion of fiber reinforced soils, depicting the influence of fiber length, at varied relative density of soil and fiber content are presented in Table 5.2. It could be observed that irrespective of density of soil and fiber content the induced apparent cohesion due to fibers (i.e. c_f) continues to increase with increase in fiber length. However, in most of cases the increase in cohesion beyond fiber length of 40 mm is relatively less. Besides, the friction angle of the soil-fiber composite, almost in all the cases, has exhibited a clear reduction. In view of this, for varied applications in geotechnical engineering, fiber length of about 40 mm can be recommended as the best.

TH-1123_10610407

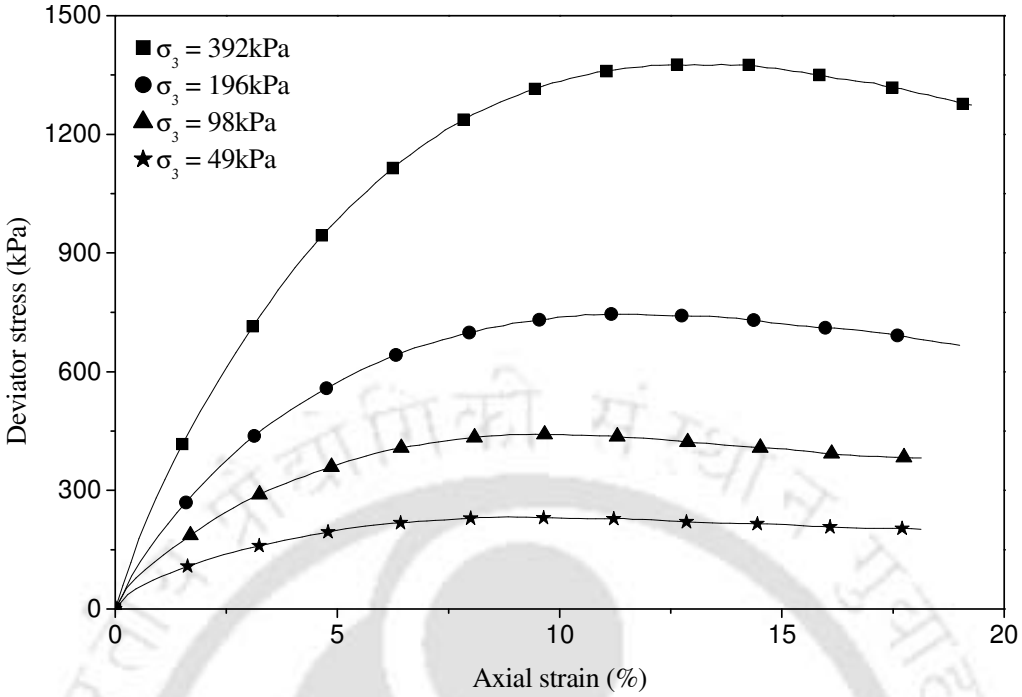

5.16 Stress-strain behavior of fiber reinforced soil (D_r = 80%, L = 10mm, f_c=5%)

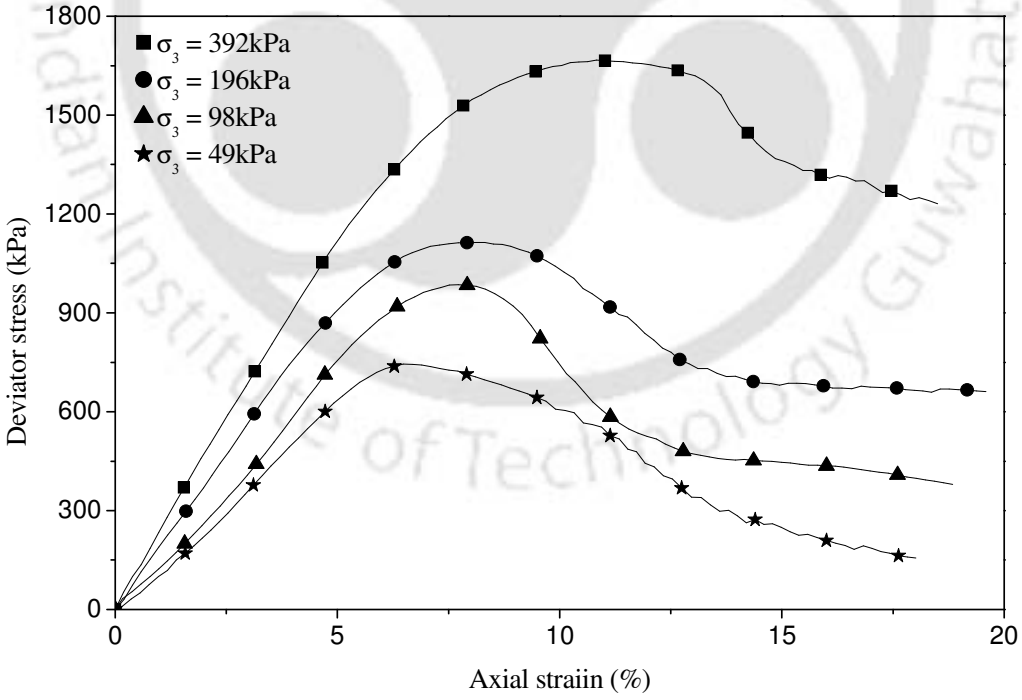

5.17 Stress-strain behavior of fiber reinforced soil (D_r = 80%, L = 80mm, f_c = 5%)

TH-1123_10610407

(a) L = 10 mm

(b) L = 20 mm

(c) L = 40 mm

(d) L = 80 mm

5.18 Failure mode of fiber reinforced soil (D_r = 80%, f_c = 5%, σ_3 = 196 kPa): Influence of fiber length

TH-1123_10610407

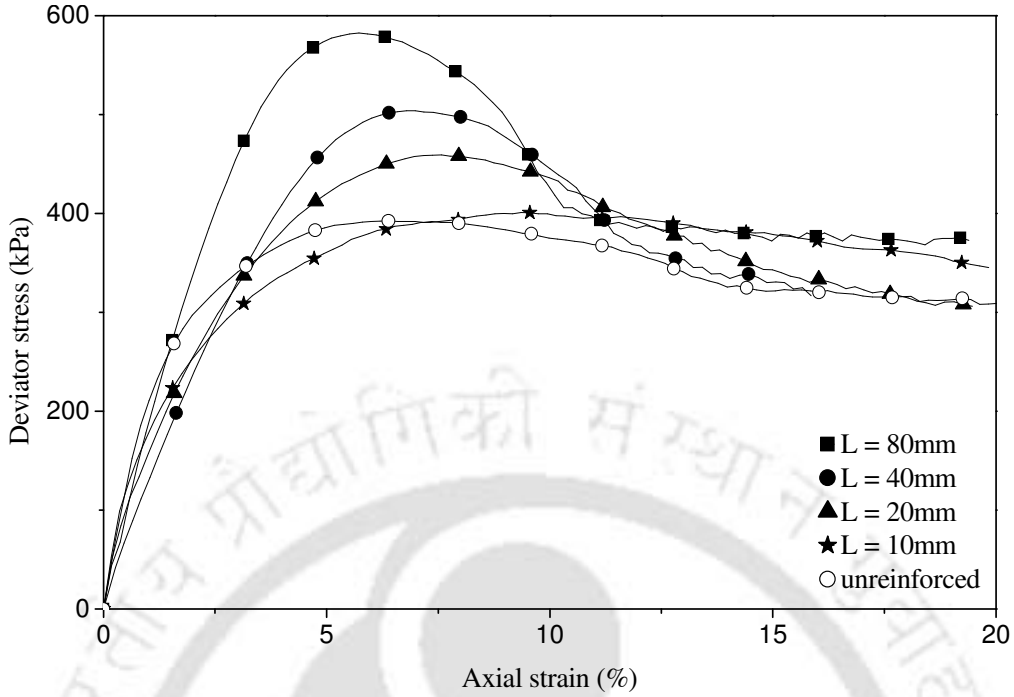

5.19 Stress-strain behavior of fiber reinforced soil (D_r = 80%, f_c = 1%, σ_3 = 98kPa): Influence of fiber length

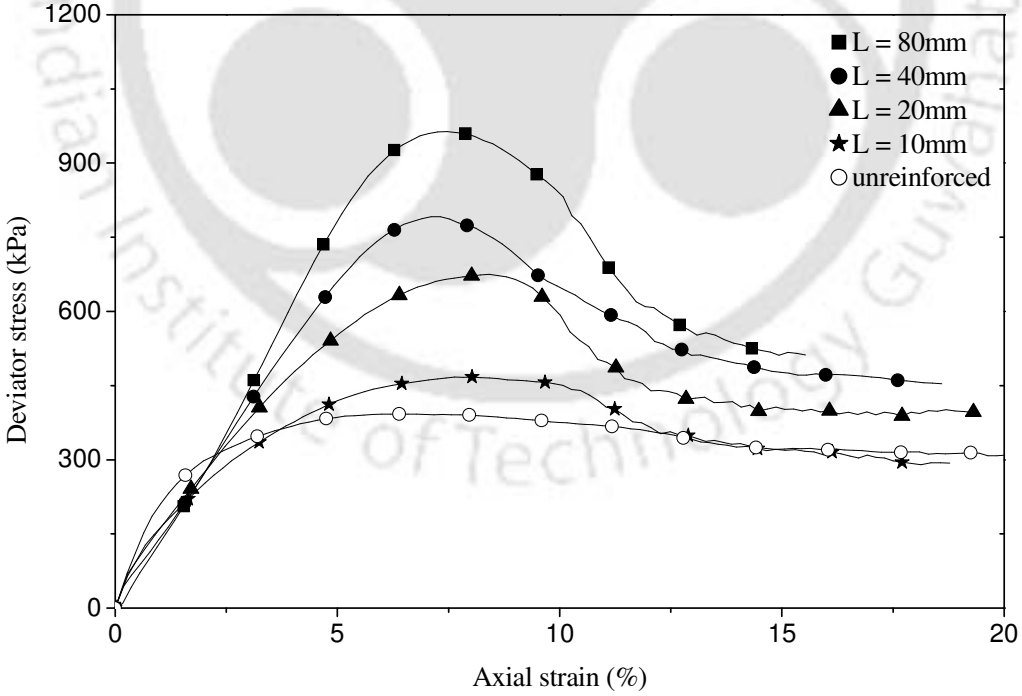

5.20 Stress-strain behavior of fiber reinforced soil (D_r = 80%, f_c = 3%, σ_3 = 98kPa): Influence of fiber length

TH-1123_10610407

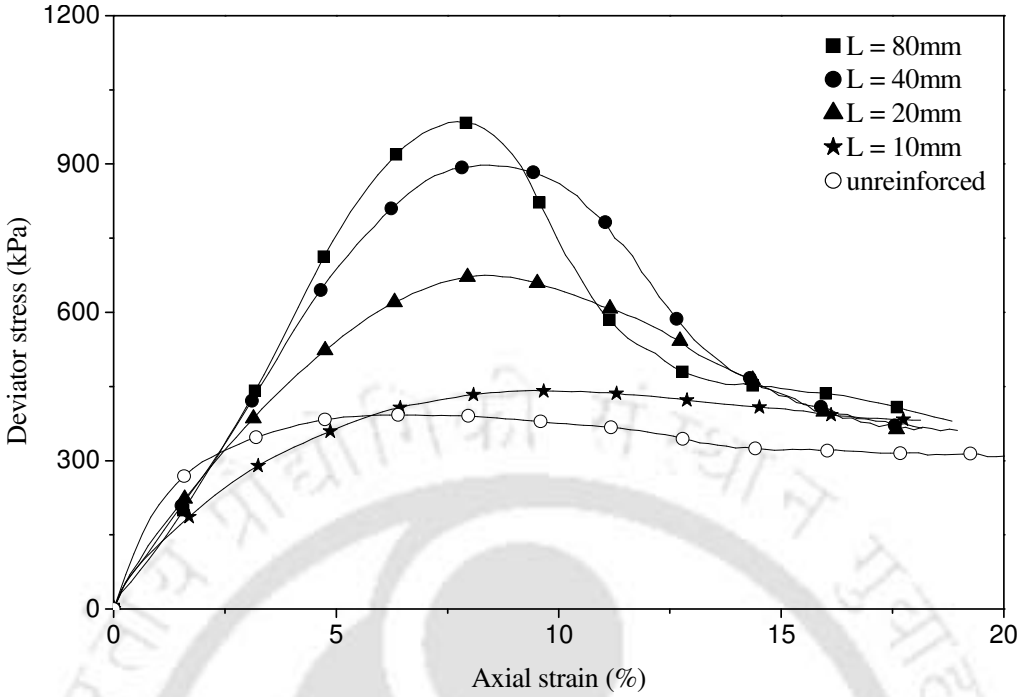

5.21 Stress-strain behavior of fiber reinforced soil (D_r = 80%, f_c = 5%, σ_3 = 98kPa): Influence of fiber length

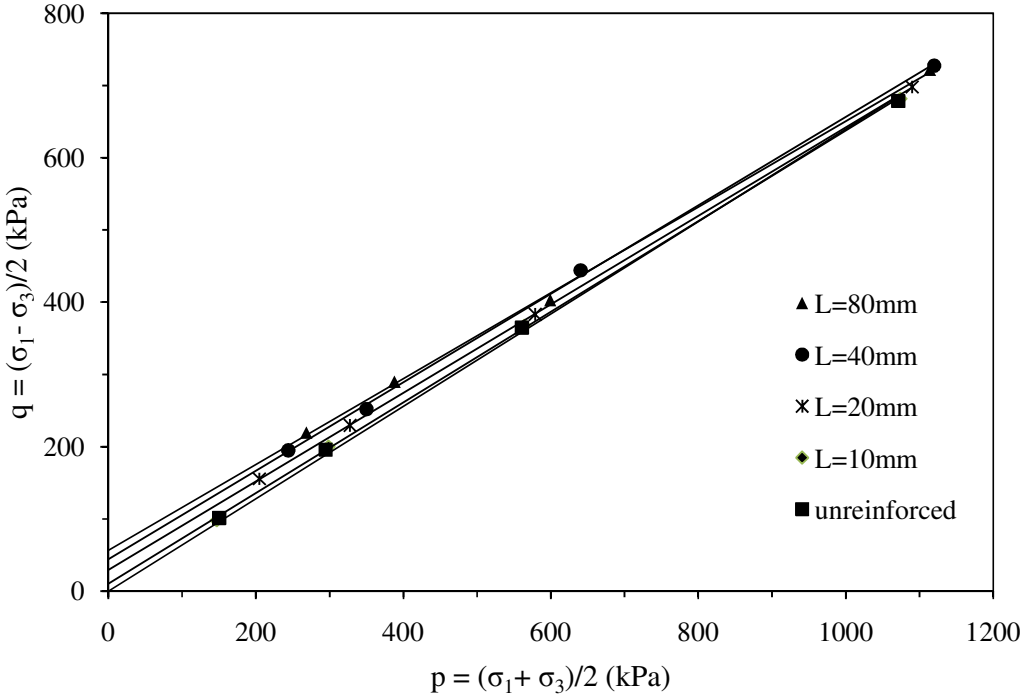

5.22 Failure strength envelopes of fiber reinforced soil (D_r = 80%, f_c = 1%): Influence of fiber length

TH-1123_10610407

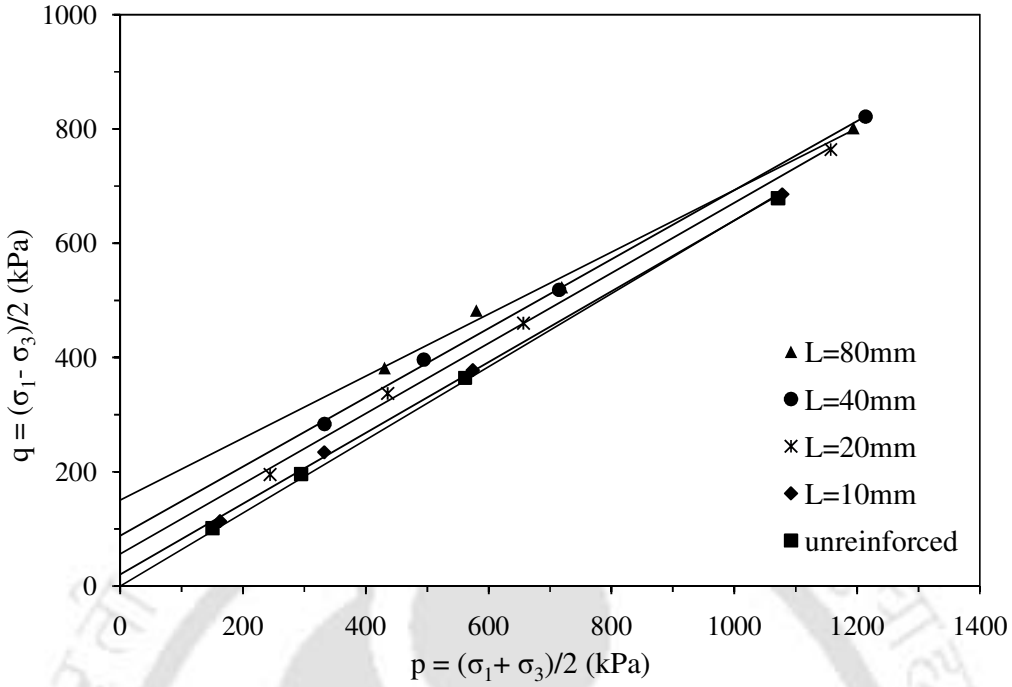

5.23 Failure strength envelopes of fiber reinforced soil (D_r = 80%, f_c = 3%): Influence of fiber length

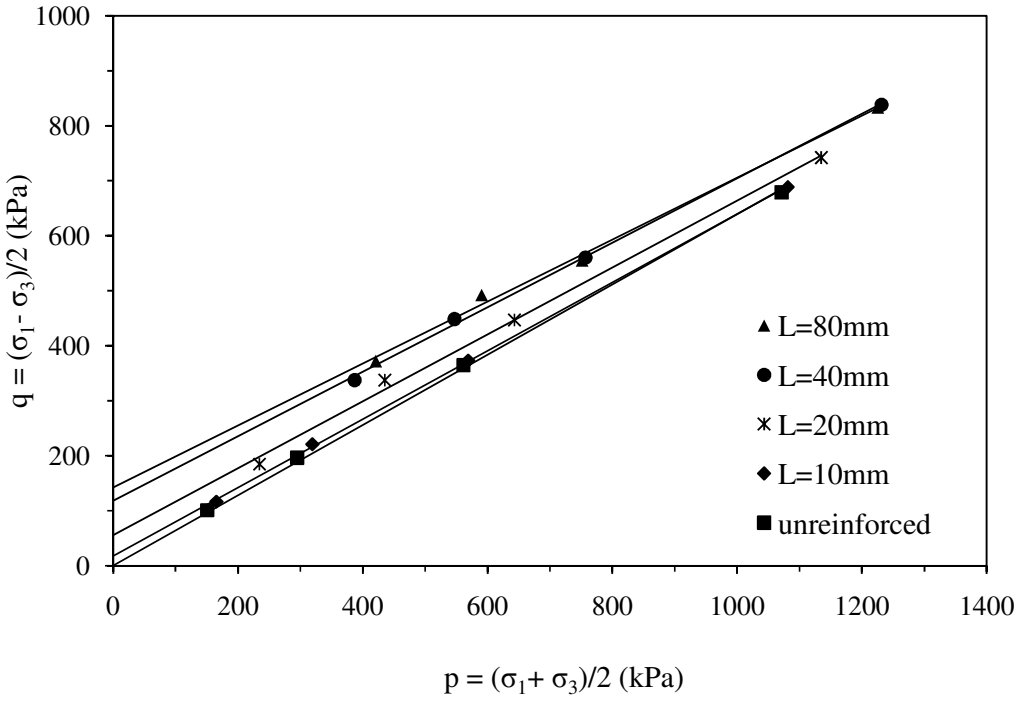

Fig. 5.24 Failure strength envelopes of fiber reinforced soil (Dr = 80%, f_c = 5%): Influence of fiber length

TH-1123_10610407

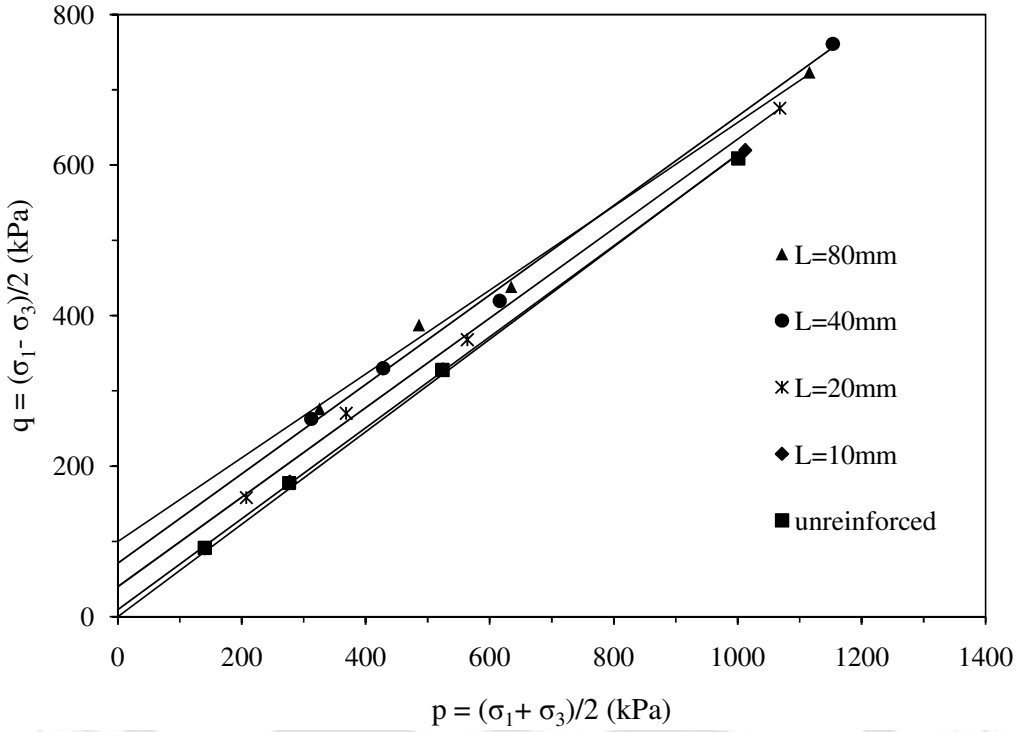

Fig. 5.25 Failure strength envelopes of fiber reinforced soil (Dr = 60%, f_c = 5%): Influence of fiber length

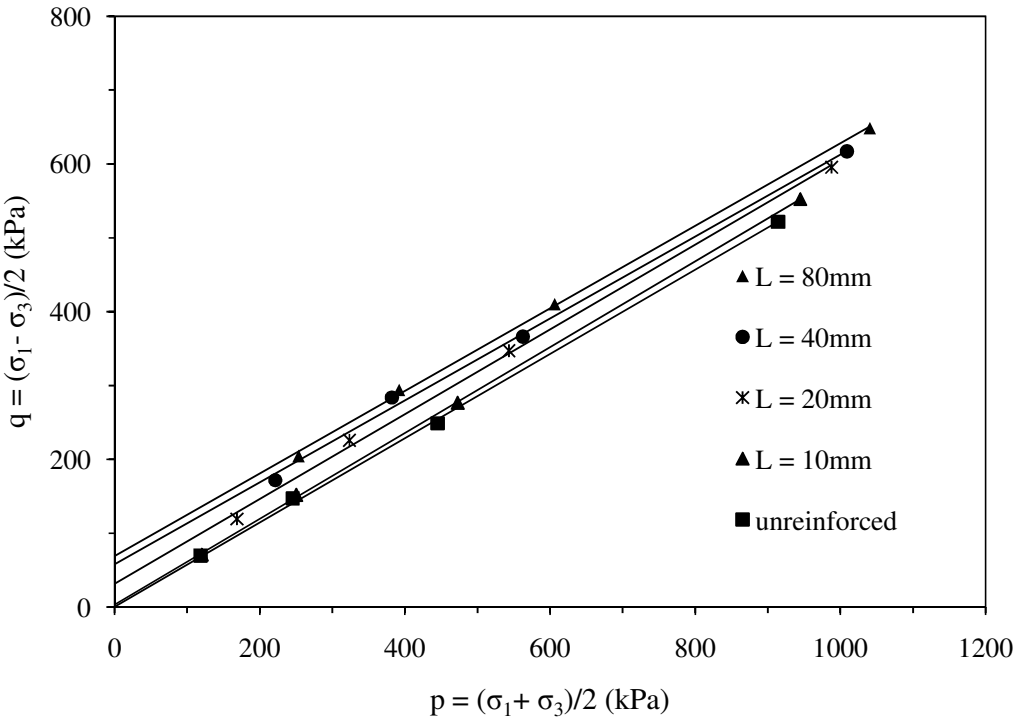

Fig. 5.26 Failure strength envelopes of fiber reinforced soil (D_r = 30%, f_c = 5%): Influence of fiber length

TH-1123_10610407

Table 5.2 Summary of shear strength parameters of fiber reinforced soil obtained from triaxial compression tests: Influence of length of fiber

Soil density D_r (%)	Fiber content f_c (%)	Fiber length L (mm)	Failure axial strain (%)	Friction angle Φ (°)	Cohesion c_f (kPa)
80	1	10	11	39	13
		20	8.5	38	37
		40	7.5	38	57
		80	7.5	36	69
	2	10	9.5	39	23
		20	8.5	38	59
		40	8.5	38	86
		80	8	35	122
	3	10	9.5	38	25
		20	9.5	38	71
		40	8	37	110
		80	7.5	35	153
	4	10	11	38	27
		20	11	38	65
		40	9	37	134
		80	9	35	164
	5	10	11	38	23
		20	10	37	70
		40	8.5	36	145
		80	8	34	171
60	1	10	12	37	14
		20	11.5	37	24
		40	10.5	37	32
		80	10	36	37
	2	10	12	37	15
		20	11.5	37	40
		40	10.5	37	55
		80	10	35	75
	3	10	12	37	13
		20	12	37	50
		40	10.5	36	94
		80	10.5	34	115
	4	10	13.5	37	10
		20	12	36	58
		40	11	36	85
		80	11.5	34	118
	5	10	13	37	11
		20	12.5	36	50
		40	12	36	88
		80	11	34	120

TH-1123_10610407

Table 5.2 (**contd.**) Summary of shear strength parameters of fiber reinforced soil obtained from triaxial compression tests: Influence of length of fiber

Soil density D_r (%)	Fiber content f_c (%)	Fiber length L (mm)	Failure axial strain (%)	Friction angle Φ(°)	Cohesion c_f (kPa)
30	1	10	14	35	5
		20	15	35	12
		40	12	35	27
		80	10	34	36
	2	10	15	35	8
		20	14	35	22
		40	12	34	48
		80	10	34	63
	3	10	15	35	6
		20	13.5	35	40
		40	12	34	73
		80	11	33	92
	4	10	14.5	35	2
		20	14	35	41
		40	13	34	65
		80	11.5	33	96
	5	10	17	35	4
		20	15	35	37
		40	13.5	34	70
		80	10	34	83

TH-1123_10610407

5.3.3 Influence of relative density of soil

The influence of relative density of soil over performance of fiber reinforced soil, with varied length and content of fiber, has been studied through twelve different series of triaxial compression tests (C_1-C_{12}) the details of which are given Table 3.3. In these tests the relative density of soil was varied as 30%, 60% and 80% representing loose, medium dense and dense condition.

Typical stress-strain responses of fiber reinforced soil with low intensity of reinforcement (i.e. short length and low content; L = 20 mm, f_c = 2%), for three different densities of the soil, D_r of 30%, 60% and 80%; are depicted in Figs. 5.27, 5.28 and 5.29 respectively. It can be seen that with loose soil (D_r = 30%, Fig. 5.27) the deviator stress is found to increase with increase the axial strain to reach a nearly asymptotic stage, typical of ductile behaviour. Whereas, with dense soil (D_r = 80%, Fig. 5.29) the stress-strain responses have shown a clear peak followed by a stress drop, akin to that of brittle behaviour. In case of medium dense soil (D_r = 60%, Fig.5.28) the constitutive behavior of the fiber reinforced soil is found to be intermediate to these extreme cases that there has taken place a mild stress drop at relatively large strain. This difference in the constitutive behavior can be attributed to the difference in the mode of failure, the specimens have undergone. Typical pictures of failure pattern as observed in the post test specimens are shown in Fig. 5.30. It can be seen that with loose soil there has taken place bulging failure while with dense soil the specimen has undergone a clear shearing. This is because the fibers initially hold the loose soil mass against lateral spreading giving rise to increased load carrying capacity. However beyond a certain limit the fibers tend to get pulled away, leading to large deformations that the specimen can no longer sustain increased loading. Once a fiber is pulled away it transfers the excess stress unto the adjacent region triggering

TH-1123_10610407

the pullout failure over there. With this process continuing there takes place increased volume expansion leading to bulging of the specimen. Whereas with dense soil around the fibers could mobilize adequate resistance against lateral deformation that the soil mass continues to take increased loading without much of volume expansion. However at one stage due to strain localization, in the critical shear plane, some of the fibers get pulled away triggering off sudden failure leading to visible stress drop (Fig. 5.29). At this stage there forms a shear band that the reinforced soil mass on both sides of the shear plane slide part as two rigid bodies (Fig. 5.30b). Hence it can be said while with looses soil the failure keeps progressing over a large part of the specimen with dense soil it is highly localized, just limited to the shear plane.

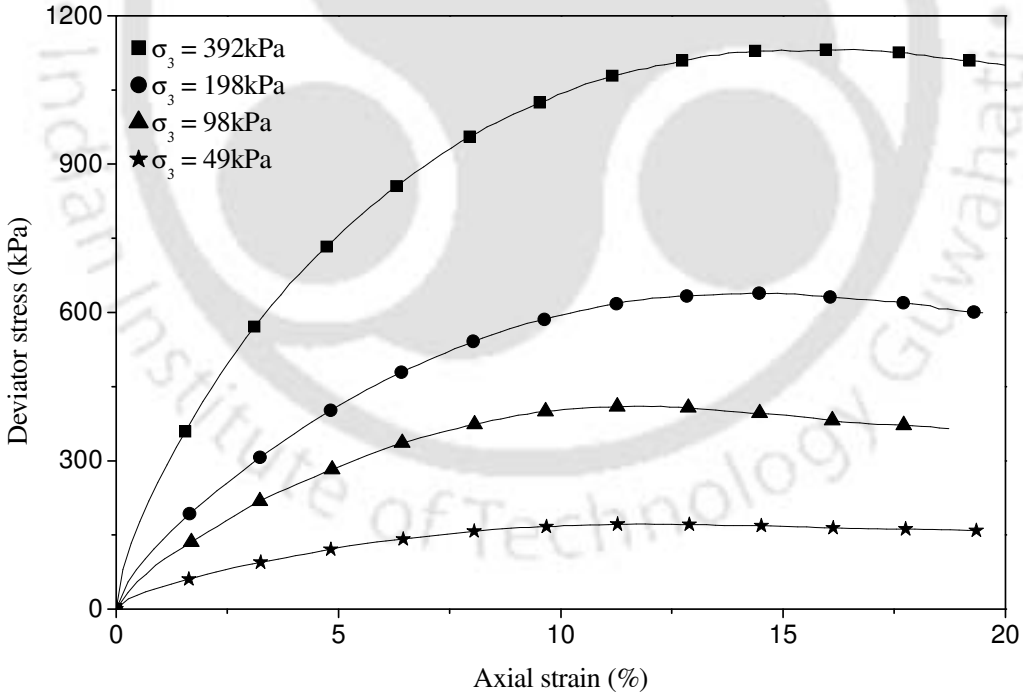

Fig. 5.27 Stress-strain behavior of fiber reinforced soil, lightly reinforced (D_r = 30%, L = 20mm, f_c = 2%).

TH-1123_10610407

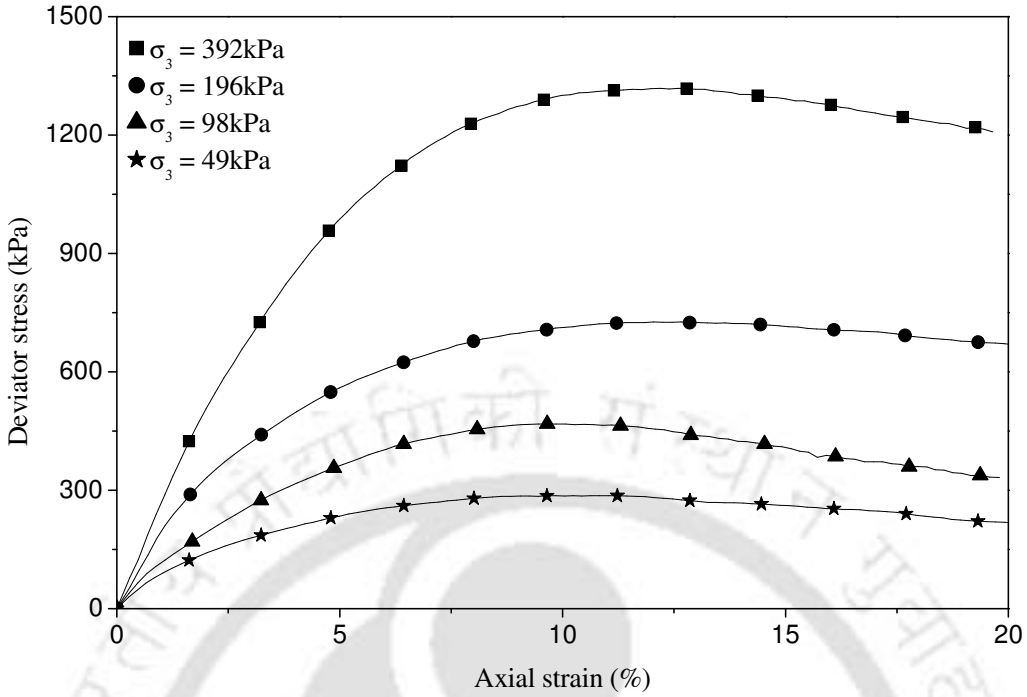

Fig. 5.28 Stress-strain behavior of fiber reinforced soil, lightly reinforced (D_r = 60%, L = 20mm, f_c = 2%).

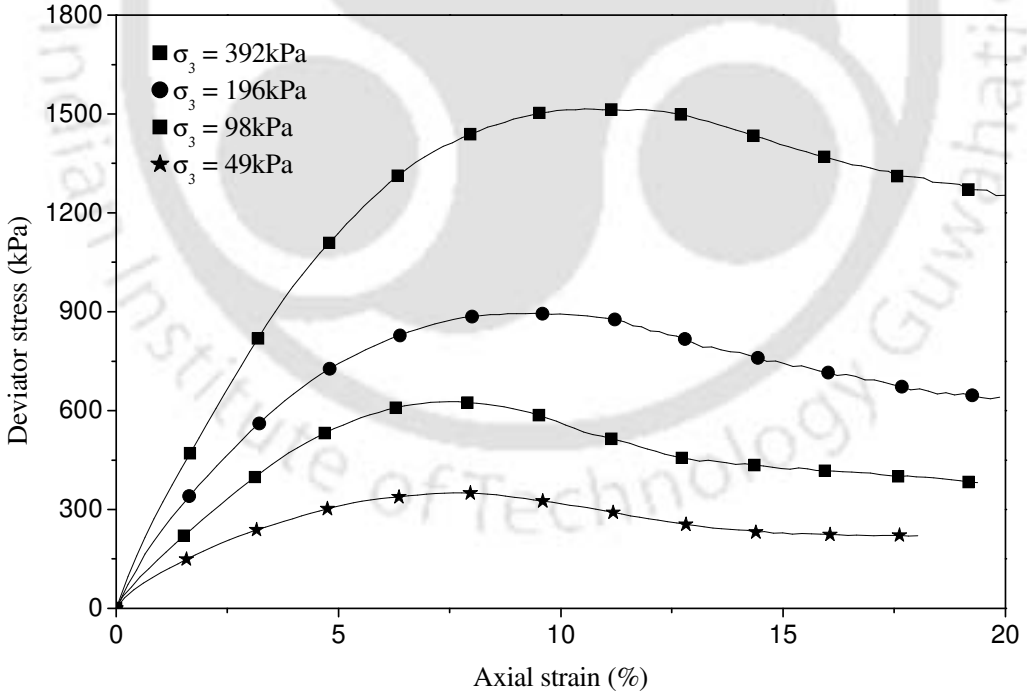

Fig. 5.29 Stress -strain behavior of fiber reinforced soil, lightly reinforced (D_r = 80%, L = 20mm, f_c = 2%).

TH-1123_10610407

(a) D_r = 30% (b) D_r = 80%

Fig. 5.30 Failure mode of fiber reinforced soil, lightly reinforced (L = 20 mm, f_c = 2%, σ_3 = 49 kPa): Influence of relative density of soil

In contrast, when the reinforcement is relatively heavy, the influence of relative density on the performance of soil-fiber composite is found to be little different (Fig. 5.31-5.33). It could be observed that with long fibers (i.e. 80 mm length) of relatively large quantity in the soil mass (f_c = 4%), irrespective of soil density, the stress-strain responses have shown brittle behavior that the stress continues to increase to peak value following which there is large drop. Even with loose soil (D_r = 30%) the fiber reinforced specimen has exhibited a clear peak followed by a visible drop in strength (Fig.5.31). With increased density of soil, the post failure stress drop is found to be relatively high. For example, for confining pressure of 392 kPa, the stress drop with 30% relative density is about 300 kPa while with 80% relative density it is as high as 600 kPa. A closed examination of the failed specimens (Fig. 5.34) indicates that the pattern of failure is relatively complex and strikingly different from that with light

TH-1123_10610407

reinforcement (Fig.5.30). With heavy reinforcement, when the soil is loose, the specimen is found to be almost intact with little bulging at the center. The little bend in the top portion indicates that the top column of soil has penetrated into the soil below leading to the bulging. It is completely different to that with lightly reinforced specimen (Fig. 5.30a) where the bulging is experienced over a much large area of the specimen. As the long fibers with large quantity have almost restrained the soil mass against lateral spreading it has continued to sustain increased loading. But there being strain localization in the central region the specimen has undergone local failure leading to the stress drop. While with dense soil, the specimen has undergone a mild shearing in the central region (Fig. 5.34b). This is primarily due to the reason that the top column of soil has penetrated into the bottom region of the specimen. Contrary to this, with light reinforcement the failure was prominent that the specimen had developed a clear shear plane (Fig. 5.30b).

Hence it can be said that with relatively heavy reinforcement, the density of soil mass does not play much of a role so far as the failure behavior of the specimen is concerned that both with loose and dense soil the fiber reinforced specimen exhibits brittle like failure that there as a peak stress followed by a visible drop. This is because the long fibers have large resistance against pull out that the bulging is effectively arrested. Besides, with large percentage of reinforcement the soil is almost encapsulated within the interwoven fiber structure that formation of a clear shear band is inhibited. The failure in both loose and dense soil condition is mostly confined to a local region which is primarily due to strain localization effect. As the strain localization induced failures are sudden in nature there has developed prominent stress drops in the constitutive responses of the fiber reinforced specimens.

TH-1123_10610407

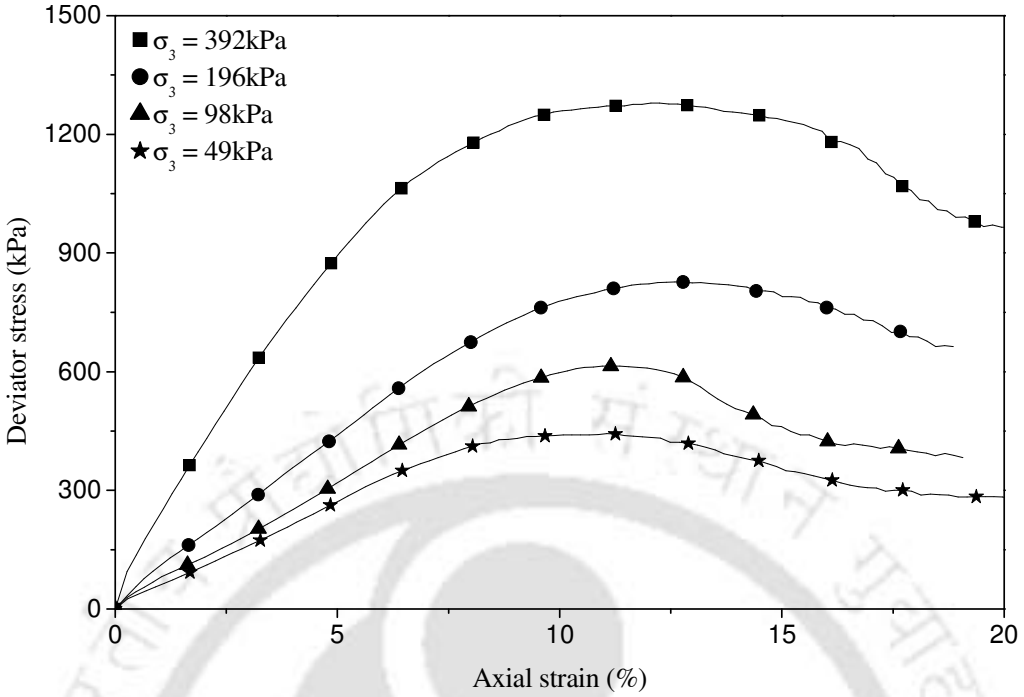

Fig.5.31 Stress-strain behavior of fiber reinforced soil, heavily reinforced (D_r = 30%, L = 80mm, f_c = 4%)

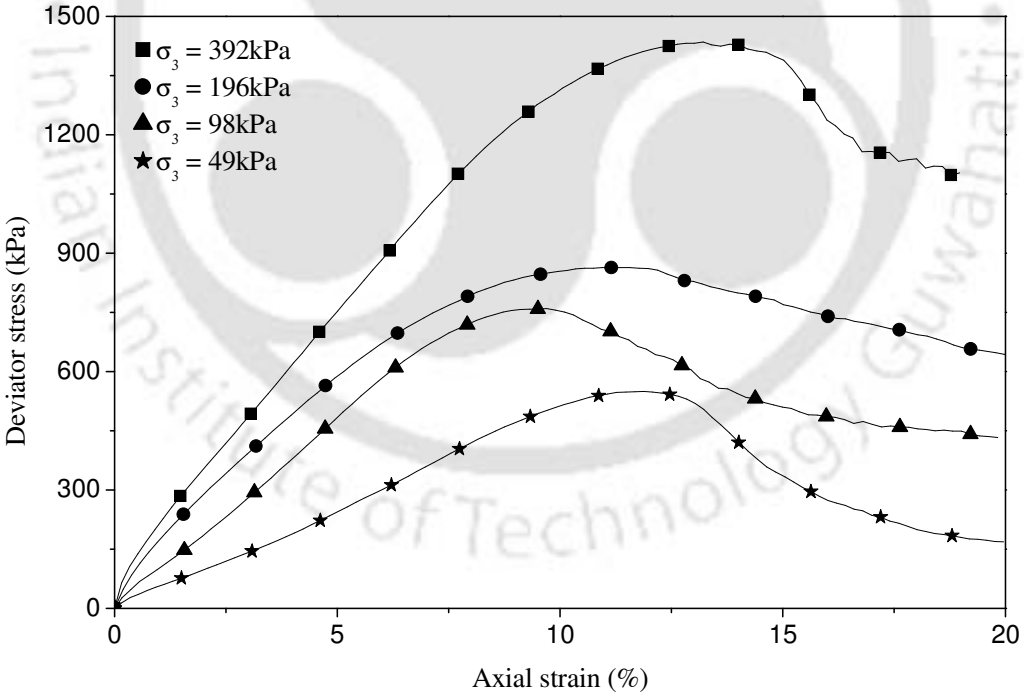

Fig. 5.32 Stress -strain behavior of fiber reinforced soil, heavily reinforced (D_r = 60%, L = 80mm, f_c = 4%)

TH-1123_10610407

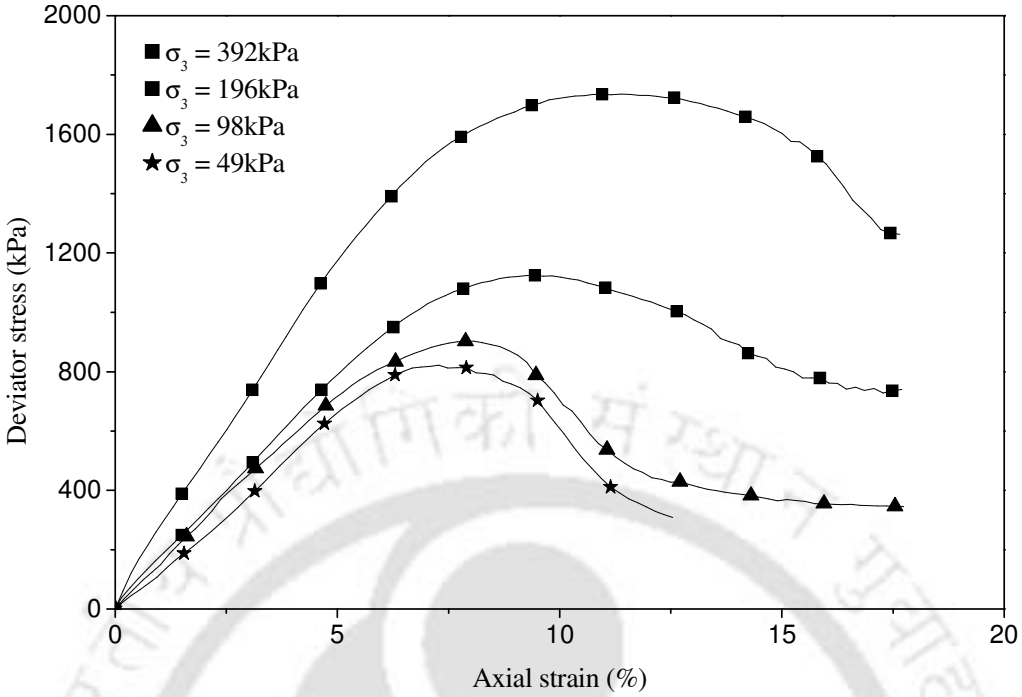

Fig. 5.33 Stress-strain behavior of fiber reinforced soil, heavily reinforced (D_r= 80%, L = 80mm, f_c = 4%).

(a) D_r = 30% (b) D_r = 80%

Fig. 5.34 Failure mode of fiber reinforced soil, heavily reinforced (L = 80 mm, f_c = 4%, σ_3 = 49 kPa): Influence of relative density of soil

TH-1123_10610407

Typical comparisons of constitutive behavior of fiber reinforced specimens with varied density of soil are shown in Figs.5.35 and 5.36. The responses presented are at a low confinement pressure that the influence of the relative density can be observed with prominence. It can be seen, both with light and heavy reinforcement the fiber reinforced specimen has exhibited visible increase in stiffness when the relative density of the soil has been increased from 30% to 80%. This is attributable to the increased frictional resistance at the fiber soil-interface that inhibits the pullout of fibers leading to reduced deformation in the specimen and hence giving rise to stiffened response. In contrast the stress-strain responses didn't so much of change in the stiffness when the fiber length and content was enhanced (Figs. 5.19-5.21, 5.9-5.10). Hence it can be said that in order to improve the stiffness of fiber reinforced soil one needs to increase the density of the soil rather than the fiber length and content. The strength too is found to increase with increased density of the soil and the strain at which the peak strength is mobilized is reduced. But the post-peak loss of strength is more when the soil is dense.

Typical peak strength envelopes depicting the influence of relative density for two different cases, lightly reinforced and heavily reinforced, are shown in Figs. 5.37 and 5.38 respectively. It can be seen that the strength envelopes for different relative densities are almost similar but with an increased cohesion intercept. Values of the induced cohesion due to fiber reinforcement, for varying soil density, and the corresponding friction angles, for different cases are summarized in Table 5.3. The induced apparent cohesion due to fiber reinforcement is found have increased significantly with increase in the density of the soil mass, more prominently when the fiber length is large. For example for 10 mm long fibers with 5% content, the increase in apparent cohesion with increase in relative density from 30% to 80% is 11 kPa

TH-1123_10610407

while with 80 mm long fibers it is as high as 88 kPa. The friction angle of the fiber reinforced soils too has exhibited an increase with increase in the relative density of the soil.

Interestingly the increase in Φ is relatively higher when the fiber length is small and it is less in quantity. For example, with 10 mm fiber of 1% content, the friction angle has increased from 35° to 39° while with 80 mm fiber of 4% content the increase in is just half (i.e. from 33° to 35°). With very high content (f_c = 5%) and long fibers (L = 80 mm) there is practically no change in the frictional angle with increase in density of soil in the soil-fiber composite.

TH-1123_10610407

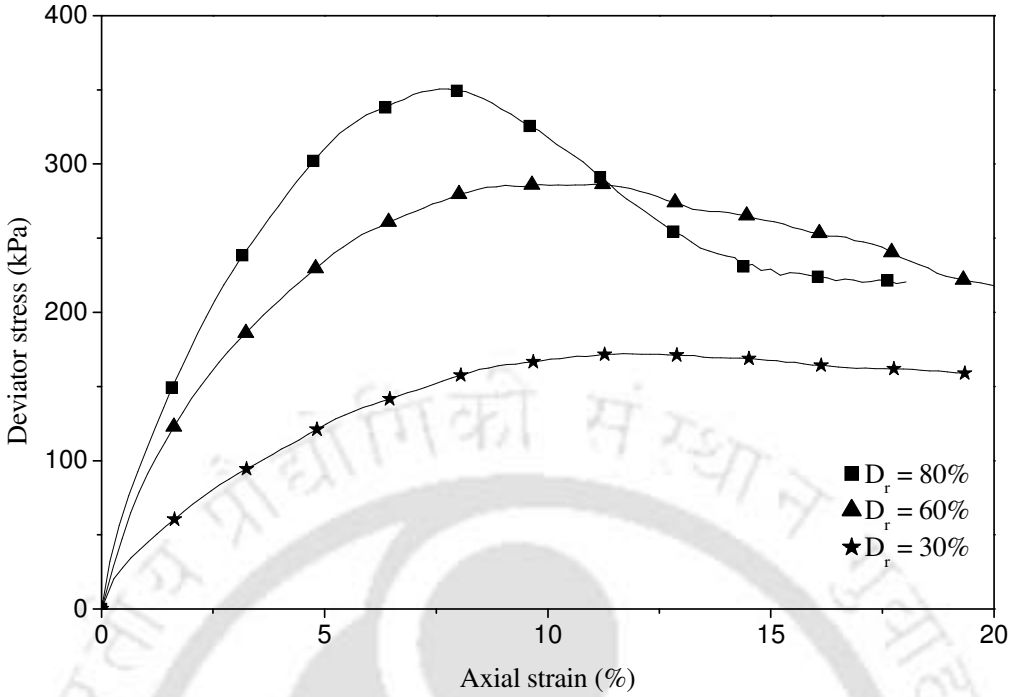

Fig. 5.35 Stress-strain behavior of fiber reinforced soil, lightly reinforced (L = 20mm, f_c = 2%, σ_3 = 49kPa): Influence of relative density of soil

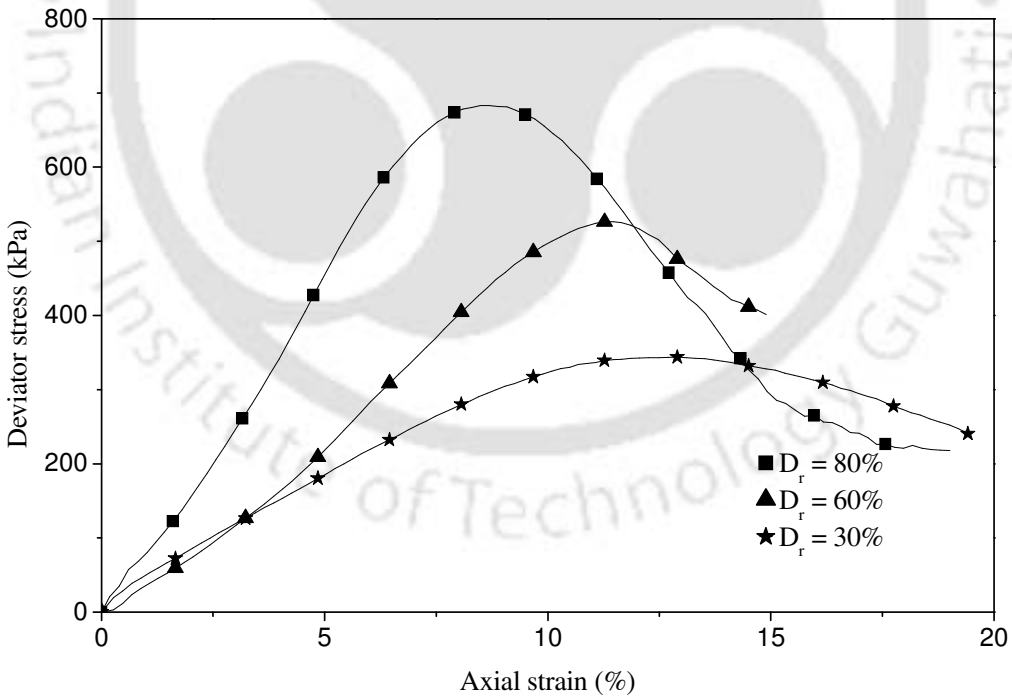

Fig. 5.36 Stress-strain behavior of fiber reinforced soil, heavily reinforced (L = 40mm, f_c = 5%, σ_3 = 49kPa): Influence of relative density of soil.

TH-1123_10610407

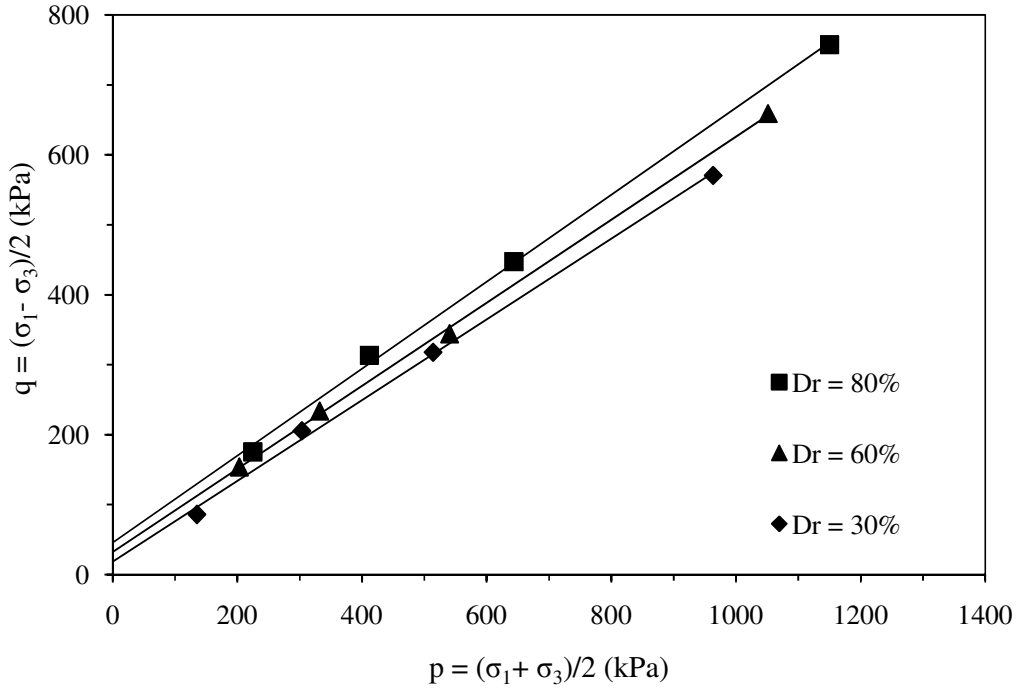

Fig. 5.37 Failure strength envelopes of fiber reinforced soil, lightly reinforced (L = 20mm, f_c = 2%): Influence of relative density of soil

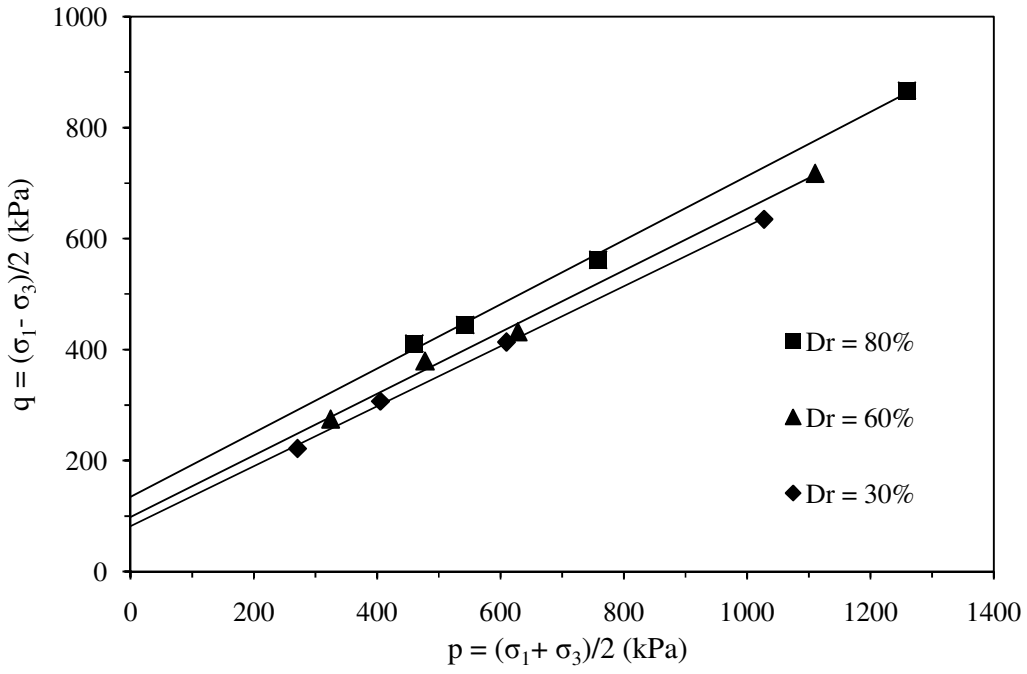

Fig. 5.38 Failure strength envelopes of fiber reinforced soil, heavily reinforced (L = 80mm, f_c = 4%): Influence of relative density of soil

TH-1123_10610407

Table 5.3 Summary of shear strength parameters of fiber reinforced soil obtained from triaxial compression tests: Influence of relative density of soil

Fiber content f_c (%)	Fiber length L (mm)	Soil density D_r (%)	Friction angle Φ (°)	Cohesion c_f (kPa)
1	10	30	35	5
		60	37	14
		80	39	13
	20	30	35	12
		60	37	24
		80	38	37
	40	30	35	27
		60	37	32
		80	38	57
	80	30	34	36
		60	36	37
		80	36	69
2	10	30	35	8
		60	37	15
		80	39	23
	20	30	35	22
		60	37	40
		80	38	59
	40	30	34	48
		60	37	55
		80	38	86
	80	30	34	63
		60	35	75
		80	35	122
3	10	30	35	6
		60	37	13
		80	38	25
	20	30	35	40
		60	37	50
		80	38	71
	40	30	34	73
		60	36	94
		80	37	110
	80	30	33	92
		60	34	115
		80	35	129

TH-1123_10610407

Table 5.3 (**contd.**) Summary of shear strength parameters of fiber reinforced soil obtained from triaxial compression tests: Influence of relative density of soil.

Fiber content f_c (%)	Fiber length L (mm)	Soil density D_r (%)	Friction angle Φ (°)	Cohesion c_f (kPa)
4	10	30	35	2
		60	37	10
		80	38	27
	20	30	35	41
		60	36	58
		80	38	65
	40	30	34	65
		60	36	85
		80	37	134
	80	30	33	96
		60	34	118
		80	35	164
5	10	30	35	4
		60	37	11
		80	38	23
	20	30	35	37
		60	36	50
		80	37	70
	40	30	34	70
		60	36	88
		80	36	145
	80	30	34	83
		60	34	120
		80	34	171

5.3.4 Influence of confining pressure

Influence of confinement pressure on the strength and deformation behavior of fiber reinforced soils was studied by conducting the triaxial compression tests at four different confinement pressures, 49 kPa, 98 kPa, 196 kPa and 392 kPa. Responses of a dense soil with varied length of fiber, at two different confinement pressures i.e. low and high, are presented in Fig. 5.39 and Fig. 5.40 respectively. Similar responses for varied fiber content are shown in Fig. 5.41 and Fig.4.42 respectively. It can be seen

TH-1123_10610407

that the stress-strain responses of the fiber reinforced soils have markedly changed when the confinement pressure is increased from 49 kPa to 392 kPa. While with low confinement pressure (49 kPa) there has developed a distinct peak deviator stress with high confinement (392 kPa) the responses are tending to be nearly asymptotic with much less strength reduction in the post failure stage. Hence it can be said that with increased confinement sudden failure in the fiber reinforced soil is restrained that the specimen tends to be more ductile in behavior. Besides the degree of improvement in the load carrying capacity is substantially less when the confinement pressure is high. For example with 49 kPa of confinement and fibers of 80 mm length, the deviator stress of the soil has increased from about 150 kPa to 760 kPa, an increment of the order of 600 kPa. In contrast with high confinement (i.e. 392 kPa) the increment in the deviator stress is much less, of the order of 300 kPa. It indicates that, with increase in the confinement pressure, the reinforcement ability of the fibers has reduced.

The above observations can better be explained through the observed failure patterns in the test specimen depicted in Fig.5.43 and fig.5.44. It can be seen that in case of the lightly reinforced specimen (Fig.5.43), there has developed visible shearing that the upper half of the specimen has slide over the lower half. But at increased confinement pressure (i.e. 392 kPa) the shear failure has completely been arrested and the specimen has undergone bulging. This indicates that with increased confinement the mode of failure is altered. This may be because with increased confinement the sudden shear failure triggered due to the pullout of the fibers is restrained. Therefore, the increased compression due to the imposed surcharge loading is accommodated through a relatively distributed volumetric expansion leading to the bulging. However in case relatively higher percentage of reinforcement (Fig.5.44) there has formed shearing in both the cases of confinement but the extent of sliding and the shear band

TH-1123_10610407

is much less when the confinement pressure is high. Hence it can be said that with increased confinement the shearing in the fiber reinforced dense soil is restrained. As a result of which the reinforcing action of the fibers is diminished that it has underperformed leading to reduced strength improvement of the soil-fiber composite. The other possible factor for the reduced strength improvement could be due to the breakage of fibers which was prominently noticed in the post test exhumed specimens particularly with long fibers (i.e. 40 mm and 80 mm).

Even with loose soil the increased confinement pressure has diminished the reinforcing ability of the fibers (Figs. 5.45, 5.46). This is primarily due to the reduced volumetric expansion with increased confinement pressure as has been observed in the post test specimens, depicted in Fig.5.47.

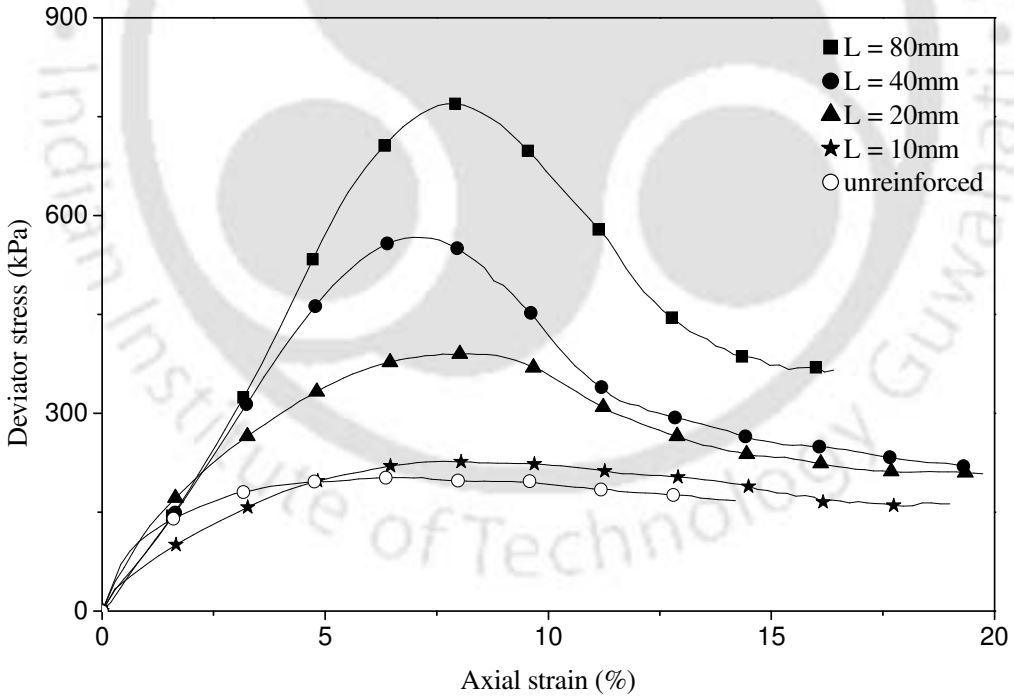

Fig. 5.39 Stress-strain behavior of fiber reinforced dense soil (D_r = 80%, f_c = 3%, σ_3 = 49kPa): Low confinement pressure.

TH-1123_10610407

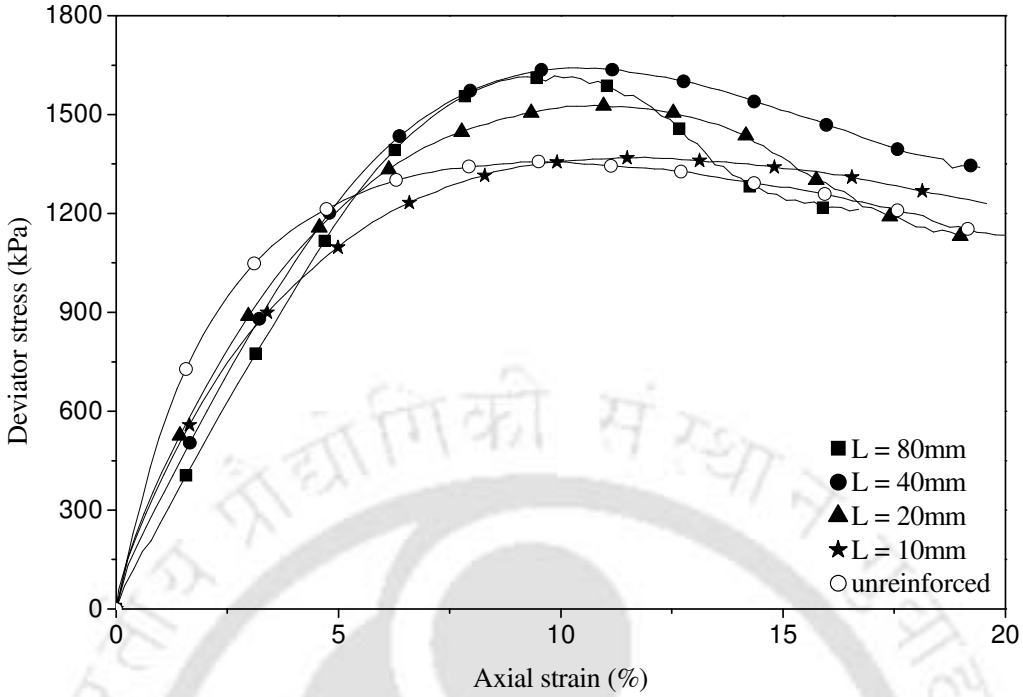

Fig. 5.40 Stress-strain behavior of fiber reinforced dense soil (D_r = 80%, f_c = 3%, σ_3 = 392 kPa): High confinement pressure

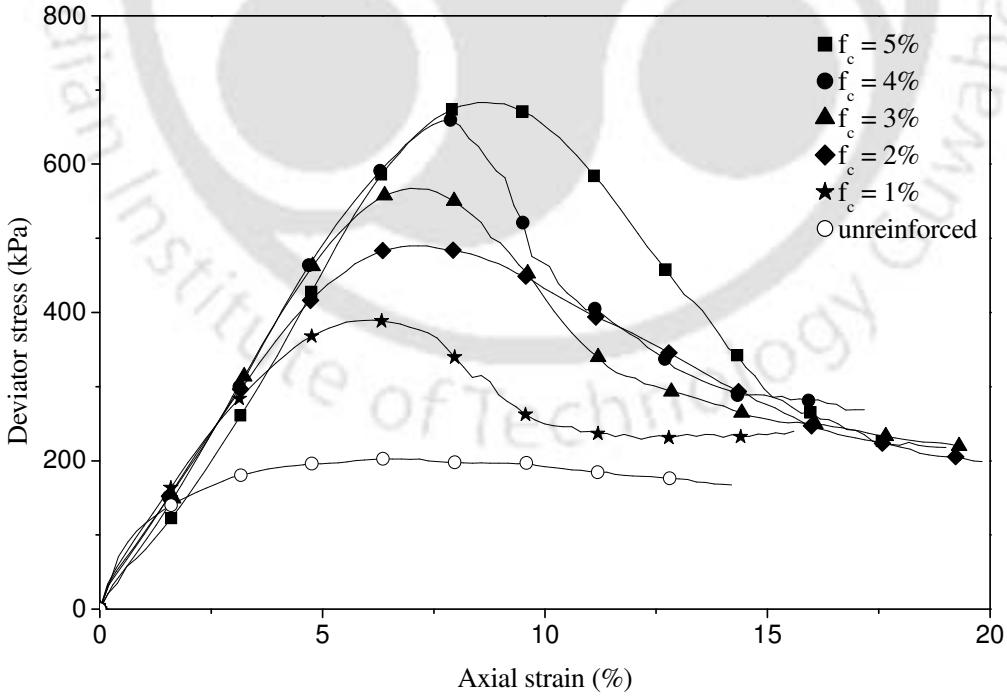

Fig. 5.41 Stress-strain behavior of fiber reinforced dense soil (D_r = 80%, L = 40mm, σ_3 = 49kPa): Low confinement pressure.

TH-1123_10610407

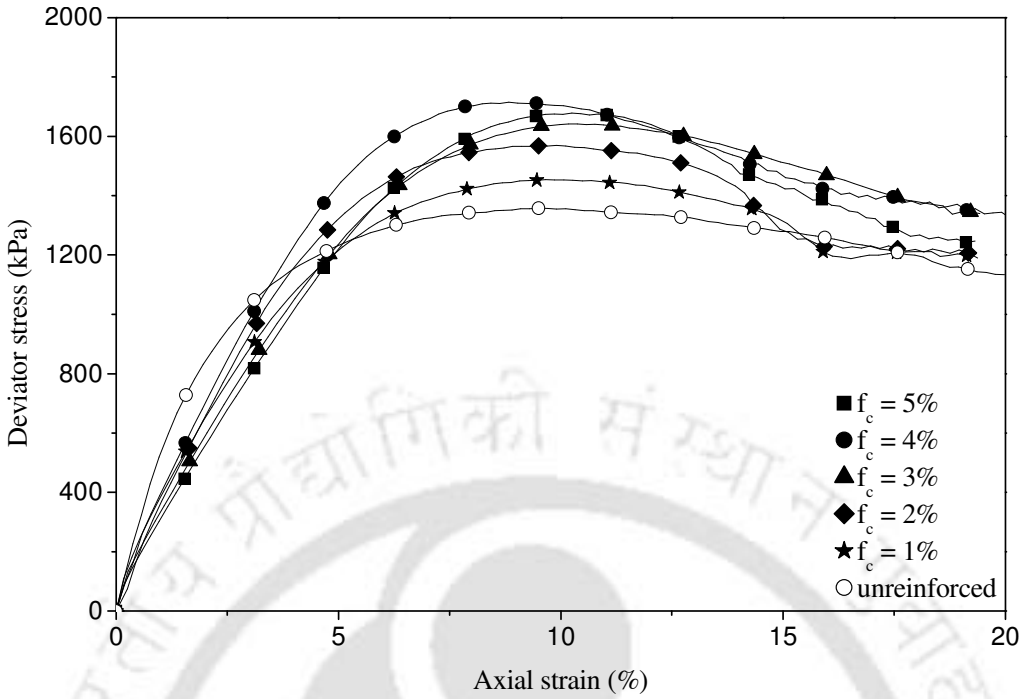

Fig. 5.42 Stress-strain behavior of fiber reinforced dense soil (D_r = 80%, L = 40mm, σ_3 = 392kPa): High confinement pressure.

(a) σ_3 = 49 kPa (b) σ_3 = 392 kPa

Fig. 5.43 Failure mode of fiber reinforced dense soil, lightly reinforced (D_r = 80%, L = 10 mm, f_c = 3%): Influence of confinement pressure.

TH-1123_10610407

(a) σ_3 = 49 kPa (b) σ_3 = 392 kPa

Fig.5.44 Failure mode of fiber reinforced dense soil, heavily reinforced (D_r = 80%, L = 40 mm, f_c = 4%): Influence of confinement pressure.

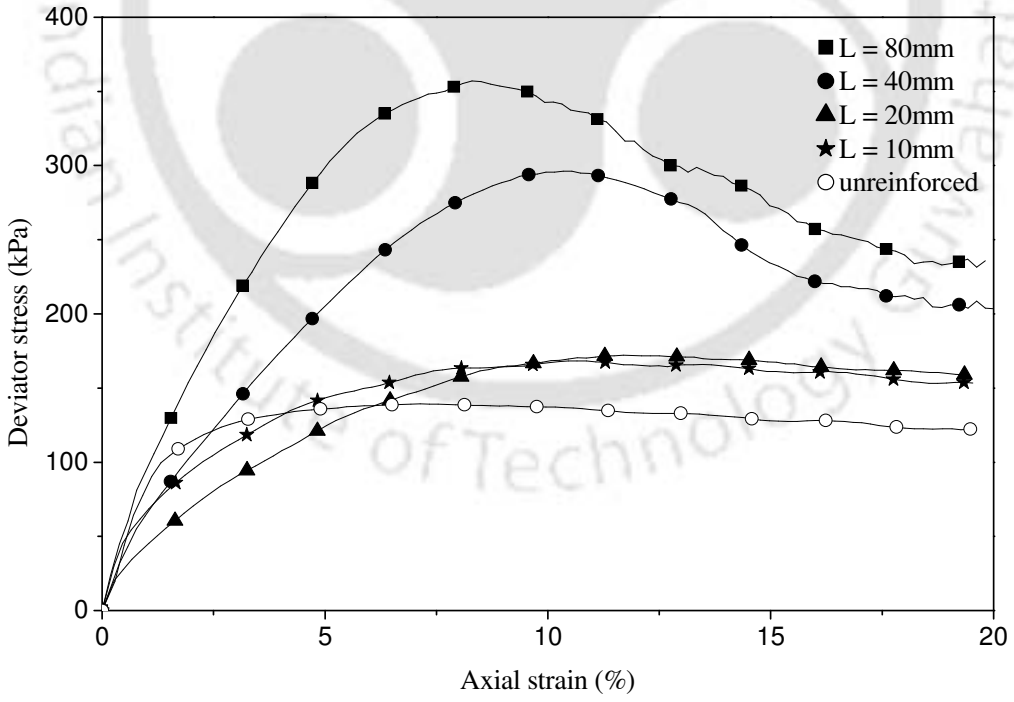

Fig. 5.45 Stress-strain behavior of fiber reinforced loose soil (D_r = 30%, f_c = 2%, σ_3 = 49 kPa): Low confinement pressure.

TH-1123_10610407

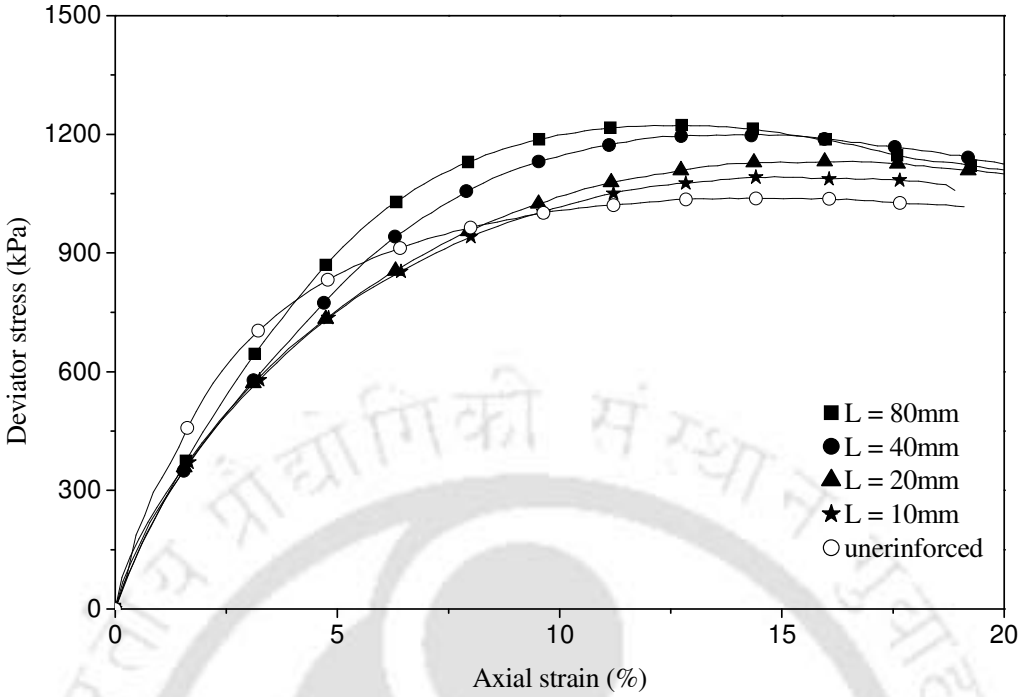

Fig. 5.46 Stress-strain behavior of fiber reinforced loose soil (D_r = 30%, f_c = 2%, σ_3 = 392kPa): High confinement pressure.

49 kPa 392 kPa

Fig.5.47 Failure mode of fiber reinforced loose soil (D_r = 30%, L = 20 mm, f_c = 2%): Influence of confinement pressure.

TH-1123_10610407

5.4 SCALE EFFECT

The important parameters that govern the strength improvement of soils due to fiber reinforcement can be assumed to be: D, L, d, S_f, γ, ϕ, G, δ, σ_1, σ_3; wherein, D is the diameter of the specimen, L is the length of the fiber, d is the diameter of the fiber, S_f is the strength/stiffness of the fiber, γ is the unit weight of soil, ϕ is the friction angle of the soil, G is the shear modulus of soil, δ is the fiber-soil interface friction angle, σ_1 is the vertical surcharge pressure, σ_3 is the confinement pressure. The function (f) that governs the system can be written as

$$f(D, L, d, S_f, \gamma, G, \sigma_1, \sigma_3, \phi, \delta) = 0 \quad (5.1)$$

Similarly as discussed in section 4.4, force and length can be considered as fundamental dimensions. As shown by Langhaar (1951) and Bukingham 1914, this system can be studied by any complete set of eight (i.e. 10-2) independent parameters (i.e. π_1, π_2, π_3,…… π_8). So as discussed by Butterfield R. 1999, R which is the set of the parameters having totally distinct dimensions will be {d, γ, σ_3} and Q which is set of the repeated variables that can be { d, σ_3} (Butterfield R. 1999). Then isolated variable will be {D, L, S_f, γ, G, σ_1, ϕ, δ} Hence Eq.5.1 can be reduced to the following form

$$g(\pi_1, \pi_2, \pi_3, \ldots\ldots \pi_8) = \left[\left(\frac{D}{d}\right), \left(\frac{L}{d}\right), \left(\frac{S_f}{\sigma_3}\right)\left(\frac{\gamma_d}{\sigma_3}\right), \left(\frac{G}{\sigma_3}\right), \left(\frac{\sigma_1}{\sigma_3}\right), \phi, \delta\right] = 0 \quad (5.2)$$

For a prototype specimen (p) with diameter N times higher than the model (m)

$$\frac{D_p}{D_m} = N \quad (5.3)$$

For similarity to be satisfied all the π terms should be same, both for the prototype and the model.

TH-1123_10610407

$$(\pi_1)_p = (\pi_1)_m \tag{5.4}$$

$$\frac{D_p}{d_p} = \frac{D_m}{d_m} \tag{5.5}$$

By rearranging equation 5.5 and substituting equation 5.3,

$$\frac{D_p}{D_m} = \frac{d_p}{d_m} = N \tag{5.6}$$

Similarly if we will compare π_4 term and consider the same density of soil in prototype and model then,

$$\frac{\gamma_p d_p}{\sigma_{3p}} = \frac{\gamma_m d_m}{\sigma_{3m}} \tag{5.7}$$

$$\frac{d_p}{\sigma_{3p}} = \frac{d_m}{\sigma_{3m}} \tag{5.8}$$

$$\frac{d_p}{d_m} = \frac{\sigma_{3p}}{\sigma_{3m}} = N \tag{5.9}$$

Now equating the π_3 term one can write that,

$$\frac{S_{fp}}{\sigma_{3p}} = \frac{S_{fm}}{\sigma_{3m}} \tag{5.10}$$

$$\frac{S_{fp}}{S_{fm}} = \frac{\sigma_{3p}}{\sigma_{3m}} = N \tag{5.11}$$

Hence, the strength of the fiber reinforcement in the prototype model should be of N times the strength of the reinforcement used in the model test, where N is the model scale. Similarly equating the π_1, π_2 terms, both in model and prototype, it can be seen

TH-1123_10610407

that the geometric parameters of the fiber reinforcement have a linear viaration with the model scale. However, large-scale tests carried out by Milligan et al. (1986) and Adams and Collin (1997) indicate that the general mechanisms and behavior observed in the model tests are generally reproduced at large scale as well.

5.5 PREDICTION OF STRENGTH OF FIBER REINFORCED SOIL

As has been seen through the experimental data discussed above the strength improvement of granular soils due to fiber reinforcement can be idealized through an induced apparent cohesion (c_f). This apparent cohesion is primarily dependent upon the length, diameter of the fibers, strength of soil and frictional resistance mobilized at the soil-fiber interface. It is difficult to predict the individual effects of theses parameters. However there are simple force-equilibrium models that can predict the combined effect of all these parameters. One such model is used by Gregory (2006). This model has been used in the present study the details of which are presented below.

The random fibers in the soil can be quantified through the statistical theory proposed by Naaman (1972). In this theory it is assumed that the fibers are distributed independently and the probability of occurrence of fibers, with reference to any axis, at all possible angles, is same. This is very close to the reality when the fibers have random distribution in the soil mass, such as the present tests.

For a given weight of fibers (w_f) the corresponding volume (V_r) can be obtained as

$$V_r = \frac{w_f}{G_f \gamma_w} \tag{5.12}$$

TH-1123_10610407

Where, w_f is weight of fiber per unit volume of fiber reinforced soil, G_f is the specific gravity of fiber, γ_w is the unit weight of water. Therefore, the number of fibers per unit volume of soil-fiber mix can be expressed as

$$N_v = \frac{4V_r}{\pi L d^2} \tag{5.13}$$

Where, L is the length of individual fiber and d is its diameter.

The probability of a single fiber making all angles is equal that when it moves in all directions with respect to its centroid shall make a sphere, Fig. 5.48 (Maher and Gray 1990).

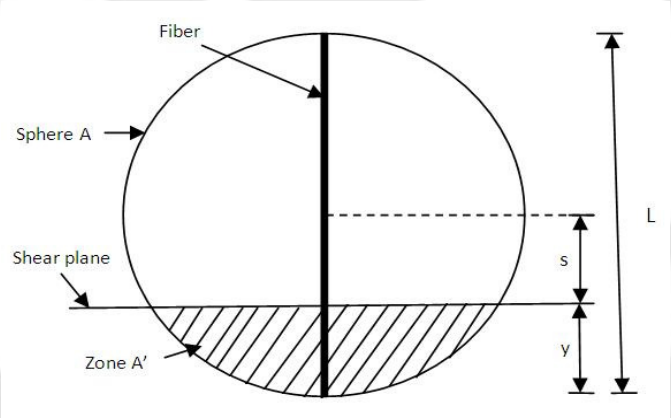

Fig. 5.48 Geometry of fiber crossing shear plane within sphere space

The shear plane located at distance s from the centre of the sphere is taken as the reference plane. The probability, P(f), that the fiber shall pass through this plane can be written as,

$$P(f) = \frac{\frac{L}{2} - s}{\frac{L}{2}} \tag{5.14}$$

That, P(f) = (1-2s/L) when s ≤ L/2, and P(f) = 0 when s > L/2 which means that the probability of fiber to intersect the plane outside the sphere is zero. Considering an

TH-1123_10610407

unit volume, on one side, the number of fibers that would intersect the plane over an unit area can written as,

$$\int_0^{L/2}(1-\frac{2s}{L})N_v A ds = N_v \frac{L}{4} \quad (5.15)$$

Therefore total number of fibers intersecting per unit area (N_f), intersecting the plane from both sides can obtained as,

$$N_f = 2N_v \frac{L}{4} = \frac{2V_r}{\pi d^2} \quad (5.16)$$

The peak interface resistance in the fiber, mobilized on the shear plane, can be written as,

$$\sigma_i = \sigma_{conf} \tan\delta \quad (5.17)$$

Where, σ_{conf} is the confinement stress applied onto the specimen and δ is the soil-fiber interface friction angle. However, the mobilized interface friction (δ) and therefore the interface shear stress (i.e. σ_i) gradually reduce to zero at the end of the fiber. Therefore the average interface shear stress mobilized on the fiber is

$$\sigma_{avg} = \frac{1}{2}\sigma_{conf} tan\delta \quad (5.18)$$

The effective length over which this average stress acts is actually half of the fiber length assuming that the fiber is middle way across the shear plane. Therefore, the effective length of the fiber can be taken as L/2.

The shear strength (τ) induced by the fiber onto the soil is primarily due to the pullout induced tensile resistance mobilized in the fiber. Hence, the induced shear stress, in the soil, can be can be expressed as

$$\tau = L_{eff}\pi d\sigma_{avg} N_f tan\Phi = \frac{L}{2}\pi d\frac{\sigma_{conf}}{2} tan\delta N_f tan\Phi \quad (5.19)$$

TH-1123_10610407

This induced shear stress (τ) can be taken as induced apparent cohesion (c_f) as the experiments have shown that the change in friction angle of soil due to fiber reinforcement is very less. Hence it can be written that

$$c_f = \frac{L}{4}\pi d\sigma_{conf}(tan\delta)N_f(tan\Phi) \quad (5.20)$$

A relatively low confinement pressure (i.e. 98 kPa) has been used in predicting the apparent cohesion in the fiber reinforced soils. This is because at this stage the reduction in friction angle negligible. It should be mentioned here that at increased confinement pressure there takes place reduction in the slope of the failure envelope indicating an apparent increase in the cohesion value. However, in the result analysis this aspect is ignored and an average failure envelope is fit through from which the apparent cohesion is obtained. In view of this assuming confinement pressure of 98 kPa in the above calculation (Eq. 5.20) is reasonable ok given that the formulation doesn't account for the reduced slope of the failure envelope that has taken place at higher confinement pressures. A comparison of the predicted values of the apparent cohesion (c_f) with experimentally obtained ones, are shown in Table 5.4 (Fig. 5.49a).

It can be seen that the predicted and the measured values (c_f), in most of the cases, have agreed well. However there is visible difference when the fiber length is relatively high. This is possibly because long fibers remain folded in the soil mass that a large portion of it remains dormant. As the model doesn't consider this factor the difference between the observed and predicted values of the apparent cohesion is relatively large. With increased fiber content this difference is found to have increased further. In view of this more work is required to refine the model, especially when the length of the fiber is relatively large.

TH-1123_10610407

Table 5.4: Apparent cohesion of fiber reinforced soil: Comparison of experimental data with the theoretically predicted values.

Density of soil, D_r (%)	Fiber length L (mm)	Fiber content f_c (%)	Cohesion, c_f (kPa) from experiment	Cohesion, c_f (kPa), predicted: Eq.5.20
30	10	1	5	5
		2	8	9
		3	6	14
		4	2	18
		5	4	22
	20	1	12	9
		2	22	18
		3	40	27
		4	41	36
		5	37	45
	40	1	27	19
		2	48	37
		3	73	55
		4	65	72
		5	70	89
	80	1	36	37
		2	63	74
		3	92	109
		4	96	144
		5	83	179
60	10	1	14	6
		2	15	13
		3	13	19
		4	10	25
		5	11	31
	20	1	24	13
		2	40	25
		3	50	38
		4	58	50
		5	50	61
	40	1	32	26
		2	55	51
		3	94	75
		4	85	99
		5	88	123
	80	1	37	51
		2	75	101
		3	115	150
		4	118	198
		5	120	245

TH-1123_10610407

Table 5.4(**contd.**): Apparent cohesion of fiber reinforced soil: Comparison of experimental data with the theoretically predicted values.

Density of soil, D_r (%)	Fiber length L (mm)	Fiber content f_c (%)	Cohesion, c_f (kPa) from experiment	Cohesion, c_f (kPa), predicted: Eq.5.20
80	10	1	13	8
		2	23	16
		3	25	24
		4	27	31
		5	23	38
	20	1	37	16
		2	59	32
		3	71	47
		4	65	62
		5	70	77
	40	1	57	32
		2	86	63
		3	110	94
		4	134	124
		5	145	154
	80	1	69	64
		2	122	127
		3	153	188
		4	164	248
		5	171	308

5.6 SUMMARY

Presented in this chapter are the strength-deformation responses of fiber reinforced soils with varied parameters such as; length and content of fiber, density of soil, confinement pressure applied. Analysis of the test data indicates that fiber reinforcement can substantially improve the soil strength, primarily in terms of an induced apparent cohesion. A theoretical model based on the principle of force-equilibrium has been used to predict the strength improvement due to fiber reinforcement. Comparison with the experimental result shows that the model can reasonably reproduce the fiber induced strength improvement of the soil.

TH-1123_10610407

CHAPTER 6

RESULTS AND DISCUSSION-III: GEOCELL-FIBER REINFORCED SOIL

6.1 INTRODUCTION

Through the test data presented in the previous two chapters (i.e. Chapter 4 and Chapter 5) it is observed that both geocell and fiber reinforcement are potential means of improving the performance of granular soils. In this chapter the combined application of both has been explored.

Triaxial compression tests have been carried out wherein the geocell is filled with fiber reinforced soils. Three different series of tests (D_1-D_3, Table 3.3) are carried out, the details of which are presented in Chapter 3. The parameters varied are the modulus of geocell which was varied from 2.2 kN/m to 51 kN/m and the relative density of the soil which was varied from 30% to 80%. But the length and content of the fiber reinforcement was kept constant, at their respective optimum values as obtained from experiments, detailed in Chapter 5. Accordingly, the content of fiber used is 3% for loose and medium dense of soils (D_r of 30%, 60%) and 4% when the soil was dense (D_r = 80%). Whereas, length of fibers was kept as 40 mm, throughout.

The combined geocell-fiber reinforcement is referred to as *composite reinforcement*. Results of the tests carried out with the composite reinforced soils are presented and discussed in the following section.

TH-1123_10610407

6.2 GEOCELL-FIBER COMPOSITE REINFORCED SOIL

Stress-strain responses of the composite reinforced soil for a typical case (i.e. M = 25kN/m, L = 40mm, f_c = 4%, D_r = 80%) are presented in Fig. 6.1. The corresponding data for geocell reinforced soil and fiber reinforced soil are depicted in Fig. 6.2 and Fig.6.3 respectively. It could be seen that the constitutive behavior in these three forms of reinforcement are strikingly different that with fibers it is mostly strain softening in nature and with geocell it is of strain hardening while with the composite reinforcement it is intermediate of these two patterns.

Besides, with fiber reinforcement the soil has undergone failure at about 8% of strain that the deviator stress has continued to decrease with further increase in axial strain. Whereas, with geocell reinforcement failure is relatively abrupt that has taken place at a strain of about 17%. But with the composite reinforcement the specimen hasn't shown any clear failure. There has taken a place a little stress drop at about 10-12% of strain following which the specimen has continued to take increased stress with further increase in the axial strain. Indeed the failure patterns of fiber-reinforced soil depicted in Fig. 6.4 shows that both at low and high confining pressures there is clear failure with formation visible shear band that runs from top to bottom of the specimen. While with additional geocell confinement, at relatively low confinement pressure (σ_3 = 49 kPa, 98 kPa), although the specimen has undergone shear but the extent of shearing has been reduced to a much smaller length (Fig.6.5 a,b). When confinement was increased to 196 kPa, shearing has completely been arrested and the specimen has under gone a little of bulging (Fig.6.5 c, d). Similar behavior is observed at confining pressure of 392 kPa as well. Hence it can be said that with the combined application of geocell and fiber reinforcement the shear failure of the soil can be inhibited to a very large extent.

TH-1123_10610407

A typical comparison of the stress strain responses with different forms of reinforcement is shown in Fig. 6.6. It could be seen that with the combined application of geocell-fiber reinforcement the peak strength has gone up substantially high as compared to that with geocell or fiber reinforcement alone. Besides, the residual strength with composite reinforcement too is much higher compared to the other two forms of reinforcement i.e. geocell, fiber. In fact, just after the post-peak stress drop the stress-strain response, with the composite reinforcement, has exhibited an increasing trend that the shear strength once again tends increasing. The initial failure marked through the post-peak stress drop is attributed to the failure of the fiber reinforced system that is primarily due to fiber pullout or breakage. Once this happens large part of the unbalanced stress is transferred to the surrounding geocell. Indeed, at this stage, the slope of the stress-strain response of composite specimen is almost same as that of the geocell reinforced specimen. This indicates that at this stage the geocell reinforcing action is substantially mobilized that has enabled the specimen to sustain increased loading.

It is of interest to note that the slope of the stress strain response with geocell-fiber composite reinforcement is much higher as compared to that with geocell or fiber reinforcement alone. Hence it can be said that the composite reinforcement can improve the stiffness of the soil, significantly.

A typical comparison of the failure strength envelops for different type of reinforcement i.e. geocell, fiber and geocell-fiber combined, along with the unreinforced case are presented in Fig. 6.7. It can be seen that the friction angle in all the cases has almost remained same, indicated through nearly similar order of slope of the strength envelopes. But the cohesion intercept has shown a significant increase. Corresponding apparent cohesion with the composite reinforcement is found to be

TH-1123_10610407

217 kPa while with geocell reinforcement it is 142 kPa and with fiber reinforcement it is 134 kPa. This indicates that with geocell-fiber composite reinforcement the induced apparent cohesion is almost double as that of the case with geocell or fiber reinforcement alone.

The influence of various parameters, on the performance of the geocell-fiber composite reinforced soil specimen are presented and analyzed in the following sub-sections.

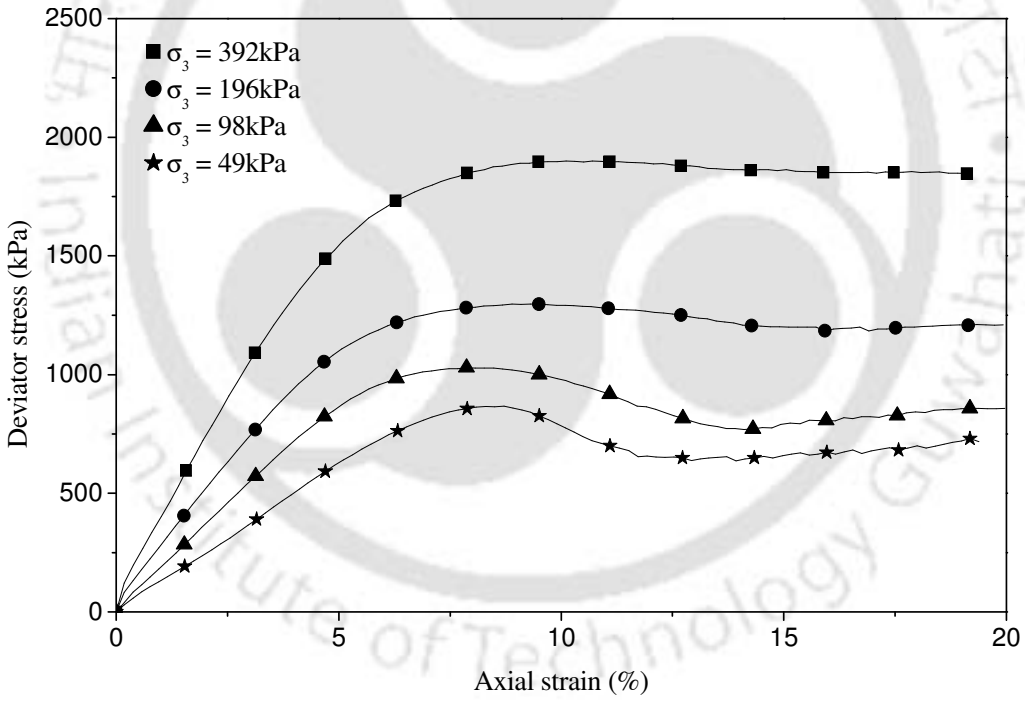

Fig.6.1 Stress-strain behavior of geocell-fiber reinforced soil (M = 25kN/m, L = 40mm, f_c = 4%, D_r = 80%)

TH-1123_10610407

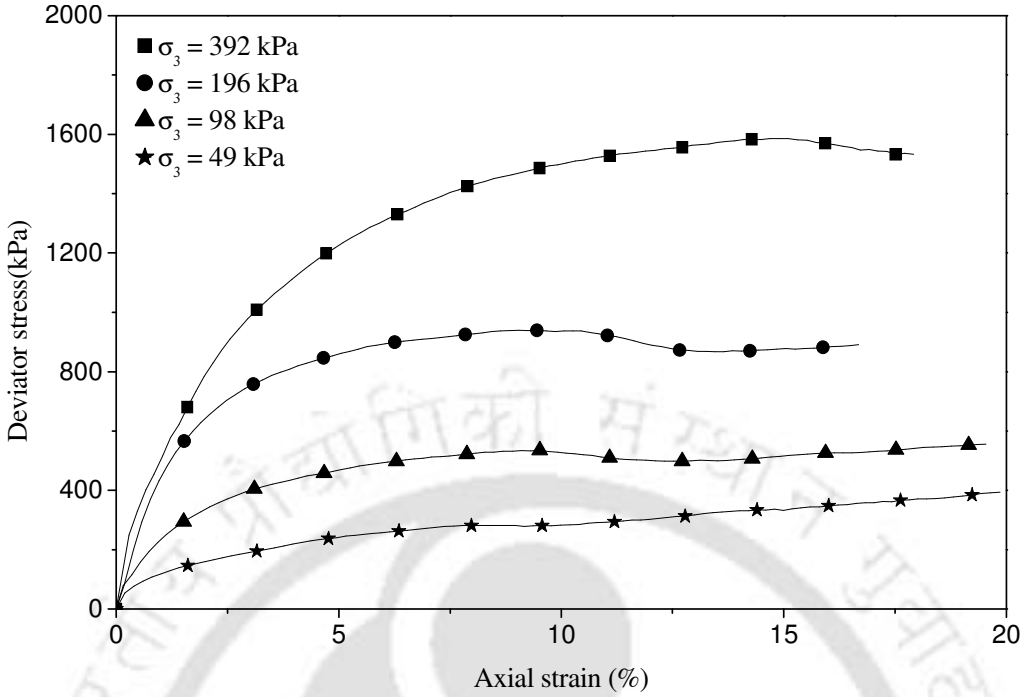

Fig. 6.2 Stress-strain behavior of geocell reinforced soil (M = 25kN/m, D_r = 80%)

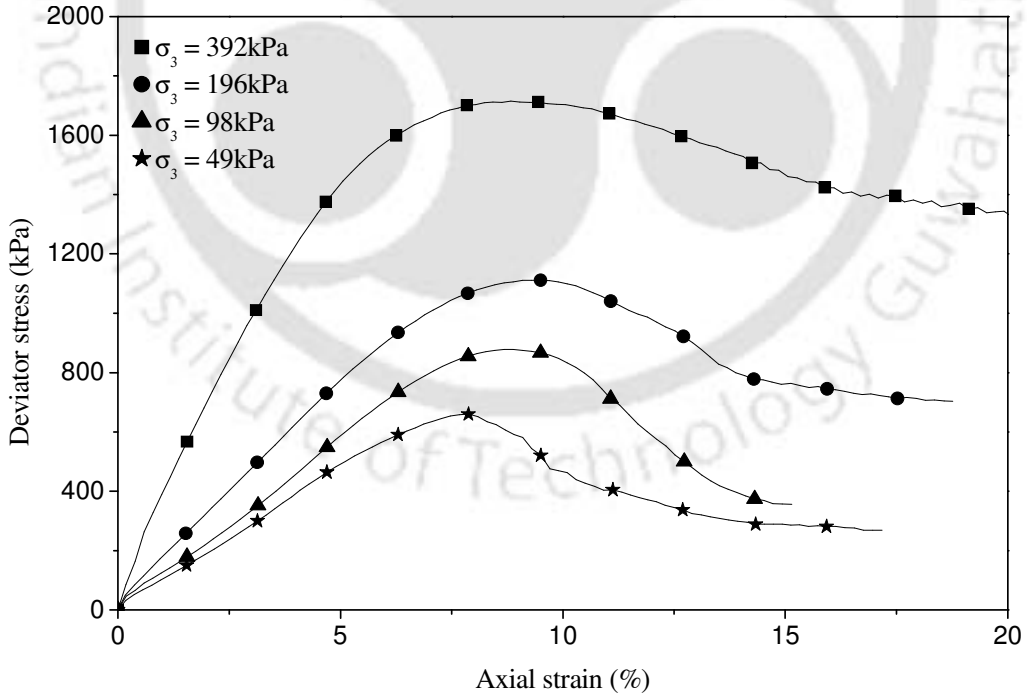

Fig. 6.3 Stress-strain behavior of fiber reinforced soil (L = 40mm, f_c = 4%, D_r = 80%)

TH-1123_10610407

(a) $\sigma_3 = 49$ kPa (b) $\sigma_3 = 98$ kPa

(c) $\sigma_3 = 196$ kPa (d) $\sigma_3 = 392$ kPa

Fig.6.4 Failure modes of fiber reinforced soil (L = 40 mm, $f_c = 4\%$, $D_r = 80\%$)

TH-1123_10610407

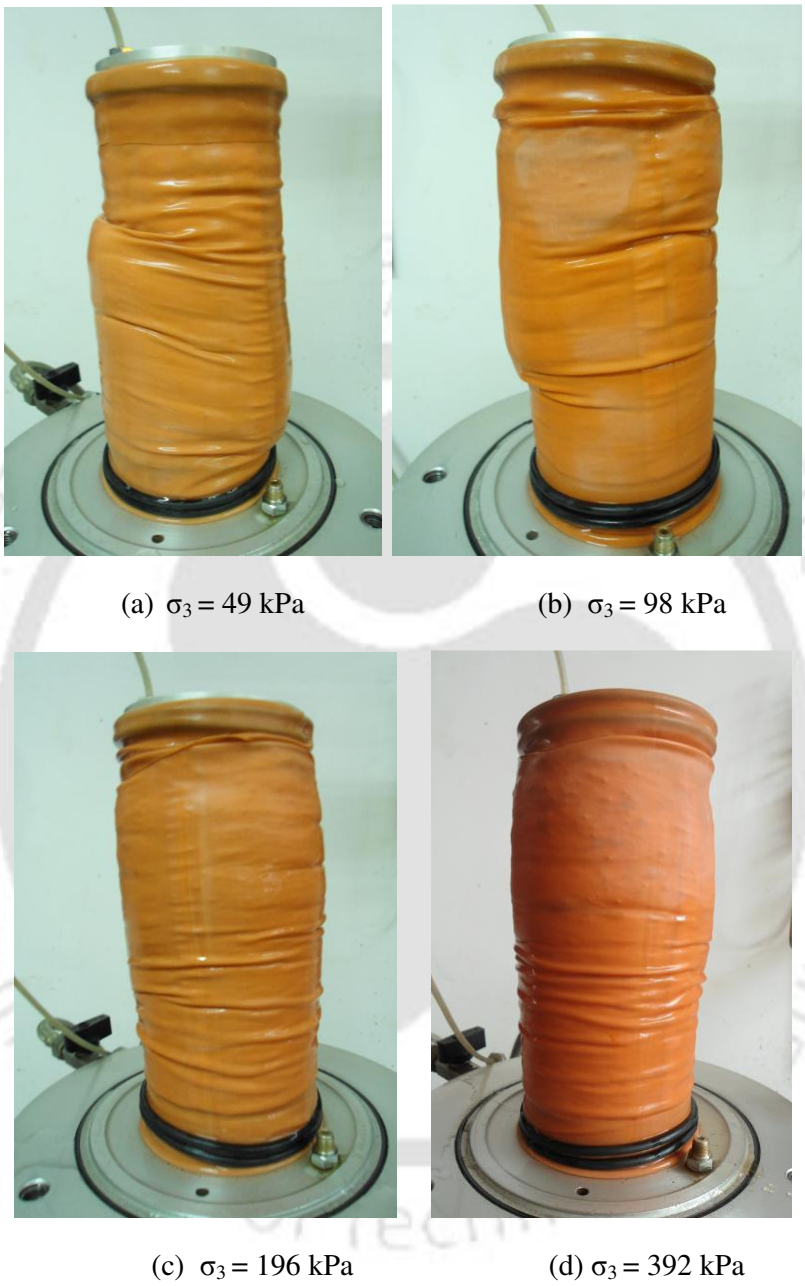

(a) σ_3 = 49 kPa (b) σ_3 = 98 kPa

(c) σ_3 = 196 kPa (d) σ_3 = 392 kPa

Fig. 6.5 Failure modes of geocell-fiber composite reinforced soil (M = 25kN/m, L = 40mm, f_c = 4%, D_r = 80%)

TH-1123_10610407

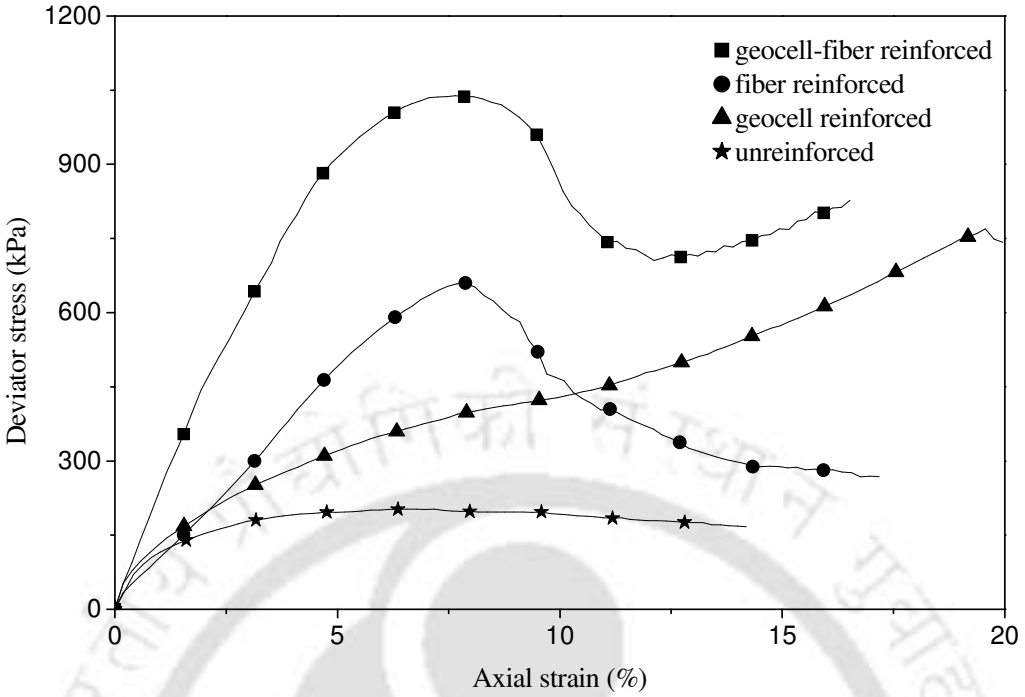

Fig. 6.6 Stress-strain behavior of soil with different form of reinforcement (M = 51kN/m, L = 40mm, f_c = 4%, D_r = 80%, σ_3 = 49kPa)

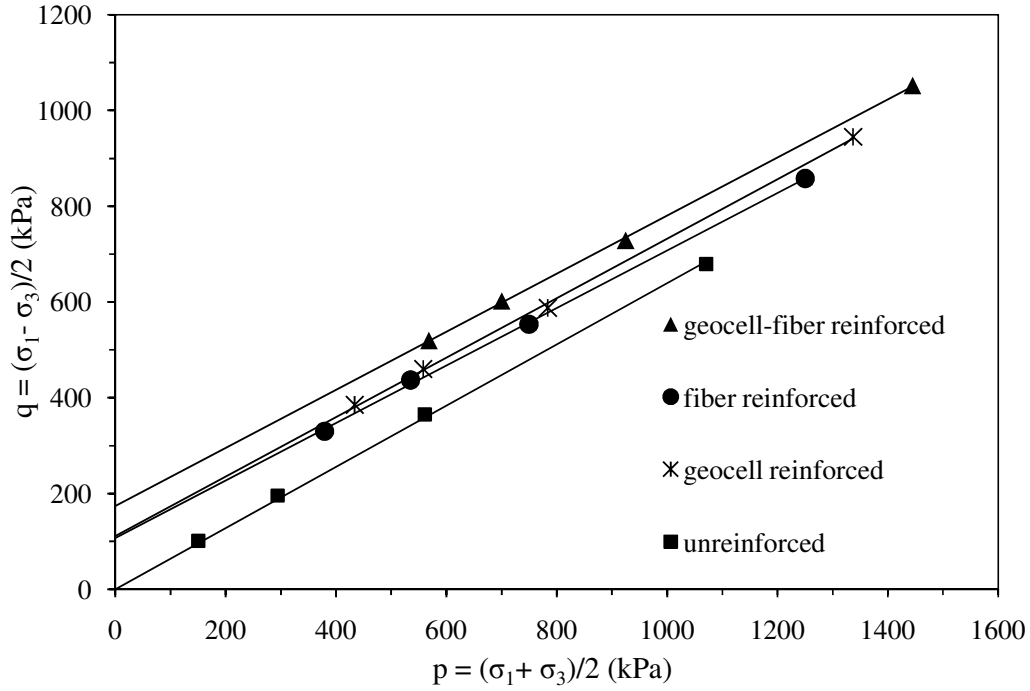

Fig. 6.7 Failure strength envelopes of soil with different form of reinforcement (M = 51kN/m, L = 40mm, f_c = 4%, D_r = 80%)

TH-1123_10610407

6.2.1 Influence of stiffness of geocell

Typical stress-strain responses of a geocell-fiber reinforced soil for two different cases i.e. geocell stiffness of 12.5 kN/m and 51 kN/m, are given Fig.6.8 and 6.9 respectively. It could be seen that with relatively weak geocell (M = 12.5 kN/m) the responses have exhibited a strain softening behavior while with a comparatively stiffer geocell (M = 51 kN/m) they tend to be of strain hardening in nature. Typical failure patterns are depicted in Fig.6.10. It can be seen that with weak geocell there has taken place a bulging cum shear failure (Fig.6.10a). As the geocell owing to low stiffness undergoes yielding the fiber reinforced soil has undergone shear failure leading to the stress drop as observed in the stress-strain responses. However with increased stiffness of the encasing geocell such shear failure is inhibited (Fig. 6.10b) that the specimen has continued to sustain increased loading, exhibiting the strain hardening behavior.

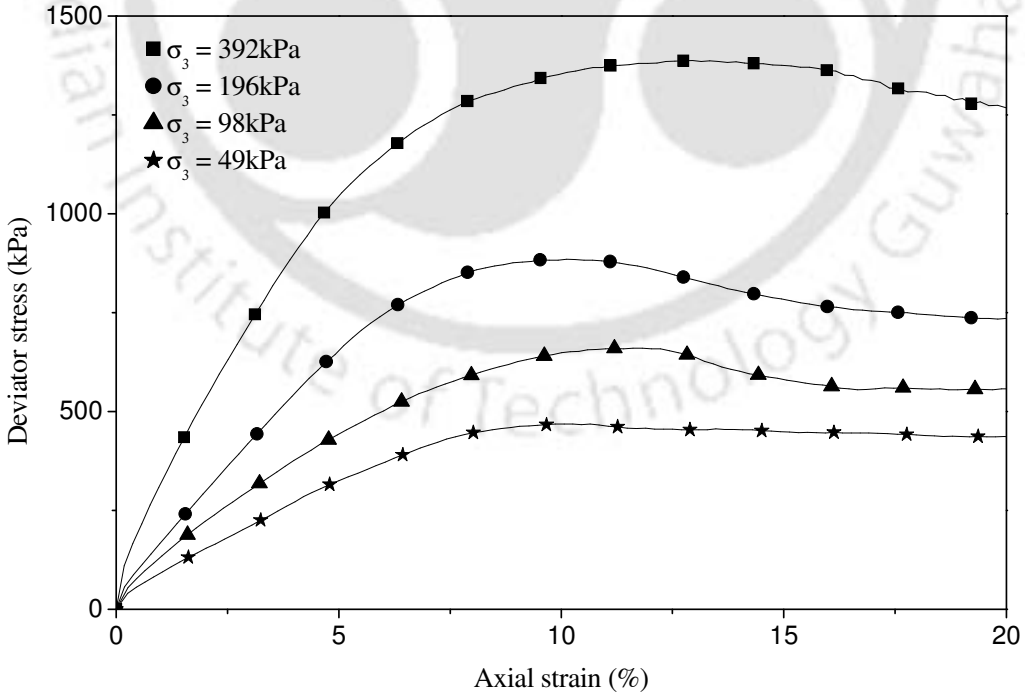

Fig. 6.8 Stress-strain behavior of geocell-fiber reinforced soil (M = 12.5 kN/m, L = 40 mm, f_c = 3 %, D_r = 30 %).

TH-1123_10610407

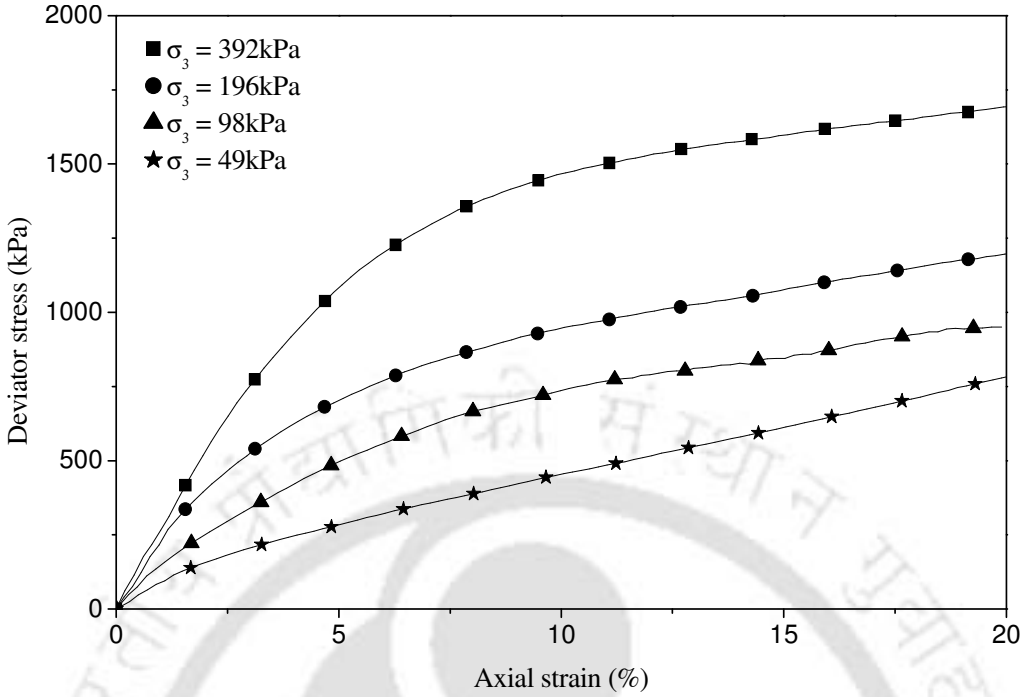

Fig. 6.9 Stress-strain behavior of geocell-fiber reinforced soil (M = 51 kN/m, L = 40 mm, f_c = 3%, D_r = 30%)

(a) M = 12.5 kN/m (b) M = 51 kN/m

Fig. 6.10 Failure modes of geocell-fiber composite reinforced soil (Dr = 30%, L = 40 mm, f_c = 3%, σ_3 = 98 kPa): Influence of stiffness of geocell.

TH-1123_10610407

Stress-strain responses of composite reinforced specimens depicting the influence of geocell stiffness for loose, medium dense and dense soil are shown in Fig. 6.11, Fig. 6.12 and Fig. 6.13 respectively. It could be observed that irrespective of the density of the soil the geocell stiffness has substantially influenced the performance. Both the peak stress and the residual stress have sown a visible increase with increase in the stiffness of the geocell. The stiffness of composite specimen too has shown improvement with increase in stiffness of the encasing geocell. However the overall performance improvement with increase in the geocell stiffness is more prominently felt when the density of the soil is less. This trend is more clearly explained, while discussing the obtained shear parameters in the following section.

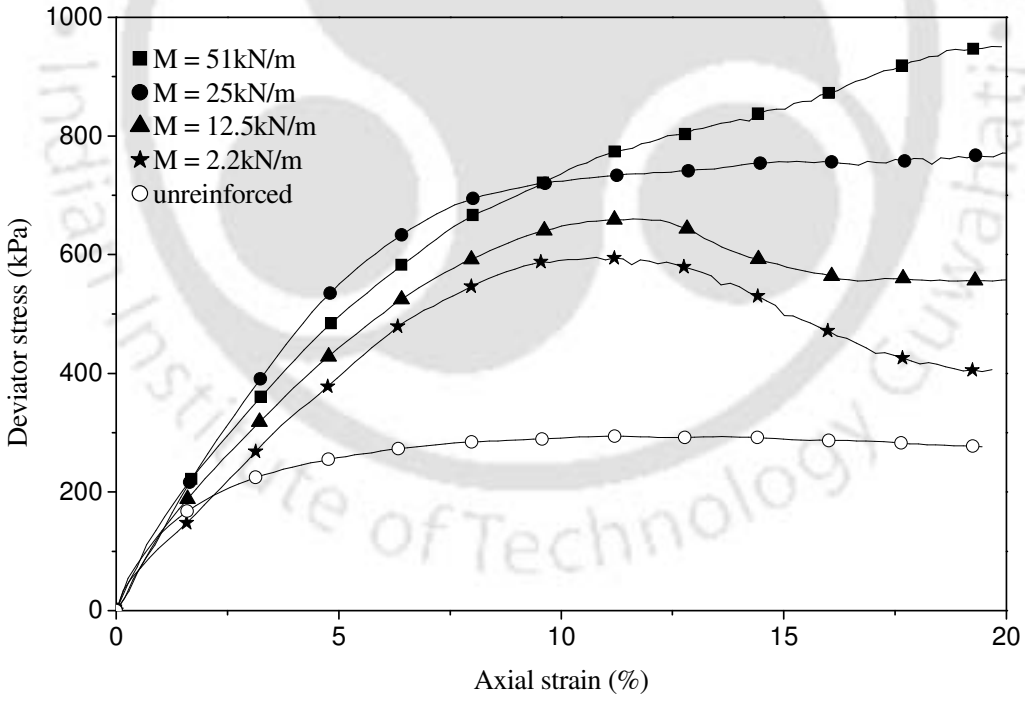

Fig. 6.11 Stress-strain behavior of geocell-fiber reinforced loose soil (D_r = 30%, L = 40mm, f_c = 3%, σ_3 = 98kPa): Influence of geocell stiffness

TH-1123_10610407

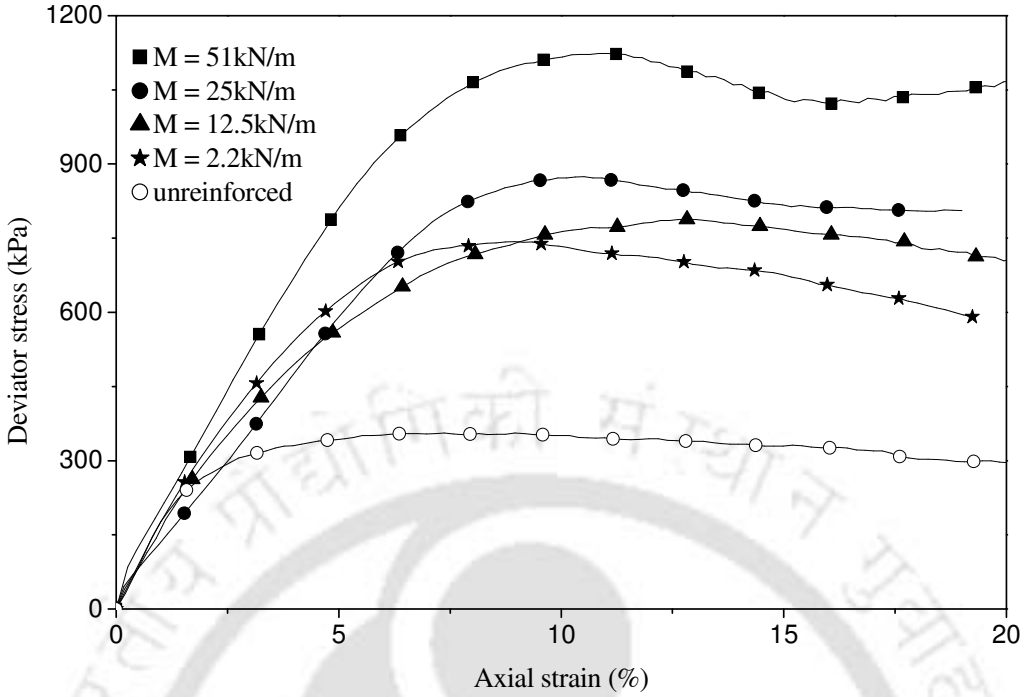

Fig. 6.12 Stress-strain behavior of geocell-fiber reinforced medium soil (D_r = 60%, L = 40mm, f_c = 3%, σ_3 = 98kPa): Influence of stiffness of geocell

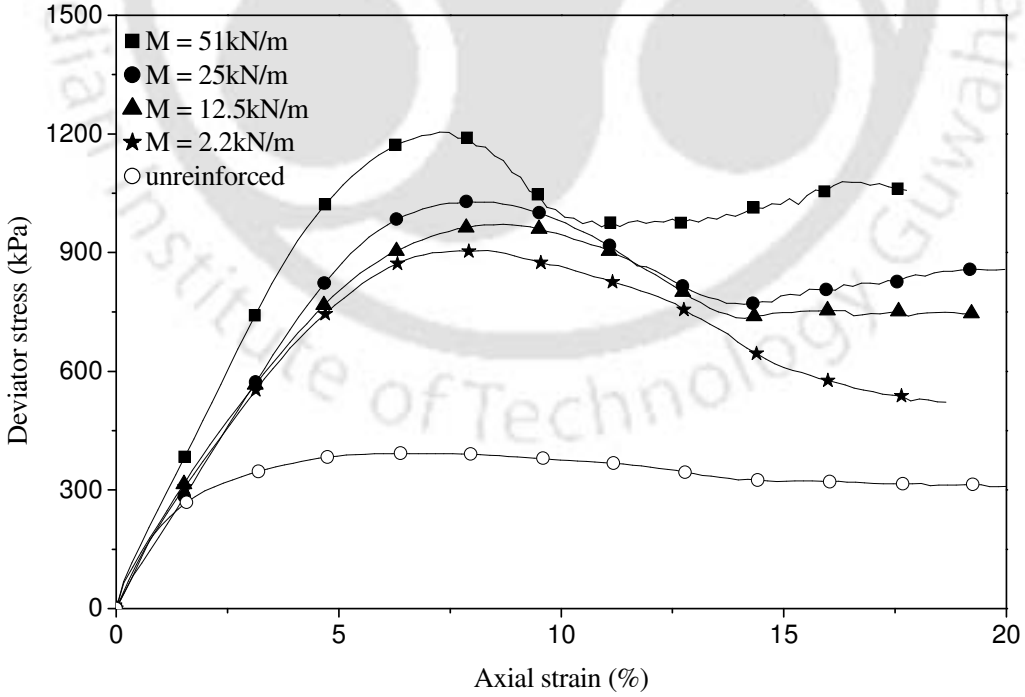

Fig. 6.13 Stress-strain behavior of geocell-fiber reinforced soil (D_r = 80%, L = 40mm, f_c = 4%, σ_3 = 98kPa)

TH-1123_10610407

Failure strength envelopes of the composite soils depicting the influence of the stiffness of the geocell, for the three different cases i.e. loose, medium dense and dense soil, are shown in Fig. 6.14, Fig. 6.15 and Fig. 6.16 respectively. It can be seen that the slope of the p-q plots are almost same for different stiffness of the geocell which indicates that the friction angle of the composite soil hasn't changed much. But the cohesion intercept has shown a visible increase with increase in the geocell stiffness. Similar behavior was observed with geocell and fiber reinforcement alone. Hence it can be said that in the geocell-fiber composite reinforcement, the qualitative behavior of the geocell and fiber reinforcement is almost retained while quantitatively the overall strength has improved substantially. The friction angle and the apparent cohesion (c_{gf}) of the composite reinforced soil, as obtained from the failure envelopes, depicting the influence of geocell stiffness for different relative density of soil, are summarized in Table. 6.1. A comparison with the apparent cohesion values presented in Table 4.1 and Table 5.1 shows that irrespective of the soil and reinforcement characteristics the geocell-fiber composite reinforcement has exhibited increased cohesion (Table 6.1). Hence it can be concluded that in general the geocell-fiber composite is a superior form of reinforcement as compared to the geocell and fiber reinforcement used in single form.

From the data presented in Table 6.1, it can be seen that, with increase in geocell stiffness, the friction angle has remained constant while the apparent cohesion has increased visibly. It is of interest to note that for relatively weak soil (D_r = 30%) composite matrix, when the geocell stiffness has increased from 2.2 kN/m to 51 kN/m the apparent cohesion (c_{gf}) has increased from 80 to 179 kPa, an increment of more than 2.2 fold. Whereas with dense composite soil (D_r = 80%), for similar increase in the geocell stiffness the induced apparent cohesion has increased from 142 kPa to 217

TH-1123_10610407

kPa, just 1.5 fold improvement. Hence it can be said that that the composite system the geocell plays an increased role when the soil is relatively weak. This is possibly because, in loose soil, the fibers due to inadequate interface friction are unable to effectively stand against the surcharge loading. Because of which a large part of the applied pressure gets transmitted to the geocell reinforcement. Given that the geocell surrounds the soil-fiber system it effectively sustains the transmitted pressure primarily through mobilization of its hoop strength. Therefore, with increased strength and stiffness of the geocell reinforcement, in the loose soil composite system, has produced increased strength improvement.

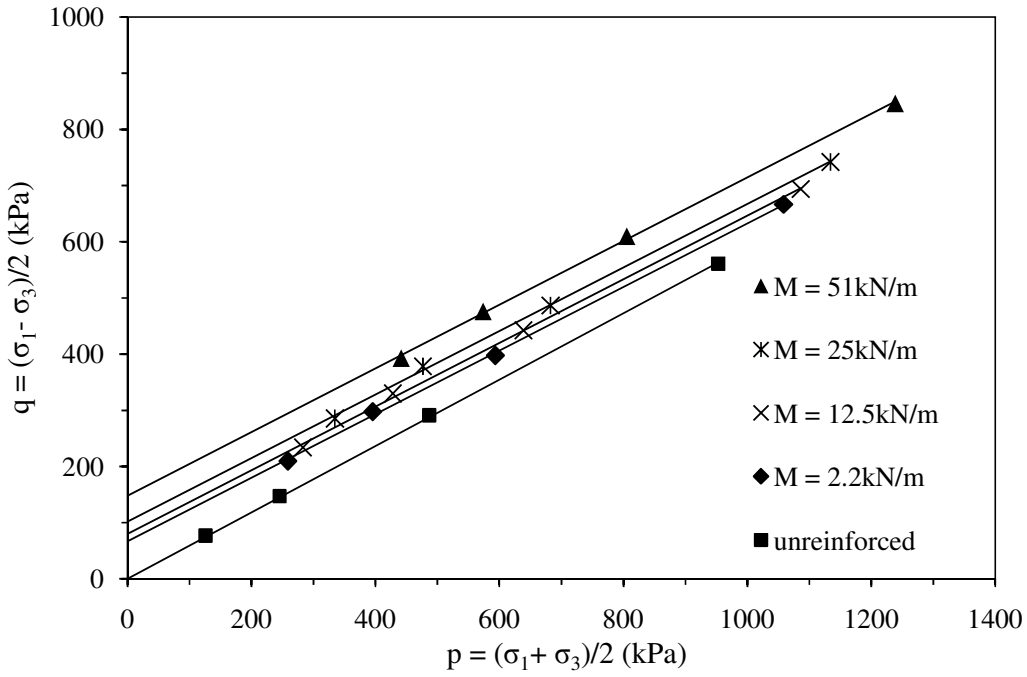

Fig. 6.14 Failure strength envelopes of geocell-fiber reinforced loose soil (D_r = 30%, L = 40mm, f_c = 3%): Influence of geocell stiffness

TH-1123_10610407

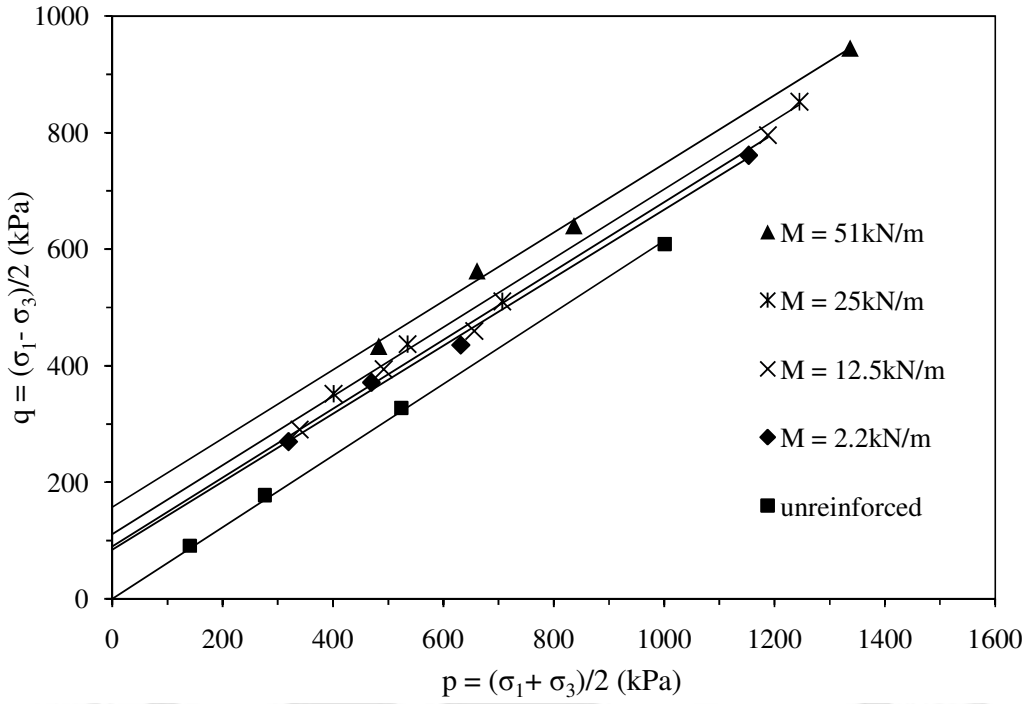

Fig. 6.15 Failure strength envelopes of geocell-fiber reinforced medium dense soil (D_r = 60%, L = 40mm, f_c = 3%): Influence of geocell stiffness.

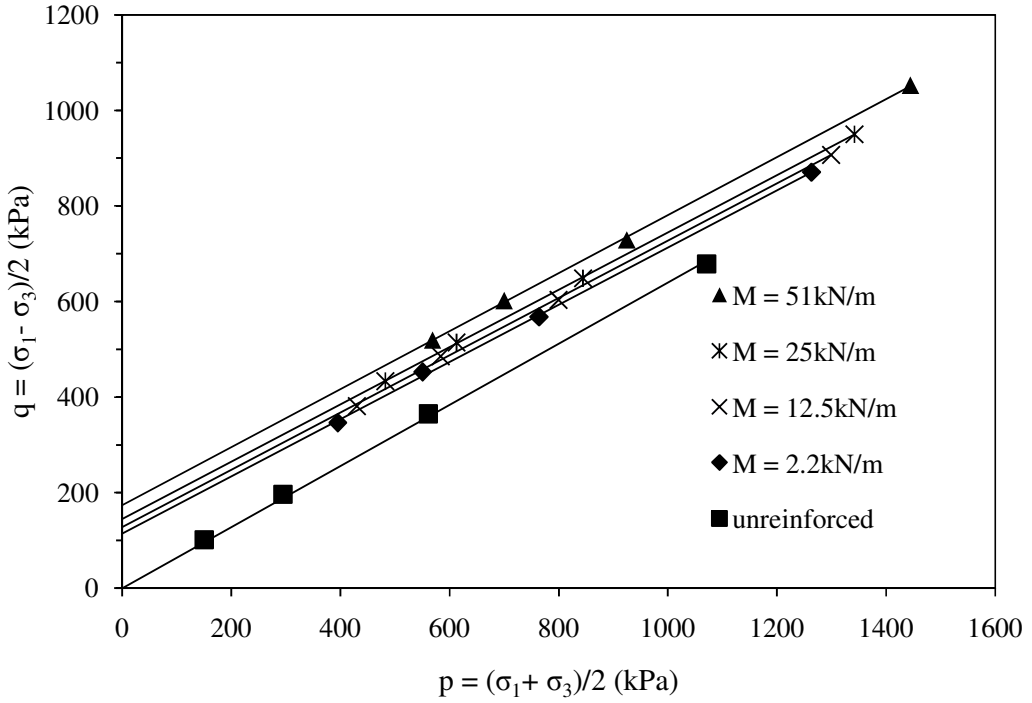

Fig. 6.16 Failure strength envelopes of geocell-fiber reinforced dense soil (D_r = 80%, L = 40mm, f_c = 4%): Influence of geocell stiffness.

TH-1123_10610407

Table: 6.1 Summary of shear strength parameters of geocell-fiber composite reinforced soils: Influence of geocell stiffness

Density of soil D_r (%)	Optimum fiber content, f_c (%)	Geocell stiffness M (kN/m)	Friction angle Φ (°)	Cohesion c_{gf} (kPa)
30	3	2.2	34	80
		12.5	34	97
		25	34	122
		51	34	179
60	3	2.2	36	103
		12.5	36	111
		25	36	137
		51	36	194
80	4	2.2	37	142
		12.5	37	159
		25	37	181
		51	37	217

Note: fiber length was kept constant as 40 mm.

6.2.2 Influence of relative density of soil

Deviator stress versus axial strain responses of composite reinforced soils with varying relative density, for two different stiffness of geocell i.e. M = 2.2 kN/m and 51 kN/m, are shown in Fig. 6.17 and Fig.6.18 respectively. The corresponding failure envelopes are shown in Fig. 6.19 and Fig. 6.20 respectively. It could be observed that, in both the cases increase in soil density has exhibited increased strength and stiffness. Besides, the failure strain is relatively less when the soil is in dense state. The loose soil contracts under deformation, therefore, more strain is required before stress transfer to the reinforcement i.e. fiber and geocell, takes place. Whereas, soil with higher relative density, being a compact structure tends to expand (i.e. dilation), under footing penetration thereby mobilises higher strength of the reinforcement leading to enhanced performance improvement. Besides, the dense soil when dilates induces

TH-1123_10610407

higher frictional resistance at the fiber soil interface as well as derives increased confinement from the geocell leading to increased load carrying capacity.

The shear parameters of the geocell-fiber reinforced soils, for different cases, along with the corresponding friction angles are summarized in Table 6.2. In general both the friction angle and the apparent cohesion have increased with increase in density of the soil in the composite system. This indicates that benefit due to increase in soil density is twofold. First, it increases the inter particle (fiber-soil) friction and interlocking leading to increase in the overall friction angle of the composite system. Second, a dense soil matrix mobilizes increased strength of reinforcement that induces increased confinement unto the soil mass leading to increased cohesion.

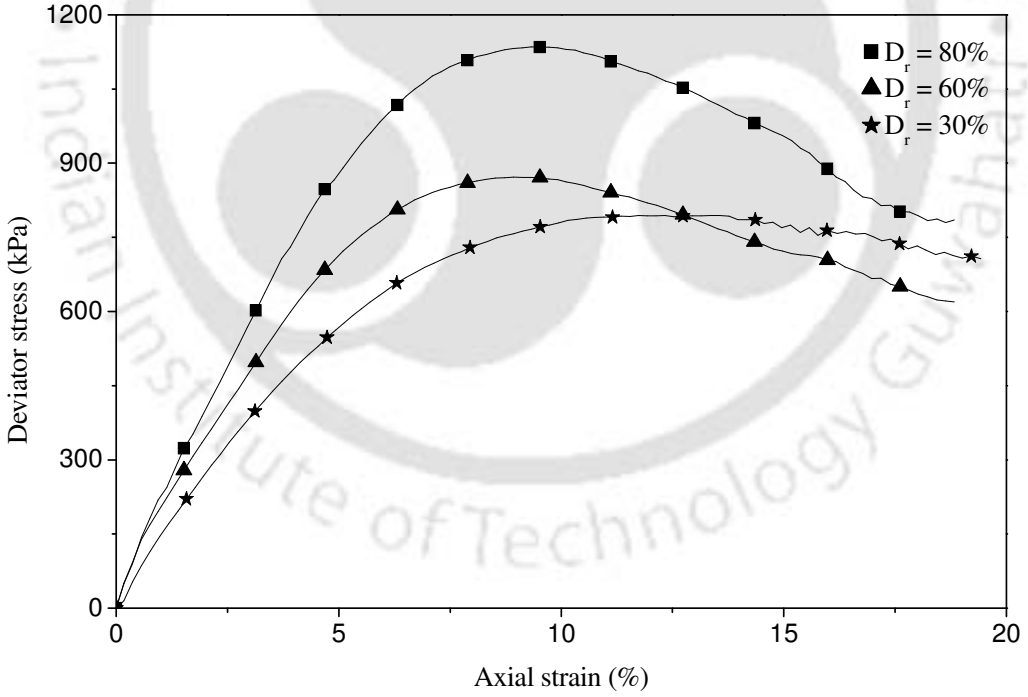

Fig. 6.17 Stress-strain behavior of geocell-fiber reinforced soil (M = 2.2kN/m, L = 40mm, f_c = optimum, σ_3 = 196kPa): Influence of relative density of soil.

TH-1123_10610407

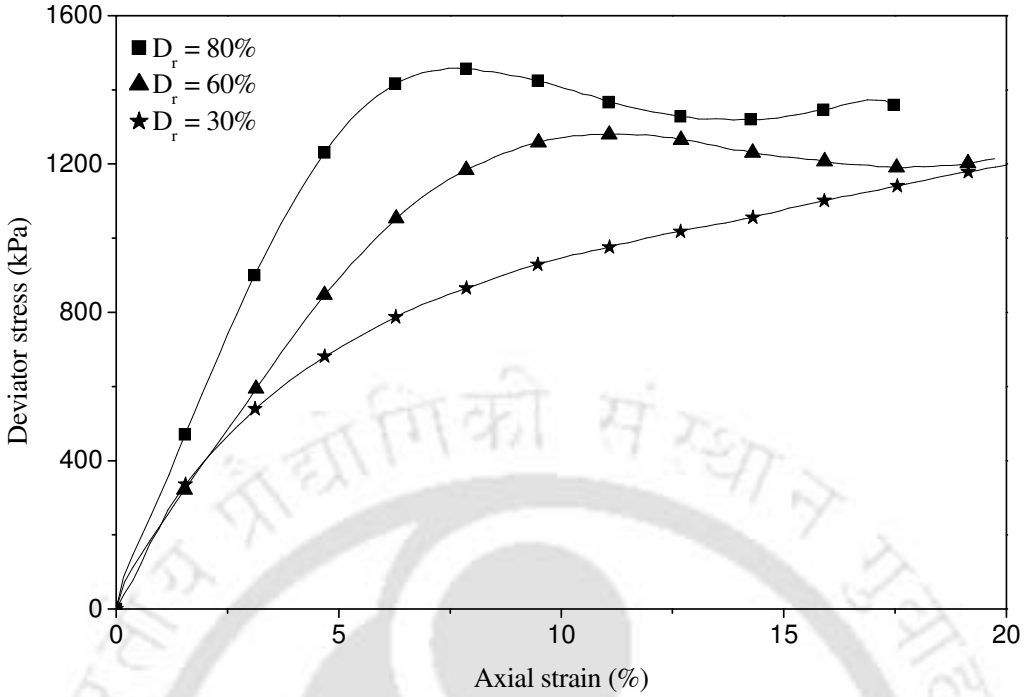

6.18 Stress-strain behavior of geocell-fiber reinforced soil (M = 51kN/m, L = 40mm, f_c = optimum, σ_3 = 196kPa): Influence of relative density of soil.

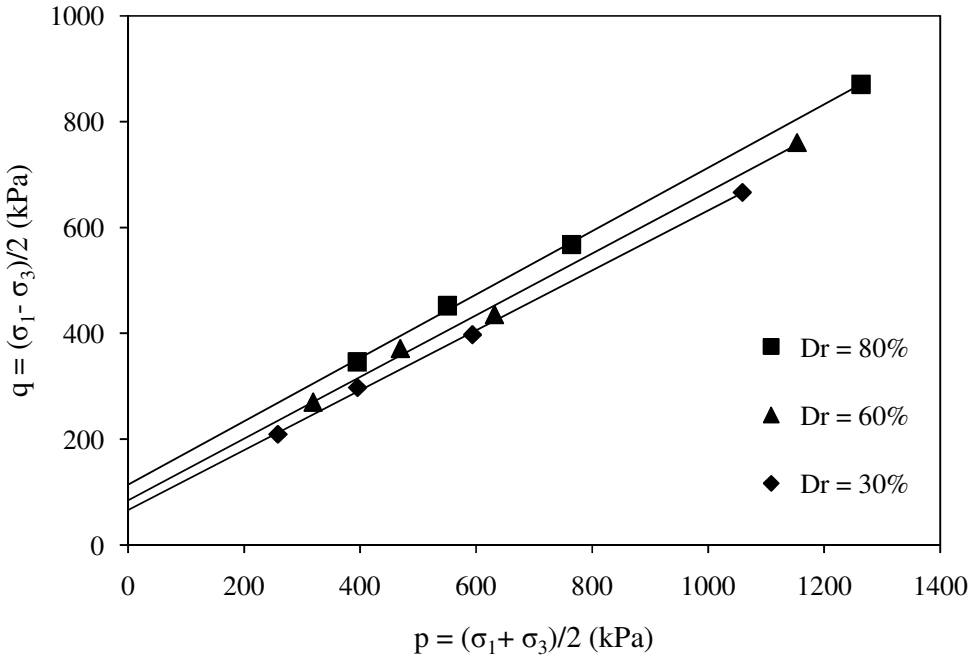

6.19 Failure strength envelopes of geocell-fiber reinforced soil (M = 2.2kN/m, L = 40mm, f_c = optimum): Influence of relative density of soil.

TH-1123_10610407

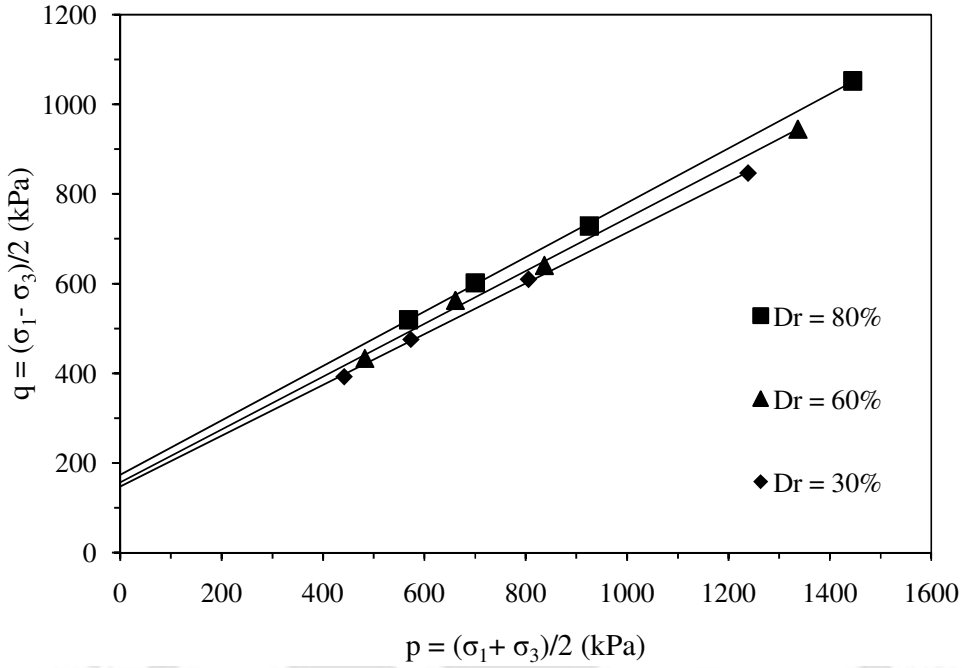

Fig. 6.20 Failure strength envelopes of geocell-fiber reinforced soil (M = 51kN/m, L = 40mm, f_c = optimum): Influence of relative density of soil

Table: 6.2 Summary of shear strength parameters of geocell-fiber composite reinforced soils: Influence of relative density of soil

Geocell stiffness M (kN/m)	Optimum fiber content, f_c (%)	Density of soil D_r (%)	Friction angle Φ(°)	Cohesion c_{gf} (kPa)
2.2	3	30	34	80
	3	60	36	103
	4	80	37	142
12.5	3	30	34	97
	3	60	36	111
	4	80	37	159
25	3	30	34	122
	3	60	36	137
	4	80	37	181
51	3	30	34	179
	3	60	36	194
	4	80	37	217

Note: fiber length was kept constant as 40 mm.

TH-1123_10610407

6.2.3 Influence of confinement pressure

Stress-strain responses of the dense soil with different forms of reinforcement i.e. geocell, fiber, geocell-fiber; for confinement pressure of 98 kPa and 392 kPa are shown in Fig. 6.21 and Fig. 6.22 respectively. Response of the unreinforced soil too is presented for comparison purpose. It can be seen that both at low and high confining pressure the geocell-fiber composite reinforcement has produced maximum strength improvement however, the degree of improvement is different. For example with 98 kPa of confinement the strength of soil has improved from about 300 kPa to more than 900 kPa, an improvement of the order of 3 fold. While with high confinement (i.e. 392 kPa) the increase is only about 1.5 fold (i.e. from 1200 to 1800 kPa). These observations indicate that with increased confinement the reinforcing efficacy of the geocell and fiber is suppressed. Higher the confining pressure, smaller is the dilatancy of the soil. As result of which the mobilized frictional on fiber and hoop stress in the geocell reduces leading to reduced load carrying capacity.

Typical failure patterns for the two different confinement pressures observed in the post test specimen are shown in Fig. 6.23. It can be observed that while with low confinement (98 kPa) the specimen has undergone a clear shear, with high confinement (392 kPa) it has just shown a mild bulging. This clearly shows that, with increased confinement, the expansion of the soil has reduced. With reduced overall strain in the specimen the reinforcement strength mobilization is reduced leading lower performance improvement. Hence it can be said that with relatively lightly loaded structures where the confining pressure is relatively less the efficacy of the geocell-fiber composite is relatively high although even at high confinement pressure its reinforcing ability is significant.

TH-1123_10610407

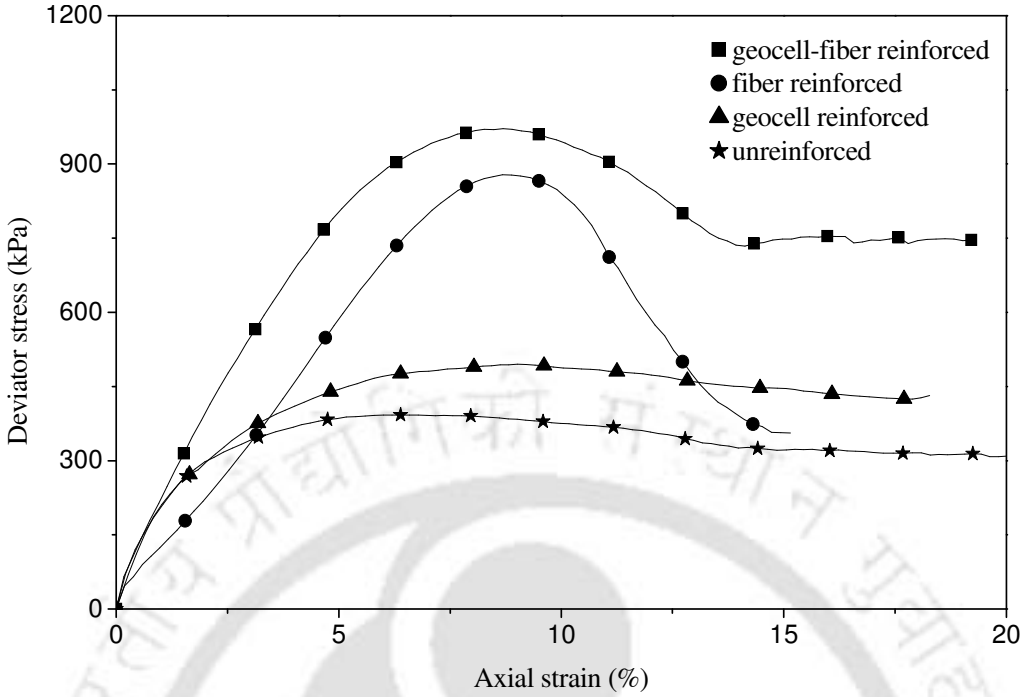

Fig. 6.21 Stress-strain behavior of geocell-fiber reinforced soil (D_r = 80%, M = 12.5kN/m, L = 40mm, f_c = 4%, σ_3 = 98kPa): Low confinement pressure.

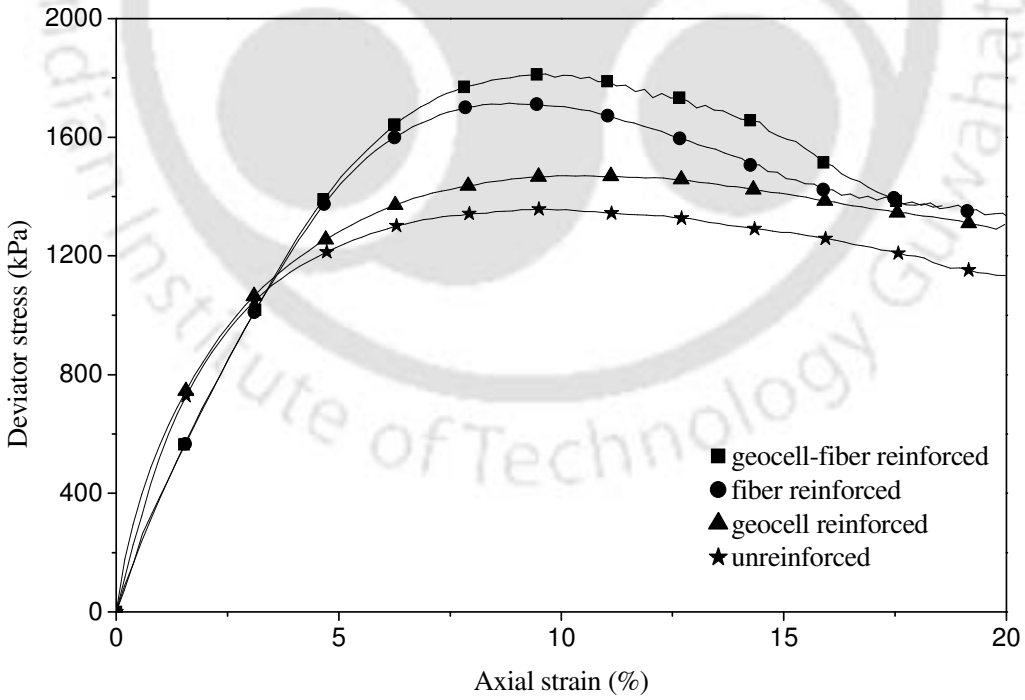

Fig. 6.22 Stress-strain behavior of geocell-fiber reinforced soil (D_r = 80%, M = 12.5kN/m, L = 40mm, f_c = 4%, σ_3 = 392kPa): High confinement pressure

TH-1123_10610407

(a) $\sigma_3 = 98$ kPa (b) $\sigma_3 = 392$ kPa

Fig. 6.23 Failure mode of geocell-fiber reinforced soil ($D_r = 80\%$, M = 12.5 kN/m, L = 40 mm, $f_c = 4\%$): Influence of confinement pressure.

6.3 SACLE EFFECT

As has been discussed above, the mechanical behavior of the composite reinforced soil is found to be governed by the interaction between the geocell and the fiber reinforced soil, contained within. In view of this, the parameters influencing the geocell-soil-fiber composite can be taken as: D, h, S_{gc} d, L, S_f, γ, ϕ, G, δ, σ_1, σ_3; wherein, D is the diameter of the geocell that same as the diameter of the specimen, h is the height of the geocell, S_{gc} is the strength/stiffness of the geocell reinforcement, L is the length of the fiber, d is the diameter of the fiber, S_f is the strength/stiffness of the fiber, γ is the unit weight of soil, ϕ is the friction angle of the soil, G is the shear modulus of soil, δ is the fiber-soil interface friction angle, σ_1 is the vertical surcharge pressure, σ_3 is the confinement pressure. Therefore, the function (f) that governs the geocell-soil-fiber composite system can be written as

$$f(D, h, S_{gc}\, d, L, S_f, \gamma, \phi, G, \delta, \sigma_1, \sigma_3) = 0 \qquad (6.1)$$

TH-1123_10610407

Following the scaling law and dimensional analysis procedures, as explained in section 4.4 of chapter 4 and section 5.4 of chapter 5, it is found that the geometric parameters of the composite system exhibit linear variation while the strength and stiffness parameters vary in second order for geocell reinforcement and first order for fiber reinforcement.

6.4 PREDICTION OF STRENGTH OF COMPOSITE REINFORCED SOIL

The test results have demonstrated that the load carried by the composite reinforced specimen is globally governed by the interaction of the geocell and the fiber reinforced soil contained within. Besides, the strength improvement of soils due to the geocell-fiber composite reinforcement is primarily through development of an apparent cohesion. Similar is the case with geocell and fiber reinforcement when used alone. Hence the apparent cohesion due to the composite reinforcement can be modeled as a function of both the geocell and fiber reinforcement coupled with the interaction between the two. Based on this the following equation is proposed to model the apparent cohesion (c_{gf}) due to the composite reinforcement.

$$c_{gf} = \frac{M}{D_o}\left[\frac{1-\sqrt{1-\varepsilon_a}}{1-\varepsilon_a}\right]\sqrt{K_p} + \frac{L}{4}\pi d(\sigma_{conf} + \Delta\sigma_3)(tan\delta)N_f(tan\varphi) \quad (6.2)$$

The terminologies used have already been defined in the sections 4.5 and 5.5 of chapter 4 and 5 respectively. However, in order to take into account the interaction between the geocell and fiber reinforcement the confinement stress acting on the fiber reinforcement is added with the confinement pressure induced by the geocell reinforcement ($\Delta\sigma_3$, Eq. 4.11). A comparison of the experimentally obtained values of the apparent cohesion (c_{gf}) with the theoretically obtained ones, are shown in Table

TH-1123_10610407

6.3 (Fig. 6.24). It can be seen that with relatively stiffer geocell in the composite reinforcement the predicted values of the cohesion is relatively close to that of the experimentally observed one. However, the difference between the two is found to be large when the stiffness of the geocell less. This is possibly because the model doesn't take into account the strain variation due to bulging of the specimen which is prominent when the geocell stiffness is low. Therefore, in order the model to predict well, further development incorporating the strain localization effect is required.

Table 6.3: Apparent cohesion of composite reinforced soil: Comparison of experimental data with the theoretically predicted values.

Density of soil D_r (%)	Fiber content f_c (%)	Geocell stiffness M (kN/m)	Cohesion c_{gf} (kPa) Experiment	Cohesion, c_{gf} kPa) Predicted: Eq.6.2
30	3	2.2	80	58
		12.5	97	74
		25	122	139
		51	179	233
60	3	2.2	103	79
		12.5	111	99
		25	137	132
		51	194	205
80	4	2.2	142	129
		12.5	159	151
		25	181	183
		51	217	238

TH-1123_10610407

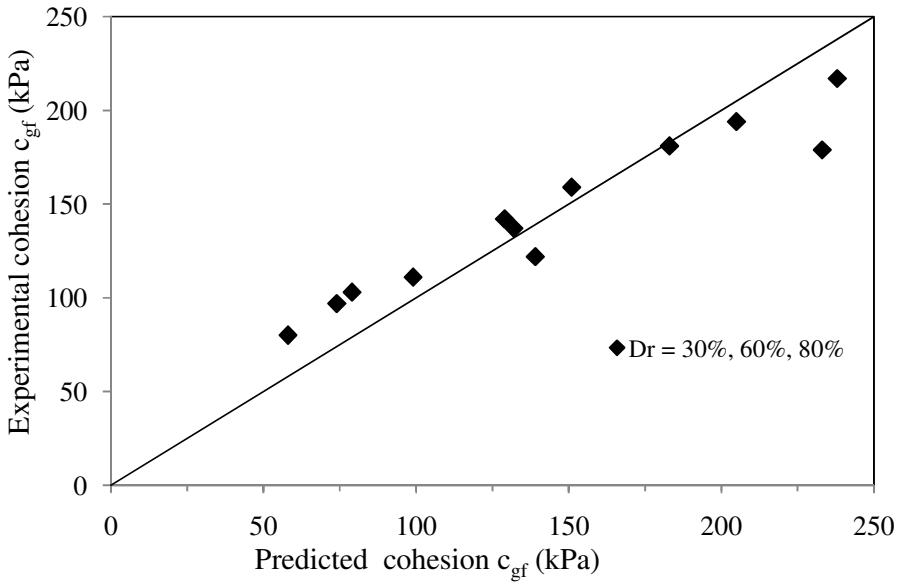

Fig. 6.24 Experimental versus predicted value of cohesion for geocell-fiber reinforced soil

6.5 SUMMARY

Presented in this chapter are the results of triaxial compression tests carried with geocell-fiber composite reinforced soils. The tests were carried out with varied density of soil and stiffness of the geocell. However the fiber length content in the fill soil was kept at their optimum values as determined from tests with fiber reinforcement alone. The obtained results are analyzed and discussed. It is found that as compared to the geocell or fiber reinforcement, the geocell-fiber composite reinforcement exhibits improved peak as well as the residual strength. The proposed theoretical model based on the combined strength improvement due to the geocell and fiber reinforcement components is found to better predict the induced apparent cohesion (c_{gf}) of the composite specimen. However with weak geocell the difference between the predicted and observed values is found to increase.

TH-1123_10610407

CHAPTER 7

SUMMARY AND CONCLUSIONS

7.1 SUMMARY

Since the pioneering work of Vidal (1969), numerous reinforced soil structures have been built across the world. Initially reinforcing of soils was primarily done through planar metallic strips and fabric sheets such as geotextiles and geogrids. Subsequent introduction of fiber reinforcement in soils was found to have effectively improved its strength and stiffness characteristics. The more recent advancement in this field is to provide three-dimensional confinement to the soil by using geocells. The details of these reinforcement techniques are presented in Chapter 1.

The review of literature presented in Chapter 2 brings out that both geocell and fiber reinforcements are effective means of improving the strength and stiffness of soils. While the geocell reinforcement primarily improves the performance of soils through three-dimensional confinement, the fiber reinforcement induced improvement is through surface interaction i.e. interlocking and frictional bond. The findings from reported literatures are summarized and the objective of the present study has been brought out.

Under the present investigation, several series of triaxial compression tests have been carried out to study the influence of different forms of reinforcements i.e. geocell, fiber, geocell-fiber composite; in the cohesionless granular soils. The details of the soil and reinforcements used, test set up and test procedures are discussed at length in Chapter 3.

TH-1123_10610407

The results of triaxial compression tests on unreinforced and geocell reinforced soils presented and discussed in Chapter 4. The parameters such as strength and stiffness of geocells, density of fill soil and the confinement pressure applied are found to have an influence on the performance of the geocell reinforced soils. In chapter 5 results of triaxial compression tests on fiber reinforced soils are presented and discussed. The influences of different parameters such as fiber content, length of fiber, density of soil and confinement pressure applied are considered. In chapter 6 results of triaxial compression tests on geocell-fiber reinforced soils are presented and discussed. The parameters investigated are stiffness of geocell, relative density of soil, and confinement pressure. It is found that these parameters have influence on the performance of geocell-fiber reinforced soil.

7.2 CONCLUSIONS

1. With geocell reinforcement the granular soil has shown visible increase in its load carrying capacity. The triaxial compression tests data when plotted onto the Mohr-Coulomb failure envelope indicates that the strength improvement due to the geocell reinforcement is primarily through an induced apparent cohesion while the friction angle remains almost same as that of the unreinforced soil.
2. While the unreinforced sand, after about 7% strain has undergone failure, with geocell encapsulation the granular soil has continued to take load until axial strain as high as 17%. This indicates that the geocell reinforcement can improve the ductility behavior of soil. Hence it can be said that an increase in the permissible strain limit in the design of structures made of geocell-reinforced soils is not likely to cause much of inconvenience.

TH-1123_10610407

3. From the failure patterns observed in the triaxial compression tests it is established that the geocell reinforcement through its three dimensional confinement can effectively inhibited the formation of rupture planes in the soil mass leading to increased performance improvement.
4. The performance improvement of the reinforced soil is found to increase with increase in the strength and stiffness of the geocell. However, there happens to be a threshold of geocell beyond which the performance improvement of the reinforced soil is visibly high.
5. With increase in the density of the fill soil there is an overall improvement in the load carrying capacity of the geocell-soil system. Therefore, the soil in the geocells should be compacted to higher density.
6. The strength improvement is primarily through an induced confinement due to the membrane stress developed in the geocell reinforcement owing to its three-dimensional geometry that encapsulates the soil within. Using this mechanism a theoretical model based on the membrane correction theory of Henkel and Gilbert (1952) is used to predict the apparent cohesion induced by the geocell onto the encapsulated soil mass. It is found that the theory can satisfactorily estimate the apparent cohesion when the geocells are relatively stiff. But, with weak geocell the prediction is substantially in the lower side of the observed value. This is attributed to the bulging induced strain variation over the specimen.
7. In general, with fiber reinforcement, the load carrying capacity of the soil is found to have improved significantly. The improvement is similar to that of geocell

TH-1123_10610407

reinforcement that the fiber reinforcement develops an apparent cohesion (c_f) in the granular soil.

8. The apparent cohesion (c_f) increases with increase in the fiber content until a certain limit beyond which further improvement is marginal. The optimum fiber content giving maximum apparent cohesion is about 2-3% when the fiber length is short i.e. 10 mm, 20 mm. But with long fibers i.e. 40 mm and 80 mm the optimum fiber content is relatively high i.e. of the order of 4-5%.
9. With increase in fiber content there takes place a reduction in the friction angle of the fiber-soil composite. This is possibly due to reduced soil to soil contact because of increased fiber content. However, except for very long fibers and dense soil matrix this reduction in friction angle is practically negligible.
10. It is observed that the strength of the soil has continued to increase with increase in fiber length till 40 mm beyond which further improvement is marginal. As such it was found that fibers longer than 40 mm are difficult to mix. Hence it can be said that the optimum length of the discrete glass fibers giving maximum performance improvement in granular soils is about 40 mm.
11. Both the strength parameters; apparent cohesion and friction angle, of the fiber reinforced soil have shown a visible increase with increase in density of the soil. But the stiffness of the soil-fiber composite has undergone a striking improvement with increase in density of soil which was not the case when the fiber length and content was increased. Hence it can be said that in order to improve the stiffness of fiber reinforced soil one needs to increase the density of the soil rather than the fiber length and content.

TH-1123_10610407

12. Combined application of geocell and fiber reinforcement can increase the peak and residual strength substantially, much ahead of the case with geocell or fiber reinforcement provided alone. Even the stiffness of the geocell-fiber composite is much superior to that of the geocell or fiber reinforced soil.
13. The performance of the geocell-soil-fiber composite has markedly increased with increase stiffness of the geocell. This is because a stiffer geocell effectively restrains the shearing in the fiber reinforced soil mass encased within.
14. The increase in density of the fill soil has also exhibited a visible increase in the performance of the composite soil mass. As the dense soil tends to dilate it induces higher frictional resistance at the fiber soil interface as well as derives increased confinement from the surrounding geocell leading to increased load carrying capacity of the composite system.
15. The theoretical model based on force-equilibrium principle is found to be reasonably good in predicting the strength improvement due to the geocell-fiber composite reinforcements in the granular soil.
16. Dimensional analysis shows that while the geometric parameters of the geocell, fiber reinforcement have a linear variation; their strength exhibits a second order variation for geocell reinforcement and linear for fiber reinforcement. Therefore, for the present test data to be valid in prototype case the strength of geocell-fiber reinforcement should be N^2 times the strength of the prototype for geocell reinforcement and N times fiber reinforcement, where N is the model scale.

TH-1123_10610407

7.3 SCOPE FOR FURTHER RESEARCH

The scope of further research is suggested as below:

- In present study only single type of fiber was used. By varying surface properties, strength properties, diameter etc. of fiber, it can be better understood about the effect of fiber properties on performance of fiber and geocell-fiber reinforcement.
- Since single geocell was used, so effect of the interaction between the geocell reinforced soil of one pocket with soil of neighborhood geocell was not considered in this study, so further investigation on multiple geocell is required.
- A numerical model can be obtained to study the behavior of geocell-fiber reinforced soil for various properties of geocell and fiber.
- Effect of volume change on the reinforcing action of geocell reinforcement, fiber reinforcement and composite reinforcement can be further investigated by performing the test under different drainage condition.
- By varying the type of soil, the effect of the different form of reinforcement and its interaction with soil can be better understand.

TH-1123_10610407

ACKNOWLEDGEMENTS

I have been associated with some handful of people, whose contribution in assorted ways to my thesis work deserves special mention.

First and foremost, I would like to express my sincere and heart-felt gratitude to my mentor and supervisor Dr. S.K. Dash for his valuable guidance, encouragement, and gracious support during this thesis phase. His valuable suggestions, effective co-operation and encouraging interactions were a great driving force for me to carry out the research work. I am also grateful to Dr. Sreedeep S. for his valuable time that he devoted with me and motivated me during my last phase of thesis work. I would like to thank my Doctoral committee members, Dr. A.K. Mishra, Dr. Bimlesh kumar, and Dr. S. Senthilvelan for sparing their valuable times in reviewing my work.

I thank to former Heads of Department Dr. S.K. Deb and present Head of Department Dr. A.K. Sarma for the facilities provided for conducting the research. I am also thankful to scientific officer of Civil Engineering Department; Mr. K. Pallav for extending all possible support. I gratefully acknowledge the unstinted help provided by Mr. Hari Ram Upadhyaya for helping me in test setup. Also, I would like to thank all Civil Engineering staff members for their support directly or indirectly.

I convey my special thanks to my friends Mr. Prabhudutta and Mr. Harinarayan for their friendly forbearance and support for my experiments. My other friends Abhijit, Arvind, Arghadeep, Asfaq, Awadhesh, Deepjyoti, Jiwan, Jitendra, Pawan, Pranjal, Rajkumar, Ramu, Shivshankar, and Suchit have made my time at IITG enjoyable and memorable. I

TH-1123_10610407

feel a lasting gratitude towards my school and graduation friends Abhay, Amrita, Mantu, Tushar and vikas who always kept me in their prayers.

It is not possible to express in words the inspirations from my parents, and my younger brother Animesh whose invaluable love, endless patience and unstinted support has brought me to this position. The concern and love of my relatives, cousins and family friends are highly appreciated. I am also grateful to all my teachers (especially Prof. K.K. jain, Mr. Ravindra K. Goliya, and Mr. Chandrabhushan SIngh) for the lessons they taught me.

Last but not least; I thank all souls of universe for giving me patience and strength directly and indirectly when I needed most.

Akash priyadarshee

TH-1123_10610407

ABSTRACT

Keywords: Reinforced soil, Geocell-fiber reinforcement, triaxial compression tests, performance improvement, apparent cohesion, scale effect, peak stress, residual stress.

Reinforcing the soil using geosynthetics is one of the fast growing techniques for ground improvement, primarily due to overall economy, simplicity and ease of construction. The geocell reinforcement is recently developed one which has a three dimensional structure that can effectively contain and confine the soil within. The other form of soil reinforcement is through randomly distributed fibers the mechanism of which is similar to that of roots in the soil. The review of literature indicates that both geocell and fiber reinforcement can effectively improving the performance of soils.

Under the present investigation, several series of triaxial compression tests have been carried out to study the influence of different forms of reinforcements i.e. geocell, fiber, geocell-fiber composite; in the sandy soil. The influence of various parameters such as; strength and stiffness of geocell reinforcement, length and content of fiber reinforcement, density of soil, ambient confinement pressure; have been studied in depth.

The test results indicate that the geocell reinforcement induces an apparent cohesion to the granular soil mass which increases with increase in the stiffness of the geocell. There is an overall improvement in the load carrying capacity of the geocell-soil system with increase in the density of the fill soil. The dimensional analysis indicates that for the present results to be valid, the strength of the reinforcement in the prototype reinforced soil foundation bed should be of N^2 times the strength of the reinforcement used in the

TH-1123_10610407

model tests, where N is the model scale. The induced apparent cohesion due to geocell reinforcement can be predicted through the membrane correction theory of Henkel and Gilbert (1952).

It has found from results that, similar to geocell reinforced soil, fiber reinforced soil also induced significant apparent cohesion onto the granular soil. With increase in the length and content of fiber, increase in strength of soil is found. But after a certain limit of length and content, improvement in load carrying capacity is marginal. With increase in the density of soil stiffness and strength of soil also increases. Similarly dimensional analysis was performed on the different parameters related to the fiber reinforced soil and which shows that for the present results to be valid, the strength of the reinforcement in the prototype reinforced soil foundation bed should be of N times the strength of the reinforcement used in the model tests, where N is the model scale Simple force-equilibrium model has used to predict the cohesion induced by fiber reinforcement.

Peak stress and residual stress both due to geocell-fiber reinforced soil is found much more, as compared to geocell and fiber reinforcement alone. The test results show that with increase in the stiffness of geocell induced cohesion also increases. It is found that with increase in the density of soil strength and stiffness both increases. Dimensional analysis for composite reinforced soil also indicates that if N is model scale, then for validation of present study strength of the prototype reinforced soil foundation bed should be of N^2 times of the strength of the geocell reinforcement and N times fiber reinforcement used in model tests. In the model for the prediction of induced cohesion it has assumed that induced cohesion will be function of the cohesion induced by geocell reinforcement, fiber reinforcement and interaction between these two reinforcements.

TH-1123_10610407

Contents

TABLE OF CONTENTS

TH-1123_10610407

Table of Contents (continued)

TH-1123_10610407

Table of Contents (continued)

TH-1123_10610407

LIST OF TABLES

TH-1123_10610407

LIST OF FIGURE

TH-1123_10610407

List of figures (continued)

TH-1123_10610407

List of figures (continued)

TH-1123_10610407

List of figures (continued)

TH-1123_10610407

List of figures (continued)

TH-1123_10610407

List of figures (continued)

TH-1123_10610407

List of figures (continued)

TH-1123_10610407

List of figures (continued)

TH-1123_10610407

List of figures (continued)

TH-1123_10610407

List of figures (continued)

TH-1123_10610407

TH-1123_10610407

ABBREVIATIONS

3D	Three dimensional
ASTM	American Society for Testing and Materials
LVDT	Linear Variable Differential Transducer
SEM	Scanning electron micrograph
SP	Poorly graded sand
UCS	unconfined compressive strength
USCS	Unified Soil Classification System

TH-1123_10610407

NOTATIONS

English Symbols

a	intercept of p-q plot
B	width of footing
c	cohesion
c_f	apparent cohesion due to fiber reinforcement
c_g	apparent cohesion due to geocell reinforcement
c_{gf}	apparent cohesion due to geocell-fiber reinforcement
C_c	coefficient of curvature
C_u	uniformity coefficient
d	diameter of fiber
D	diameter of specimen
D_o	Initial diameter of geocell
D_{50}	grain size corresponding to the 50% finer
D_r	relative density of soil
f_c	fiber content
G	shear modulus of soil
G_f	specific gravity of fiber
GT_1	geotextile 1
GT_2	geotextile 2
GM_1	geomesh 1
GM_2	geomesh 2
h	height of geocell
h_{gc}	initial height of geocell
h_s	initial height of the soil cylinder
i	angle of orientation of fiber with shear surface
k	shear distortion ratio
L	length of fiber
L_{eff}	effective length of fiber
M	secant modulus of geocell

TH-1123_10610407

N	model scale
N_c	bearing capacity factor
N_f	number of fibers per unit area
N_v	number of fibers per unit volume
p	hydrostatic stress invariant
q	shear stress invariant
S_f	strength/stiffness of the fiber
S_{gc}	strength/stiffness of the geocell reinforcement
t	initial thickness of the geocell
t_r	tensile strength per unit area of soil
V_r	volume ratio of fiber
W	weight of the specimen
W_f	Weight of fiber
W_s	Weight of soil
x	horizontal component of shear displacement
z	thickness of shear zone

Greek symbols

α	slope of p-q plot
δ	fiber soil interface friction angle
$\Delta\sigma_3$	induced confinement due to the geocell
ΔS	increased shear strength
ε_a	axial strain of the specimen
ε_c	Circumferential strain
$\emptyset$	internal angle of friction of the soil
γ	unit weight of soil
γ_d	placement density of soil and fiber mixture
γ_w	unit weight of water
σ_1	major principal stress
σ_{1max}	maximum axial stress

TH-1123_10610407

σ_3	minor principal stress
σ_{3max}	peak minor stress
σ_{avg}	average interface shear stress
σ_{conf}	confinement stress applied onto the specimen
σ_m	membrane stress
σ_r	tensile stress at fiber plane
τ	shear strength of soil

TH-1123_10610407

REFERENCES

1. **Adams, T.M.**, and **Collin, J.G.,** (1997). "Large model spread footing load tests on geosynthetic reinforced soil foundations." *Journal of Geotechnical and Geoenvironmental Engineering,* ASCE, **123**, 66-72.
2. **Ahmad, F., Bateni, F.,** and **Azmi, M.** (2010). "Performance evaluation of silty sand reinforced with fibers." *Geotextiles and Geomembranes,* **28,** 93-99.
3. **Al-Refeai, T.O.** (1991). "Behavior of granular soils reinforced with discrete randomly oriented inclusion." *Geotextiles and Geomembranes,* **10,** 319-333.
4. **Al-Refeai, T.O.,** (1992). "Model tests on strip footing on reinforced sand." *Journal King Saud university,* **4,** 155-169.
5. **ASTM standard D792,** 2008. Standard test methods for density and specific gravity (relative density) of plastics by displacement. ASTM International, West Conshohocken, PA 2010.
6. **ASTM standard D 0854,** 2006. Standard test methods for specific gravity of soil solids by water pycnometer. ASTM International, West Conshohocken, PA, 2006, vol. 04.09.
7. **ASTM standard D 2256,** 2010. Standard test method for tensile properties of yarns by the single-strand method. ASTM International, West Conshohocken, PA 2010.
8. **ASTM standard D 2487,** 2006(e1). Standard practice for classification of soils for engineering purposes (Unified Soil Classification System). ASTM International, West Conshohocken, PA, 2006, vol. 04.08.
9. **ASTM standard D 2850,** 2003. Standard test method for unconsolidated undrained triaxial compression test on cohesive soils. ASTM International, West Conshohocken, PA, 2005, vol. 04.08.
10. **ASTM standard D 4253,** 2000(2006). Standard test methods for maximum index density and unit weight of soils using a vibratory table. ASTM International, West Conshohocken, PA, 2006, vol. 04.08.

TH-1123_10610407

11. **ASTM standard D4254,** 2000 (2006). Standard test methods for minimum index density and unit weight of soils and calculation of relative density. ASTM International, West Conshohocken, PA, 2006, Vol. 04.08.
12. **ASTM standard D 4595,** 2009. Standard test methods for tensile properties of geotextiles by the wide-width strip method. ASTM International, West Conshohocken, PA, 2009.
13. **ASTM standard D 4884,** 2009. Standard test method for strength of sewn of thermally bonded seams of geotextiles. ASTM International, West Conshohocken, PA, 2009, vol. 04.13.
14. **ASTM standard D 5199,** 2011. Standard test method for measuring the nominal thickness of geosynthetics. ASTM International, West Conshohocken, PA, 2011, vol. 02.01.
15. **ASTM standard D 5261,** 2010. Standard test method for measuring mass per unit area of geotextiles. ASTM International, West Conshohocken, PA, 2010, vol. 03.01.
16. **ASTM standard D 5311,** 1992(2004e1). Standard test method for load controlled cyclic triaxial strength of soil. ASTM International, West Conshohocken, PA, 2005, vol. 04.08.
17. **ASTM standard D 6913,** 2004 (e2). Standard test methods for particle-size distribution (gradation) of soils using sieve analysis. ASTM International, West Conshohocken, PA, 2004, vol. 04.09.
18. **Bahloul, K.M.M.** (2004). "Behavior of footing resting on randomly fiber reinforced sand cushion underlaid by a layer of soft clay and adjacent to a slope."
19. **Bathurst, R.J**. and **Crowe, R.E.** (1992). "Recent case histories of flexible geocell retaining walls in North America." *Proceedings of Symposium on Recent case Histories of Permanent Geosynthetic Reinforced Soil Retaining Walls*. Tokyo, November, Balkema, Rotterdam, 1-19.
20. **Bathurst, R.J.,** and **Jarrett, P.M.** (1988). "Large scale model tests of geocomposite mattresses over peat subgrades." *Transportation Research Record*, Transportation Research Board, Washington, D.C, **1188,** 28–36.

TH-1123_10610407

21. **Bathurst, R.J.,** and **Karpurapu** (1993). "Large-scale triaxial compression testing of geocell-reinforced granular soils." *Geotechnical testing journal,* **16(3),** 296-303.
22. **Benson, C.H.** and **Khire, M.V.** (1994). "Reinforcing sand with strips of reclaimed high-density polyethylene." *Journal of Geotechnical Engineering*, **120**, 838-855.
23. **Binquet, J.,** and **Lee, K.L.** (1975). "Bearing capacity tests on reinforced earth slabs." *Journal of Geotechnical Engineering Division*, ASCE, **101(12)**, 1241-1255.
24. **Bolton, M.D.** (1986). "The strength and dilatancy of sands." *Geotechnique,* **36(1)**, 65-78.
25. **Bridgman, P.W.** (1931). "Dimensional analysis." New Haven: Yale University Press.
26. **Buckingham, E.** (1914). On physically similar systems. Physical Review, APS, 4, 345-376.
27. **Bush, D.I., Jenner, C.G.,** and **Bassett, R.H.** (1990). "The design and construction of geocell foundation mattress supporting embankments over soft ground." *Geotextiles and Geomembranes,* **9(1),** 83-98.
28. **Butterfield R.** (1999). "Dimensional analysis for geotechnical engineers" *Geotechnique,* **49 (3),** 357-366.
29. **Carroll, Jr, R.G.,** and **Curtis, V.C.** (1990). "Geogrid connections." *Geotextiles and Geomembranes*, **9(4-6),** 515-530.
30. **Chen, R.H.,** and **Chiu, Y.M.** (2008). "Model tests of geocell retaining structures." *Geotextiles and Geomembranes,* **26,** 56-70.
31. **Consoli, N. C., Casagrande M. D. T., Prietto, P. D. M.,** and **Thome**, **A.** (2003) "Plate Load Test on Fiber-Reinforced Soil." *Journal of Geotechnical and Geoenvironmental Engineering*, ASCE**, 129** (**10**), 951-955.
32. **Cowland, J.W.,** and **Wong, S.C.K.** (1993). "Performance of road embankment on soft clay supported on a geocell mattress foundation." *Geotextiles and Geomembranes,* **12(8),** 687-705.

TH-1123_10610407

33. **Das, B.M.** and **Khing, K.H**. (1994). "Foundation on layered soil with geogrid reinforcement-effect of a void." *Geotextiles and Geomembranes,* **13(8),** 545-553.
34. **Das, B.M., Puri, V.K.,** and **Evgin, E.** (1996). "Bearing capacity of strip footing on geogrid-reinforced sand-scale effects in model tests." Proceedings of 6th International Conference on offshore and Polar Engineering, Los Angles, May, 527-530.
35. **Dash, S.K., Krishnaswamy, N.R., Rajagopal, K.** (2001a). "Bearing capacity of strip footing supported on geocell-reinforced sand." *Geotextiles and Geomembranes,* **19,**235-256.
36. **Dash, S.K., Rajgopal, K.,** and **Krishnaswamy, N.R.** (2001b). "Strip footing on geocell reinforced sand beds with additional planer reinforcement." *Geotextiles and Geomembranes,* **21(4),** 197-219.
37. **Dash, S.K., Sireesh, S.,** and **Sitharam, T.G.** (2003a). "Model studies on circular footing supported on geocell reinforced sand underlain by soft clay." *Geotextiles and Geomembranes,* **21 (4),** 197-219.
38. **Dash, S.K., Sireesh, S.,** and **Sitharam, T.G.** (2003b). "Behaviour of geocell-reinforced sand beds under circular footing." *Ground Improvement,* **7(3),** 111-115.
39. **Dash, S.K., Rajgopal, K.,** and **Krishnaswamy, N.R.** (2004). "Performance of different geosynthetic reinforcement materials in sand foundations" *Geosynthetics International,* **11(1),** 35-42.
40. **Dash S. K., Rajagopal K.,** and **Krishnaswamy N. R.** (2007). "Behaviour of Geocell-Reinforced Sand Beds under Strip Loading". *Can. Geotech. J.,* **44,** 905-916.
41. **Dash, S.K., Reddy, P.D.,** and **Raghukanth, T.G.** (2008). "Subgrade modulus of geocell-reinforced sand foundation." *Ground Improvement,* **161(12),** 79-87.
42. **Dash, S.K.** (2010). "Influence of relative density of soil performance of geocell-reinforced sand foundations." *Journal of Materials in Civil Engineering division,* ASCE, **22(5),** 533-538.

TH-1123_10610407

43. **De Garidel, R.**, and **Morel, G.** (1986). "New strengthening techniques by textile elements for low-volume roads." *Proceedings of 3rd International Conference on Geotextiles, Vienna, Austria,* 1027-1032.
44. **Dean, R.** and **Lothian, E.** (1990). "Embankment construction problems over deep variable soft deposits using a geocell mattress." *Performance of reinforced soil structures.* Eds. McGown., Yeo K.c. and Andrawes, K.Z., British Geotechnical Society, Thomas Telford Ltd., London, 443-447.
45. **Dronamraju, V. S** (2008). "Studies on Field Stabilization Methods to PreventSurficial Slope Failures of Earth fill Dams". Ph.D Thesis, University of Texas atArlington, Texas, USA.
46. **Emersleben, A.**, and **Meyer, N.** (2008). "The use of geocells in road construction over soft soil: vertical stress and falling weight deflectometer measurements." *EuroGeo4,* Paper number **132,** 1-8.
47. **Fragaszy, J.R.** and **Lawton, E.** (1984) Bearing capacity of reinforced sand subgrades. *Journal of the Geotechnical Engineering Division*, ASCE, **110**, 1500-1507.
48. **Frost, J.D.,** and **Han, J.** (1999). "Behavior of interfaces between fiber-reinforced polymers and sands." *Journals of Geotechnical and Geoenvironmetal Engineering,* ASCE, **125(8),** 633-640.
49. **Forsman, J., Slunga, E.,** and **Lahtinen, P.** (1998). "Geogrid and Geocell Reinforced Secondary Road over Deep Peat Deposit." *Prooooceedings of the 6th International conference on Geosnthetics, Atlanta,* **2,** 773-778.
50. **Gray, D.H.,** and **Al-Refeai, T.** (1986). "Behavior of fabric-versus fiber-reinforced sand." *Journal of Geotechnical Engineering,* ASCE, **112(8)**, 804-820.
51. **Gray, D.H., and Ohashi, H.** (1983). "Mechanics of fiber reinforcement in sand." *Journal of Geotechnical engineering,* ASCE, **109(3)**, 335-353.
52. **Gregory, G.H.** (2006). "Shear strength, creep and stability of fiber-reinforced soil slope." PhD thesis, Oklahoma state University.
53. **Gregory, G.H**., and **Chill, D.S.** (1998) "Stabilization of earth slopes with fiber reinforcement." *Proceedings of the Sixth International Conference on Geosynthetics*, Atlanta, Georgia, 1073-1078.

TH-1123_10610407

54. **Guido, V. A.**, **Chang, D.K.** and **Sweeny, M. A.** (1986) Comparison of geogrid and geotextile reinforced earth slabs. *Canadian Geotechnical Journal*, **23**, 435-440.
55. **Gupta, A.**, and **Somnath, B.** (1994). "Bearing capacity improvement using geogrids." *Civil Engineering and Construction Review,* **7,** 12-13.
56. **Henkel, D.J. and Gilbert, G.D.** (1952) "The effect of the rubber membrane on the measured triaxial compression strength of clay samples." *Geotechnique* **3 (1),** 20-29.
57. **IS: 235,** 1989."Textiles fibers tensile characteristics of individual fibers methods of determination." BIS, New Delhi.
58. **IS: 326 (Part 3),** 2006. "Methods of sampling and test for natural and synthetic perfumery materials." BIS New Delhi.
59. **IS: 1498,** 1970. "Classification and Identification of soils for general engineering purposes." BIS, New Delhi.
60. **IS: 2720 (Part 3),** 1981. "Determination of Specific Gravity –fine,medium and coarse grained soils." BIS, New Delhi.
61. **IS: 2720 (Part 4),** 1975. "Grain size analysis." BIS, New Delhi.
62. **IS: 2720 (Part 11),** 1971."Determination of shear strength parameters of soils from consolidated-undrained triaxial compression test with measurement of pore-water pressure." BIS, New Delhi.
63. **IS: 2720 (Part 14),** 1983. "Determination of density index (Relative density) of cohesionless soils." BIS, New Delhi.
64. **IS: 13162 (Part 3),** 1992. "Determination of thickness at specified pressure." BIS, New Delhi.
65. **IS: 13162 (Part 5),** 1992. "Determination of tensile properties using a wide width strip." BIS, New Delhi.
66. **IS: 14716,** 1999. "Geotextiles-determination of mass per unit area." BIS, New Delhi.
67. **IS: 15060,** 2001."Geotextiles-Tensile test for joints/seams by wide width method." BIS, New Delhi.

TH-1123_10610407

68. **Johnson, J.E.** (1982). "Bridge and Tidal Waters." *Municipal Engineer,* **109,** 104-107.
69. **Kaniraj, S.R.,** and **Gayathri, V.** (2003). "Geotechnical behavior of fly ash mixed with randomly oriented fiber inclusions." *Geotextiles and Geomembranes,* **21**, 123-149.
70. **Khedkar, M.S.,** and **Mandal, J.N.** (2009). "Behaviour of cellular reinforced sand under triaxial loading conditions." *Geotechnical and Geological engineering,* **27**, 645-658.
71. **Khing, K.H.**, **Das, B.M.**, **Puri, V.K.**, **Cook, E.E.** and **Yen, S.C.** (1993). "The bearing-capacity of a strip foundation on geogrid reinforced sand." *Geotextiles and Geomambranes*, **12**, 351-361.
72. **Koerner R.M.** *Designing with Geosynthetics*. Prentice Hall, Englewood Cliffs, New Jersey, 1990.
73. **Krishnaswamy, N.R., Rajgopal, K.,** and **Latha, G.M.** (2000). "Model studies on geocell supported embankments constructed over a soft clay foundation." *Geotechnical Testing Journal,* GTJODJ, **23(1),** 45-54.
74. **Kumar, A., Walia, B.S.** and **Mohan, J.** (2006). "Compressive strength of fiber reinforced highly compressible clay." *Construction and Building Materials,* **20,** 1063-1068.
75. **Ladd, R.S.** (1978). "Preparing test specimens using under compaction." *Geotechnical Testing Journal,* 1(1), 16-23.
76. **Lambert, S.**, **Nicot, F.,** and **Gotteland P.** (2011). "Uniaxial compressive behavior of scrapped tire and filled wire netted geocell with a geotextile envelope." *Geotextiles and Geomembranes,* **29,** 483-490.
77. **Lambe, T.W.** and **Whitman, R.V.** (1979). "Soil Mechanics" John Wiley and Sons.
78. **Langhaar, J.L.,** 1951. "Dimensional analysis and theory of models" John wiley & sons, New York, N.Y.
79. **Latha, G.M.,** and **Murthi, V.S.** (2007). "Effects of reinforcement form on the behavior of geosynthetic reinforced sand." *Geotextiles and geomembranes,* **25(1),** 23-32.

TH-1123_10610407

80. **Latha, G.M.,** and **Somwanshi, A.** (2009). "Effect of reinforcement form on the bearing capacity of square footing on sand." *Geotextiles and Geomembranes,* **27(6),** 409-422.
81. **Lindh, E.** and **Eriksson, L.** (1990). "Sand reinforced with fibers: a field experiment." *Proceedings of the International reinforced soil conference on performance of reinforced soil structure*, Glasgow, UK., 471-474.
82. **Maher, M.H.,** and **Gray, D.H.** (1990). "Static response of sand reinforced with randomly distributed fibers." *Journal of Geotechnical Engineering,* ASCE, **116(11),** 1661-1677.
83. **Maheshwari, K.Desai, A.K.** and **Solanki, C.H. (2011).** "Application and modeling of fiber reinforced soil." *Proceeding Indian Geotechnical Conference,* 497-500.
84. **Mhaiskar, S.Y.,** and **Mandal, J.N.** (1996). "Investigations on soft clay subgrade strengthening using geocells." *Construction and Building Materials,* **10(4),** 281-286.
85. **Michalowski, R.L.,** and **Cermak, J.** (2003). "Triaxial compression of sand reinforced with fibers." *Journals of Geotechnical and Geoenvironmental Engineering,* ASCE, **129(2),** 125-136.
86. **Michalowski, R.L.,** and **Zhao, A.** (1996). "Failure of fiber-reinforced granular soils." *Journal of Geotechnical Engineering*, ASCE, **122(3),** 226-234.
87. **Milligan, G.W.E., Fannin, R.J.** and **Farrar, D.M.** (1986). "Model and full-scale tests of granular layers reinforced with a geogrid." *Proceedings of the Third International Conference on Geotextiles, Vienna,* **1,** 61-66.
88. **Minaxi, R.** (2010) "Geocell-sand mattress overlying soft clay subgrade: Behaviour under circular loading." Dissertation submitted in partial fulfillment for the requirements of the Doctoral Degree, IIT Guwahati, Guwahati.
89. **Naaman, A.E.** (1972). "A statistical theory of strength for fiber reinforced concrete," thesis submitted to Massachusetts Inst. Of Tech. at Cambridge, Mass., in partial fulfillment of the requirements for the degree of Doctor of Philosophy.
90. **Park, T.,** and **Tan, S.A.** (2005). "Enhanced performance of reinforced walls by the inclusion of short fiber." *Geotextiles and Geomembranes,* **23,** 348-361.

TH-1123_10610407

91. **Paul, J.** (1988). "Reinforced soil system in embankments-construction practices." *Proceedings of International Geotechnical Symposium on practice of Earth Reinforcement,* Fukuoka, Japan, October, 461-466.
92. **Pokharel, S.K., Han, J., Leshchinsky, D., Parsons, R.L.,** and **Halahmi, I.** (2010). "Investigation of factors influencing behavior of single geocell-reinforced bases under static loading." *Geotextiles and Geomembranes,* **28(7),** 570-578.
93. **Puppala, A. J. and Musenda, C. (2007)**. "Effects of Fiber Reinforcement on Strength and Volume Change in Expansive Soils" *Journal of the Transportation Research Board,* **1736,** 134-140.
94. **Rajagopal, K., Krishnaswamy, N.R.,** and **Latha, G.M.** (1999). "Behaviour of sand confined with single and multiple geocells." *Geotextiles and Geeomembranes,* **17(3),** 171-184.
95. **Ranjan, G.**, **Vasan, R.M.** and **Charan, H.D.** (1994). "Behaviour of plastic-fiber-reinforced sand." *Geotexiles and Geomembranes,* **13***,* 555-565.
96. **Ranjan, G., Vasan, R.M.,** and **Charan, H.D.** (1996). "Probabilistic analysis of randomly distributed fiber-reinforced soil." *Journal of Geotechnical Engineering,* ASCE, **122(6),** 419-426.
97. **Rea, C.,** and **Mitchell, J.K.,** (1978). "Sand reinforcement using paper grid cells." Reprint 3130, ASCE spring convention and exhibit, Pittsbutgh, PA, 24-28.
98. **Refai, S.M.** (2000). "Impact of polypropylene fibers on desiccation cracking and hydraulic conductivity of compacted clay liners." Dissertation submitted in partial fulfillment for the requirements of the Doctoral Degree, Wayne State University, Detroit, Michigan.
99. **Robertson, J.**, and **Gilchrist, A.J.T.** (1987). "Design and construction of a reinforced embankment across soft lakebed deposits." *Proceedings of the International Conference on Foundations and Tunnels,* London, 2, M.C. Forde Engineering Technics Press, Edinburg, pp. 84-92.
100. **Sadek, S., Najjar, S. S.,** and **Fadi Freiha** (2010). "Shear strength of fiber-reinforced sands." *Journal of Geotechnical and Geoenvironmental engineering division,* ASCE, **136(3),** 490-499.

TH-1123_10610407

101. **Santoni, R.L., Tingle, J.S.,** and **Webster, S.L.,** (2001). "Engineering properties of sand-fiber mixture for road construction." *Journal of Geotechnical and Geoenvironmental Engineering,* ASCE, **127(3),** 258-268.

102. **Shewbridge, S.E.,** and **Sitar, N.** (1990). "Deformation-based model for reinforced sand." *Journal of Geotechnical engineering,* ASCE, **116(7),** 1153-1170.

103. **Simac, M.R.** (1990). "Connections for geogrid systems." *Geotextiles and Geomembranes*, **9(4-6)**, 537-546.

104. **Sireesh, S., Sitharam, T.G.,** and **Dash S.K.** (2009). "Bearing capacity of circular footing on geocell-sand mattress overlying clay bed with void." *Geotextiles and Geomembranes,* **27(2),** 89-98.

105. **Sridharan A.** *Bearing capacity improvement* pp. 175-196 In **G.V. Rao** and **G.V.V.S. Raju**(ed.) *Engineering with Geosynthetics*, Tata McGraw-Hill, New Delhi,1990.

106. **Tafreshi, S.N.M.,** and **Dawson, A.R.** (2010a). "Behaviour of footings on reinforced sand subjected to repeated loading-comparing use of 3D and planar geotextile." *Geotextiles Geomembranes,* **28(5)**, 434 - 447.

107. **Tafreshi, S.N.M.,** and **Dawson, A.R.** (2010b). "Comparison of bearing capacity of strip footing on sand with geocell and with planar of geotextile reinforcement." *Geotextiles and Geomembranes,* **28(1),** 72-84.

108. **Tang, C., Shi, B., Gao, W., Chen F.,** and **Cai, Y.** (2007). "Strength and mechanical behavior of short polypropylene fiber reinforced and cement stabilized clayey soil." *Geotextiles and Geomembranes,* **25(3),** 194-202.

109. **Tingle, J.S., Santoni, R.L.,** and **Webster, S.L.** (2002). "Full-scale field tests of discrete fiber-reinforced sand." *Journal of Transportation Engineering,* ASCE, **128 (1),** 9-16.

110. **Vesic, A.S.** (1973). "Analysis of ultimate loads of shallow foundations." *Journal of soil mechanics and Foundations Division,* ASCE, **99(1),** .45-73.

111. **Vidal, H** (1969). The principle of reinforced earth. *Highway Research Record,* N.282, Washington D. C.

TH-1123_10610407

112. **Wang, Y.M., Chen, Y.K., and Liu W.** (2008). "Large-scale direct shear testing of geocell reinforced soil." *Journal of Central South University of Technology,* **15(6)**, 895-900.

113. **Wasti, Y.,** and **Butun, M.D.,** (1996). "Behaviour of model footings on sand reinforced with discrete inclusion." *Geotextiles and Geomembranes,* **14,** 575-584.

114. **Webster, S.L.**, (1979). "Investigation of Beach Sand Trafficability Enhancement Using Sand-grid Confinement and Membrane Reinforcement Concepts." Technical Report GL-79-20. US Army Corps of Engineers, Vicksburg, MS.

115. **Webster, S.L.,** and **Alford, S.J.,** (1978). "Investigation of construction concepts for pavements across soft ground." Technical Report **S-78-6,** US Army Corps of Engineers Waterways Experiment Station, Vicksburg, Mississippi.

116. **Webster, S.L.** and **Santoni, R.L.** (1997). "Contigency airfield and road construction using geosynthetic fiber stabilization of sand." Technical Report GL-97-4, U.S. Army Waterways Experiment Station, Vicksburg, Mississippi.

117. **Webster, S.L.,** and **Watkins, J.E.** (1977). "Investigation of construction techniques for tactical bridge approach roads across soft ground." Technical report, **S-77-1,** United state army corps of engineers, waterways experiment station, Mississippi, USA.

118. **Wesseloo, J**. (2004). "The strength and stiffness of Geocell support packs" Dissertation submitted in partial fulfillment for the requirements of the Doctoral Degree, University of Pretoria, Pretoria.

119. **Wesseloo, J., Visser, A.T.,** and **Rust, E.** (2009). "The stress-strain behaviour of multiple cell geocell packs" *Geotextiles and Geomembranes,* **27(1),** 31-38.

120. **Yetimoglu, T.,** and **Salbas, O.** (2003). "A study on shear strength of sands reinforced with randomly distributed discrete fibers." *Geotextiles and Geomembranes,* **21,** 103-110.

121. **Xie, Y.,** and **Yang, X.** (2009). "Characteristics of new-type geocell flexible retaining wall." *Journal of Materials in Civil Engineering division,* ASCE, **21(4),** 171-175.

TH-1123_10610407

122. Zhang, Z., Farrag, K. and **Morvant, M. (2008).** "Evaluation of effect of synthetic fibers and nonwoven geotextile reinforcement on the stability of heavy clay embankments." FHWA/La 03/373. Lousiana Transportation research centre, Balton, Rouge, L.A., U.S.A., 7-19.

TH-1123_10610407